UNIVERSITAT DE BARCELONA

Development and assessment of magnesium phosphate cements by using industrial by-products and wastes

Anna Alfocea Roig

ADVERTIMENT. La consulta d'aquesta tesi queda condicionada a l'acceptació de les següents condicions d'ús: La difusió d'aquesta tesi per mitjà del servei TDX (**www.tdx.cat**) i a través del Dipòsit Digital de la UB (**diposit.ub.edu**) ha estat autoritzada pels titulars dels drets de propietat intel·lectual únicament per a usos privats emmarcats en activitats d'investigació i docència. No s'autoritza la seva reproducció amb finalitats de lucre ni la seva difusió i posada a disposició des d'un lloc aliè al servei TDX ni al Dipòsit Digital de la UB. No s'autoritza la presentació del seu contingut en una finestra o marc aliè a TDX o al Dipòsit Digital de la UB (framing). Aquesta reserva de drets afecta tant al resum de presentació de la tesi com als seus continguts. En la utilització o cita de parts de la tesi és obligat indicar el nom de la persona autora.

ADVERTENCIA. La consulta de esta tesis queda condicionada a la aceptación de las siguientes condiciones de uso: La difusión de esta tesis por medio del servicio TDR (**www.tdx.cat**) y a través del Repositorio Digital de la UB (**diposit.ub.edu**) ha sido autorizada por los titulares de los derechos de propiedad intelectual únicamente para usos privados enmarcados en actividades de investigación y docencia. No se autoriza su reproducción con finalidades de lucro ni su difusión y puesta a disposición desde un sitio ajeno al servicio TDR o al Repositorio Digital de la UB. No se autoriza la presentación de su contenido en una ventana o marco ajeno a TDR o al Repositorio Digital de la UB (framing). Esta reserva de derechos afecta tanto al resumen de presentación de la tesis como a sus contenidos. En la utilización o cita de partes de la tesis es obligado indicar el nombre de la persona autora.

WARNING. On having consulted this thesis you're accepting the following use conditions: Spreading this thesis by the TDX (**www.tdx.cat**) service and by the UB Digital Repository (**diposit.ub.edu**) has been authorized by the titular of the intellectual property rights only for private uses placed in investigation and teaching activities. Reproduction with lucrative aims is not authorized nor its spreading and availability from a site foreign to the TDX service or to the UB Digital Repository. Introducing its content in a window or frame foreign to the TDX service or to the UB Digital Repository is not authorized (framing). Those rights affect to the presentation summary of the thesis as well as to its contents. In the using or citation of parts of the thesis it's obliged to indicate the name of the author.

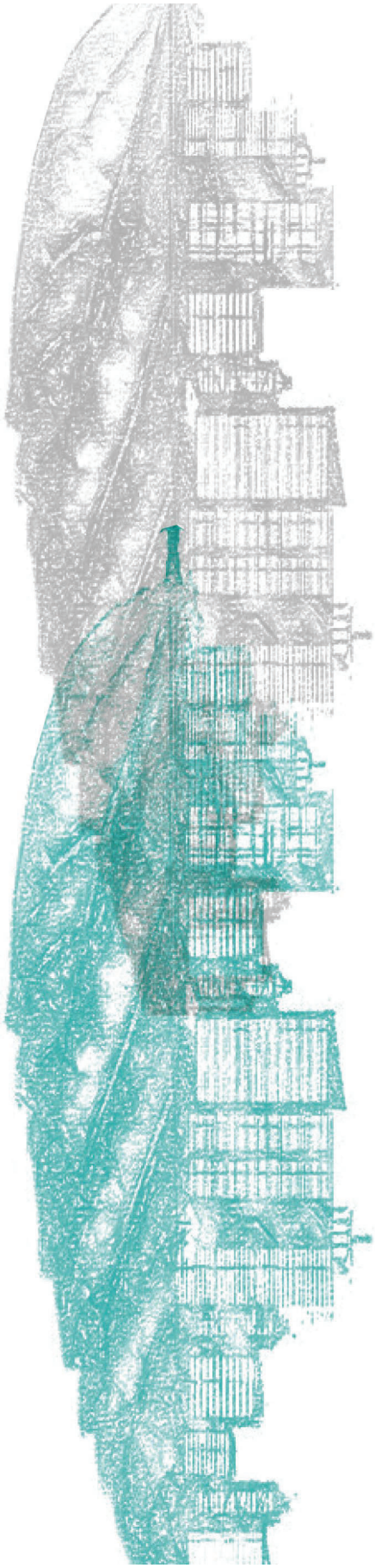

Development and assessment of magnesium phosphate cements by using industrial by-products and wastes

Anna Alfocea Roig

UNIVERSITAT DE BARCELONA

UNIVERSITAT DE BARCELONA

Doctoral Program in Engineering and Applied Sciences

Development and assessment of magnesium phosphate cements by using industrial by-products and wastes

Desenvolupament i avaluació de ciments de fosfat de magnesi mitjançant l'ús de subproductes i residus industrials

Author

Anna Alfocea Roig

Supervisors

Dr. Joan Formosa Mitjans

Dr. Jessica Giró Paloma

Departament de Ciència de Materials i Química Física, Facultat de Química, Universitat de Barcelona

2025

Recordes quan somiaves el

que ja has aconseguit?

Moltes gràcies

Moltes gràcies DIOPMA

Moltes gràcies família, sou casa

SUMMARY

The construction sector is globally recognized as a significant contributor to environmental pollution, particularly in terms of climate change and the depletion of natural resources. These environmental impacts arise from various factors, including the materials used, the technologies applied, and transportation processes involved. In response, the industry is increasingly prioritizing strategies to reduce its carbon footprint by adopting innovative solutions that minimize environmental impact and promote sustainability.

One such approach is the development of alternative cements that valorise industrial by-products and wastes. These efforts aim to conserve natural resources, protect the environment, and promote sustainable construction practices. Among these alternatives, magnesium phosphate cement (MPC) has gained recognition as a promising option. MPC is typically composed of a magnesium oxide (MgO) source and a phosphate source. However, due to the high carbon dioxide emissions associated with the production of pure magnesium oxide, identifying sustainable alternatives is essential to minimizing their environmental impact.

This PhD thesis explores the feasibility of using industrial by-products and wastes as substitutes for pure magnesium oxide in the production of MPC. Specifically, it focuses on tundish deskulling waste (TUN), a waste of the steel industry, and low-grade magnesium oxide (LG-MgO; LG), a by-product derived from magnesite calcination. This approach aligns with principles of the circular economy, promotes efficient wastes management, and contributes to the achievement of sustainable development goals (SDGs), particularly in addressing climate change.

The research began with a comprehensive evaluation of the global landscape of alternative magnesium oxide sources, offering valuable context while identifying existing opportunities and challenges. Following, a detailed investigation was conducted into the properties of TUN, marking its first-ever application as a raw material for MgO-based cements. The analysis assessed its suitability for cement formulations, its performance in mortar development, and, finally, its environmental impact through a life cycle assessment (LCA).

Subsequent chapters focused on the characterization of cements incorporating TUN and LG-MgO. The first study examined the synergistic effects of combining these materials, emphasizing their compatibility and mutual benefits. The second study shifted attention solely on LG-MgO, exploring its versatility and potential for innovative applications in the construction sector.

The present doctoral thesis highlights the transformative potential of alternative secondary sources, such as TUN and LG-MgO, as sustainable raw materials for MPC production. By minimizing the environmental footprint of conventional cement formulations, this research offers a pathway for a greener and more sustainable construction industry, emphasizing the pivotal role of industrial by-products and wastes in the advancement of cementitious materials.

Resum

El sector de la construcció és reconegut globalment com un dels principals responsables de la contaminació ambiental, especialment pel canvi climàtic i l'esgotament dels recursos naturals. Aquest impacte prové dels materials utilitzats, les tecnologies emprades i els processos de transport. En resposta, aquesta indústria busca reduir la seva petjada de carboni mitjançant solucions innovadores i sostenibles.

Una estratègia per aconseguir-ho és el desenvolupament de ciments alternatius que valoritzin residus i subproductes industrials. Aquests ciments tenen com a objectiu conservar els recursos naturals, protegir el medi ambient i fomentar pràctiques de construcció més sostenibles. El ciment de fosfat de magnesi (MPC), format per una font d'òxid de magnesi (MgO) i una font de fosfat, és una opció prometedora. No obstant això, la producció d'òxid de magnesi de pur genera elevades emissions de diòxid de carboni, per la qual cosa és essencial identificar alternatives més sostenibles.

Aquesta tesi doctoral explora la viabilitat d'utilitzar residus i subproductes industrials com a substituts de l'òxid de magnesi pur per a la producció de MPC. Concretament, analitza l'ús de residus de l'artesa del tundish (TUN), provinents de la indústria siderúrgica i un òxid de magnesi de baixa qualitat (LG-MgO; LG), derivat de la calcinació de la magnesita. Aquesta estratègia s'alinea amb els principis de l'economia circular i la gestió eficient de residus, contribuint a la consecució dels objectius de desenvolupament sostenible (ODS).

La recerca s'inicia amb una avaluació global de les fonts alternatives d'òxid de magnesi, seguida d'una anàlisi detallada del TUN per al desenvolupament de ciments, morters i l'anàlisi ambiental, marcant la primera vegada que aquest residu s'utilitza com a matèria primera en el sector de la construcció. A continuació, s'examina la possibilitat de combinar TUN amb LG-MgO per a la formulació de ciments, així com la versatilitat del LG-MgO per a noves aplicacions en la indústria de la construcció. Els resultats obtinguts evidencien el gran potencial dels residus industrials per reduir l'impacte ambiental dels ciments tradicionals i promoure un model de construcció més sostenible.

CONTENTS

Contents

Chapter 1 Preface 1
1.1. Background 3
1.1.1. General overview 3
1.1.2. Precedents and context 4
1.2. Research motivation 6
1.3. Thesis structure 9
1.4. References 11
Chapter 2 State of the art 17
2.1. Objectives 19
2.2. Introduction 21
2.2.1. Current situation 21
2.2.2. Chemically bonded ceramic (CBC) 30
2.2.3. Alternative raw materials 44
2.2.4. Challenges and future considerations 53
2.3. References 56
Chapter 3 Development of MPC-TUN 73
3.1. Cement 75
3.1.1. Introduction 75
3.1.2. Relevance 76
3.1.3. Publication 1 77
3.1.4. Additional research contribution 88
3.2. Mortar 90
3.2.1. Introduction 90
3.2.2. Relevance 91
3.2.3. Publication 2 92
3.3. Life cycle assessment 117
3.3.1. Introduction 117
3.3.2. Relevance 118
3.3.3. Publication 3 119
3.3.4. Additional research contribution 136
3.4. References 142
Chapter 4 Characterization of MPC formulations 149
4.1. Combination 151

4.1.1. Introduction 151
4.1.2. Relevance 152
4.1.3. Publication 4 153
4.2. Fibres 187
4.2.1. Introduction 187
4.2.2. Relevance 188
4.2.3. Publication 5 189
4.3. References 201
Chapter 5 Conclusions 207
5.1. Conclusions 209
5.1.1. Main findings 210
5.1.2. Future work 213
Chapter 6 Appendix 217

LIST OF FIGURES AND TABLES

List of figures

Chapter 1

Figure 1.1.Thesis structure. 10

Chapter 2

Figure 2.1.Conceptual framework of the experimental design to achieve the objectives. 20

Figure 2.2. Cembureau targets to climate neutrality by 2020 (adapted from [8]). 23

Figure 2.3. Process flow diagram for the manufacturing process of OPC. 25

Figure 2.4. Number of publications and citations of alternative cementitious materials. 27

Figure 2.5. Percentage of publications of alternative cementitious materials with respect to the country by map chart. 28

Figure 2.6. Classification of CBC families related to phosphate-based materials. 30

Figure 2.7. CBC's reaction. 31

Figure 2.8. K-struvite crystal phase (adapted from [52,53]). 35

Figure 2.9. The evolution of publications in the research field over the years. 38

Figure 2.10. Number of publications in the research field from the most relevant countries. 39

Figure 2.11. Times cited and publications over time of MPC. 42

Figure 2.12. Keyword map of MPC. 44

Figure 2.13. Simplified flow diagram for producing LG-MgO at Magnesitas Navarras S.A. company (Zubiri-Navarra, Spain). 47

Figure 2.14. Conditioning process of TUN. 50

Figure 2.15. Production of Li_2CO_3 [97,98]. 51

Figure 2.16. Process diagram of the conditioning process of MRBW. 53

Chapter 3

Figure 3.1. The research benefits of the development of MPC-TUN. 77

Figure 3.2. Headline of the article published in the journal of Environmental Chemical Engineering in October 2023, entitled "Can tundish deskulling waste be used as a magnesium oxide source to develop magnesium phosphate cement?" [6]. 78

Figure 3.3. Time evolution of the FTIR-ATR signal for the MPC-TUN sample. 89

Figure 3.4. Advantages of research on the development of MPC-TUN mortars. 91

Figure 3.5. Headline of the article under review in the journal Materials Today Sustainability, entitled "Tundish deskulling waste as a source of MgO for producing Magnesium Phosphate Cement-based mortars: advancing sustainable construction materials". 92

Figure 3.6. Systems boundaries of LCA. 118

Figure 3.7. Contributions of the environmental assessment study. 119

Figure 3.8. Article published in the journal of Sustainable Chemistry and Pharmacy in 2024, titled "Life cycle assessment of the climate change impact of magnesium phosphate cements formulated with tundish deskulling waste compared to conventional cement" [29]. 120

Figure 3.9. Contributions of mortars to the impacts on resource consumption (MJ) for the electricity scenario in 2050. 137

Figure 3.10. Results for the resource consumption category under electricity scenario. 138

Figure 3.11. Contributions of resource consumption for the electricity and fuel scenario. 139

Figure 3.12. Resource consumption category for electricity and fuel scenario. 140

Chapter 4

Figure 4.1. Advantages of research on MPC development using a combination of two alternative raw materials. 153

Figure 4.2. Headline of the article under review, entitled "Secondary sources of MgO for the development of magnesium phosphate cement: approach to sustainable construction". 154

Figure 4.3. Advantages of research on development of MPC with LG-MgO and natural fibres. 188

Figure 4.4. Headline of the article, titled "Magnesium phosphate cement incorporating sheep wool fibre for thermal insulation applications", was published in the Journal of Building Engineering in 2023 [25]. 189

List of tables

Chapter 2

Table 2.1. Clinker elemental chemical composition [12]. 24

Table 2.2. Clinker mineral phases composition [12]. 25

Table 2.3. Details of the six countries with the highest impact of MPC. 40

Table 2.4. Authors with a significant impact in the MPC field. 41

Table 2.5. Publications most cited by the four authors with the most impact. 41

Table 2.6. Highly relevant publications. 43

Chapter 3

Table 3.1. Impact categories used in this study 136

GLOSSARY

Acronyms

A	AAC	Alkali-activated cement
	ABC	Acid-base cement
	ADP	Abiotic depletion potential
	AGAUR	Agència de Gestió d'Ajuts Universitaris i de Recerca
	ATR	Attenuated total reflectance
B	BC	Belite cement
	BFS	Blast furnace slag
	B-MgO	Boron-magnesium oxide
	BOF	Basic oxygen furnace
C	CAC	Calcium aluminate cement
	CART	Citric acid reactivity test
	CBC	Chemically bonded ceramic
	CBPC	Chemically bonded phosphate cement
	CCM	Caustic calcined magnesite
	CCS	Carbon capture and storage
	CCU	Carbon capture and use
	CSAC	Calcium sulphoaluminate cement
D	DBM	Dead burned magnesite
	DIOPMA	Disseny i Optimització de Processos i Materials
	DoE	Design of Experiments
E	EAF	Electric arc furnace
	EU	European Union
F	FA	Fly Ash
	FTIR	Fourier transform infrared spectroscopy

G	GDP	Gross domestic product
	GHG	Greenhouse gases
I	IEA	International Energy Agency
J	JIF	Journal impact factor
L	LCA	Life cycle assessment
	LC^3	Limestone calcined clay cement
	LG	Low-grade magnesium oxide
	LG-MgO	Low-grade magnesium oxide
	LiB	Lithium-ion batteries
	L/S	Liquid-to-solid ratio
M	MAGNA	Magnesitas Navarras S.A.
	MAP	Monoammonium phosphate
	MKP	Monopotassium phosphate
	MKPC	Magnesium potassium phosphate cement
	MoE	Modulus of elasticity
	MPC	Magnesium phosphate cement
	MRB	Magnesia refractory brick
	MRBW	Magnesia refractory brick waste
	MSW	Municipal solid waste
O	OPC	Ordinary Porland Cement

S	SCM	Supplementary cementitious material
	SDG	Sustainable development goals
	SO	Specific objective
	SWF	Sheep wool fibres
T	TG	Thermogravimetric analysis
	TUN	Tundish deskulling waste
U	UB	Universitat de Barcelona
W	WoS	Web of Science
	W/C	Water-to-cement ratio
X	XRD	X-ray diffraction
	XRF	X-ray fluorescence

Chapter 1

CHAPTER 1

PREFACE

This chapter outlines the framework of the research, detailing its background and the motivation for the work presented in this thesis. Additionally, the preface provides an overview of the PhD thesis structure designed, carefully designed to guide the reader and ensure clarity and coherence throughout the document.

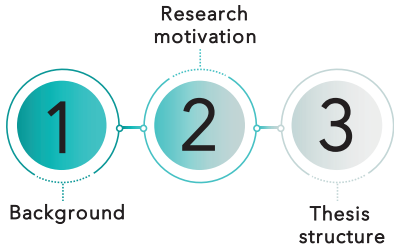

1.1. Background

1.1.1. General overview

We stand at a critical juncture in history, confronted with pressing environmental, social, and economic challenges that demand immediate and prudent actions. The coming years will be decisive as we address these issues across local, national, and global scenes. Achieving meaningful progress as a society requires a collective commitment to ethical policies and a unified effort toward shared goals [1–3].

The current doctoral thesis seeks to address one of the pressing challenges facing society today: the effective management of wastes in constructive building applications to advance the principles of a circular economy. Specifically, the research focuses on developing innovative and alternative construction materials that promote the valorisation of industrial by-products and wastes from the steel and magnesium industries, transforming them into a valuable raw material [4,5].

1.1.2. Precedents and context

This PhD research is the result of established collaboration between the DIOPMA research group (Centre de Disseny i Optimització de Processos i Materials) at Universitat de Barcelona (UB) and the company Magnesitas Navarras S.A. (MAGNA). Established in 1996, this partnership has continued to advance, focusing primarily on the development of innovative construction materials, the analysis and remediation of contaminated soils, and the treatment of wastewater. In addition, this work was supported through the Spanish Government's Grant PID2021-125810OB-C21, funded by MCIN/AEI/10.13039/501100011033 and "ERDF A way of making Europe". Other support came from the Catalan Government's Grant 2021 SGR 00708 and the *Agència de Gestió d'Ajuts Universitaris i de Recerca* (AGAUR), which provided a PhD grant (FI-DGR 2021).

Magnesitas Navarras S.A. is a leader company specialized in the mining, production, and commercialization of magnesite and its derivates, serving the steelmaking, agriculture, and environment sectors. Its main industrial activity is the production of magnesium oxide (MgO) through the calcination of magnesite-rich natural minerals ($MgCO_3$) extracted from its own mines.

Magnesite, a rare mineral, is an exceptional source for producing refractory materials fulfilling the demanding requirements of the steel industry. Among the key products derived from magnesite are refractory materials, specifically dead burned magnesite (DBM), which is produced through calcination at temperatures close to 1800 °C. These refractory masses are classified according to their applications:

- Hearth: masses designed for furnace linings and their repair, both during cold and hot conditions.
- Gunning: masses used for electric arc furnace (EAF) and basic oxygen furnace (BOF) converters.
- Tundish: spraying masses and dry vibe materials specifically tailored for tundish applications.

While the company is responsible for marketing these products, ongoing research is focused to end-of-life management of refractory materials, with the goal of finding

sustainable ways to valorise them and prevent their disposal in landfills. The research also emphasizes industrial by-products derived from magnesite calcination, aiming to develop innovative and transformative solutions. This doctoral thesis is situated within this emerging research area, specially focusing on the valorisation of tundish deskulling waste (TUN) and low-grade magnesium oxide (LG-MgO; LG) [6–8]. In this research collaboration, DIOPMA's role is to explore the potential applications of TUN and LG-MgO in the construction industry, while ensuring alignment with the principles of the circular economy and compliance with evolving environmental regulations. A key goal of the project is to develop alternative applications for TUN and LG-MgO that advance sustainability within the industry.

1.2. Research motivation

Research is a fundamental driver of progress and evolution, serving as the engine for both economic growth and societal development. Every area of research plays a pivotal role in enhancing the well-being and development of society. The doctoral thesis focuses on the development of new construction materials derived from by-products and wastes as raw material. Through this research, the aim is to drive innovation, facilitate the transfer of knowledge and technology, and ensure compliance with environmental regulations, all while promoting sustainability.

The primary motivation for this research is to address the urgent need for alternative waste valorisation methods, preventing its initial disposal in landfills. This approach aligns with the principles of the circular economy and supports the vision of a future free of emissions. The increase in wastes generation due to the human activity presents a critical environmental and social challenge that must be addressed to mitigate the negative effects on the environment, economy, public health, and society. These impacts include overexploitation of natural resources, pollution of soil, water, and air, environment degradation, and spread of bacterial contamination. While inadequate wastes management is a major contributor to these issues, sustainable wastes practices offer a viable solution to reduce their impact.

This research also encompasses to the field of environmental impact assessment within the construction industry. Cement, as a strategic material, is essential for socio-economic development, and its demand is expected to rise in the coming years. Ordinary Portland cement (OPC) represents the largest portion of global cement production [9,10]. However, the production of OPC generates significant environmental impacts, primarily due to the immense quantity of cement produced worldwide and the resource-intensive nature of its manufacturing process. Consequently, this leads to an urgent need for shift towards more sustainable cement production methods, considering the principles of zero emissions and zero wastes [11–13]. While some solutions exist to address these challenges, it is essential to unify collective efforts and

actions at all levels of society to ensure that the future cities and towns are sustainable, inclusive, and environmentally conscious.

Currently, the society is living an era marked by rapid urbanization, population growth, and economic expansion, all of which inevitably leads to a rising demand for and extraction of natural resources. Local, national, and international policymakers must address this challenge by encouraging governments, industries, financial institutions, individuals, and communities to reduce wastes and eliminate wastes mismanagement. Among the diverse types of industries, the construction sector has a pivotal role to play in advancing the circular economy, demonstrating its commitment to environmental responsibility and sustainable practices.

One possible approach to reduce the environmental impact of construction activities is the development of alternative materials with fewer adverse effects on the environment [10]. Magnesium phosphate cement (MPC) offers a viable alternative to the conventional and commercial OPC [9,10]. Composed of magnesium oxide and phosphate sources, MPC forms a cement matrix of k-struvite ($KMgPO_4 \cdot 6H_2O$) or struvite ($NaMgPO_4 \cdot H_2O$) upon reaction [14–16]. These cements exhibit favourable early-stage properties, including rapid setting, along several other advantages [17]. The materials developed in this doctoral thesis focus on MPC utilizing secondary sources of magnesium oxide, specifically tundish deskulling waste (TUN) from the steel industry, and an industrial by-product known as low-grade magnesium oxide (LG-MgO; LG) [18,19]. To guarantee their viability, safety, durability and reliability as building materials, it is necessary to conduct a thorough evaluation of their properties, to determine whether they meet the minimum requirements established by specific regulations and current standards. These evaluations analyses encompass a range of areas, including environmental assessments, and studies of structural and chemical properties, among other analyses. The use of TUN material presents an unique challenge, as this is the first time this waste has been employed in such applications, needing careful examination of its performance and suitability for its use in construction applications.

Then, the aim of this PhD thesis is to develop a new alternative construction material based on MPC, using TUN and LG-MgO as raw materials. The objective is to provide added value to these materials to promote economic circulation and effective by-products and wastes management in alignment with the principles of wastes minimization [20,21].

1.3. Thesis structure

The PhD thesis is presented as a compendium of publications, including publications that have been published or submitted to high-quality scientific journals in the fields of sustainability and construction materials.

This thesis begins with a theoretical framework, comprising of a preface in Chapter 1 and a general introduction in Chapter 2. These chapters provide the context for the research, its significance, and the application of the obtained results, followed by an outline of the research objectives.

Chapters 3 and Chapter 4 outline the experimental framework. These chapters include an introduction, relevance, and publications directly related to the research, and additional information as necessary. Chapter 3 focuses on the development of construction materials using TUN, specifically cement and mortar, alongside environmental studies. Chapter 4 presents characterization studies on the development of MPC, incorporating TUN and LG-MgO as sources of magnesium oxide.

Following, Chapter 5 summarizes the conclusions of the thesis, including observations and insights drawn from the research, as well as suggestions for future work. Chapter 6 presents additional publications and conferences that emerged during the broader course of the doctoral thesis.

A schematic representation of the thesis structure is provided in Figure 1.1, highlighting the subsections and the publications associated with each chapter.

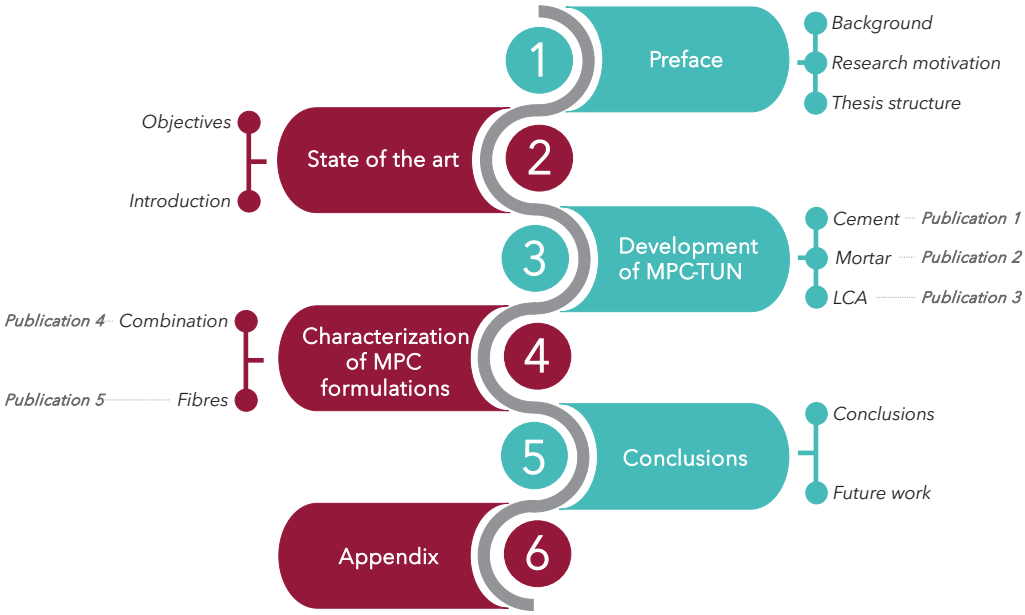

Figure 1.1.Thesis structure.

1.4. References

[1] M. Schneider, M. Romer, M. Tschudin, H. Bolio, Sustainable cement production-present and future, Cement and Concrete Research 41 (2011) 642–650. https://doi.org/10.1016/j.cemconres.2011.03.019.

[2] N. Lippiatt, T.-C. Ling, S.-Y. Pan, Towards carbon-neutral construction materials: Carbonation of cement-based materials and the future perspective, Journal of Building Engineering 28 (2020). https://doi.org/10.1016/j.jobe.2019.101062.

[3] J. de Brito, R. Kurda, The past and future of sustainable concrete: A critical review and new strategies on cement-based materials, Journal of Cleaner Production 281 (2021). https://doi.org/10.1016/j.jclepro.2020.123558.

[4] L. Horckmans, P. Nielsen, P. Dierckx, A. Ducastel, Recycling of refractory bricks used in basic steelmaking: A review, Resources, Conservation and Recycling 140 (2019) 297–304. https://doi.org/10.1016/j.resconrec.2018.09.025.

[5] G. Lopez, J. Farfan, C. Breyer, Trends in the global steel industry: Evolutionary projections and defossilisation pathways through power-to-steel, Journal of Cleaner Production 375 (2022). https://doi.org/10.1016/j.jclepro.2022.134182.

[6] A. Alfocea-Roig, S. Huete-Hernández, X. García-Zubiri, J. Giro-Paloma, J. Formosa, Can tundish deskulling waste be used as a magnesium oxide source to develop magnesium phosphate cement?, Journal of Environmental Chemical Engineering 11 (2023). https://doi.org/10.1016/j.jece.2023.110618.

[7] C. Ding, H. Lei, H. Zhang, M. Xu, Y. Zhao, Q. Li, New insight into relationship between casting speed and inclusion removal in the tundish, Journal of Materials Research and Technology 23 (2023) 5400–5412. https://doi.org/10.1016/j.jmrt.2023.02.146.

[8] Tosaka, Continuous casting (Tundish and Mold), Wikimedia (2008).

[9] D.N. Huntzinger, T.D. Eatmon, A life-cycle assessment of Portland cement manufacturing: comparing the traditional process with alternative technologies, Journal of Cleaner Production 17 (2009) 668–675. https://doi.org/10.1016/j.jclepro.2008.04.007.

[10] C. Shi, A.F. Jiménez, A. Palomo, New cements for the 21st century: The pursuit of an alternative to Portland cement, Cement and Concrete Research 41 (2011) 750–763. https://doi.org/10.1016/j.cemconres.2011.03.016.

[11] M.T. Lotz, J. Rosales Carreón, E. Worrell, A. Herbst, M. Kochański, K. Korczak, Estimating the impact range of circular economy actions for buildings on basic material demand in the European Union: A combination of qualitative and quantitative approaches, Sustainable Production and Consumption 51 (2024) 532–544. https://doi.org/10.1016/j.spc.2024.10.002.

[12] C.-C. Lin, Y.-C. Chang, Impact of circular economy network building: resilience strategy to climate action, IJCCSM 16 (2024) 337–361. https://doi.org/10.1108/IJCCSM-12-2022-0150.

[13] C.Z. Li, V.Wy. Tam, X. Lai, Y. Zhou, S. Guo, Carbon footprint accounting of prefabricated buildings: A circular economy perspective, Building and Environment 258 (2024). https://doi.org/10.1016/j.buildenv.2024.111602.

[14] B. Pang, J. Liu, B. Wang, R. Liu, Y. Yang, Effects of K-struvite on hydration behavior of magnesium potassium phosphate cement, Construction and Building Materials 275 (2021). https://doi.org/10.1016/j.conbuildmat.2020.121741.

[15] B.L. Biwan Xu Andreas Leemann, Frank Winnefeld, Reaction mechanism of magnesium potassium phosphate cement with high magnesium-to-phosphate ratio, Cement and Concrete Research 108 (2018) 140–151. https://doi.org/10.1016/j.cemconres.2018.03.013

[16] J. Formosa, M.A. Aranda, J.M. Chimenos, J.R. Rosell, A.I. Fernández, O. Ginés, Chemically bonded cements formulated with by-products of magnesium oxide, Boletin de La Sociedad Espanola de Ceramica y Vidrio 47 (2008) 293–297. https://doi.org/10.3989/cyv.2008.v47.i5.169.

[17] C. Xu, J. Han, Y. Yang, A review on magnesium potassium phosphate cement: Characterization methods, Journal of Building Engineering 82 (2024). https://doi.org/10.1016/j.jobe.2023.108284.

[18] J. Formosa, A.M. Lacasta, A. Navarro, R. Del Valle-Zermeño, M. Niubó, J.R. Rosell, J.M. Chimenos, Magnesium Phosphate Cements formulated with a low-grade MgO by-product: Physico-mechanical and durability aspects, Construction and Building Materials 91 (2015) 150–157. https://doi.org/10.1016/j.conbuildmat.2015.05.071.

[19] Y. Liu, Z. Qin, B. Chen, Influence of low-grade bauxite on the properties of magnesium phosphate cement, Construction and Building Materials 242 (2020). https://doi.org/10.1016/j.conbuildmat.2020.118052.

[20] M.R. Munaro, S.F. Tavares, A review on barriers, drivers, and stakeholders towards the circular economy: The construction sector perspective, Cleaner and Responsible Consumption 8 (2023). https://doi.org/10.1016/j.clrc.2023.100107.

[21] W.D. Oliveira Silva, D.C. Morais, Transitioning to a circular economy in developing countries: A collaborative approach for sharing responsibilities in solid waste management of a Brazilian craft brewery, Journal of Cleaner Production 319 (2021). https://doi.org/10.1016/j.jclepro.2021.128703.

Chapter 2

CHAPTER 2

STATE OF THE ART

This chapter presents the research objectives, overviews the current state of the cement industry, and emphasizes the urgent need for sustainable practices to reduce CO_2 emissions. It investigates the development of MPC incorporating by-products and wastes from secondary magnesium oxide sources as sustainable alternatives in the construction sector. This approach aligns with the objectives of this thesis, highlighting the environmental and practical benefits of these materials. Finally, the chapter examines the challenges and future considerations for their implementation.

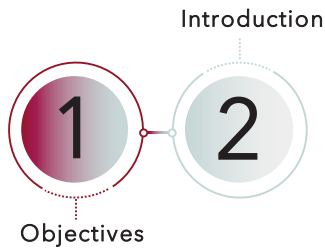

2.1. Objectives

The main objective of this PhD thesis is to investigate the feasibility of using alternative magnesium oxide sources for the development of novel magnesium phosphate cements (MPCs). This research is situated within the framework of wastes valorisation, aiming to develop a material that is environmentally sustainable. The study also focuses on evaluating the properties of the resulting MPC, with particular attention to mechanical performance, as well as chemical, physical and environmental characterization. The thesis is structured around both general and specific objectives, each addressing key aspects of the research to achieve its main aim. It is presented as a compendium of publications, comprising five research studies. Three of these studies have already been published, while two are currently under review in a high-ranking scientific journal. Figure 2.1 illustrates the methodology followed throughout the investigation.

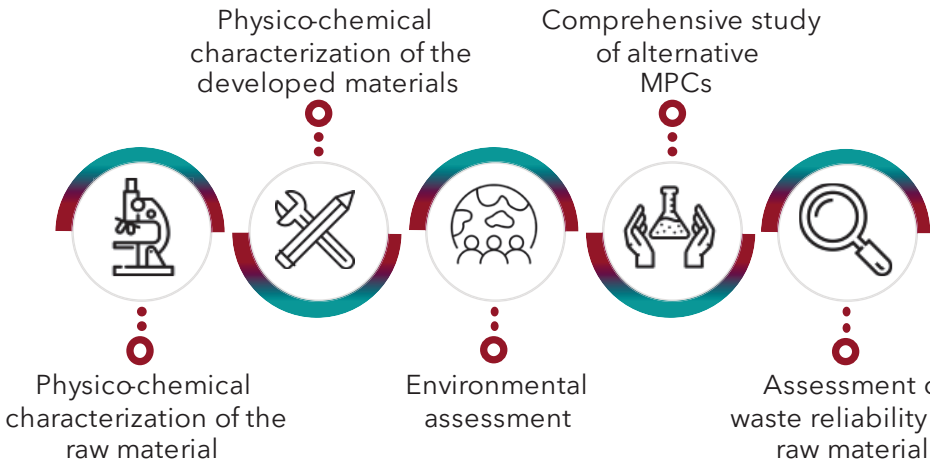

Figure 2.1.Conceptual framework of the experimental design to achieve the objectives.

The following specific objectives (SOs) are proposed to achieve the general goal:

- SO1: Contextualization of the research field through a bibliographical study on the relevance and state of MPC developed with by-products and wastes.
  Chapter 2
- SO2: Conduct a comprehensive physicochemical characterization to determine the chemical composition of TUN.
  Chapter 3 – Publication 1
- SO3: Investigate and evaluate the formulation of MPC using this waste to develop cement and mortars.
  Chapter 3 – Publication 1 and Publication 2
- SO4: Assess the impact of carbon dioxide emissions impact through a prospective life cycle assessment (LCA), comparing the sustainability of this research with conventional materials.
  Chapter 3 – Publication 3
- SO5: Evaluate the properties of MPC developed using by-products and wastes through various characterization techniques.
  Chapter 4 – Publication 4 and Publication 5

2.2. Introduction

2.2.1. Current situation

2.2.1.1. Environmental issues

What will the world be like in a few years regarding the environment? The world's future is uncertain, but the obvious fact is that there is a challenge to reverse the current trend. The population has the responsibility to fight for future generations, including the environment preservation, public health, zero pollution, and a sustainable economy, among others. The future must be focused on the human rights' principles, such as equity and sustainability. Nevertheless, climate action is one of the biggest challenges of our time. To achieve this goal, it is necessarily global or local instruments with economic and social incentives to be aligned towards the same objective. Encourage global changes by 2050 are necessary, as well as to develop international environmental laws.

The European Union (EU) and other countries have focused on targets agreed upon in regulations. Then, a high degree of consistency in policies at the global and national levels are mandatory. An example is the 17 sustainable development goals (SDG) to transform the world through different actions. Besides, at the European level exists directives and regulations with specific goals aimed to succeed.

The growing world population and materials consumption are causing negative impacts on the planet. In 2022 (latest figures available), the total wastes generated in the EU was around 2.233 Mt [1]. Preventing wastes is a part of the EU's strategy to achieve efficiency of the resources and a circular economy. The amount of wastes generation depends on the development of the society, although it is important to create solutions to ensure that waste is treated properly. The Waste Framework Directive (Directive 2018/851) defines some basic waste management principles, where the wastes prevention is the preferred option, and the worst option is landfill. The package of measures on wastes will lead to the creation of a circular economy and allow the deficiencies of the wastes sector to be corrected. By using these wastes as raw

materials, humans are dealing with another global problem: the scarcity of some resources to produce materials.

The Directive 2018/850 on the landfill of wastes specifies that all member states will implement strategies to ensure that the recycled or recovered wastes does not end up in landfills by 2030. The main goal is to reduce the negative landfills effects on the environment and human health and set out minimum responsibility requirements for all the producers. In addition, the member states have verified that waste must receive adequate treatment before being deposited in landfills. Wastes landfills are divided into three categories: hazardous, non-hazardous, and inert.

Carbon dioxide (CO_2) stands as a significant constituent among the greenhouse gases (GHGs) contributing to the global warming phenomenon. The escalation in human activities steadily amplifies the emission levels of these GHGs year by year. In 2023, global carbon dioxide emissions resulting from energy combustion and industrial processes recorded a notable increase by 1.1%, culminating in a total of 37.4 Gt [2]. In 2050, the world's population will increase to 9 billion [3]. In the context of the climate emergency and achieving of the 2030 goals focusing on the GHG emissions reduction, and the carbon neutrality by 2050, the Directive 2010/75 on industrial emissions is the main instrument for controlling and/or preventing pollutant emissions from industries to the atmosphere, water, and ground. This directive is based on the integrated approach, the use of the best available techniques, and several inspections, among others.

The production and use of energy are the principal cause of GHG emissions, along with transport. Final energy consumption in the EU decreased by 3.9% in 2022 compared to 2021 (latest figures available), reaching a total of around 37771 PJ [4]. Of this total, the three sectors that consumed the most energy were transport, households, and industry [4]. According to the IEA (International Energy Agency), industrialised economies have achieved a record decline in carbon dioxide emissions by 2023, despite GDP (gross domestic product) growth, as a result of low-emission energy generation [5]. The EU has different climate rules to ensure that the GHG emissions' reduction would be at least 40% in 2030 compared to 1990. In particular, the Directive

2018/844 pretend to achieve: i) energy consumption reduction and ii) the proportion of renewable energy consumed increases. The EU is trying to develop a decarbonized, efficient, secure, and sustainable energy system by 2050.

2.2.1.2. Cement sector

Cement stands as one of the pivotal materials significantly contributing to the social and economic development of society. World cement production has increased in the last decades, and in 2023, the estimated global production was 4.1 Gt [6]. Cement is the fundamental component in developing concrete, which acts as a binder for the concrete particles, giving cohesion and mechanical resistance through chemical and physical processes. The construction sector uses concrete, which is the most consumed material on Earth [7]. The cement sector is one of the most challenging industries, as it has multiple regulatory frameworks in Europe to achieve a carbon-neutral in 2050. The transition is accompanied to new regulations, technologies, and infrastructures.

Cembureau, the European Cement Association, recommends a 40% reduction in gross carbon dioxide emissions across the value chain by 2030, compared to the 1990 levels (783 kg $CO_2 \cdot t^{-1}$ of cement), as an intermediate step towards carbon neutrality by 2050 [8]. Some Cembureau targets to achieve climate neutrality by 2050 are based on reducing clinker and deploying innovative technologies, shown in Figure 2.2. This challenge must be faced by using renewable energy, efficiency improvements, clinker substitutes and/or development of supplementary cementitious materials (SCMs), use of sustainable alternatives, such as by-products or wastes.

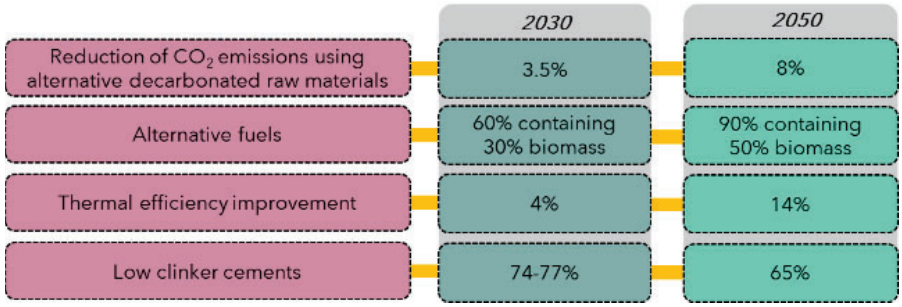

Figure 2.2. Cembureau targets to climate neutrality by 2020 (adapted from [8]).

Ordinary Portland cement industry

Cement production depends on the geographical area, the availability of raw materials, and the technologies used, among other aspects. Cement production was 1.4 Gt in 1995 and 4.1 Gt in 2023 globally, a good indicator to show the growth trend of the construction industry [6]. Cement production is closely linked to fast-growing economies. In 2023, China was the highest contributor to global production, accounting for 51% of the total of 4.1 billion tons [9]. India followed as the second-largest producer, contributing 10% [10]. Consequently, the forecast for the coming years predicts an increase in cement demand in other developing countries across Africa and Asia. The new international policies enhance international coordination and collaboration for the decarbonization roadmap of the cement industry.

Cement manufacturing is an energy-intensive process. Nowadays, OPC is the most widely used cement in the civil engineering and construction fields for its accessibility raw materials, low cost, mechanical properties, and high performance. OPC it is a well-known binder used since the 19th century, and it is manufactured mainly by calcined limestone and aluminosilicates (usually clay) [11]. OPC is a hydraulic binder that, mixed with water, forms a paste that sets, hardens, and preserves its resistance and stability. OPC is obtained by a mixing of clinker, gypsum (calcium sulphate), and other additives. The clinker is the main component, which is subjected to a series of steps before it is mixed with the other components. This process encompasses the extraction of raw materials, followed by crushing, grinding, calcination, and subsequent cooling and grinding [7]. Its composition is shown in Table 2.1, and its mineral phase's composition is shown in Table 2.2. The percentage of gypsum depends on the type of cement and serves to retard its setting time.

Table 2.1. Clinker elemental chemical composition [12].

Oxide	Name	Wt.%
CaO	Lime	60-70
SiO_2	Silica	18-22
Al_2O_3	Alumina	4-6
Fe_2O_3	Iron oxide	2-4

Table 2.2. Clinker mineral phases composition [12].

Oxide composition	Common name	Cement notation	Wt.%
$3CaO{\cdot}SiO_2$	Alite	C_3S	50-65
$2CaO{\cdot}SiO_2$	Belite	C_2S	15-25
$3CaO{\cdot}Al_2O_3$	Tricalcium aluminate	C_2A	5-15
$4CaO{\cdot}Al_2O_3{\cdot}Fe_2O_3$	Calcium alumina-ferrite	C_4AF	5-12

Figure 2.3 shows the manufacturing process flows, the energy and heat demand (inputs), and emissions associated with each stage. Cement manufacture requires large amounts of raw materials and involves high amounts of energy and carbon dioxide emissions, as depicted with icons in the Figure 2.3. Specifically, the production of a ton of clinker requires approximately 1.5 tons of raw materials. Therefore, cement manufacture entails a high consumption of natural resources [13].

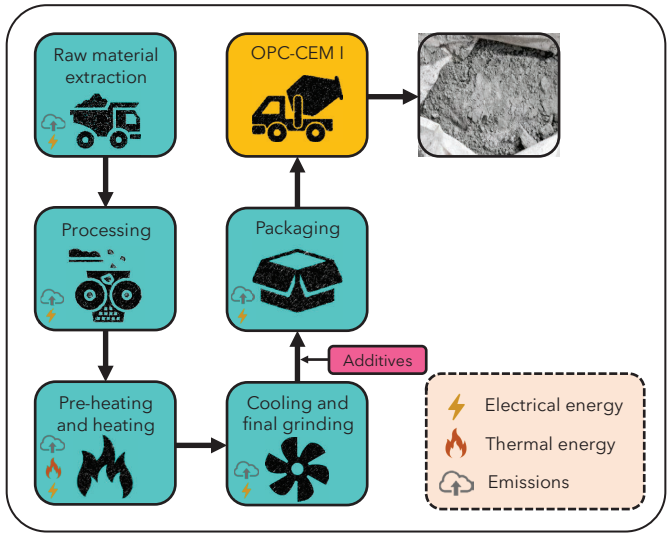

Figure 2.3. Process flow diagram for the manufacturing process of OPC.

The manufacturing process is energy intensive due to the consumption of high quantities of fuels (mainly from non-renewable sources of thermal processes). Coal is the principal energy carrier with 70% of total energy consumption, followed by oil and natural gas with 24%, and alternative fuels and biomass with just over 5% [14]. Around 3% of the global primary energy is consumed by the cement sector [15]. The global

thermal energy intensity of clinker from 2020 to 2023 was between 3.5-3.6 $GJ \cdot t^{-1}$ per year [10,16]. In the Net Zero Emissions by 2050 scenarios, the anticipated thermal energy intensity for clinker production is projected for 2030 to be 3.3 $GJ \cdot t^{-1}$ per year [10,13]. The predominant source of energy is in the form of fuel, primarily derived from fossil fuels for clinker production, alongside electricity consumption [9,10]. In cement manufacturing, the heating process consumes between 70-80% of the total energy consumption and electricity between 20-30% [14].

Manufacturing process of cement releases contaminant gases into the atmosphere (CO_2, NO_X, SO_2, and other pollutants) generated from fuel combustion in the kiln, along with fine particles carried by the kiln's exhaust gases [15]. The cement industry contributes approximately to 5-7% of the total global anthropogenic carbon dioxide emissions and 8% of the global emissions [3,17,18]. Specifically, the direct carbon dioxide intensity of cement production increased by about 1.5% per year during 2015-2023 [10]. Between 70-80% of carbon dioxide emissions come from the involved chemical reaction to obtain CaO, and the rest of the emissions come from the energy required to reach a high temperature in the rotary kiln during calcination, among other processes such as transport, and grinding [3,8].

Alternative cements

The development of alternative cements has enabled a reduction in clinker content. Partially replacing clinker with other materials can enhance both the performance and the environmental footprint of cement.

Building materials involve several environmental impacts throughout their life, including manufacturing, construction, use, maintenance, and final disposal or demolition. Nowadays, different alternatives exist to minimize the cement production's impact, including improving energy and material efficiency, adopting innovative low-carbon technologies, utilizing alternative fuels, and incorporation other materials, among others. The key actions to reduce the impact are [19]:

- Reduction of clinker by using alternative decarbonised mineral additives.

- Alternative fuel usage, promoting the circular economy and using renewable energies to replace fossil fuels.
- Optimization of energy and technology efficiency.
- Carbon capture and storage (CCS) and carbon capture and use (CCU) to transition toward a net-zero model.

This research is focused on searching for new alternative cements to reduce the use of OPC, highlighting the benefits of using sustainable cements, which have a lower environmental impact allowing moving the cement sector towards low-carbon manufacturing. A selection of publications related to alternative cementitious materials was made in 2024 by using Web of Science (WoS) webpage, considering journals and books with a total of 1720 publications. As depicted in Figure 2.4, the quantity of publications and citations pertaining to the advancement of this research field has been steadily increasing over the years. A detailed analysis was conducted on the total number of these publications to determine the percentage contribution of each country. This analysis was based on the previous results obtained from WoS and is illustrated on a world map in Figure 2.5. As evidenced in the map chart, the country with the highest number of publications on the development of alternative cementitious materials is USA, followed by China and India, respectively.

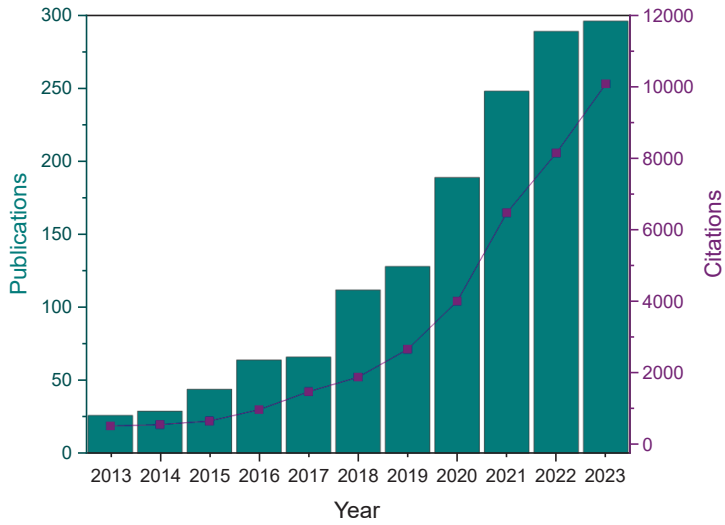

Figure 2.4. Number of publications and citations of alternative cementitious materials.

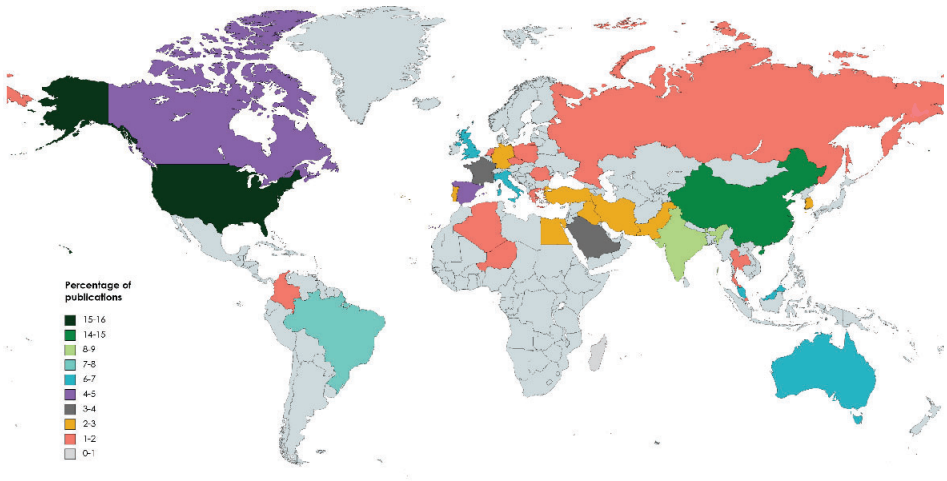

Figure 2.5. Percentage of publications of alternative cementitious materials with respect to the country by map chart.

The strategy to search sustainable alternatives to OPC has the potential to transform the cement industry into a key driver of the circular economy. It involves the development of sustainable materials made from by-products or wastes, presenting opportunities for economic viability. Some examples of alternative binders are:

- Limestone-calcined clay cement (LC^3)

LC^3 is a relatively new cement based on SCMs. Specifically, the LC^3-50 is obtained by a mixing of clinker (50 wt.%), calcined clay (30 wt.%), limestone (15 wt.%), and gypsum (5 wt.%). This binder has a high potential to reduce carbon dioxide emissions due to the reduced clinker content, replaced by calcined clays and limestone [20–22].

- Alkali-activated cement (AAC)

AAC is produced similarly to cement but exhibits properties comparable to sintered ceramics. It is produced through the reaction of amorphous aluminosilicates with alkali. The subsequent requirement is for reactive solid aluminosilicates and an alkaline activating solution. The source materials of aluminosilicate are frequently industrial by-products or wastes like municipal solid waste (MSW), blast furnace slag (BFS), and fly ash (FA), among others. Some of the technical issues associated with these cements are

their hardening rates, as well as high shrinkage. AAC is generally used as precast material [15,17–19].

- Calcium aluminate cement (CAC), and calcium sulphoaluminate cement (CSAC)

The CAC is based on aluminate, with calcium being its major component [23,24]. This type of cement exhibits both early strength and high-temperature resistance. Their applications are specifically geared towards scenarios where resistance to elevated temperatures is crucial [23,24].

The main phase of CSACs is ye'elimite ($C_4A_3\bar{S}$). Other secondary phases are belite (C_2S), calcium sulphate, and gehlenite (C_2AS). A diminished proportion of calcium and lower calcination temperature contribute to a notable reduction in the environmental footprint. Short setting time, high early strength, permeability, corrosion resistance, among others, are some of the CSAC properties. Therefore, CSAC can be applied in the solidification and stabilization of hazardous materials [23,24].

- Belite cement (BC)

BC is primarily composed of belite (C_2S), 40-50%, alongside alite (C_3S) and calcium aluminates. The impact on the environment is reduced by their lower clinker content. BC exhibits slower hydration rates, resulting in lower early-age compressive strength. This is widely applied in hydraulic concrete to control temperature cracking and reduce thermal stresses and cracking [25–27].

- Magnesium phosphate cement (MPC)

MPC belong to the chemically bonded ceramic (CBC) family, more specifically classified as chemically bonded phosphate cement (CBPC). MPC is obtained by mixing a magnesium source with a phosphate salt. MPC has remarkable properties, including fast setting and effective encapsulation of heavy metals and radioactive wastes, due to its ability to form stable, durable matrices that effectively immobilize and encapsulate hazardous materials. Additionally, MPC can be applied as repair cement [28–30].

2.2.2. Chemically bonded ceramic (CBC)

CBCs encompass a category of inorganic materials exhibiting properties to both cements and ceramics, formed by chemical reactions at low temperatures (Figure 2.6) [31]. The structure and properties of CBCs closely resemble to ceramics; however, their formation at room temperature exhibits similarities to cementitious materials [32].

CBC is formed though the reaction between an acid and a base. Therefore, acid-base cement (ABC) belong to the category of CBC [13,32]. Specifically, the bonding of CBC is a mixture of ionic and covalent bonding, as Van der Walls bonding [31,33]. The predominant types of bonding determine the properties exhibited by ceramics [31].

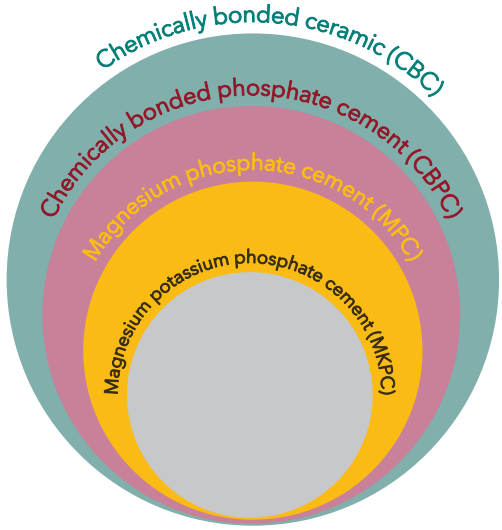

Figure 2.6. Classification of CBC families related to phosphate-based materials.

The field of interest in CBC is relatively new. Research in this area is necessary due to its environmental advantages, including reduced GHG emissions and the reduction of energy consumption. CBC hold significant importance from various perspectives, such as cost-effectiveness and the elimination of high temperatures processing requirements. CBC has been widely used in many applications including but not limited to biomedical, nuclear wastes solidification and encapsulation, and composites with fillers [34].

CBC is produced through a series of sequential steps, including the dissolution of a base salt in an acid medium, followed by gelation and precipitate formation, and culminating in crystallization, as illustrated in Figure 2.7. The resulting paste reaches a neutral pH due to the neutralization reaction between the acidic and alkaline components.

The dissolution of the basic precursor is an important control factor to verify a coherent structure and a solid product [32]. In essence, if the basic precursor dissolves at a slow rate, the formation of the reaction product will correspondingly proceed slowly. As a result, the saturation of the gel will require a longer period of time. However, if the basic precursor dissolves rapidly, precipitates will form, compromising the coherence of the structure. Therefore, the solubility of the basic precursor is a relevant factor as it directly affects the formation of the ceramic. In the context of ABC, the dissolution of the basic precursor into an acid solution is invariably partial.

As mentioned before, when phosphates are employed in the formation of CBC, this cement is referred to as chemically bonded phosphate cement (CBPC). Notably, CBPC is recognized as viable as alternative cement to conventional hydraulic cement [35,36].

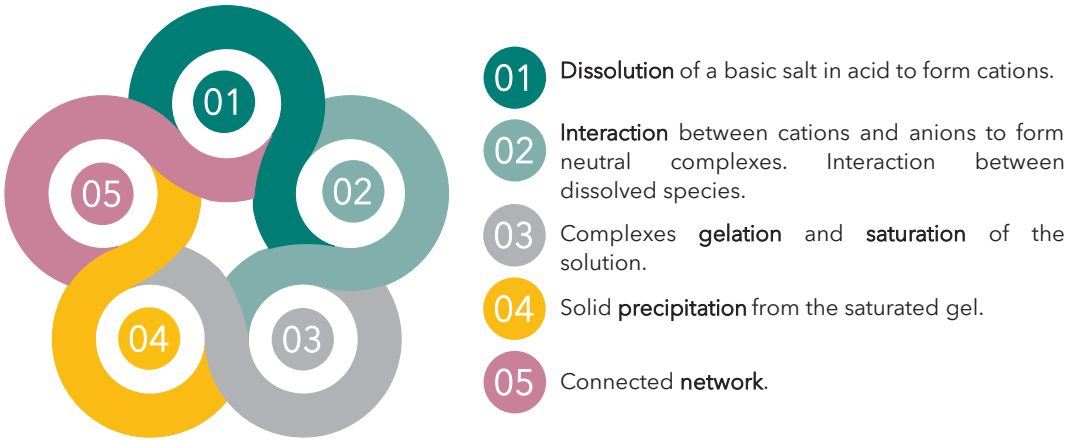

Figure 2.7. CBC's reaction.

2.2.2.1. Chemically bonded phosphate cement (CBPC)

As mentioned earlier, CBPCs are derived from an acid-base reaction and demonstrate notable characteristics such as high strength and low solubility. The acid-base reaction is between a phosphoric acid and metal oxide [31]. This reaction allows combination of phosphate anions with metal oxide cations to form a phosphate gel that crystallizes as insoluble phosphates [36,37]. Eq. 1 shows the reaction between a metal oxide and phosphoric acid. In this equation, the letter *x* refers to the valence of the metal M/n, and the letter *m* refers to an arbitrary value that defines the amount of water added to the reaction.

$$MO_{\frac{x}{2}} + nH_3PO_4 + mH_2O \rightarrow MH_{3n-x}(PO_4)_n + \left(m + \frac{x}{2}\right)H_2O \qquad \text{Eq. 1}$$

The final properties of the cement will depend on the solubility of the raw material and its pH level. CBPC can be formulated from different raw materials. There are several possible sources of phosphate [38,39]. Initially, phosphoric acid was used; however, its use was discontinued due to challenging handling as a corrosive liquid and the rapid setting it exhibited. Later, the use of ammonium phosphate salts gained prominence, but when forming the cement, ammonia gas is released, which is a toxic gas, so it has also been losing prominence [40]. Finally, potassium phosphate salts have been the phosphate source that has taken advantage over others, even though there are other interesting phosphate salts, such as sodium, aluminium, etc [39].

One of the frequent employed options is monopotassium phosphate (MKP, KH_2PO_4), among other potassium phosphate salts [41,42]. Concerning oxides, they must exhibit an appropriate solubility (i.e.: low solubility) for facilitating the formation of CBPC, because the formation of the cement depends on the dissolution kinetics of the oxide used [40]. The reduced solubility contributes to a delayed setting time, and therefore, enhances the workability of the cement [37]. If the oxides exhibit excessive solubility, they will precipitate in crystalline form, impeding the formation of a three-dimensional network. Conversely, if the solubility is too low, an insufficient supply of ions hinders the rearrangement into a three-dimensional network [31]. The main oxides used are magnesium oxide (MgO), calcium oxide (CaO), and zinc oxide (ZnO).

When mixing a phosphoric acid and a metal oxide in an aqueous solution, the formation of CBPC occurs in three stages [43,44]:

1. Dissolution of the phosphoric acid in water, phosphate releases anions and forms an anion phosphate solution of low pH.
2. Low pH increases the solubility of the alkaline component, and a gradual dissolution occurs in the solvent at the same time, which releases cations in the acidic solution.
3. The reaction to obtain precipitation of a crystalline salt or also named neutral phosphate is between the phosphate anions and the alkaline cations.

Whether the result is a well-ordered ceramic, or a crystalline precipitate depends directly on the rate of dissolution of the oxides in the acid solution and on the rate of the exothermic acid-base reaction. To obtain a well-crystallized ceramic, the following specific requirements are needed [32]:

- The solubility of the oxides should be sufficiently high to facilitate the formation of a saturated gel, yet not excessively high to allow for gradual crystallization of the gel.
- The rate of the exothermic acid-base reaction should be slow enough to enable the gradual and steady crystallization of the phosphate gel.

CBPC has extensive advantages such as rapid hardening, high early strength, and elevated temperature resistance. The CBPC strength is due to the strong covalent bonds resulting from the acid-base reaction, contrasting with the weaker bonds resulting from the hydration process in conventional cement. Initially, CBPC was used in biomedical applications, specifically in the dental sector. Currently, CBPC has found diverse applications, including repair and reinforcement cement in civil engineering, encapsulation, solidification of radioactive wastes, and in biomedical uses [36,45,46]. The essence of ABC lies in its ability to use acid and alkaline by-products or wastes as raw materials. Producing ceramics through these chemical processes demands less energy compared to conventional ceramics production. For these reasons, CBPC can contribute to diminishing environmental impact and promoting a circular economy.

2.2.2.2. Magnesium phosphate cement (MPC)

One of the most extensively studied cements among the CBPCs is MPC. MPC is obtained from the exothermic acid-base reaction between a magnesium source (typically as an oxide) and a phosphate source. In particular, MPC derived from MKP as a phosphate source stands out. It is specifically named magnesium potassium phosphate cement, or MKPC, to distinguish it from other types. Thus, MPC is the generic term, while MKPC refers to the specific case of using MKP as a phosphate source (Figure 2.6).

Magnesium oxide is the most common and widely used raw material for MPC due to its moderate solubility in an acid-phosphate solution compared to iron and calcium oxides [43]. To achieve this solubility, magnesium oxide undergoes calcination at temperatures above 1000 °C. Elevated temperatures reduce the porosity and permeability of magnesium oxide, leading to an increase in particle size. The diminished solubility of the calcined magnesium oxide powder can be attributed to a notable decrease in its surface area. A less reactive form of magnesium oxide contributes to the development of a more compact microstructure in MPC, while also extending the setting time, thus improving the mixing process [37].

MPC is usually synthesized by an acid-base neutralization reaction, involving calcined magnesia powder and a phosphate source, at room temperature and in aqueous media, Eq. 2 and Eq. 3, where the two most commonly used sources of phosphate are shown. The former, MKP, is commonly used as a fertilizer or food additive [28,47,48]. The latter, monoammonium phosphate (MAP), as mentioned above, has fallen into disuse due to the potential release of ammonia gas [30].

$$MgO\ (s) + + KH_2PO_4(s) + 5H_2O\ (l) \rightarrow MgKPO_4 \cdot 6H_2O\ (s) \qquad \text{Eq. 2}$$

$$MgO\ (s) + NH_4H_2PO_4(s) + 5H_2O\ (l) \rightarrow MgNH_4PO_4 \cdot 6H_2O\ (s) \qquad \text{Eq. 3}$$

The final product of the first reaction is a magnesium potassium phosphate binder, MKPC, and the crystal named is K-struvite ($MgKPO_4 \cdot 6H_2O$) [49]. The final product of the second reaction is struvite, which is a magnesium ammonium phosphate hexahydrate

($NH_4MgPO_4 \cdot 6H_2O$). The distinction between K-struvite and struvite lies in the presence of potassium. Specifically, in K-struvite, potassium replaces ammonium in the chemical composition, as shown in Figure 2.8. Both K-struvite and struvite have an orthorhombic structure. They have important cementitious properties and are widely used in the MPC field. Currently, K-struvite is preferred due to its reduced release of ammonia gas during setting, lower setting characteristics, and lower exothermicity. These properties enhance the ease of handling and workability of pastes while ensuring proper and controlled setting [50,51].

The formation of K-struvite takes place in three steps [31,32,40,44]:

- The interaction between magnesium oxide and an acid phosphate solution result in the creation of positive colloidal solutions. In this process, the cations of the dissolved species are surrounded by water molecules, generating positively charged aqueous sols by through hydrolysis.
- Through an acid-base reaction and gel formation by condensation, positive aqueous sols engage with phosphate anions, leading to the formation of hydrophosphate gel or binder phosphates salts.
- The gel undergoes a transformation into ceramic material as it becomes saturated, and gel crystallizes around the unreacted metallic oxide granules. This crystalline network forms a monolithic ceramic structure.

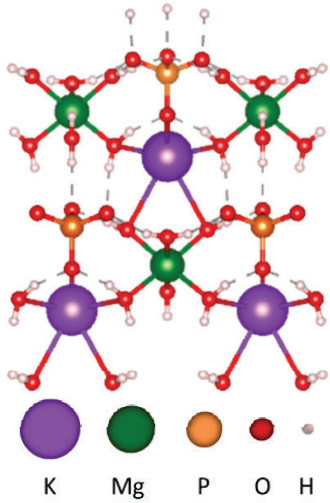

Figure 2.8. K-struvite crystal phase (adapted from [52,53]).

MPC was developed in 1940 by Prosen as ceramic materials for the moulds used in the lost casting [54]. Nowadays, MPC has captured increasing attention for its applications, such as bone substitution, stabilization, and solidification of wastes and composites cement with fibres [50,55]. Another important aspect that makes MPC and MKPC stand out are some of their characteristics, such as a practically neutral final pH, low drying shrinkage, low processing water demand, and high mechanical strength at early ages when compared to other types of cements [49]. Besides, different variables directly affect to final properties of MPC, likewise the ratio between the acid and basic components, the ratio between liquid and solid (L/S), and the reactivity of magnesium oxide [39,40,56].

MPC exhibits highly exothermic setting reactions [32,54,57]. The phosphate source must possess adequate solubility to allow controlled setting at a moderate speed, allowing the material to dissipate heat gradually during the setting process and thereby preventing thermal shock. In recent years, the scientific community has sought to reduce the production costs of MPC by using secondary sources of magnesium and introducing mineral and industrial wastes. Despite this, the high cost of this type of cement is still a factor to be considered when compared to conventional cement, such as OPC [39,40]. Therefore, for the coming years and for the sustainable development of MPC would be interesting to find phosphate sources coming from secondary sources.

Magnesium oxide can be derived from primary or secondary sources. In the case of primary sources, it involves the calcination of pure magnesium oxide from magnesite or dolomite minerals to obtain dead burned magnesia (DBM) [58]. In the case of secondary sources, magnesium oxide source is coming from industrial by-products and wastes rich in this compound, such as low-grade magnesium oxide (LG-MgO), tundish deskulling waste (TUN), boron-magnesium oxide (B-MgO) or magnesia refractory brick waste (MRB). Using by-products and wastes promotes future sustainable construction practices, advancing the principles of a circular economy environment preservation.

2.2.2.3. Significance of MPC

Research in the field of MPC has expanded significantly in recent years. MPC could play a substantial role in reducing the use of conventional cement due to the aforementioned advantages. In recent years, numerous studies have been undertaken to investigate the properties and applications of MPC.

A literature search was conducted to identify the most relevant data and advancements in the research area of MPC within the construction and building industry. This study allows us to analyse the characteristics of this field over the past decade. The main goal of this literature search is to evaluate and comprehend the progress made in this field, with a focus on its significance in the construction sector. Additionally, it aims to spotlight the most impactful publications, identify the authors with significant contributions, and highlight the regions that have been most active in this area. The data source used was WoS, considering the metadata features and the publications [59]. A total of 628 publications in significant journals and books related to MPC publications were selected from 2013 to 2024. A meticulous selection process was made to identify publications aligning with the research area, while excluding those that did not meet the criteria. The unifying factor among these documents was the presence of the term "MPC", and the required application was specifically centred on the construction sector. The results revealed a clear trend of escalating publications year by year, reaching its peak volume in 2022. Therefore, the trend in evolution indicates a likely continuation of increasing publications in the forthcoming years. Hence, the maximum number of publications was in 2022, with 112 publications, as shown in Figure 2.9.

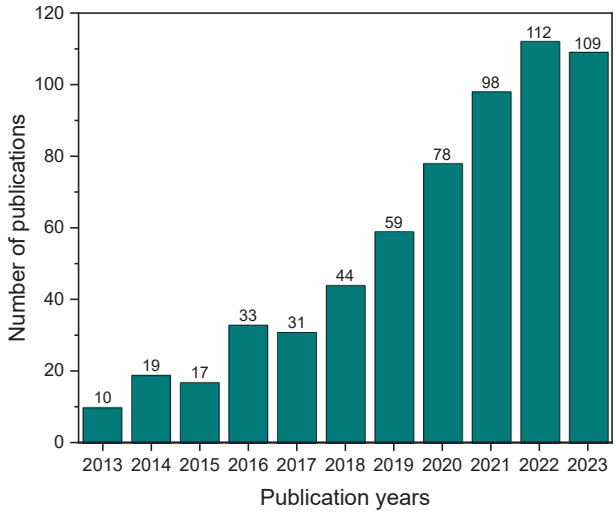

Figure 2.9. The evolution of publications in the research field over the years.

The trend in MPC research is fully associated to environmental regulations related to the reduction of the environmental impacts of the cement industry. Consequently, it also reflects the development and use of alternative cements [18].

The three most common WoS categories are "Materials Science Multidisciplinary", "Construction Building Technology", and "Engineering Civil", respectively. The top journals in the research areas are "Materials Science", "Engineering", and "Construction Building Technology". "Materials Science" stands out as the most research area, contributing to 69.9% of the total publications in this field. The most common publisher is Elsevier, followed by MDPI.

The top five recurrent publication journals are "Construction and Building Materials" (28.7%), "Materials" (6.1%), "Journal of Building Engineering" (5.6%), "Cement and Concrete Research" (4.1%), and "Journal of Materials in Civil Engineering" (3.8%). Articles make up 91.9% of the total percentage, while the remaining percentatge consist of review articles and early access publications.

Table 2.3 shows the top seven publishing countries in the selected research field, along with the number of publications and the most cited articles. China is the leading country in publishing articles, accounting for 76.8% of the total with 482 publications (Figure 2.10), representing three-quarters of the total. It shows the substancial interest in this field, particularly when compared to other countries that are considerably distant from China. The six countries that follows China are the USA (5.9%), England (3.7%), France (3.7%), Czech Republic (3.2%), Australia (2.7%), and Spain (2.5%).

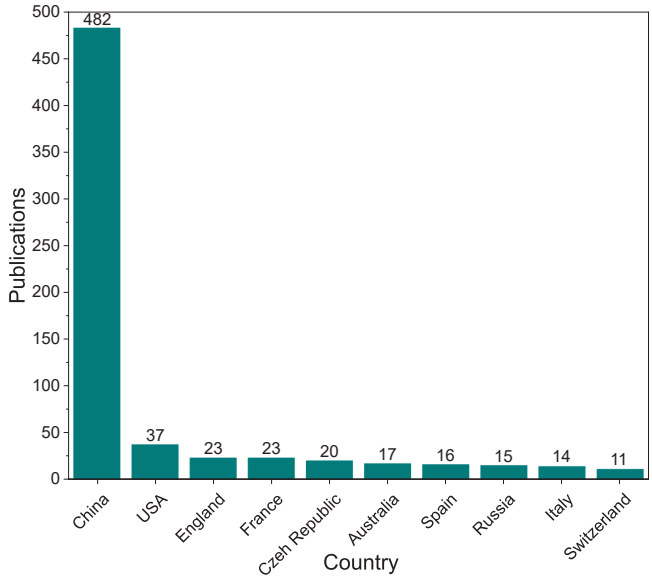

Figure 2.10. Number of publications in the research field from the most relevant countries.

While China leads in overall contributions to this field, considering the population density of each country reveals that the United States has the highest number of publications.

Table 2.3. Details of the six countries with the highest impact of MPC.

Country	Maximum number of citations	Title	Authors	Reference
China	198	Factors that affect the properties of magnesium phosphate cement	Li Yue, Chen Bing	[60]
USA	146	Influence of fly ash on compressive strength and micro-characteristics of magnesium potassium phosphate cement mortars	Biwan Xu, Hongyan Ma, Hongyu Shao, Zongjin Li, Barbara Lothenbach	[61]
England	486	Magnesia-Based Cements: A Journey of 150 Years, and Cements for the Future?	Sam A. Walling, John L. Provis	[51]
France	126	On the influence of Mg/P ratio on the properties and durability of magnesium potassium phosphate cement pastes	Mathieu Le Rouzic, Thierry Chaussadent, Lavinia Stefan, Mickaël Saillio	[62]
Czech Republic	58	Preparation of magnesium phosphate cement by recycling the product of thermal transformation of asbestos containing wastes.	Alberto Viani, Alessandro F. Gualtieri	[63]
Australia	77	Red mud-enhanced magnesium phosphate cement for remediation of Pb and As contaminated soil	Lei Wang, Liang Chen, Binglin Guo, Daniel C.W. Tsang, Longbin Huang, Yong Sik Ok, Viktor Mechtcherine	[64]
Spain	45	Preliminary study of the mechanical and hygrothermal properties of hemp-magnesium phosphate cements	Ricardo del Valle-Zermeño, Jean Emmanuel Aubert, Aurélie Laborel-Préneron, Joan Formosa, Josep Maria Chimenos	[41]

The top three authors with the highest number of publications on MPC are Chen Bing with 58 articles (9.2%), Li Yue with 34 articles (5.4%), Qian Jueshi with 32 articles (5.1%), and Jian-Ming Yang with 31 articles (4.9%), respectively. Chen Bing, started publishing in year 2020, Li Yue in year 1999, Qian Jueshi in year 1999 and Jian-Ming Yang in year 2009; therefore, it is observed that this field of research is increasingly

gaining more maturity and more relevance. Table 2.4 illustrates various indicators of the top authors, including their affiliation, number of total publication, number of citations, and the h-index. Finally, the three most recurring affiliations in the publications are Shanghai Jiao Tong University (10.2%), Chongqing University (6.7%), and Beijing University of Technology (4.9%).

Table 2.4. Authors with a significant impact in the MPC field.

Author	Affilation	N° publications	N° Citations	h-index
Chen Bing	Shanghai Jiaotong University, Shanghai, China	235	9103	51
Li Yue	Beijing University of Technology, Beijing, China	239	2403	31
Qian Jueshi	Chongqing University, Chongqing, China	227	3945	36
Jian-Ming Yang	Sanjiang University, Nanjing, China	64	1077	17

Table 2.5 shows the three most impactful publications for each of the four most prominent authors in this research area, along with their titles, citations, publication years, and references.

Table 2.5. Publications most cited by the four authors with the most impact.

Author	Title	Citations	Year	Reference
Chen Bing	Research progresses on magnesium phosphate cement: A-review	151	2019	[65]
	A comprehensive study of basalt fiber reinforced magnesium phosphate cement incorporating ultrafine fly ash	128	2019	[66]
	Experimental research on magnesium phosphate cements modified by red mud	116	2020	[67]
Li Yue	Effects of fly ash and quartz sand on water-resistance and salt-resistance of magnesium phosphate cement	97	2016	[68]
	Experimental study on mechanical properties and fracture toughness of magnesium phosphate cement	75	2015	[69]
	The effect of slag on the properties of magnesium potassium phosphate cement	56	2016	[70]

Qian Jueshi	Influence of fly ash and metakaolin on the microstructure and compressive strength of magnesium potassium phosphate cement paste	147	2018	[71]
	Effect of early hydration temperature on hydration product and strength development of magnesium phosphate cement (MPC)	110	2015	[72]
	Bond behavior and interfacial micro-characteristics of magnesium phosphate cement onto old concrete substrate	94	2018	[73]
Jian-Ming Yang	Research progresses in magnesium phosphate cement-based materials	103	2014	[74]
	Effect of waterglass on water stability of potassium magnesium phosphate cement paste	88	2014	[75]
	Effect of curing regime on water resistance of magnesium–potassium phosphate cement	74	2017	[76]

The highest number of citations related to this selection occurred in 2023, reaching 3508 citations, as demostrated in Figure 2.11.

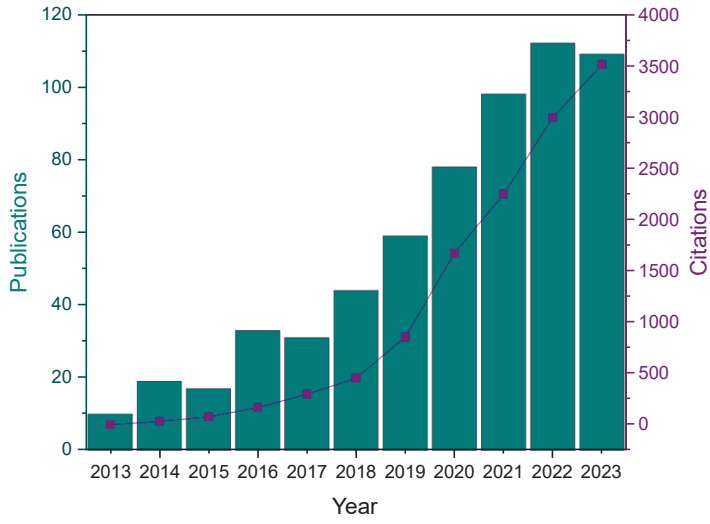

Figure 2.11. Number of citations and publications over time of MPC.

Table 2.6 presents the five most cited publications, all of which are highly relevant to the research field. The top-ranked publication is a review, while the remaining four are research articles.

Table 2.6. Highly relevant publications.

Citations	Tittle	Authors	Reference	Year	Country
486	Magnesia-Based Cements: A Journey of 150 Years, and Cements for the Future?	Walling, SA and Provis, JL	[51]	2016	England
198	Factors that affect the properties of magnesium phosphate cement	Li Yue, Chen Bing	[60]	2013	China
173	Magnesium potassium phosphate cement paste: Degree of reaction, porosity and pore structure	Hongyan Ma, Biwan Xu, Zongjin Li	[77]	2014	China
172	Effects of water content, magnesia-to-phosphate molar ratio and age on pore structure, strength and permeability of magnesium potassium phosphate cement paste	Hongyan Ma, Biwan Xu, Jun Liu, Huafu Pei, Zongjin Li	[78]	2014	China
151	Research progresses on magnesium phosphate cement: A review	M. Aminul Haque, Chen Bing	[65]	2019	China

Finally, a keyword map was created for all the selected publications to visualize the trends and advancements in keywords, and showed in Figure 2.12. The map showcases different circles, each representing a keyword within the chosen research field. The connecting lines between circles indicate the number of publications featuring each keyword. Furthermore, the color scheme represents the appearance year of the keyword. Specifically, yellow refers to recent terms, while blue corresponds to older ones. Figure 2.12 highlights the most frequently used keywords, including “Magnesium phosphate cement”, “Magnesium potassium phosphate cement”, and “Microstructure”. After evaluating the trends and the specific keywords such as porosity, durability, and

3D printing, it becomes evident that there has been notable improvement and progress in this field in recent years. The keywords "Microstructure", "Compressive stregth", and "Mechanical properties" are closely linked to material properties and characteristics, which, in turn, can be linked to the application requirements.

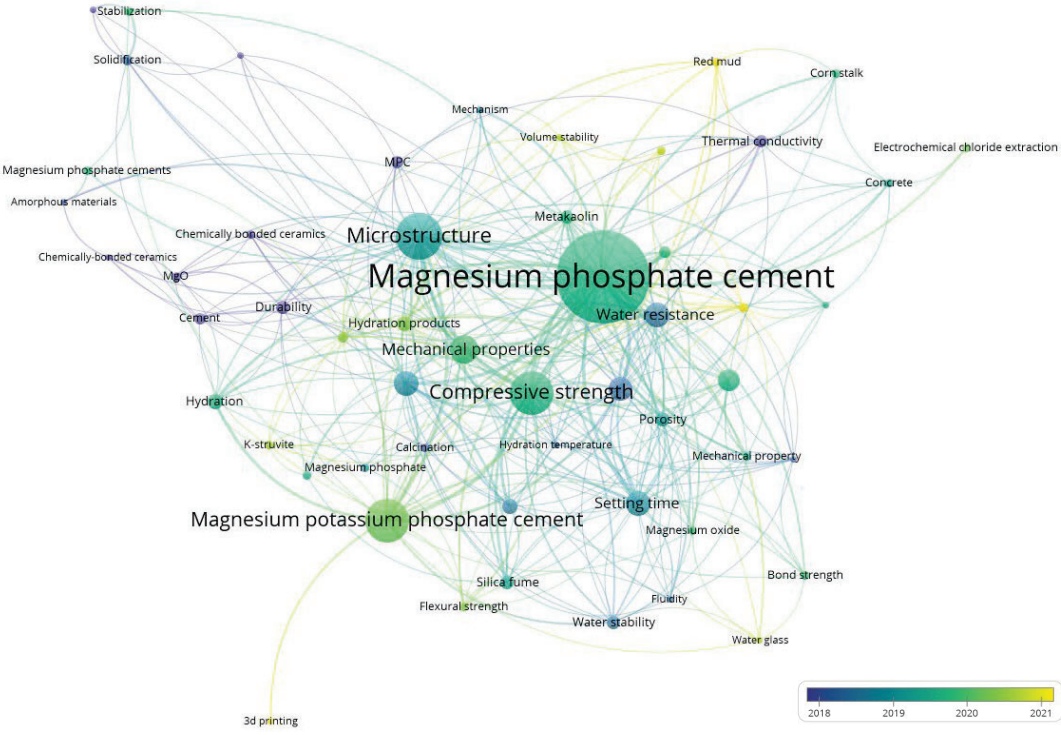

Figure 2.12. Keyword map of MPC.

2.2.3. Alternative raw materials

The following section presents alternative materials to high-purity magnesium oxide. The materials presented are industrial by-products and wastes that have been identified in the literature as potential alternatives for the development of MPC. Although the four alternative raw materials are presented to provide a general understanding of the context and situation, it is important to emphasize that this thesis focuses exclusively on two of them, LG-MgO and TUN. The methods of obtaining and conditioning these materials for use as a source of magnesium oxide to obtain MPC are therefore

described. It is important to note that although the conditioning processes of these secondary materials incur an energy cost, pure magnesium oxide also requires a conditioning process, including a high-temperature thermal treatment (above 1000 °C), to achieve the necessary reactivity for the proper formation of the cementitious matrix.

2.2.3.1. Low-grade magnesium oxide (LG-MgO)

Magnesite ($MgCO_3$) is one of the most important raw material sources for magnesia refractory production [79]. After its calcination, two principal products are commonly obtained, calcined magnesite and sintered magnesite. Below are the sequential steps involved in obtaining magnesium oxide [79]:

1. Mineral Extraction

Several minerals are extracted from various opencast mines rich in magnesite ($MgCO_3$), the primary source of magnesium. However, magnesium can also be obtained from seawater and brines in the form of magnesium hydroxide ($Mg(OH)_2$). After extraction, the minerals are ground.

2. Separation

The minerals are discharged into hoppers at the factory. To remove impurities, they are sorted by size using a classifier/washer, producing a carbonate suitable for the process. The classified minerals are then separated using two wet sieves, resulting in four distinct fractions (greater than 12 mm, 4-12 mm, 1-4 mm, and 0.3-1 mm).

3. Enrichment of magnesium carbonate

The two smaller fractions are sent to cyclones, where the minerals are dehydrated. The smaller fractions cannot be further enriched; hence, they are either stored to feed the ovens, or dried and sold as carbonate.

The two greater fractions pass-through conveyor belts, to enrich the treatment plant for dense media that contains water and mineral. These fractions are also used to feed the ovens.

4. Calcination and/or sintering of magnesium carbonate to obtain magnesium oxide

The separated minerals are introduced in different rotating cylindrical kilns at temperatures between 1100 °C to 1950 °C. Finer materials are compacted to prevent

the oven from dragging them. The thermal decomposition that occurs in the kiln is shown below (Eq. 4):

$$MgCO_{3\,(s)} \rightarrow MgO_{(s)} + CO_{2\,(g)} \qquad \text{Eq. 4}$$

Depending on the calcination temperature, magnesium oxide is produced with different reactivity:

- The caustic calcined magnesite (CCM), high reactive magnesium oxide, is treated around 1300 °C. It is used in agriculture, livestock applications, and innovative products for the environment.
- The sintered magnesite or dead burned magnesite (DBM) is treated at temperatures higher than 1800 °C. It is essential for the steel industry in the refractory materials manufacture.

The high-temperature air current circulates in an opposite direction to the movement of the material. The combustion gases are led to a purification system before their emission into the atmosphere, where the flying particles are retained, initially in a system of cyclones and later in a bag filter. The by-product, mainly composed of low-grade or low content magnesium oxide, is collected as cyclone dust, as shown in Figure 2.13, named low-grade magnesium oxide (LG-MgO). Therefore, LG-MgO, an industrial by-product obtained from the calcination of natural $MgCO_3$, plays a crucial role in the production of magnesium oxide.

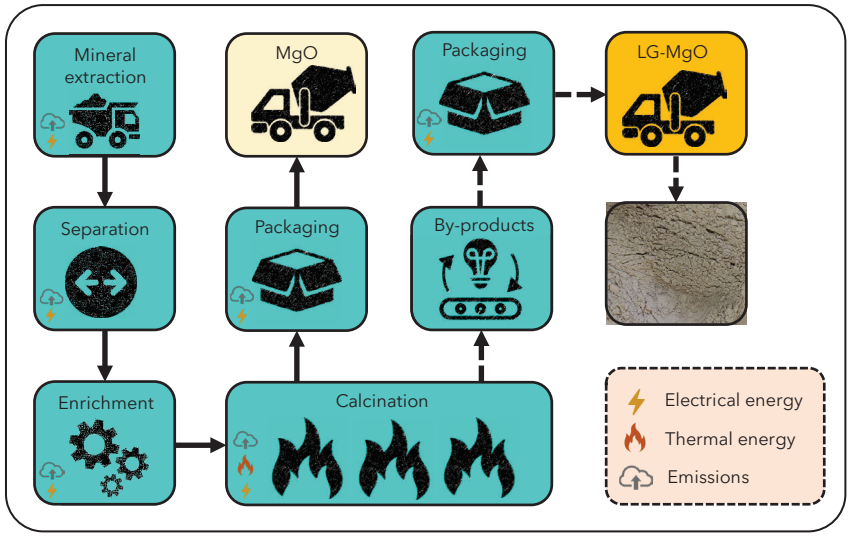

Figure 2.13. Simplified flow diagram for producing LG-MgO at Magnesitas Navarras S.A. company (Zubiri-Navarra, Spain).

LG-MgO has different environmental applications such as stabilization of metal-contaminated soils, desulfurization of gases, production of hydromagnesite, and for CBPC development as a precursor for MKPC, among others [80]. Using LG-MgO instead of pure magnesium oxide has many benefits. The use contributes to environmental sustainability by valorising industrial by-products while also offering a significant economic benefit, being ten times more cost-effective [43,44]. Taking this into account, the production of 1 ton of magnesium oxide from $MgCO_3$ results in approximately 1.08 tons of carbon dioxide emissions. This translates to a higher emission level compared to the emissions from OPC [81].

2.2.3.2. Tundish deskulling waste

Steel production significantly increased in the last decade [82,83]. Steel is indispensable for numerous sectors, including energy, transportation, and construction. This material is usually produced in a BOF or in an EAF [83]. Refractory materials are essential for steel manufactories. Refractory materials function is to form a protective lining layer in high temperature containers. The final refractory material depends on the main materials and its composition. Refractories materials can be acid, neutral, or basic.

Refractories based on magnesia (MgO) are basic ones, and present resistance to steelmaking slags [84]. Pure magnesium oxide is used in steelmaking industries due to its excellent slag corrosion resistance, thermal shock resistance, and low corrosion [85]. Around 90% of the world's steel production goes through a continuous casting process [86]. Tundish is usually covered from a basic refractory material, known as tundish mass, with more than 60% of magnesium oxide [84].

Tundish mass is an indispensable component for regulating the right amount of molten steel. It is the last metallurgical container where the steel liquid flows from the ladle to the continuous casting mould before solidifying. The interactions between molten steel and tundish are fundamental for the steel industry [87]. Thus, the material and design of the tundish are crucial in defining the composition and quality of the steel, with the refractory material needing to exhibit the correct properties, such as thermal shock resistance, to ensure optimal results [86]. The flow field within the tundish plays a critical role in removing any inclusion [88]. Due to the importance of this material, many innovations have been introduced in the steelmaking sector [89,90].

The refractory material (tundish mass) used in the steel industry deteriorates over time and becomes waste, referred to as tundish deskulling waste (TUN), which is disposed of in landfills [36]. Consequently, there is a global issue that requires management and prevention to avoid its disposal in landfill. Nevertheless, TUN could be considered a by-product, given its considerable potential for further processing and value addition [91,92]. The entire scientific environment is looking for applications for this waste to reduce the environmental footprint. Besides, by-products or wastes use as raw materials replaces the impact associated with the natural mineral resource extraction. Hence, TUN can be used as a magnesium oxide source, but it must be properly conditioned to achieve an adequate quality with the desired particle size to be used as a component of the MPC [91]. The TUN conditioning process, provided by Magnesitas Navarras, S.A. company, is based on different steps and shown in Figure 2.14:

1. Collection and manual separation

Tundish deskulling waste (TUN) is collected in the steel industry after its use. Fractions of visible undesirables are removed manually before moving into the next phase. Once the raw material is picked up, it is transported by truck to the conditioning plant.

2. Screening

The material is sieved into two size fractions: particles larger than 10 mm, referred to as blocks, and those smaller than 10 mm, classified as fines. These two fractions will be handled separately from this point onward.

3. Grinding

Each fraction is automatically crushed and sieved into two particle sizes, firstly 1 to 3 mm and then particles below 1 mm.

4. Magnetic separation

Magnetic separation is the final stage in the conditioning plant. Both fractions go separately through a magnetic machine to remove part of the remaining steel to increase the purity of the outgoing materials. After separating the magnetic and non-magnetic components, the non-magnetic fractions are recombined.

Subsequently, the non-magnetic material is transported by truck to another plant to mix it with the other components to obtain MPC considering the specific proportions.

Anyway, it is important to note that this process is specifically designed to utilize the material as a source of magnesium oxide for the development of MPC. However, in the case of Magnesitas Navarras S.A. company, this fraction is currently used as feedstock for the furnace.

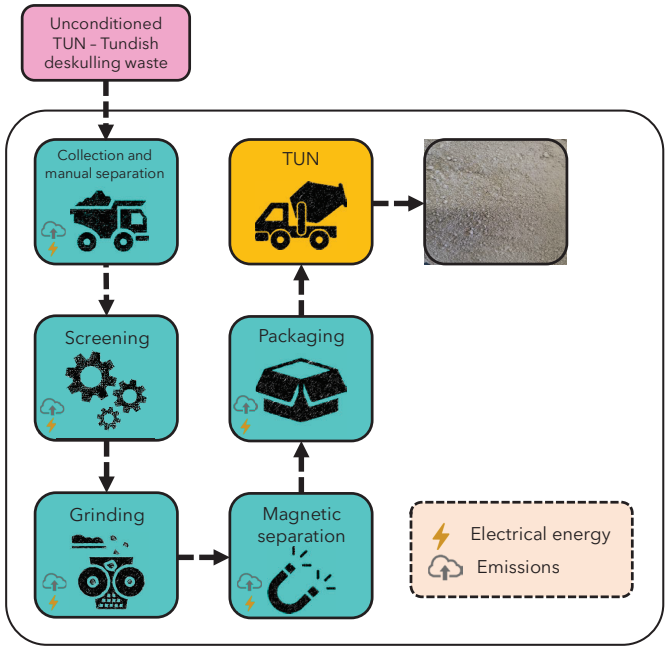

Figure 2.14. Conditioning process of TUN.

2.2.3.3. Boron-containing magnesium oxide by-product (B-MgO)

Lithium, is emerging as a pivotal energy material, mainly employed in lithium-ion batteries (LiBs) for electric vehicles [93]. These new vehicles have the potential to reduce the environmental footprint associated with conventional fossil-fuel vehicles [106]. Lithium is a key component to the energy transition in the coming years, for this reason, nowadays is one of the most critical metals.

Global lithium production in 2020 reached $82 \cdot 10^3$ metric tons and is expected to increase significantly due to the ongoing revolution in the transportation sector. Consequently, a substantial volume of by-products and wastes is being generated and is expected to increase further [107]. Lithium is produced from brine (Li_2CO_3) or from hard-rock one (concentrate of Li_2CO_3 and LiOH) [94]. The brines are the main source of lithium such as from the salt lakes brines, for their cheaper production cost and their availability [95].

Approximately 40% of the world's Li_2CO_3 production in 2020 was sourced from brine-based resources [94]. The Li_2CO_3 production is based on different processes, shown in Figure 2.15 [95]. Specifically, the process starts with lithium containing brines, followed by the lithium containing $MgCl_2$, continuing with the Li-containing magnesium oxide, to obtain the dilute LiCl solution that will later be obtained the LiCl concentrate to get Li_2CO_3 [96].

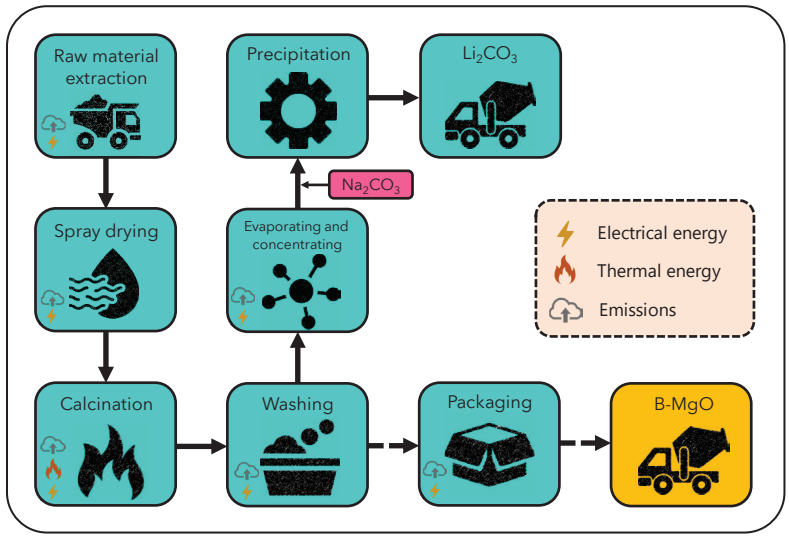

Figure 2.15. Production of Li_2CO_3 [97,98].

One of the by-products of the production of $LiCO_3$ from salt lakes is boron-containing magnesium oxide, known as a B-MgO [58]. B-MgO needs to undergo calcination within a temperature range between 800 °C and 1400 °C to achieve the desired surface area, ensuring the appropriate reactivity for its use as a raw material [99,100]. It should be noted that the calcination conditions are totally linked to the properties of the magnesium oxide source. The main components of B-MgO by-product are magnesium oxide and trimagnesium diborate ($Mg_3B_2O_6$) [96]. Ideally, the optimal approach would involve removing impurities from the by-product. However, the high cost associated with the purification process prevents the separation of boron and magnesium [101].

In the coming years, this technology is expected to mature and become increasingly significant. Consequently, it is crucial to explore alternative approaches for developing new applications to employ the by-products and wastes generated.

2.2.3.4. Magnesia refractory brick waste (MRBW)

Magnesia refractory brick (MRB) is used in the metallurgy sector due to its service conditions, such as excellent fire resistance, superior high-temperature strength, and strong absorption of thermomechanical stresses [102]. As a key component, its demand is expected to rise, particularly for use in furnace equipment operating in high-temperature environments. After their useful life, the refractory materials must be replaced by others to guarantee the operating conditions. It is at this point that magnesium refractory brick waste (MRBW) is produced.

MRBW is formed by different refractory materials based on MgO, MgO-C, MgO-Al_2O_3, MgO-CaO, MgO-SiO_2, or MgO-Cr_2O_3 [103,104]. The specific properties of the refractories may be tuned depending on their composition. Several studies demonstrate the high-quality magnesium oxide content in the composition of MRB [104–106]. Then, it is an alternative and promising source of magnesium oxide to develop MPC.

Nevertheless, it is important to emphasize that a conditioning process is essential to obtain an adequate granulometry, as shown in Figure 2.16. This process relies on crushing, sorting, and grinding procedures. The wastes valorisation is beneficial for avoiding the landfilling treatment and reducing the environmental impact associated with the extraction of natural resources.

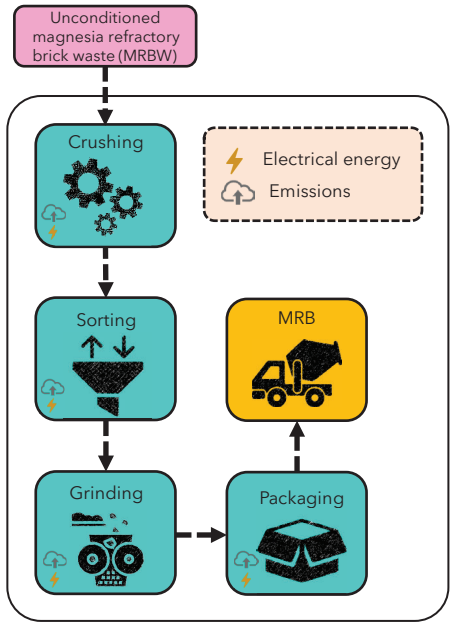

Figure 2.16. Process diagram of the conditioning process of MRBW.

2.2.4. Challenges and future considerations

The implementation and development of MPC that utilize alternative magnesium sources, rather than pure DBM, aligns with the Sustainable Development Goals (SDGs). Specifically, the present thesis aims to contribute to the following SDGs, which are part of the 17 goals set by United Nations member states to be achieved by 2030:

- Goal 9: Build resilient infrastructure, promote inclusive and sustainable industrialization and foster innovation.

The valorisation of by-products and wastes presented in this doctoral thesis promotes a more sustainable construction industry by enhancing the efficient use of the planet's resources. It reduces the reliance on primary production materials, supported by innovative infrastructure and sustainable industrialization. Additionally, this research contributes to the advancement of scientific knowledge and innovation in the field of materials.

- Goal 11: Make cities and human settlements inclusive, safe, resilient and sustainable.

The primary goal of this research on new sustainable construction materials is to apply these innovations to infrastructure projects, such as paving and urban furniture, to create resilient and sustainable cities. Achieving sustainable development requires a fundamental transformation in how urban spaces are designed, constructed, and managed. For this reason, the present doctoral thesis aims to develop construction materials with a lower carbon footprint using secondary sources.

- Goal 12: Ensure sustainable consumption and production patterns.

The research conducted promotes sustainable consumption by utilizing alternative sources, contributing to the transition towards sustainable economic models and helping to reduce current global consumption patterns.

- Goal 13: Take urgent action to combat climate change and its impacts.

The momentum for change is constantly growing, with an increasing number of individuals and organizations adopting diverse strategies to reduce emissions and enhance adaptation efforts towards a more sustainable society. Ultimately, this work aims to contribute to climate change mitigation and support this progress by raising awareness of its causes and effects, while sharing research results and potential solutions to expand knowledge.

Despite the numerous advantages of MPC developed with alternative sources, its implementation on a large industrial scale still faces certain challenges. Addressing these obstacles is essential to unlocking the potential of alternative materials for use in sustainable construction. Some of the most pressing challenges and future considerations to be addressed include:

1. Local resource availability: ensuring the availability and quality of local raw materials is essential to standardize the production of MPC. Given the widespread availability of alternative sources across many regions, MPC offers several advantages, making it easier to adopt globally by utilizing locally sourced materials.

However, the variability of resources can affect the homogeneity and consequently the performance of the final product. Therefore, it is essential to develop strategies for sourcing and material characterization to ensure the viability and reliability of MPC formulations.

2. Alternative phosphate sources: the use of alternative phosphate sources is vital for enhancing sustainability and reducing costs. Identifying and optimizing secondary or recycled phosphate materials could mitigate dependence on primary resources while lowering the environmental footprint.
3. Pilot testing for properties and durability: rigorous pilot-scale testing of MPC formulations is required to evaluate their mechanical properties, durability, and long-term performance under real-world conditions. These studies are essential for building confidence in MPC suitability for diverse applications.
4. Adoption barriers: overcoming adoption barriers in the construction industry is a key challenge. This includes addressing cost considerations, adapting production techniques, complying with regulatory standards, and increasing awareness of MPC's environmental and performance benefits among stakeholders.

By addressing these challenges, MPC technology can advance toward becoming a widely adopted solution in sustainable construction practices. This progress would not only significantly reduce the environmental footprint of the construction industry but also promote the principles of a circular economy by integrating by-products and wastes valorisation and resource efficiency.

2.3. References

[1] Eurostat - Statistics Explained, Waste statistics 2022, (2022). https://ec.europa.eu/eurostat/statistics-explained/Total_waste_generation (accessed November 7, 2024).

[2] International Energy Agency, World Energy Outlook 2021, 2021. www.iea.org/weo.

[3] A. Favier, C. De Wolf, K. Scrivener, G. Habert, A sustainable future for the European Cement and Concrete Industry: Technology assessment for full decarbonisation of the industry by 2050, ETH Zurich, 2018. https://doi.org/10.3929/ETHZ-B-000301843.

[4] Eurostat Statistics Explained, Energy statistics - an overview, 2024 (2024). https://ec.europa.eu/eurostat/statisticsexplained/Final_energy_consumption (accessed November 7, 2023).

[5] International Energy Agency, Major growth of clean energy limited the rise in global emissions in 2023, https://www.iea.org/News/Major-Growth-of-Clean-Energy-Limited-the-Rise-in-Global-Emissions-in-2023 (2023).

[6] Statista, Production volume of cement worldwide from 1995 to 2022, (2023). https://www.statista.com/statistics/1087115/global-cement-productionvolume/ (accessed November 7, 2023).

[7] C. Tregambi, R. Solimene, F. Montagnaro, P. Salatino, M. Marroccoli, N. Ibris, A. Telesca, Solar-driven production of lime for ordinary Portland cement formulation, Solar Energy 173 (2018) 759–768. https://doi.org/10.1016/j.solener.2018.08.018.

[8] Cembureau (The European Cement Association), Cementing the European Green Deal, (2023).

[9] International Energy Agency, Cement, (2023). https://www.iea.org/energy-system/industry/cement#tracking (accessed March 4, 2024).

[10] International Energy Agency, Cement report, https://www.iea.org/Reports/Cement (2024).

[11] A. Gladwin Alex, A. Kedir, T. Gebrehiwet Tewele, Review on effects of graphene oxide on mechanical and microstructure of cement-based materials, Construction and Building Materials 360 (2022). https://doi.org/10.1016/j.conbuildmat.2022.129609.

[12] A. Cadix, S. James, Cementing additives, in: Fluid Chemistry, Drilling and Completion, Elsevier, 2022: pp. 187–254. https://doi.org/10.1016/B978-0-12-822721-3.00008-3.

[13] A.S. Wagh, Recent Progress in Chemically Bonded Phosphate Ceramics, ISRN Ceramics 2013 (2013) 1–20. https://doi.org/10.1155/2013/983731.

[14] R.T. Kusuma, R.B. Hiremath, P. Rajesh, B. Kumar, S. Renukappa, Sustainable transition towards biomass-based cement industry: A review, Renewable and Sustainable Energy Reviews 163 (2022). https://doi.org/10.1016/j.rser.2022.112503.

[15] M. Torres-Carrasco, F. Puertas, La activación alcalina de diferentes aluminosilicatos como una alternativa al Cemento Portland: cementos activados alcalinamente o geopolímeros, Revista Ingeniería de Construcción 32 (2017) 05–12. https://doi.org/10.4067/S0718-50732017000200001.

[16] International Energy Agency, Global thermal energy intensity and fuel consumption of clinker production in the Net Zero Scenario, 2015-2030, (2030). https://www.iea.org/data-and-statistics/charts/global-thermal-energy-intensity-and-fuel-consumption-of-clinker-production-in-the-net-zero-scenario-2015-2030 (accessed March 4, 2024).

[17] Z. He, X. Zhu, J. Wang, M. Mu, Y. Wang, Comparison of CO_2 emissions from OPC and recycled cement production, Construction and Building Materials 211 (2019) 965–973. https://doi.org/10.1016/j.conbuildmat.2019.03.289.

[18] A. Alsalman, L.N. Assi, R.S. Kareem, K. Carter, P. Ziehl, Energy and CO_2 emission assessments of alkali-activated concrete and Ordinary Portland Cement concrete: A comparative analysis of different grades of concrete, Cleaner Environmental Systems 3 (2021). https://doi.org/10.1016/j.cesys.2021.100047.

[19] J.H.A. Rocha, R.D. Toledo Filho, N.G. Cayo-Chileno, Sustainable alternatives to CO_2 reduction in the cement industry: A short review, Materials Today: Proceedings 57 (2022) 436–439. https://doi.org/10.1016/j.matpr.2021.12.565.

[20] A.M.S. Hassan, H. Shoukry, P. Perumal, M.M. Abd El-razik, R.M.H. Aly, A.M.Y. Alzahrani, Evaluation of the thermo-physical, mechanical, and fire resistance performances of limestone calcined clay cement (LC^3)-based lightweight rendering mortars, Journal of Building Engineering 71 (2023). https://doi.org/10.1016/j.jobe.2023.106495.

[21] K. Scrivener, F. Martirena, S. Bishnoi, S. Maity, Calcined clay limestone cements (LC^3), Cement and Concrete Research 114 (2018) 49–56. https://doi.org/10.1016/j.cemconres.2017.08.017.

[22] J. Mañosa, A. Calderón, R. Salgado-Pizarro, A. Maldonado-Alameda, J.M. Chimenos, Research evolution of limestone calcined clay cement (LC^3), a promising low-carbon binder – A comprehensive overview, Heliyon (2024). https://doi.org/10.1016/j.heliyon.2024.e25117.

[23] M. Khan, J. Lao, M. Riaz Ahmad, M.F. Kai, J.G. Dai, The role of calcium aluminate cement in developing an efficient ultra-high performance concrete resistant to explosive spalling under high temperatures, Construction and Building Materials 384 (2023). https://doi.org/10.1016/j.conbuildmat.2023.131469.

[24] Y. Xu, T. He, X. Ma, R. Luo, The influence of calcium sulphoaluminate cement on the hydration process of cement paste mixed with alkali free liquid accelerator, Materials Today Communications 33 (2022). https://doi.org/10.1016/j.mtcomm.2022.104622.

[25] A. Cuesta, A. Ayuela, M.A.G. Aranda, Belite cements and their activation, Cement and Concrete Research 140 (2021). https://doi.org/10.1016/j.cemconres.2020.106319.

[26] A. Goncharov, S. Zhutovsky, Eco-friendly belite cement from crude calcareous oil shale with low calorific value, Cement and Concrete Research 159 (2022). https://doi.org/10.1016/j.cemconres.2022.106874.

[27] C. Jiang, L. Jiang, S. Li, X. Tang, L. Zhang, Impact of cation type and fly ash on deterioration process of high belite cement pastes exposed to sulfate attack, Construction and Building Materials 286 (2021). https://doi.org/10.1016/j.conbuildmat.2021.122961.

[28] S. Huete-Hernández, A. Maldonado-Alameda, J. Giro-Paloma, J.M. Chimenos, J. Formosa, Fabrication of sustainable magnesium phosphate cement micromortar using design of experiments statistical modelling: Valorization of ceramic-stone-porcelain containing waste as filler, Ceramics International 47 (2021) 10905–10917. https://doi.org/10.1016/j.ceramint.2020.12.210.

[29] S. Huete-Hernández, A. Maldonado-Alameda, A. Alfocea-Roig, J. Giro-Paloma, J.M. Chimenos, J. Formosa, Sustainable magnesium phosphate micromortars formulated with PAVAL® alumina by-product as micro-aggregate, Boletin de La Sociedad Espanola de Ceramica y Vidrio (2023) 1–15. https://doi.org/10.1016/j.bsecv.2023.02.001.

[30] Q. Zhang, X. Cao, R. Ma, S. Sun, L. Fang, J. Lin, J. Luo, Solid waste-based magnesium phosphate cements: Preparation, performance and solidification/stabilization mechanism, Construction and Building Materials 297 (2021). https://doi.org/10.1016/j.conbuildmat.2021.123761.

[31] P. Kinnunen, A. Ismailov, S. Solismaa, H. Sreenivasan, M.L. Räisänen, E. Levänen, M. Illikainen, Recycling mine tailings in chemically bonded ceramics – A review, Journal of Cleaner Production 174 (2018) 634–649. https://doi.org/10.1016/j.jclepro.2017.10.280.

[32] A.S. Wagh, Introduction to Chemically Bonded Ceramics, in: Chemically Bonded Phosphate Ceramics, Elsevier, 2016: pp. 1–16. https://doi.org/10.1016/B978-0-08-100380-0.00001-4.

[33] X. Huang, H. Wu, D. Lu, Preparation of novel chemically bonded ceramics with steel slag and potassium hydrogen oxalate, Journal of Hazardous Materials 403 (2021). https://doi.org/10.1016/j.jhazmat.2020.124042.

[34] H.A. Colorado, J. Pleitt, C. Hiel, J.M. Yang, H.T. Hahn, C.H. Castano, Wollastonite based-Chemically Bonded Phosphate Ceramics with lead oxide contents under gamma irradiation, Journal of Nuclear Materials 425 (2012) 197–204. https://doi.org/10.1016/j.jnucmat.2011.08.043.

[35] C.A. Cárdenas Balaguera, M.A. Gómez Botero, Engineering applications of chemically-bonded phosphate ceramics, Ing. Inv. 39 (2019) 10–19. https://doi.org/10.15446/ing.investig.v39n3.81424.

[36] A.P. Machado, S. Arcaro, F. Raupp-Pereira, C.P. Bergmann, O.R.K. Montedo, Chemically-Bonded Magnesium Phosphate Ceramics from Magnesium Oxide-Graphite Refractory Brick Waste, Mat. Res. 24 (2021). https://doi.org/10.1590/1980-5373-mr-2021-0162.

[37] J. Formosa, Formulaciones de nuevos morteros y cementos especiales basadas en suproductos de magnesio, Universitat de Barcelona, 2012.

[38] C. Yan, H. Ma, Z. Luo, X. Zhou, L. Wang, Influence of Phosphorus Sources on the Compressive Strength and Microstructure of Ferronickel Slag-Based Magnesium Phosphate Cement, Materials 15 (2022). https://doi.org/10.3390/ma15051965.

[39] Y. Zheng, Y. Zhou, X. Huang, H. Luo, Effect of raw materials and proportion on mechanical properties of magnesium phosphate cement, Journal of Road Engineering 2 (2022) 243–251. https://doi.org/10.1016/j.jreng.2022.06.001.

[40] X. Meng, Y. Jiang, B. Chen, L. Wang, Research progress on the setting time and solidification mechanism of magnesium phosphate cement: A review, Construction and Building Materials 408 (2023). https://doi.org/10.1016/j.conbuildmat.2023.133612.

[41] R. Del Valle-Zermeño, J.E. Aubert, A. Laborel-Préneron, J. Formosa, J.M. Chimenos, Preliminary study of the mechanical and hygrothermal properties of hemp-magnesium phosphate cements, Construction and Building Materials 105 (2016) 62–68. https://doi.org/10.1016/j.conbuildmat.2015.12.081.

[42] M. Wang, L. Liang, Q. Liu, X. Liang, H. Guo, Z. Li, R. Liang, G. Sun, Influence of dipotassium hydrogen phosphate on properties of magnesium potassium phosphate cement, Construction and Building Materials 320 (2022). https://doi.org/10.1016/j.conbuildmat.2021.126283.

[43] S.O. Amiandamhen, M. Meincken, L. Tyhoda, Phosphate bonded natural fibre composites: a state of the art assessment, SN Appl. Sci. 1 (2019). https://doi.org/10.1007/s42452-019-0910-9.

[44] D.V. Ribeiro, G.R. Paula, M.R. Morelli, Effect of boric acid content on the properties of magnesium phosphate cement, Construction and Building Materials 214 (2019) 557–564. https://doi.org/10.1016/j.conbuildmat.2019.04.113.

[45] Z. Ding, Y.-Y. Li, C. Lu, J. Liu, An Investigation of Fiber Reinforced Chemically Bonded Phosphate Ceramic Composites at Room Temperature, Materials 11 (2018). https://doi.org/10.3390/ma11050858.

[46] Y. Tao, L. Zhenyu, R. Chunrong, W. Yuanyuan, H. Zhichao, H. Xin, W. Jie, L. Mengliang, D. Qiubai, K. Khan, L. Zhongyuan, L. Shuzhen, Study on solidification properties of chemically bonded phosphate ceramics for cesium radionuclides, Ceramics International 46 (2020) 14964–14971. https://doi.org/10.1016/j.ceramint.2020.03.025.

[47] Y. Li, G. Zhang, Z. Wang, Z. Guan, Experimental-computational approach to investigate compressive strength of magnesium phosphate cement with nanoindentation and finite element analysis, Construction and Building Materials 190 (2018) 414–426. https://doi.org/10.1016/j.conbuildmat.2018.09.145.

[48] Y. Li, J. Sun, B. Chen, Experimental study of magnesia and M/P ratio influencing properties of magnesium phosphate cement, Construction and Building Materials 65 (2014) 177–183. https://doi.org/10.1016/j.conbuildmat.2014.04.136.

[49] L.J. Gardner, S.A. Walling, C.L. Corkhill, S.A. Bernal, V. Lejeune, M.C. Stennett, J.L. Provis, N.C. Hyatt, Temperature transformation of blended magnesium potassium phosphate cement binders, Cement and Concrete Research 141 (2021). https://doi.org/10.1016/j.cemconres.2020.106332.

[50] L.J. Gardner, S.A. Walling, S.M. Lawson, S. Sun, S.A. Bernal, C.L. Corkhill, J.L. Provis, D.C. Apperley, D. Iuga, J.V. Hanna, N.C. Hyatt, Characterization of and Structural Insight into Struvite-K, $MgKPO_4 \cdot 6H_2O$, an Analogue of Struvite, Inorganic Chemistry 60 (2021) 195–205. https://doi.org/10.1021/acs.inorgchem.0c02802.

[51] S.A. Walling, J.L. Provis, Magnesia-Based Cements: A Journey of 150 Years, and Cements for the Future?, Chemical Reviews 116 (2016) 4170–4204. https://doi.org/10.1021/acs.chemrev.5b00463.

[52] D. Leng, X. Li, Y. Lv, H. Tan, N. Li, Z. Liu, W. Jiang, D. Jiang, Cesium immobilization by K-struvite crystal in aqueous solution: Ab initio calculations and experiments, Journal of Hazardous Materials 387 (2020). https://doi.org/10.1016/j.jhazmat.2019.121872.

[53] K. Momma, F. Izumi, VESTA 3 for three-dimensional visualization of crystal, volumetric and morphology data, Journal of Applied Crystallography 44 (2011) 1272–1276. https://doi.org/10.1107/S0021889811038970.

[54] S. Fan, B. Chen, Experimental study of phosphate salts influencing properties of magnesium phosphate cement, Construction and Building Materials 65 (2014) 480–486. https://doi.org/10.1016/j.conbuildmat.2014.05.021.

[55] J.W. Bullard, H.M. Jennings, R.A. Livingston, A. Nonat, G.W. Scherer, J.S. Schweitzer, K.L. Scrivener, J.J. Thomas, Mechanisms of cement hydration, Cement and Concrete Research 41 (2011) 1208–1223. https://doi.org/10.1016/j.cemconres.2010.09.011.

[56] X. Huang, G. Liu, Y. Zheng, H. Luo, The performance of magnesium phosphate cement in negative temperature environment: A state-of-the-art review, Journal of Building Engineering 76 (2023). https://doi.org/10.1016/j.jobe.2023.107278.

[57] M. Le Rouzic, T. Chaussadent, G. Platret, L. Stefan, Mechanisms of k-struvite formation in magnesium phosphate cements, Cement and Concrete Research 91 (2017) 117–122. https://doi.org/10.1016/j.cemconres.2016.11.008.

[58] B. Fang, Z. Hu, T. Shi, Y. Liu, X. Wang, D. Yang, K. Zhu, X. Zhao, Z. Zhao, Research progress on the properties and applications of magnesium phosphate cement, Ceramics International 49 (2023) 4001–4016. https://doi.org/10.1016/j.ceramint.2022.11.078.

[59] R. Salgado-Pizarro, A. Calderón, A. Svobodova-Sedlackova, A.I. Fernández, C. Barreneche, The relevance of thermochemical energy storage in the last two decades: The analysis of research evolution, Journal of Energy Storage 51 (2022). https://doi.org/10.1016/j.est.2022.104377.

[60] Y. Li, B. Chen, Factors that affect the properties of magnesium phosphate cement, Construction and Building Materials 47 (2013) 977–983. https://doi.org/10.1016/j.conbuildmat.2013.05.103.

[61] B. Xu, H. Ma, H. Shao, Z. Li, B. Lothenbach, Influence of fly ash on the compressive strength and micro-characteristics of magnesium potassium phosphate cement mortars, Cement and Concrete Research 99 (2017) 86–94. https://doi.org/10.1016/j.cemconres.2017.05.008.

[62] M. Le Rouzic, T. Chaussadent, L. Stefan, M. Saillio, On the influence of Mg/P ratio on the properties and durability of magnesium potassium phosphate cement pastes, Cement and Concrete Research 96 (2017) 27–41. https://doi.org/10.1016/j.cemconres.2017.02.033.

[63] A. Viani, A.F. Gualtieri, Preparation of magnesium phosphate cement by recycling the product of thermal transformation of asbestos containing wastes, Cement and Concrete Research 58 (2014) 56–66. https://doi.org/10.1016/j.cemconres.2013.11.016.

[64] L. Wang, L. Chen, B. Guo, D.C.W. Tsang, L. Huang, Y.S. Ok, V. Mechtcherine, Red mud-enhanced magnesium phosphate cement for remediation of Pb and As contaminated soil, Journal of Hazardous Materials 400 (2020). https://doi.org/10.1016/j.jhazmat.2020.123317.

[65] M.A. Haque, B. Chen, Research progresses on magnesium phosphate cement: A review, Construction and Building Materials 211 (2019) 885–898. https://doi.org/10.1016/j.conbuildmat.2019.03.304.

[66] M.R. Ahmad, B. Chen, J. Yu, A comprehensive study of basalt fiber reinforced magnesium phosphate cement incorporating ultrafine fly ash, Composites Part B: Engineering 168 (2019) 204–217. https://doi.org/10.1016/j.compositesb.2018.12.065.

[67] Y. Liu, Z. Qin, B. Chen, Experimental research on magnesium phosphate cements modified by red mud, Construction and Building Materials 231 (2020). https://doi.org/10.1016/j.conbuildmat.2019.117131.

[68] Y. Li, T. Shi, J. Li, Effects of fly ash and quartz sand on water-resistance and salt-resistance of magnesium phosphate cement, Construction and Building Materials 105 (2016) 384–390. https://doi.org/10.1016/j.conbuildmat.2015.12.154.

[69] Y. Li, Y. Li, T. Shi, J. Li, Experimental study on mechanical properties and fracture toughness of magnesium phosphate cement, Construction and Building Materials 96 (2015) 346–352. https://doi.org/10.1016/j.conbuildmat.2015.08.012.

[70] Y. Tan, H. Yu, Y. Li, W. Bi, X. Yao, The effect of slag on the properties of magnesium potassium phosphate cement, Construction and Building Materials 126 (2016) 313–320. https://doi.org/10.1016/j.conbuildmat.2016.09.041.

[71] L. Mo, L. Lv, M. Deng, J. Qian, Influence of fly ash and metakaolin on the microstructure and compressive strength of magnesium potassium phosphate cement paste, Cement and Concrete Research 111 (2018) 116–129. https://doi.org/10.1016/j.cemconres.2018.06.003.

[72] C. You, J. Qian, J. Qin, H. Wang, Q. Wang, Z. Ye, Effect of early hydration temperature on hydration product and strength development of magnesium phosphate cement (MPC), Cement and Concrete Research 78 (2015) 179–189. https://doi.org/10.1016/j.cemconres.2015.07.005.

[73] J. Qin, J. Qian, C. You, Y. Fan, Z. Li, H. Wang, Bond behavior and interfacial micro-characteristics of magnesium phosphate cement onto old concrete substrate, Construction and Building Materials 167 (2018) 166–176. https://doi.org/10.1016/j.conbuildmat.2018.02.018.

[74] N. Yang, C. Shi, J. Yang, Y. Chang, Research progresses in magnesium phosphate cement – based materials, Journal of Materials in Civil Engineering 26 (2014). https://doi.org/10.1061/(ASCE)MT.1943-5533.0000971.

[75] C. Shi, J. Yang, N. Yang, Y. Chang, Effect of waterglass on water stability of potassium magnesium phosphate cement paste, Energy and CO_2 Emission 53 (2014) 83–87. https://doi.org/10.1016/j.cemconcomp.2014.03.012.

[76] L. Chong, J. Yang, C. Shi, Effect of curing regime on water resistance of magnesium–potassium phosphate cement, Construction and Building Materials 151 (2017) 43–51. https://doi.org/10.1016/j.conbuildmat.2017.06.056.

[77] H. Ma, B. Xu, Z. Li, Magnesium potassium phosphate cement paste: Degree of reaction, porosity and pore structure, Cement and Concrete Research 65 (2014) 96–104. https://doi.org/10.1016/j.cemconres.2014.07.012.

[78] H. Ma, B. Xu, J. Liu, H. Pei, Z. Li, Effects of water content, magnesia-to-phosphate molar ratio and age on pore structure, strength and permeability of magnesium potassium phosphate cement paste, Materials & Design 64 (2014) 497–502. https://doi.org/10.1016/j.matdes.2014.07.073.

[79] P. An, Z. Han, K. Wang, J. Cheng, Z. Zhao, Y. Andre Situmorang, J. Rizkiana, A. Abudula, G. Guan, Energy-saving strategy for a transport bed flash calcination process applied to magnesite, Carbon Resources Conversion 4 (2021) 122–131. https://doi.org/10.1016/j.crcon.2021.03.004.

[80] R. Del Valle-Zermeño, J. Formosa, J.A. Aparicio, J.M. Chimenos, Reutilization of low-grade magnesium oxides for flue gas desulfurization during calcination of natural magnesite: A closed-loop process, Chemical Engineering Journal 254 (2014) 63–72. https://doi.org/10.1016/j.cej.2014.05.089.

[81] J. Nobre, H. Ahmed, M. Bravo, L. Evangelista, J. De Brito, Magnesia (MgO) Production and Characterization, and Its Influence on the Performance of Cementitious Materials: A Review, Materials 13 (2020) 4752. https://doi.org/10.3390/ma13214752.

[82] F. Ravazzolo, J. Vespignani, World steel production: A new monthly indicator of global real economic activity, Canadian J of Economics 53 (2020) 743–766. https://doi.org/10.1111/caje.12442.

[83] M. Yellishetty, G.M. Mudd, P.G. Ranjith, A. Tharumarajah, Environmental life-cycle comparisons of steel production and recycling: sustainability issues, problems and prospects, Environmental Science & Policy 14 (2011) 650–663. https://doi.org/10.1016/j.envsci.2011.04.008.

[84] M. Musmeci, N.M. Rendtorff, L. Musante, L. Martorello, P. Galliano, E.F. Aglietti, Characterization of MgO-based tundish working lining materials, microstructure and properties, Ceramics International 40 (2014) 14091–14098. https://doi.org/10.1016/j.ceramint.2014.05.138.

[85] A.R. Pal, S. Bharati, N.V.S. Krishna, G.C. Das, P.G. Pal, The effect of sintering behaviour and phase transformations on strength and thermal conductivity of disposable tundish linings with varying compositions, Ceramics International 38 (2012) 3383–3389. https://doi.org/10.1016/j.ceramint.2011.12.049.

[86] Y. Sahai, Tundish Technology for Casting Clean Steel: A Review, Metall Mater Trans B 47 (2016) 2095–2106. https://doi.org/10.1007/s11663-016-0648-3.

[87] Y. Liu, G. Li, L. Wang, Z. Zhang, Effect of the Tundish Gunning Materials on the Steel Cleanliness, High Temperature Materials and Processes 37 (2018) 313–323. https://doi.org/10.1515/htmp-2016-0137.

[88] P.K. Jha, S. Rao, A. Dewan, Effect of Height and Position of Dams on Inclusion Removal in a Six Strand Tundish, ISIJ International 48 48 (2008) 154–160. https://doi.org/10.2355/isijinternational.48.154

[89] D. Mazumdar, Review, Analysis, and Modeling of Continuous Casting Tundish Systems, Steel Research Int. 90 (2019) 1800279. https://doi.org/10.1002/srin.201800279.

[90] Continuous casting: Find suppliers, processes & material, Manufacturing (2021). https://www.manufacturingguide.com/en/continuous-casting.

[91] A. Alfocea-Roig, S. Huete-Hernández, X. García-Zubiri, J. Giro-Paloma, J. Formosa, Can tundish deskulling waste be used as a magnesium oxide source to develop magnesium phosphate cement?, Journal of Environmental Chemical Engineering 11 (2023). https://doi.org/10.1016/j.jece.2023.110618.

[92] A.C. Quintero-Payan, S. Huete-Hernández, V.B. Aguilar-Pozo, S. Astals, J.M. Chimenos, Stabilization of metal and metalloids from contaminated soils using magnesia-based tundish deskulling waste from continuous steel casting, Chemosphere 348 (2024). https://doi.org/10.1016/j.chemosphere.2023.140750.

[93] B.E. Lebrouhi, S. Baghi, B. Lamrani, E. Schall, T. Kousksou, Critical materials for electrical energy storage: Li-ion batteries, Journal of Energy Storage 55 (2022). https://doi.org/10.1016/j.est.2022.105471.

[94] D. Gielen, M. Lyons, International Renewable Energy Agency, Critical materials for the energy transition: Lithium, (2022).

[95] C. Dessemond, F. Lajoie-Leroux, G. Soucy, N. Laroche, J.F. Magnan, Spodumene: The lithium market, resources and processes, Minerals 9 (2019). https://doi.org/10.3390/min9060334.

[96] Y. Tan, H. Yu, Y. Li, C. Wu, J. Dong, J. Wen, Magnesium potassium phosphate cement prepared by the byproduct of magnesium oxide after producing Li_2CO_3 from salt lakes, Ceramics International 40 (2014) 13543–13551. https://doi.org/10.1016/j.ceramint.2014.05.063.

[97] Y.Z. Huaiyou Wang Baoqiang Du, Youjing Zhao, Min Wang, Recovery of both magnesium and lithium from high Mg/Li ratio brines using, Hydrometallurgy 175 (2018). http://dx.doi.org/10.1016/j.hydromet.2017.10.017.

[98] D. Fuentealba, C. Flores-Fernández, E. Troncoso, H. Estay, Technological tendencies for lithium production from salt lake brines: Progress and research gaps to move towards more sustainable processes, Resources Policy 83 (2023). https://doi.org/10.1016/j.resourpol.2023.103572.

[99] D.V. Ribeiro, G.R. Paula, M.R. Morelli, Use of microwave oven in the calcination of MgO and effect on the properties of magnesium phosphate cement, Construction and Building Materials 198 (2019) 619–628. https://doi.org/10.1016/j.conbuildmat.2018.11.289.

[100] W. Zheng, J. Dong, J. Wen, C. Chang, X. Xiao, Effects of water-to-cement ratios on the properties of magnesium potassium phosphate cement prepared with lithium-extracted magnesium residue, Applied Sciences (Switzerland) 11 (2021). https://doi.org/10.3390/app11094193.

[101] P. Liu, J. Dong, C. Chang, W. Zheng, X. Liu, X. Xiao, J. Wen, Preparation of low-cost magnesium oxychloride cement using magnesium residue byproducts from the production of lithium carbonate from salt lakes, Materials 14 (2021). https://doi.org/10.3390/ma14143899.

[102] A.L. Luza, L. Simão, J. Acordi, F. Raupp-Pereira, M.D.M. Innocentini, O.R.K. Montedo, Synthesis of chemically bonded porous ceramics from MgO–C refractory bricks waste, Ceramics International 48 (2022) 3426–3434. https://doi.org/10.1016/j.ceramint.2021.10.119.

[103] S. Nanda, A. Choudhury, K.S. Chandra, D. Sarkar, Raw materials, microstructure, and properties of MgO–C refractories: Directions for refractory recipe development, Journal of the European Ceramic Society 43 (2023) 14–36. https://doi.org/10.1016/j.jeurceramsoc.2022.09.032.

[104] X. Wang, X. Li, L. Lian, X. Jia, J. Qian, Recycling of waste magnesia refractory brick powder in preparing magnesium phosphate cement mortar: Hydration activity, mechanical properties and long-term performance, Construction and Building Materials 402 (2023). https://doi.org/10.1016/j.conbuildmat.2023.133019.

[105] X. Bing Dai, L. Lian, X. Wen Jia, J. Hui Qin, J. Shi Qian, Preparation and properties of magnesium phosphate cement with recycled magnesia from waste magnesia refractory bricks, Journal of Building Engineering 63 (2023). https://doi.org/10.1016/j.jobe.2022.105491.

[106] S. Sinha, S. Ghosh, A.K. Samanta, Influence of waste refractory brick on the destructive and non-destructive properties of sustainable eco-friendly concrete, Materials Today: Proceedings (2023). https://doi.org/10.1016/j.matpr.2023.03.508.

Chapter 3

CHAPTER 3

DEVELOPMENT OF MPC-TUN

This chapter examines the development of alternative materials using TUN as a secondary source of magnesium oxide, with a particular focus on binders and mortars. It evaluates their physical, chemical, and mechanical properties, while also conducting an environmental assessment to provide insights into their potential impacts.

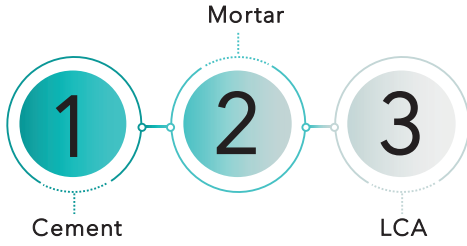

3.1. Cement

3.1.1. Introduction

MPC has gained attention for their ability to incorporate industrial by-products and wastes as sources of magnesium oxide [1,2]. A critical requirement for the MPC is a sufficient magnesium oxide content to facilitate the formation of K-struvite [3,4]. However, due to the complex nature of these materials, other components are often present, needing comprehensive chemical characterization to assess their suitability as a raw material. In this context, the citric acid reactivity test (CART) has proven effective in classifying TUN as a material with appropriate reactivity. Techniques such as X-ray fluorescence (XRF), X-ray diffraction (XRD), and thermogravimetric analysis (TG) have been employed to determine the composition and estimate the magnesium oxide content. Additionally, various physical, mechanical, and environmental characterization methods have been employed to comprehensively evaluate the material properties and its potential applications.

The potential of TUN as a source of magnesium oxide has been demonstrated through the development and characterization of MPC-TUN binders. Specifically, this study marks the first application of this waste material in the constructive materials field, which explains the absence of prior literature on its use. However, there is a wide variety of literature regarding MPC, which has been used to inform the evaluation techniques, analysed the material behaviour, and assess its suitability for use in construction applications.

The initial research conducted as part of this PhD thesis was focused on evaluating whether TUN could serve as a suitable and effective material for developing MPC binders with desirable mechanical and environmental properties. The following section provides a concise summary of the key findings from first study, highlighting the potential use of TUN as a raw material in this context.

3.1.2. Relevance

In recent years, the field of alternative cements has garnered significant attention from the global scientific community [5]. As a result, numerous researchers have contributed publishing into this area, particularly, on the use of industrial by-products and wastes as raw materials for sustainable cement development. The incorporation of TUN into MPC represents a novel approach, expanding the possibilities for valorising a waste material that has yet to find application in the construction industry. Figure 3.1 shows the key advantages of developing MPC using TUN (MPC-TUN).

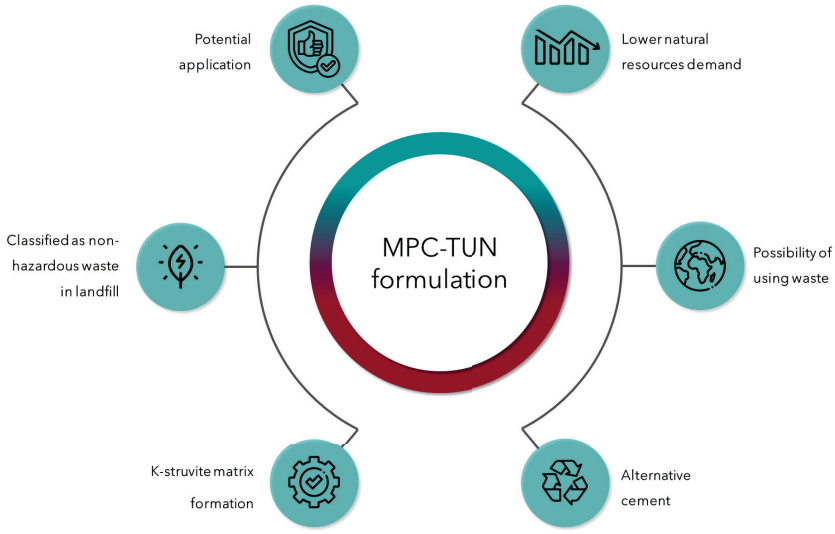

Figure 3.1. The research benefits of the development of MPC-TUN.

3.1.3. Publication 1

Publication 1 titled "Can tundish deskulling waste be used as a magnesium oxide source to develop magnesium phosphate cement?" was published under open access in the journal of Environmental Chemical Engineering (journal impact factor (JIF) of 7.4 in 2023, ranked in Q1) in October 2023, volume 11, issue 5. The title of the publication is displayed in Figure 3.2, and the full text is included in this document.

Journal of Environmental Chemical Engineering
Volume 11, Issue 5, October 2023, 110618

Can tundish deskulling waste be used as a magnesium oxide source to develop magnesium phosphate cement?

A. Alfocea-Roig [a], S. Huete-Hernández [a], Í.X. García-Zubiri [b], J. Giro-Paloma [a], J. Formosa [a]

[a] Departament de Ciència de Materials i Química Física, Universitat de Barcelona, Martí i Franquès 1-11, 08028 Barcelona, Spain
[b] Magnesitas Navarras, S.A., Av. Roncesvalles, 31630 Zubiri, Spain

Figure 3.2. Headline of the article published in the journal of Environmental Chemical Engineering in October 2023, entitled "Can tundish deskulling waste be used as a magnesium oxide source to develop magnesium phosphate cement?" [6].

Journal of Environmental Chemical Engineering 11 (2023) 110618

Contents lists available at ScienceDirect

Journal of Environmental Chemical Engineering

journal homepage: www.elsevier.com/locate/jece

Can tundish deskulling waste be used as a magnesium oxide source to develop magnesium phosphate cement?

A. Alfocea-Roig [a], S. Huete-Hernández [a], Í.X. García-Zubiri [b], J. Giro-Paloma [a], J. Formosa [a,*]

[a] Departament de Ciència de Materials i Química Física, Universitat de Barcelona, Martí i Franquès 1-11, 08028 Barcelona, Spain
[b] Magnesitas Navarras, S.A., Av. Roncesvalles, 31630 Zubiri, Spain

ARTICLE INFO

Editor: Apostolos Giannis

Keywords:
Circular economy
Refractory waste
Magnesium phosphate cement
Steel industry waste
Valorisation

ABSTRACT

Ordinary Portland cement (OPC) has a significant environmental impact since approximately 0.81 kg of CO_2 is generated for every kilogram produced. Thus, it is mandatory to look for sustainable alternative cements. One of the most promising materials in this sense is magnesium phosphate cement (MPC). This study evaluates the possibility of revaluing a waste obtained from the tundish deskulling (TUN) as a raw material for formulating alternative MPC. This approach aims to promote the circular economy and minimizing the environmental impact of MPC. The tundish working lining is a crucial refractory material used in continuous steel casting. An optimal cement formulation was achieved by maximizing the compressive strength (CS) at 7 days, resulting in the combination of 60 wt% of TUN and 40 wt% of KH_2PO_4, with a water/cement (W/C) ratio of 0.27. The physical and mechanical properties were evaluated at three different stages: after 1, 7, and 28 days of curing. Furthermore, an exhaustive physicochemical characterization was conducted to investigate the feasibility of using it as an alternative cement. This study confirms the feasibility of formulating MPC using TUN as raw material due to the main product obtained, which is K-struvite. The use of TUN implies important economic savings and enhances sustainability criteria avoiding its management in landfills.

1. Introduction

The Industry current new lines of research are mainly focused on the circular economy, energy efficiency, and greenhouse gas (GHG) emissions reduction. Primary resources from mining activities remain a significant prerequisite to appease the growing global demand for raw materials. Hence, mining is crucial, even more so in a circular economy tendency. Improving the production processes and product design of a product can minimise the amount and volume of the demanded raw materials. More efficient reuse, repair, and recycling of waste and by-products can be accomplished. In this sense, it is necessary to continue studying for better efficiency in mining operations to achieve the goal of zero waste mining, using secondary resources from mine waste to its fullest potential.

The steel industry is the largest consumer of refractory materials (about 70 %). The refractory materials are divided into two types: unshaped (monolithic refractories) with 45 % and shaped refractories with 55 % [1]. These are classified by their chemical composition, density, or type of blend [2,3]. Specifically, non-shaped includes also refractories made of magnesia (47 %). Following a study on critical raw materials in the EU in 2020, it is estimated that 57 % of EU magnesite consumption comes from steelmaking [4]. These refractories are used in this industry as they exhibit high temperature resistance (> 1500 ºC), slag resistance, and chemical and physical resistance to molten metals.

The highest consumption (42 %) of refractories in steelmaking corresponds to the tundish masses coating [5]. Tundish is an essential component for the process of continuous casting of steel, as it is the last container with refractory material to deliver molten metal at a controlled speed to the moulds [6]. Fig. 1. A shows the process of steel production and Fig. 1. B shows the container before its use. The functions of the container include smoothing the outflow, regulating the feeding of the metal to the moulds, and cleaning the metal, among other operations. For this reason, the refractories in the container must be renewed periodically since the slag generated in the process can interfere with them, therefore, making them less effective. The service lifetime of the tundish masses depends on the service conditions and the

Abbreviations: MPCs, Magnesium phosphate cements; MKP, Monopotassium phosphate; OPC, Ordinary portland cement; MKPC, Magnesium potassium phosphate cement; TUN, Tundish deskulling waste; MPC-TUN, Magnesium phosphate cement - Tundish deskulling waste.

* Corresponding author.
E-mail address: joanformosa@ub.edu (J. Formosa).

https://doi.org/10.1016/j.jece.2023.110618
Received 11 May 2023; Received in revised form 30 June 2023; Accepted 20 July 2023
Available online 22 July 2023
2213-3437/© 2023 The Author(s). Published by Elsevier Ltd. This is an open access article under the CC BY-NC-ND license (http://creativecommons.org/licenses/by-nc-nd/4.0/).

Fig. 1. A (right). Scheme of steel production which the number 2 is related to the Tundish container. B (left). Tundish based on MgO refractory container (supplied by Magnesitas Navarras, S.A.).

performance of the material, but once it exceeds the quality and safety conditions, the masses are replaced with new material. Therefore, a high amount of waste is generated, containing significant impurities, and being difficult to separate and recycle. This waste is known as tundish deskulling (TUN).

The raw materials demand for the manufacture of refractory materials is only covered with 5–8 % of recycled materials, which is approximately 2.5 million tons [1,7]. The utilization of TUN as a raw material after its service life enables a reduction in the extraction of new minerals, water pollution, waste associated with mineral extraction, and ground degradation. Hence, this leads to a reduction in the environmental impact associated. The EU Directive on the landfill of waste (Directive 2018/850) classifies landfill sites into three different types: inert waste, hazardous waste and, non-hazardous waste [8]. Refractories are considered non-hazardous waste, and the Directive establishes targets to introduce restrictions on landfilling. The objective of the European Parliament is to incentivize the circular economy and waste management. In that regard, the valorization of TUN can contribute to the achievement of various goals outlined in Directive 2008/98/EC on waste and Directive 1999/31/EC on the landfilling of waste [8,9].

As abovementioned, the primary sector driving the demand for magnesia globally is the steel industry, but the cement sector also plays a significant role [4]. Hence, it is important to seek for new applications for magnesia refractory waste. Consequently, TUN could be a sustainable alternative to the raw materials traditionally employed for developing Magnesium Phosphate Cement (MPC), which has a high potential to reduce the use of Ordinary Portland Cement (OPC) in some applications, such as for example in precast cements, repair cements, among others. OPC is one of the most manufactured materials in the world [10]. The OPC industry emits around 7 % of global anthropogenic CO_2 emissions and it is the third-largest industrial energy consumer [3]. This is attributed to the calcination of raw materials that leads to the formation and release of CO_2, as well as the high energy demand to maintain high temperatures in the clinkerization process. To manufacture 1 ton of OPC, approximately 900 kg CO_2 is emitted, and 1.5 tons of raw material are required [11]. Therefore, the scientific and technological community is looking for alternative types of cement to reduce GHG emissions, energy demand, and consumption of natural resources from the manufacture of cement. The challenges faced by industries include the utilization of alternative fuels instead of conventional fossil fuels and partially substituting clinker with waste or industrial by-products. The implementation of these solutions can contribute to the achievement of Sustainable Development Goals (SDG) and reducing CO_2 levels and other GHG emissions in the atmosphere, among other challenges [12,13].

MPCs are hydraulic cements that are formed through an acid-base reaction. In particular, the reaction between MgO and monopotassium phosphate (KH_2PO_4, MKP) in an aqueous solution at room temperature leads to the formation of magnesium potassium phosphate cement (MKPC), with $MgKPO_4{\cdot}6H_2O$, also known as K-struvite, as the main reaction product, as shown in Eq. (1) [14,15].

$$MgO_{(s)} + KH_2PO_{4(s)} + 5H_2O \quad {}_{(l)} \rightarrow MgKPO_4{\cdot}6H_2O_{(s)} \tag{1}$$

MPCs have several advantages such as neutral pH, low water demand, fast setting, high early strength, good waste encapsulation, and low drying shrinkage, among others features [16–18]. Due to these properties, the applications of MPCs are highly diverse as they have been extensively used as a repair and reinforcement cements in civil engineering, as stabilizers/solidifiers of radioactive waste, and in biomedical applications [15–20].

The objective of this study is to assess the potential of using TUN, which is defined as tundish deskulling waste, as a MgO source for developing an alternative magnesium phosphate cement; named as MPC-TUN. The assessment of its potential was conducted from various perspectives, including morphological, physical, chemical, environmental, and mechanical viewpoints. Different formulations were

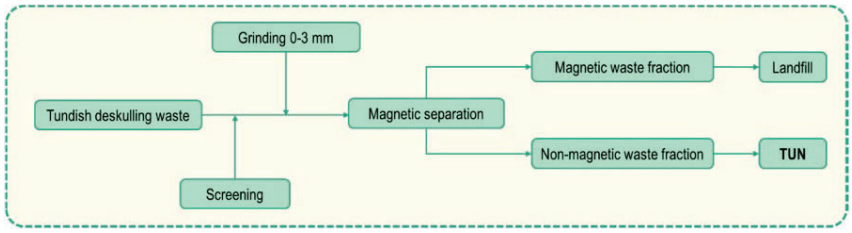

Fig. 2. Conditioning of TUN.

performed by maximizing the compressive strength (CS) at 7 days. The resultant optimal formulation was characterized at 1, 7, and 28 days of curing. In addition, it should be noted that this alternative material can reduce the CO_2 emissions, energy demand, and resource consumption by following the challenges and agreements set internationally, such as the Paris Agreement. In addition, the MPC-TUN alternative cement contributes positively to the challenge of carbon neutral concrete in 2050 [21].

2. Materials and methods

2.1. Materials

TUN was supplied by Magnesitas Navarras, S.A. company (Navarra, Spain). It originates from a Basauri steel mill, located in Bizkaia (Spain), which has an annual steel production of approximately 700 kt and consumes 2.7 kt of tundish masses [22]. After its recollection, it has to be screened, milled (to obtain a particle size below 3 mm) and subsequently demagnetized (to remove magnetic impurities from the slag), as shown in Fig. 2. On one hand, various wastes are generated during the conditioning process, primarily from screening and grinding operations, which are subsequently disposed of in landfills, accounting for 22.46 % of the total waste. Additionally, the magnetic waste fraction (13.66 %) is also disposed of in landfills. On the other hand, the TUN utilized as a raw material in this study comprises solely the non-magnetic fraction (63.88 %) of the original waste material. At the end of the conditioning process, the non-magnetic fraction is quartered and homogenized to obtain a representative chemical composition.

The phosphate source was KH_2PO_4, known as MKP and was supplied by Norken, S.L. (food-grade, purity: 99.8 wt%). Boric acid (H_3BO_3, HB) was supplied by Borax España, S.A., is used as a setting retarder and to control thermal expansion [23].

2.2. TUN characterization

To characterize the chemical composition and to determine the content of the most stable oxides, X-ray fluorescence spectroscopy (XRF) was employed using a Philips PW 2400 sequential X-ray spectrometer. TUN was characterized by X-ray diffraction (XRD) using a PANalytical X'Pert PRO MPD alpha1 powder diffractometer, with CuKα_1 radiation. The resulting diffraction pattern was analyzed using the X'Pert HighScore software, and the main mineral and crystalline phases were determined by referencing the PDF2 database. Moreover, thermogravimetric analysis with derivative thermogravimetry (TG/DTG) was conducted with a TA Instruments Q-600 SDT from 30° to 1400°C at a heating rate of 10 °C min^{-1} in air and nitrogen atmosphere with gas flow of 50 mL·min^{-1}.

Besides, Fourier transformed infrared spectroscopy in attenuated total reflectance mode (FTIR-ATR) was used by means of Spectrum Two™ equipment from Perkin Elmer to detect the symmetric and asymmetric stretching vibration bonds. A 32-scan average was collected with a resolution of 4 cm^{-1}.

The specific surface area (SSA) was evaluated using the Brunauer-Emmett-Teller (BET) model with a TriStar 3000 V6.04 A. The particle size distribution (PSD) was determined with a Beckman Coulter® LSTM 13 320 device with a universal liquid module. Citric acid reactivity test (CART) was performed to study the reactivity of magnesium oxide and, consequently, to classify TUN from high reactivity (< 60 s) to dead-burnt, i.e., low reactivity (> 900 s) [17]. During the test, 2 g of TUN was combined with 100 mL of a citric acid solution. The resulting mixture was stirred at 500 rpm·min^{-1} at 30 °C and monitored using a pH-meter from Hannah Instruments to determine the time necessary to achieve a pH of 9 [17].

Leaching tests to determine the environmental potential impact were performed following the EN 12457–2 standard. The leachates were subsequently analysed employing inductively coupled plasma mass spectrometry (ICP-MS) with the NexION 350D equipment from Perkin Elmer.

Finally, the microstructure of TUN was analysed using scanning electron microscopy (SEM) and energy-dispersive X-ray spectroscopy (EDS). The TUN sample was carbon-coated to evaluate the particle morphology and elemental composition. This analysis was conducted using the ESEM FEI Quanta 200 equipment.

Table 1
Compressive strength of the preliminary study of different formulations.

W/C	TUN/MKP (MPa)					
	60/40	±	**55/45**	±	**50/50**	±
0.25	31.87	2.77	30.00	2.68	31.89	4.58
0.27	35.32	2.31	27.17	3.12	25.32	5.82
0.29	29.30	1.63	28.87	0.15	23.41	3.77
0.31	26.42	1.43	23.55	2.30	22.84	2.53
0.33	24.03	0.79	23.16	0.87	19.81	0.42
0.35	22.30	3.56	21.63	3.22	21.70	2.02

2.3. Samples preparation

The methodology for preparing the MPC-TUN formulations was thoroughly followed to ensure that there were no alterations in the variables that could potentially impact the final properties of the cements. MPC-TUN formulations were prepared in two steps. Firstly, a preliminary study was conducted by preparing small batches of 200 g of solid (MKP and TUN) in order to determine the proper dosage for conducting this study. The preliminary study was focused on obtaining the maximum CS at 7 days of curing with the absence of efflorescence.

In the preliminary study, the TUN/MKP ratios ranged from 80/20–20/80, with a 10 wt% variation for each dosage. The water/cement (W/C) ratio was set at 0.20 and 0.30. For each preliminary dosage, three specimens measuring 2.5 × 2.5 × 2.5 cm^3 were evaluated. Better results were obtained within the TUN/MKP ratio range of 60/40 and 50/50. Subsequently, a more detailed study was conducted within this range, following the same procedure outlined in Table 1, but with a W/C ratio between 0.25 and 0.35. The aim was to determine the appropriate TUN/MKP and W/C ratios for evaluating the properties of the MPC-TUN. The dosages of 50/50 presented efflorescence; for this reason, they were discarded. As shown in Table 1, the 60/40 TUN/MKP formulations achieved higher CS after 7 days of curing compared to the 55/45 formulations with the same W/C ratio. Hence, the formulation with 60 wt% of TUN and 40 wt% of KH_2PO_4 with a W/C ratio of 0.27 was chosen for the further study of MPC-TUN.

It should be highlighted that to increase the workability of this formulation (TUN/MKP = 60/40, and W/C = 0.27) a new batch was prepared by adding 1 wt% of HB relative to the total of solids (TUN and MKP). As it is reported in the literature, HB acts as a setting retarder and improves the workability of the mixture [14]. Three new MPC-TUN batches of 2000 g each were prepared using the best dosage above mentioned to obtain a total of nine 16 × 4 × 4 cm^3 prismatic specimens.

One important characteristic of MPCs, as mentioned earlier, is their ability to develop early strength, resulting in rapid setting. Consequently, a low final setting time is expected for MPC-TUN. The results of VICAT testing, following the UNE-EN 196–3 standard, reveal that the initial setting time is 3150 s, and the final setting time is 3690 s. This MPC-TUN formulation was prepared as it is shown Fig. 3. The solid cement components (i.e.: TUN, MKP, and HB) and the kneading water were weighed separately. Subsequently, the solid cement components were poured and homogenized for 60 s at low speed in a planetary mortar mixer. Then, the kneading water was added and the mixture was mixed during 180 s. The fresh mixture was moulded in three 16 × 4×4 cm^3 moulds, and cured in laboratory conditions. After 24 h of curing, the samples were demoulded. Then, the samples were cured up

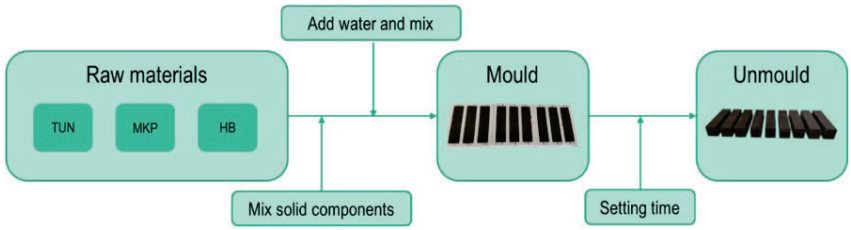

Fig. 3. Methodology to formulate the MPC-TUN.

Table 2
Characterization of TUN and MPC-TUN.

Techniques	TUN	MPC-TUN		
		Day 1	Day 7	Day 28
BET	✓	-	-	-
CART	✓	-	-	-
CS	-	✓	✓	✓
FS	-	✓	✓	✓
FT-IR	✓	-	-	✓
Leaching test	✓	-	-	✓
PSD	✓	-	-	-
SEM	✓	-	-	✓
TG/DTG	✓	-	-	✓
XRD	✓	-	-	✓
XRF	✓	-	-	-

to for 1, 7, and 28 days at room temperature under the same conditions. In total nine prismatic samples were performed, three per each specific cured time. The laboratory conditions (25 °C ± 1 °C and 50 % ± 5 % relative humidity) were kept constant during the experimental process. Finally, the samples were tested and analysed to evaluate the different physical, chemical, mechanical, and environmental properties.

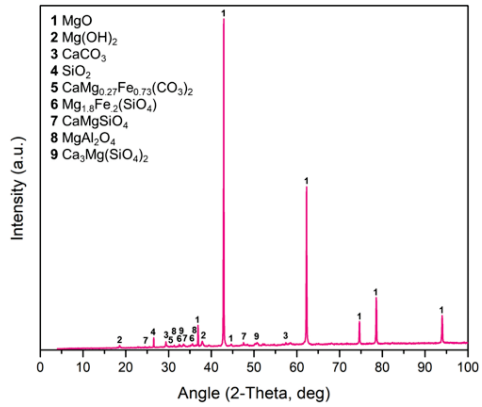

Fig. 4. XRD pattern of TUN.

2.4. Characterization of the MPC-TUN formulation

MPC-TUN formulation was characterized to determine physical, mechanical, chemical, and leaching properties, as shown in Table 2. The flexural strength (FS) and CS were evaluated with an Incotecnic MULTI-R1 universal testing machine, equipped with a 200 kN load cell, following the UNE-EN 196–1 standard. The FS and CS test speed was 5 kg·s^{-1} and 240 kg·s^{-1}, respectively. Apparent density following EN1936:2006, FS, and CS were evaluated at 1, 7, and 28 days of curing. On the other hand, the samples corresponding to the batch of 28 days of curing were thoroughly analysed by means of XRD, TG/DTG, FT-IR, BET, leaching test, and SEM-EDS.

In this regard, XRD analysis was performed using a Bragg-Brentano Siemens D-500 powder diffractometer with CuKα1 radiation. The resulting diffraction pattern was interpreted using the X'Pert HighScore software, with reference to the PDF2 database, to analyse the main crystalline phases of the MPC-TUN reaction products.

The TG/DTG analysis was performed using the same equipment employed for the characterization of raw materials. The analysis was performed in both air and nitrogen atmospheres (at a flow rate of 50 mL·min^{-1}) with a heating rate of 10 °C·min^{-1} up to 1400 °C. Furthermore, FTIR-ATR was conducted in the same conditions as TUN was analysed to determine the atomic bonds vibrations in order to understand more the chemical structure of MPC-TUN. The potential release of heavy metals and metalloids was assessed according to the EN 12457–2 standard, which enabled the simulation of leaching behaviour after the service lifetime of the material. MPC-TUN was crushed below 4 mm following the UNE-EN 12457–2. The leaching procedure involves the extraction heavy metals from the solids using deionized water with a liquid-to-solid ratio of 10 L·kg^{-1}. This extraction process was conducted for 24 h under continuous stirring at 10 rpm and at room temperature. Subsequently, the leachate was separated and filtered using a 0.45 mm pore membrane, and analysed by means of ICP-MS with the NexION 350D Perkin Elmer equipment. The following elements were evaluated, as specified by the standard: As, Ba, Cd, Cr, Cu, Hg, Mo, Ni, Pb, Sb, Se, V, and Zn.

Finally, the microstructure and morphology of the samples were characterized through SEM using ESEM FEI Quanta 200 equipment. Backscattered electron images were collected and combined with EDS elemental mapping (20 kV, working distance of 15 mm) to obtain high contrast micrographs, where each colour corresponds to the different elemental composition found in the sample. SEM-EDS was used to determine the elemental composition in different areas of the developed MPC-TUN samples after 28 days of curing. The fragments of MPC-TUN

Table 3
XRF analysis of TUN expressed in wt%.

Compounds	MgO	CaO	SiO_2	Al_2O_3	Fe_2O_3	SO_3	P_2O_5	Cr_2O_3	Na_2O	LOI
wt%	68.70	9.43	8.67	4.68	3.56	0.15	0.11	0.07	0.02	4.61

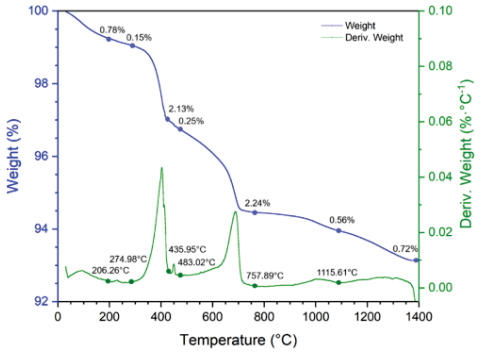

Fig. 5. TG/DTG of TUN.

were fixed on a carbon adhesive and carbon-coated. Additionally, polished samples were examined to reveal the internal structure of the MPC-TUN matrix and embedded particles.

3. Results and discussion

3.1. Raw material characterization

The chemical composition of TUN determined by XRF is shown in Table 3 as the most stable oxide for each element. As expected, the most abundant element is magnesium, with an average MgO content of 68.70 wt%. Following MgO, the most abundant elements are calcium, silicon, aluminium, and iron as CaO (9.43 wt%), SiO_2 (8.66 wt%), Al_2O_3 (4.68 wt%), and Fe_2O_3 (3.56 wt%), respectively. The Loss on Ignition (LOI) refers to the mass loss up to 1050 °C, resulting in 4.61 wt%.

Fig. 4 presents the XRD pattern of TUN, indicating the primary crystalline phases, which are magnesium oxide (MgO, 01-078-0430), brucite ($Mg(OH)_2$, 01-082-2453), and calcite ($CaCO_3$, 01-083-0578). In addition, other crystalline phases are compatible with the following phases: silicon oxide (SiO_2, 01-081-0065), ankerite ($CaMg_{0.27}Fe_{0.73}(CO_3)_2$, 01-084-2067), forsterite ($Mg_{1.8}Fe_{0.2}(SiO_4)$, 01-079-2184), monticellite ($CaMgSiO_4$, 01-084-1321), spinel ($MgAl_2O_4$, 01-077-0436), and merwinite ($Ca_3Mg(SiO_4)_2$, 01-074-0382).

The TG/DTG analysis showed a total mass loss of 6.82 wt% in N_2 atmosphere when heated from 30 ºC to 1400 ºC. Seven different mass losses are shown in Fig. 5 (blue dots), as well as the temperature range of each one (green dots). The first step is related to water loss due to the moisture of the sample from 30 ºC to 206 ºC (0.78 wt%). The following decompositions are from 206 ºC to 275 ºC (0.15 wt%, not assigned), from 275 ºC to 436 ºC (2.13 wt%) due to the $Mg(OH)_2$ decomposition, as well as $Ca(OH)_2$ decomposition from 436 ºC to 483 ºC (0.25 wt%). The following two decompositions are assigned to two different carbonates decomposition (ankerite and calcite, respectively) from 483 ºC to 1116 ºC (2.8 wt%), and the last loss up to 1400 ºC (0.72 wt%) is attributed to sulphates, which is probably due to the presence of $CaSO_4$ in TUN, and it could be also related to the not assigned weight loss from 206 to 275 ºC.

The TG/DTG results in combination with the XRD and XRF results were used to estimate the chemical composition of TUN, as shown in Table 4. The TG/DTG results allow an approximate percentage of compounds that decomposed thermally up to 1400 ºC, the XRF results were used to calculate the remaining composition, and finally, the XRD results enables the recognition of the chemical compounds that were decomposed thermally during the TG/DTG tests. Although the presence of sulphates is not determined by XRD (see Fig. 4), its presence is interpreted in the previous TG/DTG analysis with a weight loss of 0.723 % above 1100 °C (see Fig. 5). The TUN analysis results point out that the main compound obtained is MgO. Besides, the presence of $Mg(OH)_2$ is attributed to a hydration process on the surface of MgO particles of TUN that occurs due to atmospheric exposure during the conditioning process. The presence of $Mg(OH)_2$ does not interfere with the development of MPC-TUN. The crystalline phases containing Si do not decompose below 1400 ºC, for this reason they are not indicated per separate in Table 4, included as other compounds (15.54 wt%) as well as the spinel phase determined by XRD (see Fig. 4).

Table 4
Estimated composition of TUN by means of XRD-TG/DTG-XRF.

Compounds	MgO	$Mg(OH)_2$	CaO	$CaMg_{0.27}Fe_{0.73}(CO_3)_2$	$CaSO_4$	$CaCO_3$	$Ca(OH)_2$	Others
wt%	61.42	6.90	6.05	5.27	2.51	1.27	1.04	15.54

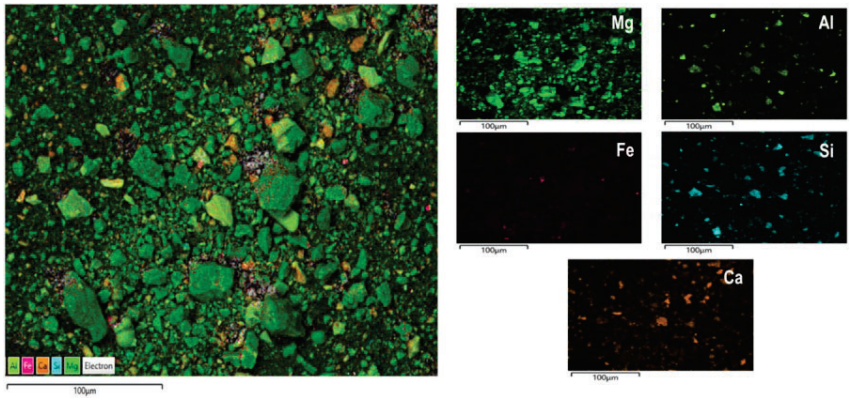

Fig. 6. SEM-EDS of TUN (x450). General elemental mapping (left) and the elemental mapping (right).

Table 5
Density values of MPC-TUN.

Fresh bulk density	Bulk density Day 7	Bulk density Day 28
	$kg \cdot m^{-3}$	
1920 ± 0.01	1840 ± 0.01	1760 ± 0.01

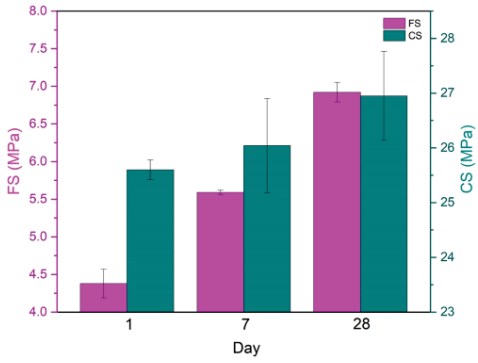

Fig. 7. Mechanical properties of MPC-TUN.

In addition, the SSA of the raw material was 3.57 $m^2 \cdot g^{-1}$. The SSA determined by BET analysis indicates that TUN exhibits a very low reactivity in terms of surface area. PSD analysis revealed that 10 % of particles (d_{10}), 50 % of particles (d_{50}), and 90 % of particles (d_{90}) were below 0.72 μm, 3.31 μm, and 7.85 μm, respectively. TUN CART result is greater than 900 s, which classifies the waste as dead-burned MgO, with low reactivity. Pure MgO exhibits high reactivity and tends to agglomerate when used in the development of MPC, resulting in poor workability of the paste and a non-homogeneous material. Therefore, pure MgO needs to undergo precalcination processes to obtain a suitable reactivity. However, the low reactivity of TUN, as far as we know, can be advantageous for the effective development of MPC. This characteristic helps minimize the environmental impact as it eliminates the need for precalcination, leading to a reduction in energy consumption during the manufacturing process [14].

Fig. 6 presents the SEM-EDS elemental mapping of TUN particles. The micrograph shows a high dispersion of particles with varying sizes, consistent with the results obtained from the PSD analysis. In addition, the particles present an angular shape due to the grinding process in the conditioning stage. In relation to elemental mapping, the main element is Mg, but it is also possible to observe others such as Al, Fe, Si, and Ca. These elements agree with the above-mentioned crystalline phases determined by XRD, mainly originating from silicon oxide, ankerite, forsterite, monticellite, spinel, and merwinite.

3.2. MPC-TUN characterization

The density values of MPC-TUN are shown in Table 5. As the curing time progresses, the density of TUN-MPC decreases, which is attributed to an increase in porosity resulting from the release of water during the drying process [24].

The mechanical characterization results, in terms of FS and CS of the formulation tested after 1, 7, and 28 days are shown in Fig. 7. An increasing trend in FS and CS results is observed with the curing time. The FS and the CS after 28 days of curing are approximately 7 and 27 MPa, respectively. It is essential to understand that the difference between the CS results of the preliminary study and the final formulation is due to the difference in sample size, as well as the shape of the samples, which directly impact the results. It should be mentioned that as the curing days increase, both FS and CS results show higher values. However, the increase is more pronounced in the FS test compared to the CS test, which can be attributed to the nature of each test and the porosity of the samples. These findings are consistent with previously reported mechanical results for MPCs formulated with similar waste and/or by-products [25]. Other studies with different by-products of MgO, such as low-grade magnesium oxide (LG-MgO), achieved similar responses with same specimen size. These findings suggest that the use of LG-MgO and similar by-products could be relevant for specific construction applications [17].

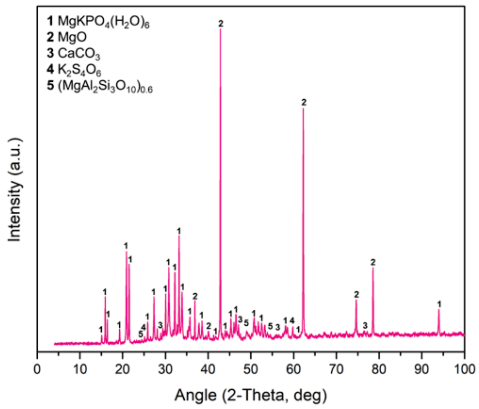

Fig. 8. XRD MPC-TUN.

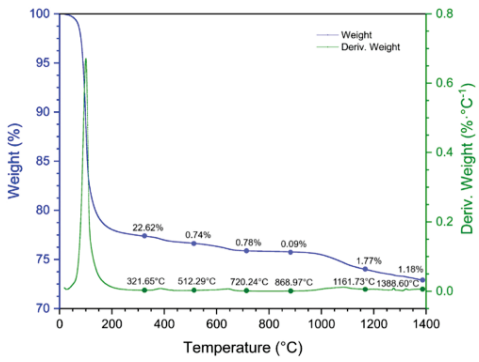

Fig. 9. TG/DTG MPC-TUN.

The XRD results are shown in Fig. 8, which confirms that the K-struvite ($MgKPO_4(H_2O)_6$, 01-075-1076) is the majority phase, but also other minor phases, such as unreacted magnesium oxide (MgO, 01-078-0430), carbonates ($CaCO_3$, 01-081-2027), potassium sulphate ($K_2S_4O_6$, 00-002-0441), and aluminosilicates ($(MgAl_2Si_3O_{10})_{0.6}$, 01-073-2337) are identified as a compatible crystalline phases. K-struvite is detected in different 2-Theta degrees, the most significant is located at 20.8° [26]. Although in Fig. 4 the aluminosilicates are not observed, due to the high number of phases, they are derived from the TUN as can be visualised in the SEM-EDS analysis of TUN shown in Fig. 6.

The TG/DTG characterization of the cement at 28 days is shown in

Table 6
Estimated composition of MPC-TUN by means of XRD-TG/DTG.

Compounds	$MgKPO_4$ $(H_2O)_6$	$CaCO_3$	$CaSO_4$	Mg $(OH)_2$	$CaMg_{0.27}Fe_{0.73}$ $(CO_3)_2$	Others
wt%	55.76	4.21	2.51	2.39	1.83	33.3

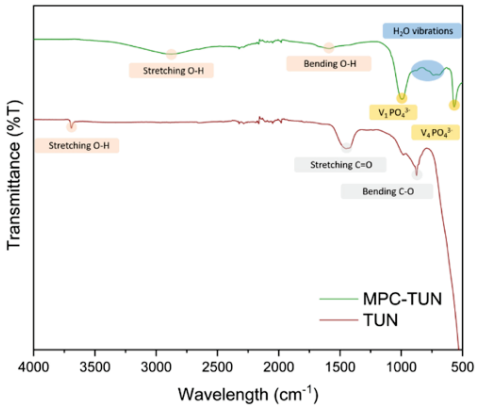

Fig. 10. FT-IR of TUN and MPC-TUN.

Fig. 9. Thermogravimetric analysis confirmed the presence of K-struvite, which has a dehydration temperature from 105 to 136 °C [27,28]. However, it is possible to identify other non-reactive phases from raw materials. The TG/DTG results revealed the following mass losses and temperature ranges of decomposition: a loss of 22.62 wt% between 25 and 322 °C, attributed to the loss of water from K-struvite; a loss of 0.74 wt% between 322 and 512 °C, attributed to the loss of water from $Mg(OH)_2$ decomposition; and other losses were attributed to the decomposition of carbonates [29,30]. Therefore, the XRD-TG/DTG results show the formation of K-struvite; hence, the MPC was successfully developed. Specifically, the estimated amount of K-struvite in the MPC-TUN is 55.76 wt%, as shown in Table 6. But it also shows the presence of other phases and an increase of the amount of $CaCO_3$ compared to the amount present in TUN, which may be indicative of possible carbonation.

FT-IR spectrum of TUN and MPC-TUN are shown in Fig. 10. On the one hand, TUN spectrum shows the presence of a peak related to the Mg–O vibration (850–600 cm^{-1}) [31]. The peaks around 3700 cm^{-1}, 1450 cm^{-1}, and 870 cm^{-1} are associated with the O–H stretching vibration, with the C═O stretching vibration and with the bending vibration of C–O related to carbonates, respectively [32–34]. The –OH group is attributed to the $Mg(OH)_2$ previously identified in XRD analysis [32]. On the other hand, in the case of MPC-TUN after 28 days of curing, the characteristic bands of K-struvite can be observed in Fig. 10. The phosphate (PO_4^{3-}) peak in K-struvite appears between 1000 and 1200 cm^{-1} [35–37]. Besides, the asymmetrical deformation of PO_4^{3-} is located at 1000 cm^{-1} and the symmetrical one is identified at 575 cm^{-1} [38]. The peaks located around 2900 cm^{-1} and 2300 cm^{-1} are associated to the H–O–H stretching of crystallization water molecules. The peak located around 1700 cm^{-1} corresponds to the H–O–H bending modes of vibrations [33,38]. The Mg–O bond peak is located around 600 cm^{-1} and the vibrations of coordinated water are at 750 cm^{-1} [36, 37,39].

Table 7 shows the leaching results and the regulatory limits following the European Commission legislation (Directive 2018/850). Also, the results of the duplicates and the limits are shown in Table 7. The analysis shows that TUN would be accepted in landfills but it would be classified as non-hazardous waste, as Se exceeds the established limit, but the other metal(oid)s are classified as inert waste. In the case of MPC-TUN, after its useful life, it should be managed as hazardous waste, because the Se concentration is quite above the threshold limit. Note that Mo and Sb should be classified as non-hazardous. To reduce the Sb content, a pH reduction would be convenient (around pH=10) to avoid Sb (V) compounds precipitation. It should be noted that the concentrations of all the other metal(oid)s are classified as inert. The trend of increasing concentrations of Mo, Sb, and Se in relation to the raw material has been also observed in other studies involving MPCs developed with various waste and industrial by-products, including LG-MgO [25]. In the coming future, research should be conducted to investigate the internal reaction of these cements and determine the chemical response to this trend.

Fig. 11 shows the different morphology and microstructure of MPC-TUN samples. The surface shows the non-reactive particles are

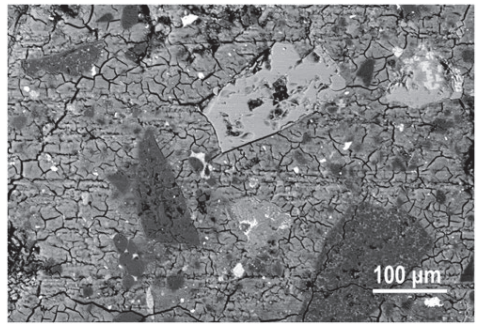

Fig. 11. Backscattered electron micrograph obtained by SEM of MPC formulated with TUN polished sample (x200).

Table 7
Leachates in water following the EN 12457–2 standard.

Sample		mg·kg^{-1}											
	pH	As	Ba	Cd	Cr	Cu	Hg	Mo	Ni	Pb	Sb	Se	Zn
TUN	12.54	< 0.010	2.201	< 0.020	0.019	0.052	< 0.010	0.286	0.032	< 0.050	0.014	0.489	< 0.100
MPC-TUN	11.28	0.411	< 0.050	< 0.020	< 0.050	< 0.050	< 0.010	1.804	< 0.050	< 0.050	0.092	0.989	< 0.100
Limits according to the EN 12457–2													
Inert limit	-	0.5	20	0.04	0.5	2	0.01	0.5	0.4	0.5	0.06	0.1	4
Non-hazardous limit	-	2	100	1	10	50	0.2	10	10	10	0.7	0.5	50
Hazardous limit	-	25	300	5	70	100	2	30	40	50	5	7	200

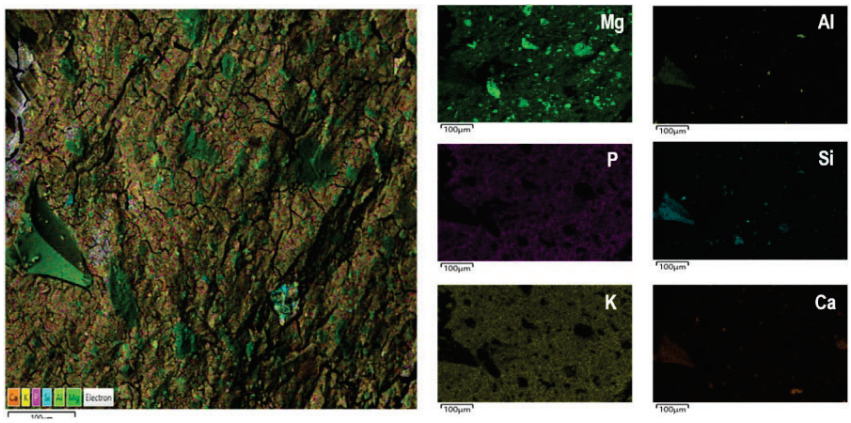

Fig. 12. MPC-TUN SEM-EDS general elemental mapping (left) and the elemental mapping (right) (x200).

embedded in the cementitious matrix. Likewise, the SEM micrograph allows for the observation of microcracking produced by water evaporation during the exothermic setting and curing period. Fig. 12 presents the EDS elemental mapping of MPC-TUN, where the expected elements (Mg, K, P, and O) are observed. Therefore, it is verified that a differentiated matrix of K-struvite predominates with non-reactive nuclei (as can be seen with the green, violet, and yellow colours that refer to magnesium, phosphorus, and potassium, respectively) [29]. Therefore, it is possible to identify the cementitious matrix with the representative morphology of K-struvite by embedding the non-reactive phases from the TUN providing adequate cohesion. On the left side of the Fig. 12, is possible to see a non-reactive particle which is assigned to calcium aluminosilicate particle.

4. Conclusions

In this study, an experimental investigation of MPC-TUN is developed. The results verify that is feasible to formulate MPC-TUN using TUN as raw material. This implies the valorisation of the waste contributes to the evaluation of a potential method for its recovery and reduces its shipment to landfill. Therefore, this valorization can contribute to the sustainability of the planet and promote a future, with a smaller environmental footprint, following the goals of sustainable development.

The results of the study show that TUN is a magnesium oxide-rich waste with adequate reactivity for developing MPC. Therefore, it is a suitable residue for its use as a source of MgO. It is important to highlight that the use of TUN instead of pure MgO promotes the circular economy by reducing CO_2 emissions. Furthermore, K-struvite is successfully obtained using TUN as raw material. Subsequently, it is possible to confirm the correct formulation of an MPC. The microstructure analyses evidence that the main product is the K-struvite matrix, although other non-reactive phases from TUN are identified in the cementitious matrix.

Finally, it is crucial to emphasize that the present study opens up an opportunity to formulate a new alternative cement that can be utilized in various applications within the field of construction. Moreover, the CS performance (~27 MPa at 28 days) suggests its potential use for applications such as cobblestones and street furniture, among other prefabricated materials. In addition, after its service life could be accepted in landfills classified as hazardous waste. Future investigations should be focused on the durability study and the life cycle assessment (LCA) of the MPC-TUN to verify its potential application.

Funding

This work is supported by the Spanish Government with the Grant PID2021-125810OB-C21 funded by MCIN/AEI/10.13039/501100011033 and by "ERDF A way of making Europe". Furthermore, the Agència de Gestió d'Ajuts Universitaris i de Recerca (AGAUR) contributed through Ms A. Alfocea-Roig's PhD grant (FI-DGR 2021). This work is also partially supported by Magnesitas Navarras, S.A. (FBG312160).

CRediT authorship contribution statement

A. Alfocea-Roig: Data curation, Formal analysis, Investigation, Writing - original draft. **S. Huete-Hernández**: Conceptualization, Resources, Visualization, Investigation, Writing - review & editing. **Í .X. García-Zubiri**: Resources, Visualization, Writing - review & editing. **J. Giro-Paloma**: Conceptualization, Visualization, Supervision, Writing - review & editing. **J. Formosa**: Conceptualization, Visualization, Supervision, Methodology, Writing - review & editing, Funding acquisition.

Declaration of Competing Interest

The authors declare that they have no known competing financial interests or personal relationships that could have appeared to influence the work reported in this paper.

Data availability

Data will be made available on request.

Acknowledgments

The authors would like to thank Magnesitas Navarras, S.A. company for material supply. Dr. Jessica Giro-Paloma is a Serra Húnter Fellow. The authors would like to thank the Catalan Government for the quality accreditation given to their research group DIOPMA (2017 SGR 0118, 2021 SGR 00708). DIOPMA is a certified agent TECNIO in the category of technology developers from the Government of Catalonia.

References

[1] 5REFRACT, Systematic and integral valorization of refractories under the "5R" approach, 2018. ⟨http://www.conama.org/conama/download/files/conama2018/CT2018/1222224770.pdf⟩.
[2] F. Mora, Revestimiento refractario en horno de solera galopante, Universidad Carlos III de Madrid (UC3M), 2008. ⟨http://hdl.handle.net/10016/10746⟩.
[3] D. Mazumdar, Review, analysis, and modeling of continuous casting tundish systems, Steel Res. Int. 90 (2019) 1–14, https://doi.org/10.1002/srin.201800279.
[4] D. Blengini Gian Andrea, El. Latunussa Cynthia, Eynard Umberto, Torres De. Matos Cristina, Wittmer Dominic, Georgitzikis Konstantinos, Pavel Claudiu, Carrara Samuel, Mancini Lucia, Unguru Manuela, Blagoeva Darina, Mathieux Fabrice Pennington, Study on the EU's list of Critical Raw Materials (2020), Eur. Com. (2020), https://doi.org/10.2873/867993.
[5] J. Madías, Reciclado de materiales refractarios utilizados en la siderurgia, Acero Lat. (2010) 46–55. ⟨https://www.academia.edu/31032934/Reciclado_de_materiales_refractarios_utilizados_en_la_siderurgia⟩.
[6] M. Musmeci, N.M. Rendtorff, L. Musante, L. Martorello, Characterization of MgO-based tundish working lining materials, microstructure and properties, Ceram. Int. 40 (2014) 14091–14098, https://doi.org/10.1016/j.ceramint.2014.05.138.
[7] EU project REFRASORT, How to turn refractory waste back into raw materials, Innov. Sep. Technol. High Grade Recycl. Refract. Waste Using Non Destr. Technol. (2016). ⟨https://cordis.europa.eu/article/id/197342-how-to-turn-refractory-waste-back-into-raw-materials/es⟩.
[8] THE COUNCIL OF THE EUROPEAN UNION, Directive 1999/31/EC on the landfill of waste, (1999).
[9] THE COUNCIL OF THE EUROPEAN UNION, Directive 2008/98/EC on waste, (2008) 3–30.
[10] R. Maddalena, J.J. Roberts, A. Hamilton, Can Portland cement be replaced by low-carbon alternative materials? A study on the thermal properties and carbon emissions of innovative cements, J. Clean. Prod. 186 (2018) 933–942, https://doi.org/10.1016/j.jclepro.2018.02.138.
[11] A. Naqi, J.G. Jang, Recent Progress in green cement technology utilizing low-carbon emission fuels and raw materials: a review, Sustainability 2 (2019), https://doi.org/10.3390/su11020537.
[12] U. Nations, Sustainable Development Goals, 17 Goals to Transform Our World. (2015). ⟨https://www.un.org/sustainabledevelopment/⟩.
[13] B. Xiao, Y. Chen, Q. Fang, Z. Ding, Research progresses on magnesium phosphate cement-based composites: a review, Gongneng Cailiao/J. Funct. Mater. 51 (2020) 885–898, https://doi.org/10.3969/j.issn.1001-9731.2020.08.002.
[14] S.A. Walling, J.L. Provis, Magnesia-based cements: a journey of 150 years, and cements for the future? Chem. Rev. 116 (2016) 4170–4204, https://doi.org/10.1021/acs.chemrev.5b00463.
[15] M. Le Rouzic, T. Chaussadent, G. Platret, L. Stefan, Mechanisms of k-struvite formation in magnesium phosphate cements, Cem. Concr. Res. 91 (2017) 117–122, https://doi.org/10.1016/j.cemconres.2016.11.008.
[16] Y. Liu, Z. Qin, B. Chen, Experimental research on magnesium phosphate cements modified by red mud, Constr. Build. Mater. 231 (2020), https://doi.org/10.1016/j.conbuildmat.2019.117131.
[17] S. Huete-Hernández, A. Maldonado-Alameda, J. Giro-Paloma, J.M. Chimenos, J. Formosa, Fabrication of sustainable magnesium phosphate cement micromortar using design of experiments statistical modelling: Valorization of ceramic-stone-porcelain containing waste as filler, Ceram. Int. 47 (2021) 10905–10917, https://doi.org/10.1016/j.ceramint.2020.12.210.
[18] M. Riaz, B. Chen, J. Yu, A comprehensive study of basalt fiber reinforced magnesium phosphate cement incorporating ultra fine fly ash, Composites 168 (2019) 204–217, https://doi.org/10.1016/j.compositesb.2018.12.065.
[19] M.A. Haque, B. Chen, Research progresses on magnesium phosphate cement: a review, Constr. Build. Mater. 211 (2019) 885–898, https://doi.org/10.1016/j.conbuildmat.2019.03.304.
[20] Y. Su, J. Yang, D. Liu, S. Zhen, N. Lin, Y. Zhou, Effects of municipal solid waste incineration fly ash on solidification/stabilization of Cd and Pb by magnesium potassium phosphate cement, J. Environ. Chem. Eng. 4 (2016) 259–265, https://doi.org/10.1016/j.jece.2015.11.025.
[21] GCCA, Global Cement and Concrete Association, GCCA 2050 Cem. Concr. Ind. Roadmap Net Zero Concr. (2021). ⟨https://gccassociation.org/concretefuture/⟩.
[22] L.P. Iñigo X. García-Zubiri, Mikel Arandigoyen, Roiner Racedo, Presen Amezketa, Marcelo Lagier, Luciano Disante, Mariano Comas, Silvia Murialdo, Coldmag ®, the easy way to cast, in: Jorn. Mater. Refract. '11 - Refract. Mater. Semin. '11 IAS, 2011, Rosario, Santa Fe, Argentina., 2011. ⟨https://www.magnesitasnavarras.es/wp-content/uploads/coldmag_paper_english.pdf⟩.
[23] J. Formosa, J.M. Chimenos, A.M. Lacasta, M. Niubó, Interaction between low-grade magnesium oxide and boric acid in chemically bonded phosphate ceramics formulation, Ceram. Int. 38 (2012) 2483–2493, https://doi.org/10.1016/j.ceramint.2011.11.017.
[24] A. Maldonado-Alameda, A.M. Lacasta, J. Giro-Paloma, J.M. Chimenos, L. Haurie, J. Formosa, Magnesium phosphate cements formulated with low grade magnesium oxide incorporating phase change materials for thermal energy storage, Constr. Build. Mater. 155 (2017) 209–216, https://doi.org/10.1016/j.conbuildmat.2017.07.227.
[25] S. Huete-Hernández, A. Maldonado-Alameda, A. Alfocea-Roig, J. Giro-Paloma, J. M. Chimenos, J. Formosa, Sustainable magnesium phosphate micromortars formulated with PAVAL® alumina by-product as micro-aggregate, Bol. La Soc. Esp. Ceram. Y. Vidr. (2023) 1–15, https://doi.org/10.1016/j.bsecv.2023.02.001.
[26] Y.J. Du, M.L. Wei, K.R. Reddy, F. Jin, H.L. Wu, Z.Bin Liu, New phosphate-based binder for stabilization of soils contaminated with heavy metals: leaching, strength and microstructure characterization, J. Environ. Manag. 146 (2014) 179–188, https://doi.org/10.1016/j.jenvman.2014.07.035.
[27] H. Lahalle, C. Patapy, M. Glid, G. Renaudin, M. Cyr, Microstructural evolution/durability of magnesium phosphate cement paste over time in neutral and basic environments, Cem. Concr. Res. 122 (2019) 42–58, https://doi.org/10.1016/j.cemconres.2019.04.011.
[28] B. Xu, B. Lothenbach, A. Leemann, F. Winnefeld, Reaction mechanism of magnesium potassium phosphate cement with high magnesium-to-phosphate ratio, Cem. Concr. Res. 108 (2018) 140–151, https://doi.org/10.1016/j.cemconres.2018.03.013.
[29] O. Mgkpo, L.J. Gardner, S.A. Walling, S.M. Lawson, S. Sun, S.A. Bernal, C. L. Corkhill, J.L. Provis, D.C. Apperley, D. Iuga, J.V. Hanna, N.C. Hyatt, Characterization of and Structural Insight into Struvite-K, Inorg. Chem. 4 (2021).
[30] D. Dollimore, S. Lerdkanchanaporn, Thermal Analysis, William Andrew Publishing/Noyes Publications, 1998, https://doi.org/10.1021/a19800038.
[31] G. Balakrishnan, R. Velavan, K. Mujasam Batoo, E.H. Raslan, Microstructure, optical and photocatalytic properties of MgO nanoparticles, Results Phys. 16 (2020), 103013, https://doi.org/10.1016/j.rinp.2020.103013.
[32] M.H. Zahir, M.M. Rahman, K. Irshad, M.M. Rahman, Shape-stabilized phase change materials for solar energy storage: MgO and $Mg(OH)_2$ mixed with polyethylene glycol, Nanomaterials 9 (2019) 1–21, https://doi.org/10.3390/nano9121773.
[33] Y. Yuanquan, Z. Guanhua, G. Jinbo, Q. Dingwen, L. Runqing, An insight into the thermal properties of struvite-k by Rietveld refinement method, J. Mater. Res. Technol. 24 (2023) 3683–3690, https://doi.org/10.1016/j.jmrt.2023.04.032.
[34] P. Makreski, G. Jovanovski, Minerals from Macedonia. Distinction between some rhombohedral carbonates by FT-IR spectroscopy, Bull. Chem. Technol. Maced. (2003).
[35] V.B. Suryawanshi, R.T. Chaudhari, Synthesis and Characterization of Struvite-k Crystals by Agar Gel, J. Cryst. Process Technol. 04 (2014) 212–224, https://doi.org/10.4236/jcpt.2014.44026.
[36] A. Siciliano, C. Limonti, Is K-Struvite precipitation a plausible nutrient recovery method from potassium-containing wastes?—A review, Sustainability (2022), https://doi.org/10.3390/su141811680.
[37] P. Zhang, W.P. Liu, T.L. Zhao, Q.Z. Yao, H. Li, S.Q. Fu, G.T. Zhou, Biomineralization of struvite by Shewanella oneidensis MR-1 for phosphorus recovery: Cr(VI) effect and behavior, J. Environ. Chem. Eng. 10 (2022) 1–9, https://doi.org/10.1016/j.jece.2021.106923.
[38] R.C. de, S. Meira, S.P.A. da Paz, J.A.M. Corrêa, XRD-Rietveld analysis as a tool for monitoring struvite analog precipitation from wastewater: P, Mg, N and K recovery for fertilizer production, J. Mater. Res. Technol. 9 (2020) 15202–15213, https://doi.org/10.1016/j.jmrt.2020.10.082.
[39] N.K. Nga, N.T. Thuy Chau, P.H. Viet, Preparation and characterization of a chitosan/MgO composite for the effective removal of reactive blue 19 dye from aqueous solution, J. Sci. Adv. Mater. Devices 5 (2020) 65–72, https://doi.org/10.1016/j.jsamd.2020.01.009.

3.1.4. Additional research contribution

Additional measurements, not included in the publication, were performed to analyse K-struvite formation and complement the material's investigation. The nomenclature used aligns with that stablished in *Publication 1*.

Fourier transform infrared spectroscopy in attenuated total reflectance mode (FTIR-ATR) was performed using the PerkinElmer Spectrum Two™ instrument to analyse symmetric and asymmetric stretching vibration bonds during setting. The Top Plate SP2 UATR Arrow device was used for the analysis, covering a spectral range from 4000 to 450 cm^{-1} with a resolution of 4 cm^{-1}. Each spectrum was obtained by averaging 4 scans, with a total of 1008 spectra collected over 360 minutes, at approximately 15-second intervals between scans. The time evolution of the collected FTIR-ATR spectra, showed in Figure 3.3 illustrates the emergence of the main phosphate group vibrations as the cement reaction progresses. The results indicate that the primary phosphate vibrations (1200-800 cm^{-1}) become apparent in the later stages of the experiment's initiation [7–9]. Specifically, four characteristic peaks associated with phosphates were identified: the first, between 404–470 cm^{-1}, corresponds to the symmetric bending vibration of PO_4^{3-}; the second, at 509–554 cm^{-1}, is related to asymmetric bending modes; the third, from 930–995 cm^{-1}, is attributed to the symmetric stretching vibration of PO_4^{3-} units; and the final peak, between 1017 and 1163 cm^{-1}, is associated with the asymmetric stretching vibration of PO_4^{3-} units [10,11]. In addition, it was observed that over time, the intensity of the vibration bands associated with water increased, particularly the H-O-H stretching vibrations of water near 3000 cm^{-1}.

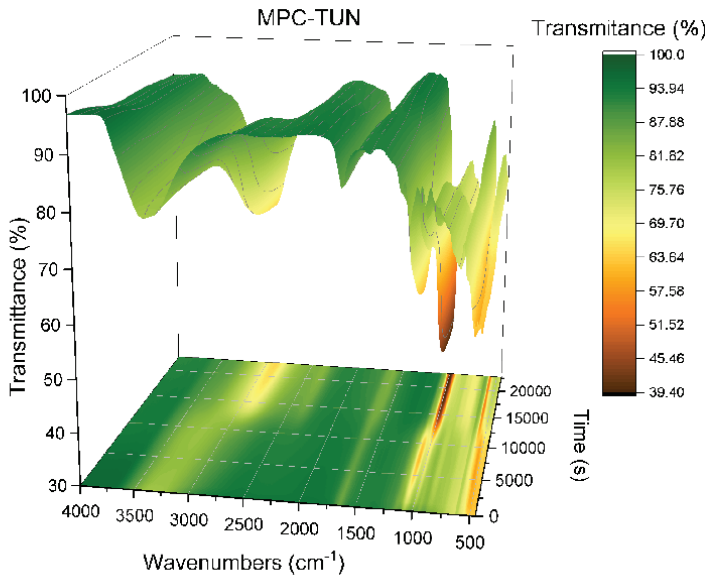

Figure 3.3. Time evolution of the FTIR-ATR signal for the MPC-TUN sample.

3.2. Mortar

3.2.1. Introduction

Cement is a fundamental material in construction, serving for infrastructure development. Key applications include mortar and concrete, which are integral to the construction and/or building sectors [12]. Mortar, a mixture of cement, sand, and water, is highly versatile and plays a crucial role in various applications [13]. The proportions of its components, the preparation process, and the selection of raw materials enable the formulation of mortars with specific properties and versatile characteristics tailored to diverse uses [14]. In order to ensure the optimal performance in practical applications, a critical factor is the precise definition of component proportions and adherence to a standardized mixing protocol [15].

The increasing environmental concerns and increased awareness of industrial pollution have prompted the search for innovative, sustainable materials that reduce reliance on conventional resources [16,17]. A promising approach to lower the environmental impact of construction materials involves incorporating wastes into the development of alternative mortars. Consequently, the second investigation in this PhD focused on developing mortars based on MPC, utilizing TUN as a magnesium oxide source to obtain an alternative binder.

The primary objectives of this research were to determine the optimal water-to-cement (W/C) ratio and to characterize different formulations by contributing to the knowledge of this material through detailed analyses. This study successfully demonstrated the feasibility of developing MPC-TUN mortars, as the K-struvite matrix was consistently formed across different formulations. Test conducted on these formulations primarily focused on chemical characterisation techniques, such as XRD and FTIR-ATR, to confirm the formation of K-struvite and secondary reaction products. Furthermore, a comprehensive evaluation of both fresh and hardened states of the mortars was carried out using various characterization techniques. Key parameters assessed included density, physicochemical properties, isothermal calorimetry, and

leaching behaviour, among others. The following section provides a concise overview and summary of the main findings from this study.

3.2.2. Relevance

Understanding the material and determining its dosage and optimal composition is fundamental and crucial for this study. The originality of this research was based on the investigation of various W/C ratios to demonstrate the feasibility of formulating MPC-TUN binders for non-structural mortars. Figure 3.4 summarizes the key findings of this research on the development of MPC-TUN mortars. As a result, this research highlights the potential of various mixtures in the construction and/or building sectors, providing valuable insights into the properties of MPC-TUN to advance its understanding and practical applications. Moreover, the development of these mortars represents an innovative approach to waste valorisation, enabling the integration of alternative, sustainable materials into the construction industry sector.

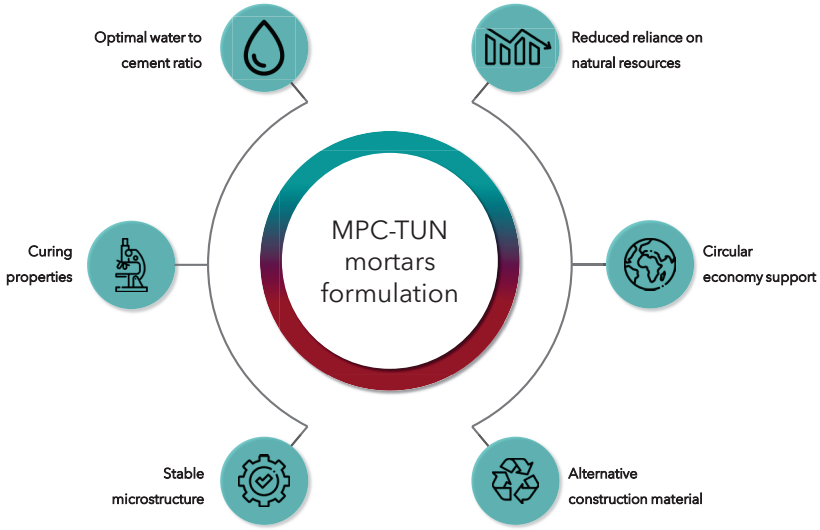

Figure 3.4. Advantages of research on the development of MPC-TUN mortars.

3.2.3. Publication 2

Publication 2, titled "Tundish deskulling waste as a source of MgO for producing Magnesium Phosphate Cement-based mortars: advancing sustainable construction materials", is currently under review in the journal of Materials Today Sustainability (JIF of 7.1 in 2023, Q1), submitted on December 4th 2024. The publication's title is presented in Figure 3.5, and the complete text is included in the manuscript.

Materials Today Sustainability

Tundish deskulling waste as a source of MgO for producing Magnesium Phosphate Cement-based mortars: advancing sustainable construction materials

--Manuscript Draft--

Manuscript Number:	
Article Type:	Research Paper
Keywords:	Circular economy; refractory waste, magnesium phosphate cement, mortars, alternative construction materials
Corresponding Author:	Joan Formosa Universitat de Barcelona Barcelona, SPAIN
First Author:	Anna Alfocea-Roig, PhD student
Order of Authors:	Anna Alfocea-Roig, PhD student
	David Vera-Rivera, PhD student
	Sergio Huete-Hernández, Ph.D.
	Jessica Giro-Paloma, Ph.D.
	Joan Formosa, Ph.D.

Figure 3.5. Headline of the article under review in the journal Materials Today Sustainability, entitled "Tundish deskulling waste as a source of MgO for producing Magnesium Phosphate Cement-based mortars: advancing sustainable construction materials".

Tundish deskulling waste as a source of MgO for producing Magnesium Phosphate Cement-based mortars: advancing sustainable construction materials

A. Alfocea-Roig[1], D. Vera-Rivera[1], S. Huete-Hernández[1], J. Giro-Paloma[1], J. Formosa[1*]

[1]Departament de Ciència de Materials i Química Física, Universitat de Barcelona, Martí i Franquès 1-11, 08028, Barcelona, Spain.

Ph: +34-934021316

*Corresponding author

E-mail address: joanformosa@ub.edu

ABSTRACT

Currently, the cement industry stands as one of the sectors with the most significant environmental impact, primarily due to its substantial greenhouse gas emissions and energy consumption. To mitigate this impact, a roadmap has been followed in recent years, outlining a set of objectives aimed at diminishing the environmental footprint of the construction industry. This research focuses on the development of mortars with different water/cement ratio employing an alternative cement, specifically magnesium phosphate cement (MPC) formulated with secondary sources. The goal of this research relays in developing mortars based on MPC by using a waste from the metallurgical industry, named tundish deskulling waste (TUN), as a MgO source. The results revealed the optimal water/cement (W/C) ratio for MPC-TUN mortars production through the assessment of various characterisation techniques, which was 0.55. This ratio resulted in the highest compressive strength after 28 days of curing and the formation of a stable K-struvite matrix. Furthermore, it demonstrated the effectiveness of aluminium sulphate in preventing efflorescence caused by carbonates. The development of alternative masonry mortars for application in building materials represents a significant stride towards advancing the principles of a circular economy, in alignment with the objectives laid out in the 2030 roadmap.

KEYWORDS

Circular economy; refractory waste, magnesium phosphate cement, mortars, alternative construction materials.

1. INTRODUCTION

Currently, cement is one of the most widely used materials worldwide, serving as the primary component in the production of mortars and concrete. The cement industry consumes 2% of global energy consumption and 5% of industrial electrical uses [1,2].To mitigate its environmental impact to promote a future carbon-neutral cement, exploring alternative cements developed with secondary sources are a viable approach [1,3–6]. One of the possible alternative materials includes the Magnesium Phosphate Cements (MPCs) which belong to the Chemically Bonded Ceramics (CBCs) family and are specifically classified under Chemically Bonded Phosphate Cements (CBPCs) [1,3–

5,7–9]. To obtain MPCs, it is necessary to initiate a reaction between a magnesium oxide source and a phosphate salt in a water medium. In this research, the developed MPCs were obtained by mixing MgO and MKP (KH_2PO_4). The reaction takes place in an acid-base reaction between MgO and KH_2PO_4, resulting in the formation of K-struvite ($MgKPO_4 \cdot 6H_2O$) [10–12]. When examining the setting reaction steps of MPCs, they can be divided into five primary stages, as illustrated in Figure 1 [10,13]:

A) Dissolution of MgO particles: in the initial step, MgO particles react with water, dissolving into Mg^{2+} and 2 OH^- ions.
B) Formation of aquosols: cations can react with water to form positively charged species, such as $[Mg{\leftarrow}OH_2]^{2+}_{(aq)}$.
C) Acid-Base reaction and condensation: in this step, the magnesium phosphate forms and subsequently condenses to produce the initial particle aggregates.
D) Gel formation and percolation: the newly formed salt particles interact to create a network, which subsequently leads to the formation of a gel.
E) Crystallization: the formation of the gel increases saturation, leading to the creation of crystals.

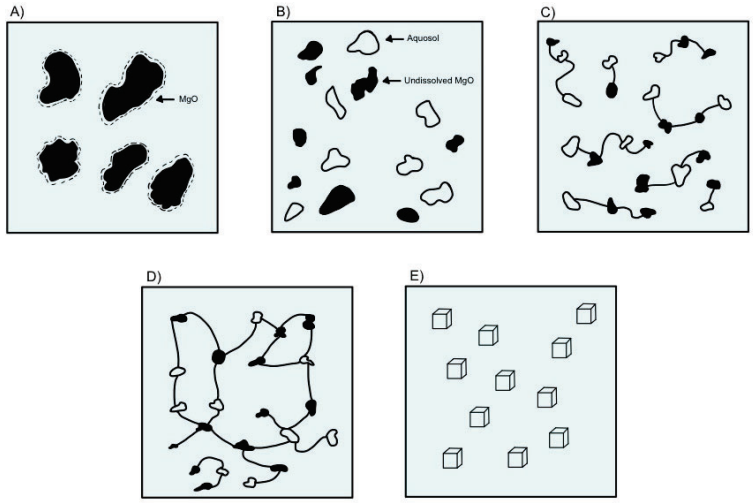

Figure 1. MPC formation (adapted by [14]).

The incorporation of waste materials into MPCs can contribute to a circular economy aligned with the Sustainable Development Goals (SDGs), while also addressing the high energy consumption and CO_2 emissions associated with the use of dead burned magnesite (DBM) by exploring solid waste alternatives as substitutes [15,16]. This practice has been increasingly applied in construction materials in recent years [17] . Common waste materials utilized in the construction industry include

blast furnace slag, steelmaking dust, coal ash, and steel slag, all of which originate from of the steel industry. Steel is one of the most demanded materials worldwide, extensively produced due to its critical role in numerous industries and sectors [18,19]. In the metallurgical industry, the refractory material plays a pivotal function in withstanding high temperatures of melted steel during production processes [20,21]. The tundish mass, which is a refractory material, is an essential component in the steel continuous casting process as it serves as the final vessel to regulate the flow of molten metal into the moulds (Figure 2) [22–26].

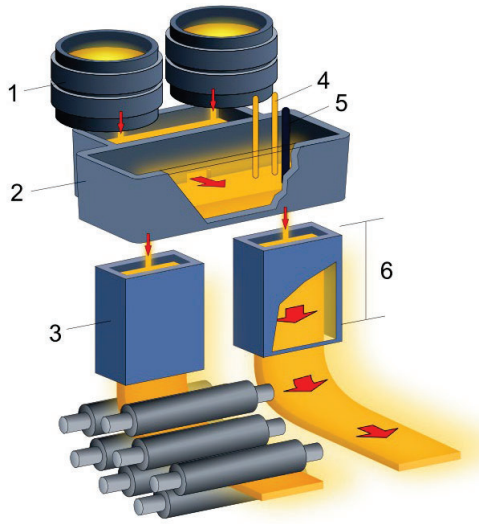

Figure 2. Continuous casting: 1. Ladle; 2. Tundish; 3. Mould; 4. Plasma torch; 5. Stopper; 6. Straight zone.

The service life of the tundish mass relies on several factors, including the operating conditions and the performance characteristics of the material used. After reaching the end of its useful life, it must be replaced with new material, generating a large amount of waste, known as tundish deskulling (TUN), which currently ends up in landfills.

The present research aims to use the industrial waste TUN as a MgO source instead of pure DBM for developing MPC with the objective of promoting the valorisation of this waste and contributing to the circular economy. This study evaluates the use of TUN in MPC as a MgO source for synthesizing alternative mortars, focusing on properties such as mechanical performance, hydration behaviour, and leaching, to determine its suitability for use as a building material [7,22–25,27].

2. MATERIALS AND METHODS

2.1. Materials

TUN was supplied by Magnesitas Navarras, S.A. (Navarra, Spain) after their conditioning processes to obtain the homogeneous non-magnetic fraction with the required particle size. The phosphate source, potassium dihydrogen phosphate (KH_2PO_4), commonly referred to as MKP, was supplied by Norken, S.L. (food grade, 99.8 wt.% purity). Boric acid (H_3BO_3, HB) was supplied by Borax España, S.A.

2.2. TUN characterisation

To determine TUN composition accurately, XRF (X-Ray Fluorescence) and XRD (X-Ray Diffraction) analyses were employed in previous studies published in the literature mortars, showing that it is a suitable component to be used as a source of MgO [23,26]. Additionally, BET analysis determined an SSA of 3.57 $m^2 \cdot g^{-1}$ for the raw material, confirming TUN's low reactivity due to its minimal surface area. PSD results indicated that particle size distribution followed these thresholds: 10% (d_{10}) measured under 0.72 µm, 50% (d_{50}) was below 3.31 µm, and 90% (d_{90}) did not exceed 7.85 µm. To assess the reactivity of this waste material and verify its suitability as an MgO source, a citric acid test was conducted [23,26,28,29]. Depending on its reactivity, MgO can be classified based on its reaction time as follows: soft-burned (below 60 seconds), moderately reactive (between 180-300 seconds), hard-burned (around 600 seconds), and dead-burned (below 900 seconds) [30,31]. This characterisation was executed in the previous studies, and the principal findings of them indicated that TUN is qualified as a MgO-rich waste, and that it possesses an adequate reactivity since it is classified as DBM for the advancement of MPC-TUN mortars [23,26,32].

2.3. Samples preparation

Figure 3 summarises the formulation composition of the mortars developed. The cement (C) formulation consisted of 60 wt.% of TUN and 40 wt.% of MKP, a dosage that has been previously developed in earlier studies by the authors, which has proven to be the most promising formulation [19]. Additionally, 1 wt.% of H_3BO_3 (HB) was incorporated into the total cement content to retard the setting time, thereby counteracting rapid setting and hardening. The aggregate used was sand, added in a 1:3 Cement:Aggregates (C/A) mass ratio. Three different formulations were developed using water/cement ratios (W/C) of 0.55, 0.60, and 0.65 as shown in Figure 3 and Figure 4 during the first trials, efflorescence was detected on the surface of the samples, attributed to the presence of carbonated salts, as shown in Figure 5 [33]. To address this issue, aluminium sulphate (AS, 52-57% $Al_2(SO_4)_3 \cdot 16\text{-}18H_2O$) was incorporated into the mixing water at a concentration of 0.35 M, a method proven effective in preventing efflorescence in the literature [34]. This effectiveness is evident in Figure 4, where no efflorescence is observed. The presence of this efflorescence can lead to a loss of properties in the long-term, such as a reduction of the mechanical strength [34].

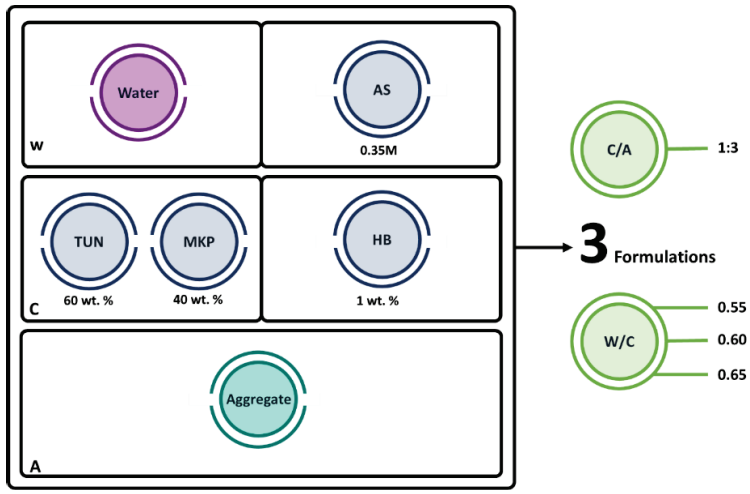

Figure 3. Experimental design.

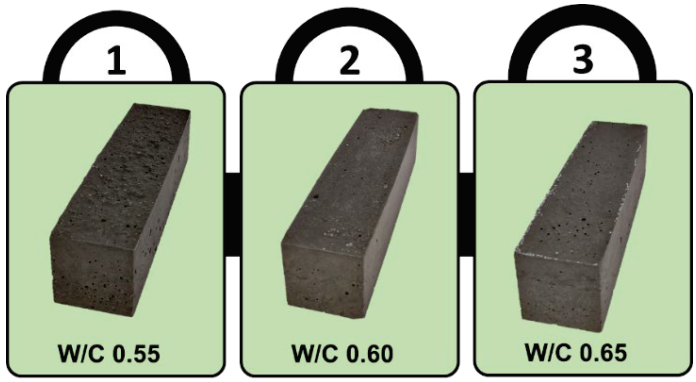

Figure 4. Three formulations developed.

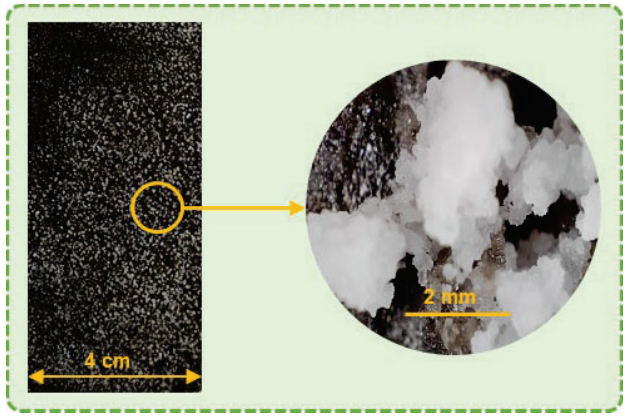

Figure 5. Sample with efflorescence.

The efflorescence was characterised by using XRD, as shown in Figure 6. The main structures observed were carbonates such as Buetschliite ($K_2Ca(CO_3)_2$, 01-070-2051), Dolomite ($MgCa(CO_3)_2$, 01-071-1662) and Magnesite ($MgCO_3$, 01-081-2273), sulphates such as Epsomite ($MgSO_4{\cdot}7H_2O$, 00-036-0419) and Plolyhalite ($K_2Ca_2Mg(SO_4)_4{\cdot}(H_2O)_2$, 01-070-2158), silicates as Magnesium Silicate (Mg_2SiO_4, 01-075-1447), Calcium Silicate (Ca_2SiO_4, 00-003-0753) and Grossular ($Ca_3Al_2Si_3O_{12}$, 01-083-2209), and Magnesium Aluminum Sulfide ($MgAl_2S_4$, 01-077-0289).

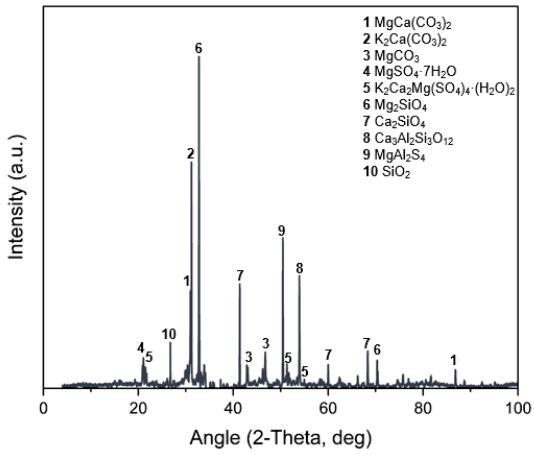

Figure 6. XRD of the efflorescence presents on the surface.

MPC-TUN mortars were cast into prismatic specimens measuring 16 x 4 x 4 cm^3. After 2, 7, and 28 days of curing, three specimens per curing period were tested to ensure reliable results and to comprehensively evaluate the mechanical performance and property evolution of MPC over time. The laboratory conditions were maintained at a constant temperature of 25 ± 1 ºC and a relative humidity (RH) of 50 ± 5% throughout the experimental procedure.

2.4. Characterisation of the MPC-TUN mortars formulations

MPC-TUN mortars were characterised to determine physical, mechanical, chemical, and leaching properties by different techniques, as shown in Table 1, to evaluate their suitability as masonry mortars for building material applications.

In the fresh state, workability was determined using the slump test, following the EN 1015-3 standard. Additionally, apparent density was evaluated according to the EN 1936:2006 standard.

Table 1. Characterisation of MPC-TUN mortars.

	Techniques	MPC-TUN mortars		
Fresh state	Slump test	-	-	-
	Apparent fresh density	-	-	-
	Techniques	**2d**	**7d**	**28d**
Hardened state	Apparent density	✓	✓	✓
	MoE	✓	✓	✓
	CS (σ_c)	✓	✓	✓
	FS (σ_f)	✓	✓	✓
	FTIR-ATR	✓	✓	✓
	XRD	✓	✓	✓
	TG	-	-	✓
	Isothermal Calorimetry	✓	✓	✓
	Leaching tests	-	-	✓
	SEM	-	-	✓

In the hardened state, a mechanical characterisation was performed by evaluating the Modulus of Elasticity (MoE) following the harmonic frequencies method, in accordance with the UNE-EN 12504-4 standard an ultrasonic pulse velocity tester (C368 by Matest, equipped with a 55 kHz transceiver sensor) was used to conduct the test. This approach was employed to ascertain the material's ability to tolerate deformation when subjected to external strength. The experimental procedure involves applying strength perpendicular to the reader and, subsequently, assessing the impulse excitation of vibration and the resulting analysis of the fundamental resonant frequency [35,36]. This measurement facilitates the estimation of MoE, considering the Poisson's coefficient.

Flexural strength (FS or σ_f) and compressive strength (CS or σ_c) were measured following the UNE-EN 196-1 standard using an Incotecnic MULTI-R1 universal testing machine, equipped with a 200 kN load cell. The specimens that were split in half during the flexural test were subsequently used for the compression test. The test speeds for the FS and CS were 5 $kg \cdot s^{-1}$ and 240 $kg \cdot s^{-1}$, respectively.

Chemical and structural characterisation was also carried out specifically to the cement, as the aggregate was previously separated. Fourier-transformed infrared spectroscopy in attenuated total reflectance mode (FTIR-ATR) was employed using the Spectrum Two™ equipment from Perkin Elmer. The data was collected with a resolution of 4 cm^{-1} in the range 4000-450 cm^{-1}. This technique enables the determination of functional groups and chemical bonds in the samples. The analysis through X-ray diffraction (XRD) was conducted using Bragg-Brentano Siemens D-500 powder

diffractometer device with $CuK_{\alpha 1}$ radiation, to determine the mineral and crystalline phases. Afterwards, thermogravimetric analysis (TG) was performed using an SDT Q600 device from TA instruments in an air atmosphere (50 mL·min^{-1}) with a heating rate of 10 ºC·min^{-1} ranging from 30º C to 1100 ºC.

An isothermal conduction calorimetry (ICC) experiment was conducted to evaluate the heat changes that could occur during the initial setting of the mortar, as well as the chemical reaction kinetics. This experiment was performed using an 8-channel TAM-Air calorimeter from TA Instruments. The internal thermostat temperature was maintained at 20 ºC throughout the entire experiment. For this experiment, fresh batches were prepared directly inside the calorimeter. Water was injected into a sealed glass ampoule which contained the mortar formulation, and subsequently mixed using an Ad-Mix system equipped with a stirring rotor and a syringe for liquid injection. Data recording commenced immediately after the injection of water, marking the initial contact with the dry materials and the onset of the reaction. Following this, the paste was mixed for a duration of 180 s, and the heat flow was continuously recorded for a period of 140 h.

The microstructure characterisation was performed through Scanning Electron Microscope (SEM) using EOL JSM-7100F equipment. The samples evaluated were polished and embedded in epoxy resin. SEM and energy-dispersive X-ray spectroscopy (SEM-EDS) were employed to analyse the elemental composition across various sections of the developed MPC-TUN mortars following a curing period of 28 days.

Finally, the environmental characterisation was conducted through leaching tests at 28 days of curing, to evaluate the environmental risk associated with these mortars. This is achieved by quantifying the amount of hazardous elements that are released upon exposure to water. The procedure for this analysis was carried out in following the UNE EN 12457-2 standard using an OVAN RHDE rotator, rotating the containers which contained the mortars samples with a particle size below 4 mm and deionized water, spinning for 24 hours at 40 rpm. The leaching process entails extracting heavy metals from the solids utilizing deionised water at a liquid-to-solid ratio of 10 L·kg^{1}. Following this, the leachate was isolated and filtered utilizing an 0.45 mm pore membrane, then subjected to analysis through Inductively Coupled Plasma mass spectrometry (ICP-MS) using the NexION 350D Perkin Elmer equipment. The metals studied were the subsequent elements: As, Ba, Cd, Cr, Cu, Hg, Mo, Ni, Pb, Sb, Se, V, and Zn.

3. RESULTS AND DISCUSSION

3.1. Slump test

The slump test results are showed in Table 2, revealing that the mixture presents greater workability for the 0.65 formulation, since it has higher amount of water. Nevertheless, the three formulations exhibit closely matched consistencies, differing by less than 10%. This similarity indicates similar behaviours and workability in their fresh state, making them suitable for the same applications.

Table 2. Base expansion of slump test of MPC-TUN mortar formulations.

Formulation	Base width (mm)
0.55	112.53
0.60	120.88
0.65	126.78

3.2. Apparent fresh density

The apparent fresh density exhibits similar values across all three formulations, as depicted in Table 3. The slight variations in the apparent fresh density results, despite a different W/C, are due to the significant impact of the compaction process depending on the consistency of the mortars.

Table 3. Apparent density of each MPC-TUN mortar formulation.

Formulation	Apparent fresh density ($g \cdot cm^{-3}$)
0.55	2.044 ± 0.034
0.60	2.042 ± 0.025
0.65	2.054 ± 0.019

3.3. Apparent density

The calculated density for each formulation reveals a general decrease in density as curing time increases, as shown in Table 4, with the exception of day 7. This trend can be attributed to the evaporation of free water during the curing process, leads to the formation of pores. The exception observed on day 7 may be due to intermediate hydration processes, where some degree of consolidation or ongoing chemical reactions temporarily counterbalance the effects of evaporation.

Table 4. Apparent density of MPC-TUN mortars at different curing ages.

Apparent density (g·cm^{-3})			
Formulation	**2d**	**7d**	**28d**
0.55	2.064 ± 0.005	2.034 ± 0.040	1.954 ± 0.030
0.60	2.024 ± 0.003	2.030 ± 0.020	1.932 ± 0.020
0.65	1.985 0.009	2.150 ± 0.002	1.947 ± 0.010

3.4. Modulus of elasticity, flexural strength, and compressive strength

Figure 7 illustrates the performance of the MoE, demonstrating a decreasing trend as the W/C ratio increases. This trend is associated with a reduction in density and an increase in porosity, attributable to the higher water content in the various formulations. However, concerning curing time, the MoE values show an opposite trend compared to the other mechanical properties (σ_f and σ_c), according to the data provided in Figure 8. This fact could be attributed to the presence of more free water within the structure during the early days of curing. This free water increases the apparent density of the specimen, significantly influencing its vibration during measurement and thereby affecting the results. In contrast, at later stages of curing, the evaporation of this water leads to the formation of a porous network, thereby reducing the density [37].

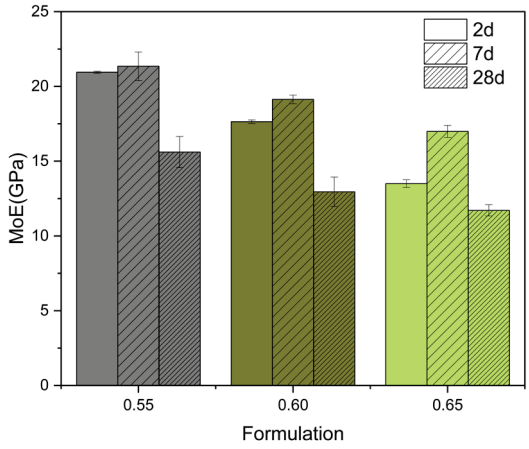

Figure 7. MoE results of MPC-TUN mortars at different ages of curing.

Both σ_f and σ_c results showed in Figure 8 elucidate, in general, the same trends: as the W/C ratio increases the strength decreases, and as the curing time increases, the strength increases as well. The primary reason for the observed decrease in mechanical properties is attributed to the increased water content in the mortar formulations, which leads to a more extensive porous network. Additionally, extended curing times result in a higher strength increases due to the continued

hardening of the specimens, likely attributed to cement carbonation. The highest σ_c value, 14.3 ± 0.4 MPa, is associated with the 0.55 formulation after 28 days of curing, and its σ_f value is 5.2 ± 0.2 MPa. All formulation results indicate that, according to UNE-EN 998-1:2018, they can be classified as M-7.5 masonry mortars, making them suitable for building applications, as their 28-day σ_c exceeds 7.5 MPa. However, the 0.55 and 0.60 formulations could also be categorized as M-10, given their σ_c values exceed 10 MPa.

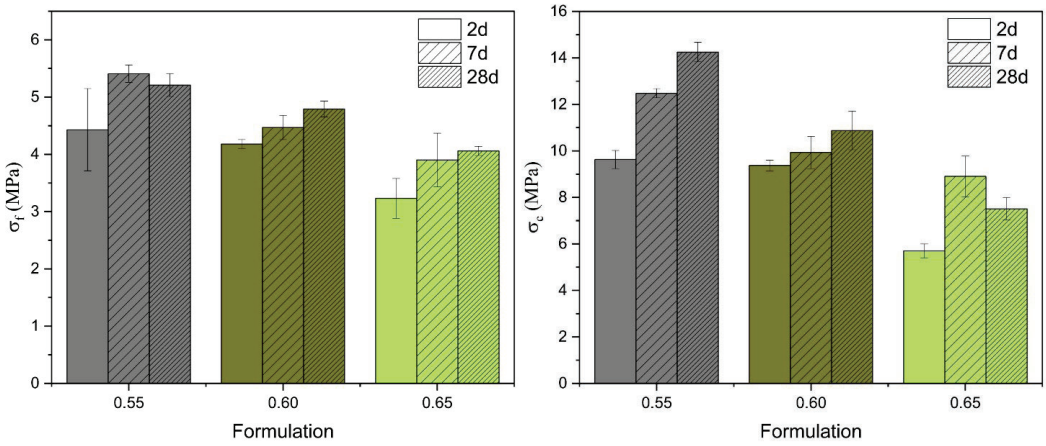

Figure 8. Flexural strength (σ_f, left) and compressive strength (σ_c, right) of MPC-TUN mortars at different ages of curing.

3.5. Fourier-transformed infrared spectroscopy in attenuated total reflectance (FTIR-ATR)

The FTIR-ATR spectra of each sample at different test day (2, 7, and 28), showed no significant differences in the resulting bands at different ages. Therefore, only the FTIR-ATR spectra corresponding to day 28 are presented in Figure 9.

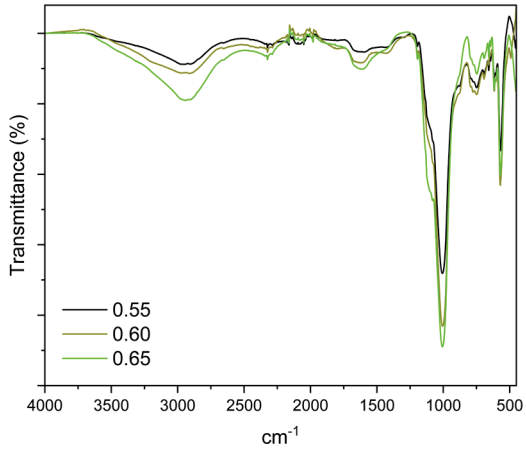

Figure 9. FTIR-ATR of 28 days MPC-TUN mortars.

As a result, only the spectral bands associated with the MPC-TUN paste at 28 days are shown, facilitating a precise analysis of its composition. The functional groups identified in the samples, shown in Table 5, were attributed to the presence of the O-H stretching and bending from H_2O, and the stretching from PO_4^{3-} bands [38]. These groups are directly associated with the formation of K-struvite ($MgKPO_4 \cdot 6H_2O$), previously mentioned as the product result from the acid-base reaction between MgO and KH_2PO_4. [12,39,40].

Table 5. Assignation of FTIR-ATR bands.

Band (cm^{-1})	Assignation
2940-3250	ν O-H from water
1590-1680	δ O-H from water
1000-1010	ν_1 P-O_4 from K-struvite
575-560	ν_4 P-O_4 from K-struvite

3.6. X-Ray Diffraction (XRD)

The XRD patterns obtained at different testing days (2, 7, and 28) showed no significant changes in the diffraction peaks, indicating stable phase formation over time. Therefore, only the data at 28 days are presented, confirming the formation of crystalline phases without significant alterations. The XRD analysis shown in Figure 10 confirms the presence of seven common structures found in all the formulations analysed in different ages. On the one hand, the presence of magnesium oxide (MgO, 01-078-0430) is indicative of an incomplete dissociation reaction and an excess of this reagent on a molar basis, which needs to be added in larger quantities to ensure the completion of the MKP-TUN reaction. On the other hand, the presence of K-struvite ($MgKPO_4 \cdot 6H_2O$, 01-075-1076) confirms the successful reaction between MKP-TUN [11,41,42]. The silicon oxide (SiO_2, 01-078-

2315) structure is derived from sand, which is used as an aggregate, being the main compound. The presence of both, aluminium phosphate ($AlPO_4$, 01-076-0228) and potassium sulphate (K_2SO_4, 00-005-0613) are related to the addition of aluminium sulphate (AS) to prevent the efflorescence and secondary phases of TUN, as reported in the literature [23,26,34]. Finally, calcium hydroxide ($Ca(OH)_2$, 01-084-1275) and calcite ($CaCO_3$, 01-083-1762), originating from the raw material composition, were identified in all the developed formulations. These compounds gradually hydrated and carbonated over time.

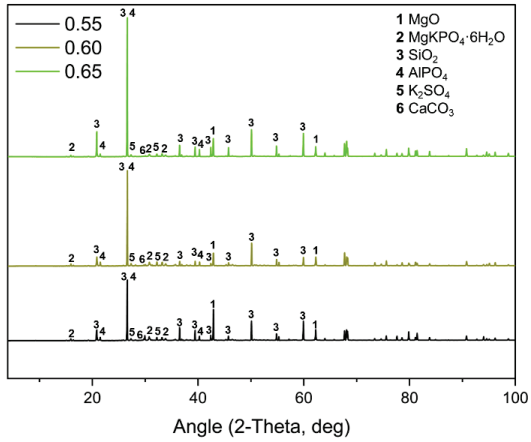

Figure 10. XRD analysis after 28 days of curing for the MPC-TUN mortars.

3.7. Thermogravimetric analysis (TG)

The thermogravimetric analysis with derivative thermogravimetry (TG/DTG) carried out for each formulation at 2, 7 and 28 days do not exhibit significant differences between the different curing days. Figure 11 presents the results of the TG analysis for MPC-TUN mortar after a curing time of 28 days at different formulations.

The results for the 28 day curing time in all the formulations showed the following decomposition profile: the first weight loss, observed between 25-260 ºC, is attributed to K-struvite decomposition; the second weight loss, observed between 260-530 ºC, is attributed to the water loss from $Mg(OH)_2$; the third weight loss, occurring between 530-790 ºC, is related to the decomposition of the present carbonates in the samples; and the fourth loss, observed between 790-1200 ºC, is associated to the sulphate decomposition and other carbonates [43-46]. Furthermore, an overlap of the second peak may occur between $Mg(OH)_2$ and the $Ca(OH)_2$ previously observed in the XRD results. This overlap is expected, as the mass loss occurs within the 330-480 ºC range [51]. However, in this study, it has been estimated to correspond to $Mg(OH)_2$, as it is more abundant in the raw material.

Table 6. Estimated composition of MPC-TUN mortars in weight percentage.

	Wt.%			
Formulations	**$MgKPO_4 \cdot 6H_2O$**	**$Mg(OH)_2$**	**$CaCO_3$**	**K_2SO_4**
0.55	27.77	1.27	1.03	5.66
0.60	28.72	1.05	1.01	5.55
0.65	28.83	1.33	0.61	7.15

Table 6 shows the estimated composition of the different formulations. The formation of K-struvite increases with a higher W/C ratio, as well as $Mg(OH)_2$. Although $Mg(OH)_2$ was not directly identified in the XRD results (Figure 10), the detection of MgO suggests that it may have undergone hydration, leading to the observed presence of hydroxide. In contrast, the concentration of $CaCO_3$, decreases further as the W/C ratio increases. Finally, the increasing presence of K_2SO_4 as the W/C ratio increases is attributed to the larger volume of $Al_2(SO_4)_3$ solution added, which promotes increased of the sulphates formation.

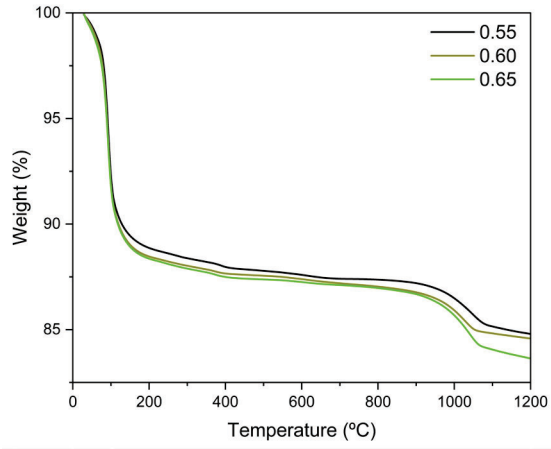

Figure 11. Thermogravimetric analysis of MPC-TUN at 28 days.

The weight losses values of the different formulations are shown in Figure 11. Focusing on the first loss related to the decomposition of K-struvite, it is possible to observe a trend towards a slight increase as the W/C ratio increases, which is related to a higher humidity in the analysed samples.

3.8. Isothermal conduction calorimetry (ICC)

Isothermal conduction calorimetry was carried out to compare the thermodynamic behaviour, focusing on the heat flow and the cumulative heat of the process.

Figure 12 shows the heat flow comparison, where the reaction starts with an endothermic peak, being larger for 0.60, followed by the 0.65 and almost unappreciable for the 0.55. This minimum is related to the dissolution of the MKP, which requires energy [47]. Additionally, it allows for the examination of the faster dissolution of MKP, along with the increased presence of K^+, H^+, and HPO_4^{2-}.

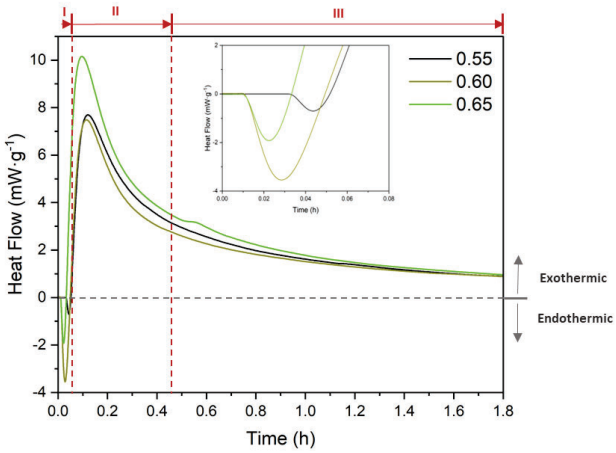

Figure 12. Heat flow of reaction of MPC-TUN mortars.

After the first endothermic peak, it follows an exothermic maximum peak. The formulation with the larger exothermic peak is the 0.65 followed by 0.55, and very close to the W/C=0.60. This peak is related to the dissolution process of MgO by H^+ ions present in the medium, where the dissociation of magnesia to Mg^{2+} is a significant exothermic reaction [47,48]. There is also a second exothermic peak, less intense and practically unappreciable, related to the reaction between the present ions to produce $MgKPO_4 \cdot 6H_2O$. All these three steps take place in the first experimental hour and the experiments is considered completed after three hours.

The cumulative heat curves shown in Figure 13 confirm that the 0.65 formulation reaches the end of the reaction earlier, being much faster than the other two formulations. However, the 0.60 formulation ultimately achieves the highest cumulative heat values. A possible explanation would be that the 0.65 formulation allows the correct dissolution of the different components by presenting a greater amount of water. Although formulations with more water typically exhibit slower reactions, the isothermal nature of the test allows the excess water to promote dissolution, accelerating the reaction process.

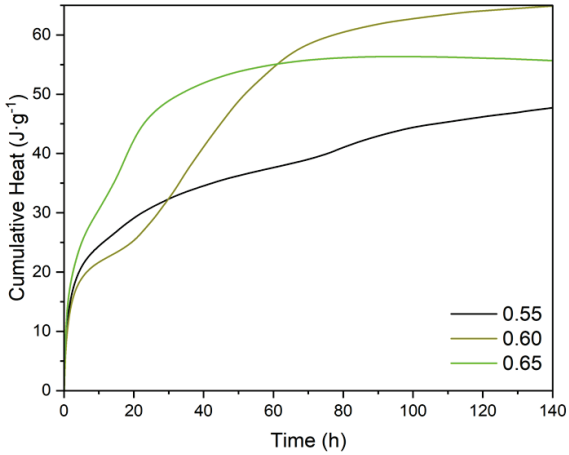

Figure 13. Cumulative heat of reaction of MPC-TUN mortars.

3.9. SEM-EDS

The three formulations were evaluated by SEM-EDS (Figure 14 for the 0.55 formulation, Figure 15 for the 0.60 formulation, and Figure 16 for the 0.65 formulation). There were no significant differences between them. The elemental distribution mapping (Figure 14 - Figure 16) shows the presence of K, P, and Mg as main elements in the matrix, which is attributed to K-struvite structure [49]. Furthermore, it is evident that the matrix is surrounding of embedded particles primarily composed of SiO_2, attributed to the aggregate, while unreacted MgO particles originating from TUN are also noticeable. The presence of S and Al in the sample are related to the addition of aluminium sulphate (AS) to avoid the efflorescence. Besides, the observed fracture surfaces are attributed to the rapid exothermic reaction due to thermal expansion, commented in the isothermal conduction calorimetry section [50].

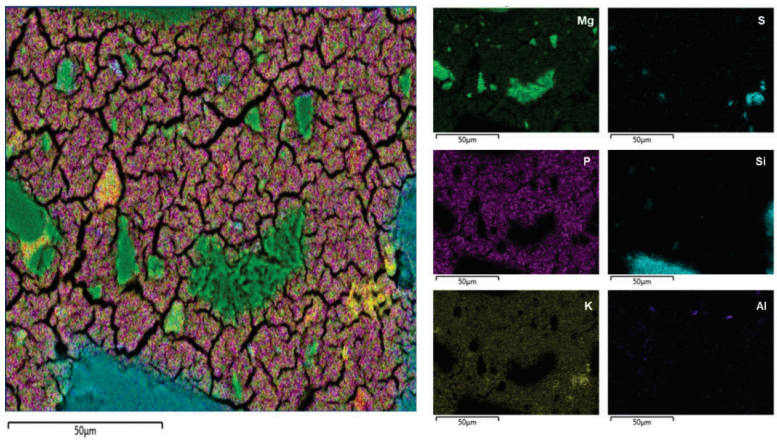

Figure 14. SEM-EDS elemental distribution mapping of 0.55 formulation.

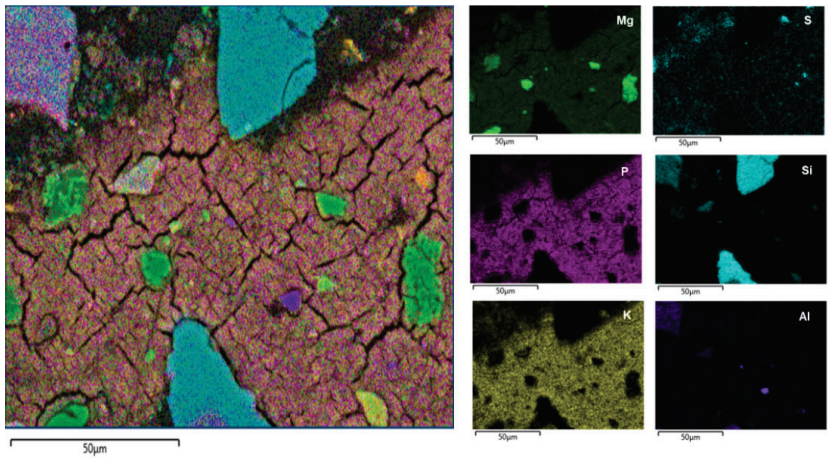

Figure 15. SEM-EDS elemental distribution mapping of 0.60 formulation.

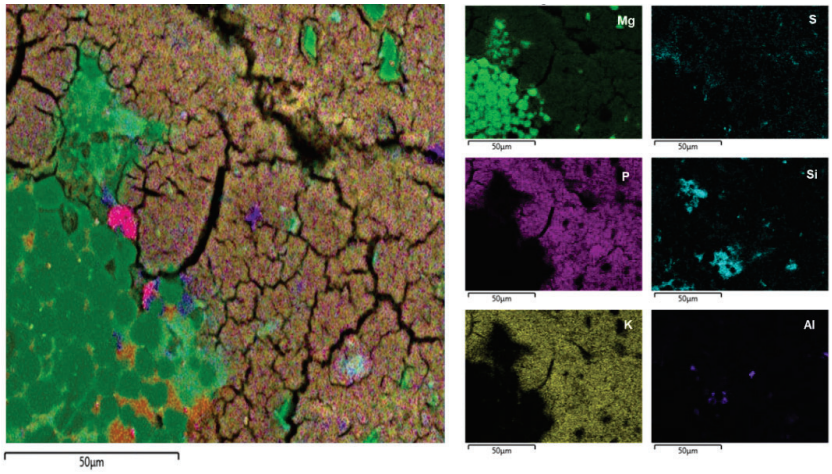

Figure 16. SEM-EDS elemental distribution mapping of 0.65 formulation.

3.10. Dynamic leaching test

As shown in Table 7, the concentration values for the studied elements are within inert limits except for Se, which slightly exceeds the inert limit. Consequently, the MPC-TUN mortars are classified as non-hazardous.

Comparing the values of the mortars with the MPC-TUN pastes (obtained in previous published studies), a dilution effect is observed, attributed to the lower concentration of TUN in the mortar due to the addition of the aggregate [23]. This effect reduces the concentrations of Se and Sb in MPC-TUN cement, categorizing it as a hazardous. However, in the case of the MPC-TUN mortars, the concentration of Sb does not exceed the inert limit, while Se surpasses the inert limit but does not

reach the hazardous limit. In the case of Ba, its concentration in the mortars increases compared to the MPC-TUN paste, probably due to the influence of the aggregate.

Similarly, the increase in pH observed in the mortars compared to the MPC-TUN paste is attributed to the previously mentioned dilution effect. With a lower cement content, fewer OH^- ions are produced, resulting in a more acidic pH.

Table 7. Leaching test for TUN, MPC-TUN paste and mortars.

Sample	pH	As	Ba	Cd	Cr	Cu	Hg	Mo	Ni	Pb	Sb	Se	Zn
TUN	12.54	< 0.01	2.2	< 0.02	0.02	0.05	< 0.01	0.29	0.03	< 0.05	0.01	0.49	< 0.10
MPC-TUN (paste)	11.28	0.41	< 0.05	< 0.02	< 0.05	< 0.05	< 0.01	1.8	< 0.05	< 0.05	0.09	0.99	< 0.10
0.55	10.74	0.02	10.86	< 0.01	< 0.01	< 0.01	< 0.02	0.33	< 0.02	< 0.01	< 0.01	0.35	< 0.10
0.6	10.63	0.01	9.18	< 0.01	< 0.01	< 0.01	< 0.02	0.4	< 0.02	< 0.01	< 0.01	0.42	< 0.10
0.65	10.54	< 0.01	9.69	< 0.01	< 0.01	< 0.01	< 0.02	0.38	< 0.02	< 0.01	< 0.01	0.42	< 0.10
Inert limit (mg/kg)	-	0.5	20	0.04	0.5	2	0.01	0.5	0.4	0.5	0.06	0.1	4
Non-hazardous limit (mg/kg)	-	2	100	1	10	50	0.2	10	10	10	0.7	0.5	50
Hazardous limit (mg/kg)	-	25	300	5	70	100	2	30	40	50	5	7	200

4. CONCLUSIONS

The main conclusions of this study are as follows:

- The utilization of TUN waste from the metallurgical industry as a residual source of MgO allows to produce a binder, named MPC-TUN, which is adequate for developing mortars. MPC-TUN mortars exhibit properties that make them suitable for its utilization as precast material. Consequently, this research marks the beginning of a path toward exploring alternative mortars, which may play an important role in the development of alternative construction materials.
- There is a correlation between the progression of curing days and the increase in mechanical strengths, with the 0.55 formulation yielding the best mechanical performance at 28 days among the tested compositions. The consistency results further support this, as the 0.55 formulation achieves an optimal balance between adequate fluidity and adequate strength development. Moreover, this formulation meets the compressive strength requirements to be classified as M-10 masonry mortars, making it suitable for building applications.
- The characterization of MPC-TUN mortars, including FTIR-ATR, XRD, TG, ICC, and SEM-EDS, was essential for a comprehensive analysis. These techniques provided key insights, confirming K-struvite as the main phase and identifying secondary phases derived from TUN.
- The development of mortars using TUN waste demonstrates the potential for future MPC applications, promoting the principles of the circular economy, sustainability, and implementing proper waste management practices. By incorporating solid waste materials as substitutes for pure DBM, these strategies address the high energy consumption and CO_2 emissions typically associated with MPC production. The implementation of waste recovery strategies not only promotes the efficient management of natural resources but also highlights a paradigm shift

towards sustainable practices, contributing to the preservation of environmental ecosystems and the mitigation of climate change.

Acknowledgments

The authors would like to thank Magnesitas Navarras, S.A. company for the information supply. Dr. Jessica Giro-Paloma is a Serra Húnter Fellow.

Funding

This work is supported by the Spanish Government with the Grant PID2021-125810OB-C21 funded by MCIN/AEI/10.13039/501100011033 and by “ERDF A way of making Europe”. Grant CNS2022-135800 funded by MICIU/AEI /10.13039/501100011033 and by the "European Union NextGenerationEU/PRTR”. The authors would like to thank the Catalan Government for the quality accreditation and funding given to their research group DIOPMA (2021 SGR 00708). DIOPMA is a certified agent TECNIO in the category of technology developers from the Government of Catalonia. Furthermore, the Agència de Gestió d’Ajuts Universitaris i de Recerca (AGAUR) contributed through Ms A. Alfocea-Roig’s PhD grant (FI-DGR 2021). This work is also partially supported by Magnesitas Navarras, S.A. (FBG312160).

Credit authorship contribution statement

A. Alfocea-Roig: Data curation, Formal analysis, Investigation, Writing - original draft. D. Vera-Rivera: Data curation, Visualization, Investigation, Writing - review & editing. S. Huete-Hernández: Resources, Visualization, Investigation, Writing - review & editing. J. Giro-Paloma: Conceptualization, Visualization, Supervision, Writing - review & editing, Funding acquisition. J. Formosa: Conceptualization, Visualization, Supervision, Methodology, Writing - review & editing, Funding acquisition.

Declaration of Competing Interest

The authors declare that they have no known competing financial interests or personal relationships that could have appeared to influence the work reported in this paper.

References

[1] Z. He, X. Zhu, J. Wang, M. Mu, Y. Wang, Comparison of CO_2 emissions from OPC and recycled cement production, Construction and Building Materials 211 (2019) 965–973. https://doi.org/10.1016/j.conbuildmat.2019.03.289.

[2] E. Worrell, L. Price, N. Martin, C. Hendriks, L.O. Meida, Carbon dioxide emissions from the global cement industry, (2021). www.annualreviews.org.

[3] Supriya, R. Chaudhury, U. Sharma, P.C. Thapliyal, L.P. Singh, Low-CO_2 emission strategies to achieve net zero target in cement sector, Journal of Cleaner Production 417 (2023). https://doi.org/10.1016/j.jclepro.2023.137466.

[4] J. Mañosa, A. Calderón, R. Salgado-Pizarro, A. Maldonado-Alameda, J.M. Chimenos, Research evolution of limestone calcined clay cement (LC3), a promising low-carbon binder – A comprehensive overview, Heliyon (2024). https://doi.org/10.1016/j.heliyon.2024.e25117.

[5] E. Bernard, H. Nguyen, S. Kawashima, B. Lothenbach, H. Manzano, J. Provis, A. Scott, C. Unluer, F. Winnefeld, P. Kinnunen, MgO-based cements – Current status and opportunities, RILEM Technical Letters 8 (2023) 65–78. https://doi.org/10.21809/rilemtechlett.2023.177.

[6] M. Yang, L. Chen, J. Lai, A.I. Osman, M. Farghali, D.W. Rooney, P.-S. Yap, Advancing environmental sustainability in construction through innovative low-carbon, high-performance cement-based composites: A review, Materials Today Sustainability 26 (2024). https://doi.org/10.1016/j.mtsust.2024.100712.

[7] S. Huete-Hernández, A. Maldonado-Alameda, J. Giro-Paloma, J.M. Chimenos, J. Formosa, Fabrication of sustainable magnesium phosphate cement micromortar using design of experiments statistical modelling: Valorization of ceramic-stone-porcelain containing waste as filler, Ceramics International 47 (2021) 10905–10917. https://doi.org/10.1016/j.ceramint.2020.12.210.

[8] S. Griffiths, B.K. Sovacool, D.D. Furszyfer Del Rio, A.M. Foley, M.D. Bazilian, J. Kim, J.M. Uratani, Decarbonizing the cement and concrete industry: A systematic review of socio-technical systems, technological innovations, and policy options, Renewable and Sustainable Energy Reviews 180 (2023). https://doi.org/10.1016/j.rser.2023.113291.

[9] P. Kinnunen, A. Ismailov, S. Solismaa, H. Sreenivasan, M.L. Räisänen, E. Levänen, M. Illikainen, Recycling mine tailings in chemically bonded ceramics – A review, Journal of Cleaner Production 174 (2018) 634–649. https://doi.org/10.1016/j.jclepro.2017.10.280.

[10] Z. Ding, B. Dong, F. Xing, N. Han, Z. Li, Cementing mechanism of potassium phosphate based magnesium phosphate cement, Ceramics International 38 (2012) 6281–6288. https://doi.org/10.1016/j.ceramint.2012.04.083.

[11] M. Le Rouzic, T. Chaussadent, G. Platret, L. Stefan, Mechanisms of k-struvite formation in magnesium phosphate cements, Cement and Concrete Research 91 (2017) 117–122. https://doi.org/10.1016/j.cemconres.2016.11.008.

[12] B. Pang, J. Liu, B. Wang, R. Liu, Y. Yang, Enhancement of magnesium phosphate cement solidification of Pb^{2+} by K-struvite whisker in lead-contaminated solution, Journal of Cleaner Production 320 (2021). https://doi.org/10.1016/j.jclepro.2021.128848.

[13] A.S. Wagh, S.Y. Jeong, Chemically Bonded Phosphate Ceramics: I, A Dissolution Model of Formation, Journal of the American Ceramic Society 86 (2003) 1838–1844. https://doi.org/10.1111/j.1151-2916.2003.tb03569.x.

[14] B. Fang, Z. Hu, T. Shi, Y. Liu, X. Wang, D. Yang, K. Zhu, X. Zhao, Z. Zhao, Research progress on the properties and applications of magnesium phosphate cement, Ceramics International 49 (2023) 4001–4016. https://doi.org/10.1016/j.ceramint.2022.11.078.

[15] P. Schroeder, K. Anggraeni, U. Weber, The Relevance of Circular Economy Practices to the Sustainable Development Goals, J of Industrial Ecology 23 (2019) 77–95. https://doi.org/10.1111/jiec.12732.

[16] H. Qiu, J. Yu, H. Chen, D. Kuang, R. He, Investigation on a sustainable magnesium phosphate cement (MPC) with recycled waste MPC powders, Journal of Environmental Chemical Engineering 12 (2024). https://doi.org/10.1016/j.jece.2024.114160.

[17] M.B. Fahad, A.M. Abdulkarem, T.H. Hamed, A review on wastes as sustainable construction materials, IOP Conf. Ser.: Earth Environ. Sci. 779 (2021). https://doi.org/10.1088/1755-1315/779/1/012014.

[18] S. Seifert, S. Dittrich, J. Bach, Recovery of raw materials from ceramic waste materials for the refractory industry, Processes 9 (2021) 1–17. https://doi.org/10.3390/pr9020228.

[19] L. Horckmans, P. Nielsen, P. Dierckx, A. Ducastel, Recycling of refractory bricks used in basic steelmaking: A review, Resources, Conservation and Recycling 140 (2019) 297–304. https://doi.org/ 10.1016/j.resconrec.2018.09.025.

[20] G. Lopez, J. Farfan, C. Breyer, Trends in the global steel industry: Evolutionary projections and defossilisation pathways through power-to-steel, Journal of Cleaner Production 375 (2022). https://doi.org/10.1016/j.jclepro.2022.134182.

[21] I. Muñoz, A. Soto, D. Maza, F. Bayón, Life cycle assessment of refractory waste management in a Spanish steel works, Waste Management 111 (2020) 1–9. https://doi.org/10.1016/j.wasman. 2020.05.023.

[22] C. Ding, H. Lei, H. Zhang, M. Xu, Y. Zhao, Q. Li, New insight into relationship between casting speed and inclusion removal in the tundish, Journal of Materials Research and Technology 23 (2023) 5400–5412. https://doi.org/10.1016/j.jmrt.2023.02.146.

[23] A. Alfocea-Roig, S. Huete-Hernández, X. García-Zubiri, J. Giro-Paloma, J. Formosa, Can tundish deskulling waste be used as a magnesium oxide source to develop magnesium phosphate cement?, Journal of Environmental Chemical Engineering 11 (2023). https://doi.org/10.1016/j.jece.2023.110618.

[24] Y. Zou, H. Gu, A. Huang, L. Fu, G. Li, L. Wang, D. Chen, Simultaneous enhance of the thermal shock resistance and slag-penetration resistance for tundish flow-control refractories: The role of microporous magnesia, Materials and Design 233 (2023). https://doi.org/10.1016/j.matdes.2023. 112245.

[25] A.C. Quintero-Payan, S. Huete-Hernández, V.B. Aguilar-Pozo, S. Astals, J.M. Chimenos, Stabilization of metal and metalloids from contaminated soils using magnesia-based tundish deskulling waste from continuous steel casting, Chemosphere 348 (2024). https://doi.org/10.1016/j.chemosphere.2023.140750.

[26] V. Muñoz-Ruiz, E. Cifrian, A. Alfocea-Roig, J. Santos, J. Formosa, J.M. Chimenos, A. Andres, Ecotoxicity assessment of sustainable magnesium phosphate cements (Sust-MPCs) using luminescent bacteria and sea urchin embryo-larval development tests, Journal of Environmental Chemical Engineering 12 (2024). https://doi.org/10.1016/j.jece.2024.113995.

[27] B.L. Biwan Xu Andreas Leemann, Frank Winnefeld, Reaction mechanism of magnesium potassium phosphate cement with high magnesium-to-phosphate ratio, Cement and Concrete Research 108 (2018) 140–151.

[28] D.V. Ribeiro, G.R. Paula, M.R. Morelli, Effect of boric acid content on the properties of magnesium phosphate cement, Construction and Building Materials 214 (2019) 557–564. https://doi.org/10.1016/j.conbuildmat.2019.04.113.

[29] J. Formosa, J.M. Chimenos, A.M. Lacasta, M. Niubó, Interaction between low-grade magnesium oxide and boric acid in chemically bonded phosphate ceramics formulation, Ceramics International 38 (2012) 2483–2493. https://doi.org/10.1016/j.ceramint.2011.11.017.

[30] S.A. Walling, J.L. Provis, Magnesia-Based Cements: A Journey of 150 Years, and Cements for the Future?, Chemical Reviews 116 (2016) 4170–4204. https://doi.org/10.1021/acs.chemrev.5b00463.

[31] C.A. Strydom, E.M. Van Der Merwe, M.E. Aphane, The effect of calcining conditions on the rehydration of dead burnt magnesium oxide using magnesium acetate as a hydrating agent, J Therm Anal Calorim 80 (2005) 659–662. https://doi.org/10.1007/s10973-005-0710-x.

[32] A. Alfocea-Roig, A. Müller, B. Steubing, S. Huete-Hernández, J. Giro-Paloma, J. Formosa, Life cycle assessment of the climate change impact of magnesium phosphate cements formulated with tundish deskulling waste compared to conventional cement, Sustainable Chemistry and Pharmacy 42 (2024). https://doi.org/10.1016/j.scp.2024.101802.

[33] A. Andrés, M.C. Díaz, A. Coz, M.J. Abellán, J.R. Viguri, Physico-chemical characterisation of bricks all through the manufacture process in relation to efflorescence salts, Journal of the European Ceramic Society 29 (2009) 1869–1877. https://doi.org/10.1016/j.jeurceramsoc.2008.11.015.

[34] B. Xu, F. Winnefeld, B. Ma, D. Rentsch, B. Lothenbach, Influence of aluminum sulfate on properties and hydration of magnesium potassium phosphate cements, Cement and Concrete Research 156 (2022). https://doi.org/10.1016/j.cemconres.2022.106788.

[35] S. Huete-Hernández, A. Maldonado-Alameda, A. Alfocea-Roig, J. Giro-Paloma, J.M. Chimenos, J. Formosa, Sustainable magnesium phosphate micromortars formulated with PAVAL® alumina by-product as micro-aggregate, Boletin de La Sociedad Espanola de Ceramica y Vidrio (2023) 1–15. https://doi.org/10.1016/j.bsecv.2023.02.001.

[36] J.R. Rosell, I.R. Cantalapiedra, Método simple para determinar el módulo de Young dinámico a partir de una excitación por impacto, aplicado a morteros de cal y cemento, Mater. Construcc. 61 (2011) 39–48. https://doi.org/10.3989/mc.2010.53509.

[37] C.K. Chau, F. Qiao, Z. Li, Microstructure of magnesium potassium phosphate cement, Construction and Building Materials 25 (2011) 2911–2917. https://doi.org/10.1016/j.conbuildmat.2010.12.035.

[38] X. Wang, L. Meng, M. Hu, L. Gao, B. Lian, The competitive and selective adsorption of heavy metals by struvite in the Pb(II)-Cd(II)-Zn(II) composite system and its environmental significance, Water Research (2023). https://doi.org/10.1016/j.watres.2023.121087.

[39] Y. Yuanquan, Z. Guanhua, G. Jinbo, Q. Dingwen, L. Runqing, An insight into the thermal properties of struvite-K by Rietveld refinement method, Journal of Materials Research and Technology 24 (2023) 3683–3690. https://doi.org/10.1016/j.jmrt.2023.04.032.

[40] I. Kabdaşlı, A. Siciliano, C. Limonti, O. Tünay, Is K-Struvite Precipitation a Plausible Nutrient Recovery Method from Potassium-Containing Wastes? A Review, Sustainability (Switzerland) 14 (2022). https://doi.org/10.3390/su141811680.

[41] C. Xu, J. Han, Y. Yang, A review on magnesium potassium phosphate cement: Characterization methods, Journal of Building Engineering 82 (2024). https://doi.org/10.1016/j.jobe.2023.108284.

[42] M.-V. Le, T.H.T. Duy, B.-T. Dang, V.H. Luan, N.-D.-T. Huynh, N.Q. Long, L.C.N. Phuong, Phosphorus recovery from fertilizer industrial wastewaters using bittern: Influence of wastewater composition and pH on struvite formation, Bioresource Technology Reports (2023). https://doi.org/10.1016/j.biteb.2023.101752.

[43] V. Pimentel Lages, F. de Campos Vitorino, R. Bentes Carvalho, A.L.C. da Cunha, J. Dweck, A new thermogravimetric method to quantify SO_2 absorption capacity by limestone, Thermochimica Acta 667 (2018) 140–147. https://doi.org/10.1016/j.tca.2018.07.024.

[44] J. Dweck, M.B.M. Melchert, M.M. Viana, F.K. Cartledge, P.M. Büchler, Importance of quantitative thermogravimetry on initial cement mass basis to evaluate the hydration of cement pastes and mortars, in: Journal of Thermal Analysis and Calorimetry, 2013: pp. 1481–1490. https://doi.org/10.1007/s10973-013-3112-5.

[45] H. Lahalle, C. Patapy, M. Glid, G. Renaudin, M. Cyr, Microstructural evolution/durability of magnesium phosphate cement paste over time in neutral and basic environments, Cement and Concrete Research 122 (2019) 42–58. https://doi.org/10.1016/j.cemconres.2019.04.011.

[46] D. Dollimore, S. Lerdkanchanaporn, Thermal Analysis, Anal. Chem. 70 (1998) 27–36. https://doi.org/10.1021/a19800038.

[47] A.S. Wagh, Recent Progress in Chemically Bonded Phosphate Ceramics, ISRN Ceramics 2013 (2013) 1–20. https://doi.org/10.1155/2013/983731.

[48] F. Qiao, C.K. Chau, Z. Li, Calorimetric study of magnesium potassium phosphate cement, Materials and Structures/Materiaux et Constructions 45 (2012) 447–456. https://doi.org/10.1617/s11527-011-9776-z.

[49] D. Wang, Y. Yue, J. Qian, Effect of carbonation on the corrosion behavior of steel rebar embedded in magnesium phosphate cement, Composites Part B: Engineering 268 (2024). https://doi.org/10.1016/j.compositesb.2023.111088.

[50] J. Zhang, Y. Qi, Y. Yang, W. Long, B. Dong, Enhancement of magnesium phosphate cement composites with sintered sludge ash, Developments in the Built Environment (2023). https://doi.org/10.1016/j.dibe.2023.100313.

3.3. Life cycle assessment

3.3.1. Introduction

In recent years, global population growth and economic expansion have led to increased energy demand, resource extraction, and contributions to global warming. Cement remains one of the most widely used materials worldwide, playing an essential role in the construction and maintenance of buildings, infrastructures, and transport systems [18]. However, the production of OPC is a significant contributor to its large environmental footprint [19,20]. As previously discussed, the development of alternative cements presents a promising path to mitigate this impact. To facilitate this transition, it is essential to exhaustively evaluate and determine whether alternative cements offer a more sustainable manufacturing process with a reduced environmental footprint.

This research, which was conducted during a research stay at the Leiden University, is aligned with the 2030 Agenda for sustainable development and the reduction of the carbon footprint [21–23]. A key objective of this third phase of the doctoral research was to evaluate the impact of climate change, particularly in terms of carbon dioxide emissions, associated with both conventional and alternative cement production [24,25]. To achieve this, a comparative study was carried out using life cycle assessment (LCA) tool, which allowed for the analysis and quantification of the environmental footprint across different functional units and potential future scenarios [26]. LCA can be conducted with varying scopes (Figure 3.6); however, this study specifically focuses on a defined system boundary, from cradle-to-gate, to accurately assess the environmental impact [27]. The materials evaluated included OPC CEM I, MPC formulated with pure magnesium oxide (MPC-MgO), and MPC-TUN for the same application. However, it is important to note that for MPC-TUN, certain estimations were required, as it is still under development at laboratory scale. Nevertheless, every effort was made to ensure these estimations were as accurate and rigorous as possible. The following section provides an overview of the results of the prospective LCA,

emphasizing the environmental benefits related to climate change impact for cements developed with TUN as raw material [28].

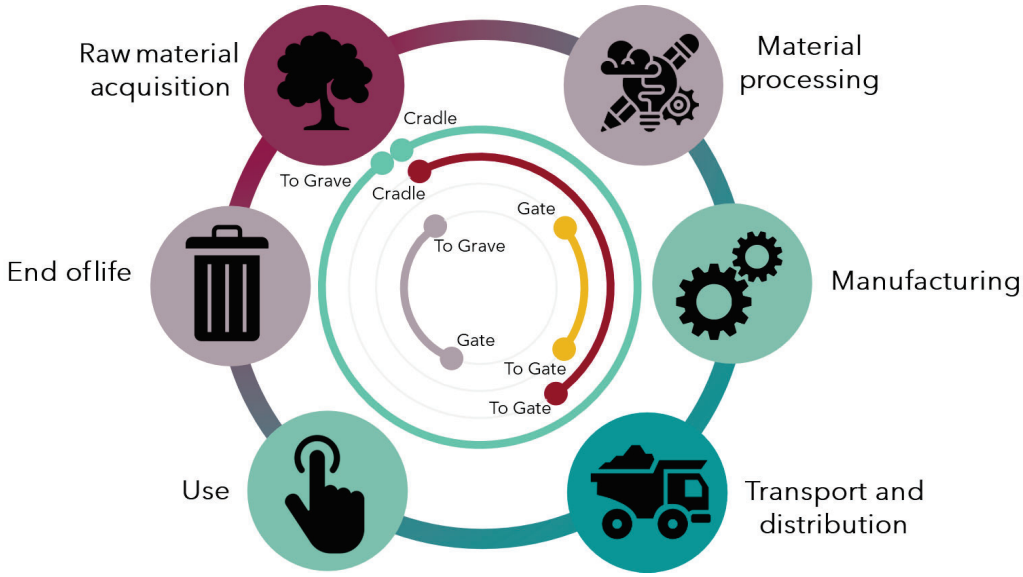

Figure 3.6. Systems boundaries of LCA.

3.3.2. Relevance

The novelty of this research lies in the environmental assessment of an alternative cement developed using TUN as a raw material. To the best of the authors' knowledge, this is the first study in the literature to evaluate the environmental impact of this material in comparison to conventional industrialized cements. Furthermore, this study introduces an innovative approach to environmental analysis by conducting a prospective LCA, distinguishing it from traditional environmental assessments typically performed on OPC. Figure 3.7 summarizes the key achievements of this pioneering research.

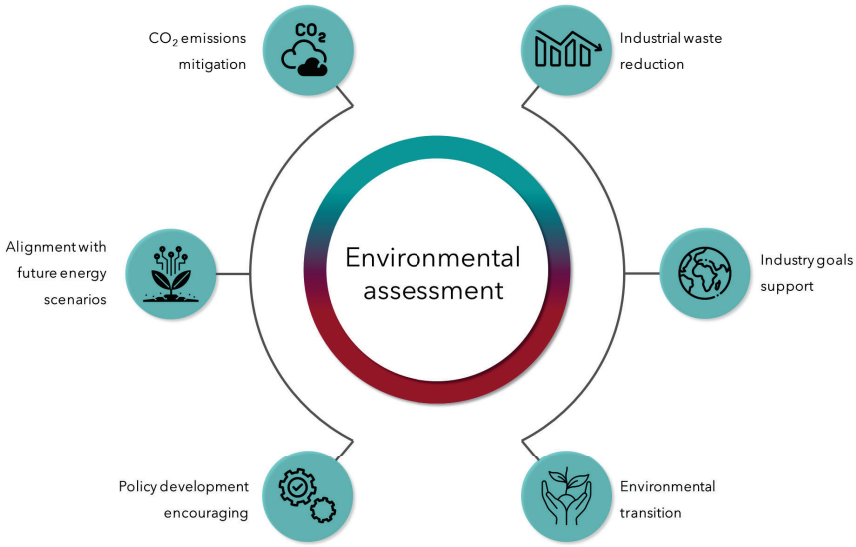

Figure 3.7. Contributions of the environmental assessment study.

3.3.3. Publication 3

Publication 3, titled "Life cycle assessment of the climate change impact of magnesium phosphate cements formulated with tundish deskulling waste compared to conventional cement" was published in open access in December 2024 issue (volume 42) in the Sustainable Chemistry and Pharmacy journal (JIF of 5.5 in 2023, Q1). The publication's title is shown in Figure 3.8, and the full text is included in this manuscript.

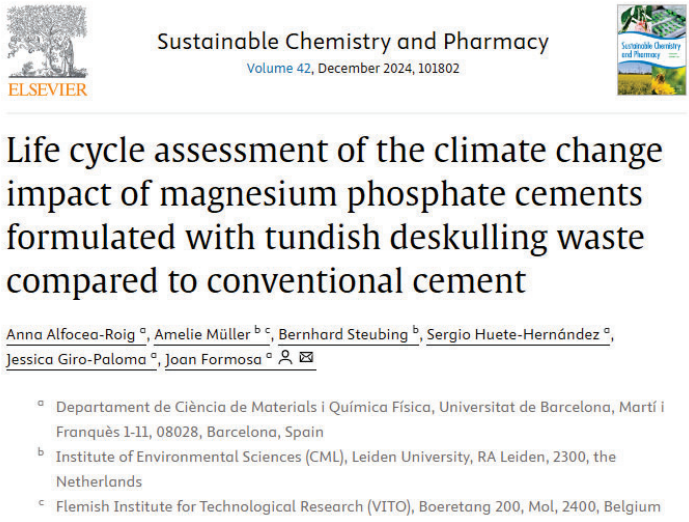

Sustainable Chemistry and Pharmacy
Volume 42, December 2024, 101802

Life cycle assessment of the climate change impact of magnesium phosphate cements formulated with tundish deskulling waste compared to conventional cement

Anna Alfocea-Roig [a], Amelie Müller [b c], Bernhard Steubing [b], Sergio Huete-Hernández [a], Jessica Giro-Paloma [a], Joan Formosa [a]

[a] Departament de Ciència de Materials i Química Física, Universitat de Barcelona, Martí i Franquès 1-11, 08028, Barcelona, Spain
[b] Institute of Environmental Sciences (CML), Leiden University, RA Leiden, 2300, the Netherlands
[c] Flemish Institute for Technological Research (VITO), Boeretang 200, Mol, 2400, Belgium

Figure 3.8. Article published in the journal of Sustainable Chemistry and Pharmacy in 2024, titled "Life cycle assessment of the climate change impact of magnesium phosphate cements formulated with tundish deskulling waste compared to conventional cement" [29].

Sustainable Chemistry and Pharmacy 42 (2024) 101802

Contents lists available at ScienceDirect

Sustainable Chemistry and Pharmacy

journal homepage: www.elsevier.com/locate/scp

Life cycle assessment of the climate change impact of magnesium phosphate cements formulated with tundish deskulling waste compared to conventional cement

Anna Alfocea-Roig [a], Amelie Müller [b,c], Bernhard Steubing [b], Sergio Huete-Hernández [a], Jessica Giro-Paloma [a], Joan Formosa [a,*]

[a] Departament de Ciència de Materials i Química Física, Universitat de Barcelona, Martí i Franquès 1-11, 08028, Barcelona, Spain
[b] Institute of Environmental Sciences (CML), Leiden University, RA Leiden, 2300, the Netherlands
[c] Flemish Institute for Technological Research (VITO), Boeretang 200, Mol, 2400, Belgium

ARTICLE INFO

Handling Editor: Borhane Mahjoub

Keywords:
Life cycle assessment
Circular economy
Refractory waste
Tundish deskulling waste

ABSTRACT

Ordinary Portland cement (OPC) production significantly contributes to greenhouse gas emissions due to high resource consumption and CO_2 output. It is therefore imperative to investigate alternative cements, such as magnesium phosphate cement (MPC), as a potential solution. This study is based on Life Cycle Assessment (LCA) methodology, comparing OPC with alternative magnesium phosphate cements (MPC) developed at the laboratory scale. The novelty of this study considers two types of alternative cements that use two different sources of MgO: MPC-MgO, developed with pure MgO, and MPC-TUN, formulated using tundish deskulling waste from steelmaking industry.

The evaluated functional units are 1 tonne of cement, 1 m^3 of cement paste, and 1 m^3 of mortar, all of them are designed for the same function, which is as non-structural precast elements. The study assesses climate change impacts under two future scenarios: 1) electricity decarbonisation in the background economy using projections from Integrated Assessment Models and 2) electricity decarbonisation and a fuel switch in the cement kilns.

The results indicate that MPC-TUN exhibits a lower impact of climate change in terms of CO_2 emissions across all functional units and scenarios compared to the other materials. In the most ambitious climate scenario, MPC-TUN mortar exhibits 42% and 56% lower climate change impacts than OPC-CEM I and MPC-MgO mortars, respectively, demonstrating its potential as a more sustainable construction material. Although further research is needed on the applicability of MPC-TUN in construction, regulatory frameworks are advised to simplify barriers to expedite the adoption of sustainable alternative cements.

1. Introduction

The construction sector, which provides the infrastructure needed for our society's daily activities, is accountable for approximately 40% of the total natural resources utilized, and 40% of the total energy consumed by humans (Eberhardt et al., 2020; Gong et al., 2012). Additionally, the construction sector is responsible for generating approximately 40% of the total waste produced by

* Corresponding author.
E-mail address: joanformosa@ub.edu (J. Formosa).

https://doi.org/10.1016/j.scp.2024.101802
Received 29 July 2024; Received in revised form 1 October 2024; Accepted 10 October 2024
2352-5541/© 2024 The Authors. Published by Elsevier B.V. This is an open access article under the CC BY-NC-ND license (http://creativecommons.org/licenses/by-nc-nd/4.0/).

human activities (Gong et al., 2012). Given the high resource and waste intensity of this sector, it is essential to alter the trajectory of the construction sector to minimize the associated environmental impacts (Hossain and Poon, 2018).

Cement, a fundamental and essential component in concrete, is a crucial material for the construction sector. Ordinary Portland cement (OPC) possesses various advantages, such as its affordability, mechanical properties, durability, and more (Valipour et al., 2014). Currently, conventional cement is a major contributor to climate change (Folliet and Milagros Rivas Saiz, 2017). Specifically, the cement industry is accountable for 8% of anthropogenic carbon dioxide (CO_2) emissions, primarily originating from two main contributions: the calcination process to obtain clinker and the energy consumption during manufacturing (Sousa et al., 2023). In response to the demand for OPC and its associated impact, the industrial community has established a roadmap to achieve Net Zero CO_2 emissions by 2050 (International Energy Agency, 2023; de Brito and Kurda, 2021; El-Dieb and Kanaan, 2018). This roadmap is based on the "Focus of the 5Cs", which encourages collaboration throughout the entire value chain of "Clinker-Cement-Concrete--Construction-(re)Carbonation" to realize climate neutrality in the industrial sector (Agrupación de fabricantes de cemento de España, 2021; CEMBUREAU, 2021).

CEMBUREAU, the European Cement Association, has developed a roadmap for 2050 that outlines the opportunities and actions depicted in Fig. 1 (CEMBUREAU, 2021). The aim of this roadmap is to reduce the emissions along the value chain by 2030 by 30–40% compared to 1990 and to achieve carbon neutrality by 2050. Particularly, Fig. 1 outlines CO_2 emissions reductions for each 5C by 2030 and 2050, aiming to achieve zero CO_2 emissions per tonne of cement produced in 2050. These targets align with various policies of the European Union (EU), in line with the Paris Agreement's objective of limiting the global temperature increase to well below 2 °C and striving to achieve 1.5 °C, as well as other agreements (Amanatidis, 2019; Anna Nilsson et al., 2020; Brugger et al., 2021). The successful achievement of these goals relies on the implementation of different regulations and policy frameworks, along with investments in technologies that are currently being undertaken at local, national, and international levels.

When it comes to cement, there are conventional options available that utilize alternative materials such as blast furnace slag (BFS) from the steel industry and fly ash (FA) from coal-fired power plants, resulting in a lower clinker content. However, the replacement potential of these conventional substitution materials is limited in the future as the processes, of which they are by-products, are expected to decline in a future decarbonized economy (Font et al., 2020; Kermeli et al., 2019). Additionally, there are supplementary cementitious materials (SCM) options available, as well as other alternative binders (Kermeli et al., 2019). One such alternative binders is magnesium phosphate cement (MPC) (Formosa et al., 2012; Huete-Hernández et al., 2021; Maldonado-Alameda et al., 2017). MPCs is produced by combining magnesium oxide (MgO), monopotassium phosphate (MKP, KH_2PO_4), and water.

In the last decades, circular economy has emerged as another mean to reach environmental sustainability, by minimizing material waste and maximizing material reuse at all stages of production and consumption(Ma et al., 2023). Utilizing waste as a raw material instead of extracting natural resources is an important strategy to reduce landfill waste and decrease the extraction of new natural resources. As a result, there is a growing body of research focused on developing alternative cements that utilize waste as a raw material, aligning with new environmental policies (Giro-Paloma et al., 2019; Huete-Hernández et al., 2021; Maldonado-Alameda et al., 2018). This study compares magnesium phosphate cement (MPC) formulated with pure magnesium oxide (MPC-MgO) to MPC-TUN which uses refractory waste from the steel industry, specifically tundish deskulling waste (TUN), as a source of magnesium oxide. TUN is a refractory material used in the last metallurgical vessel through which liquid steel flows before being shaped (Formosa et al., 2012).

Life cycle thinking is a valuable tool for addressing social, economic, and environmental challenges. To comprehensively examine the various impacts of conventional and alternative cements, a life cycle assessment (LCA) approach is necessary. LCA has been widely used to assess the environmental impacts throughout the life cycle of a product or system. Different approaches to LCAs exists, contingent upon the study's objectives. Conventional LCA is structured around current environmental impacts derived from historical

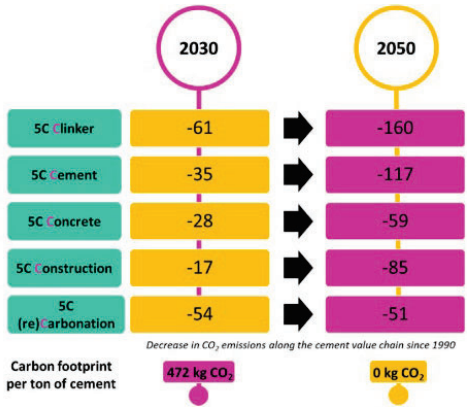

Fig. 1. CEMBUREAU 2050 roadmap related to the CO_2 savings for each 5C (adapted from (CEMBUREAU, 2021)).

or present data, while prospective LCA (pLCA) is oriented towards future scenarios, considering potential alterations that may happen (Arvidsson et al., 2018). Hence, pLCA offers the opportunity to assess whether an alternative cement can be classified as sustainable or not considering future developments (Langkau et al., 2023; Mendoza Beltran et al., 2020; Sacchi et al., 2022). PLCA is particularly beneficial for evaluating the environmental performance of emerging materials that have not yet been widely implemented.

The objective of this study is to compare the differences in current and potential future climate change impact and energy consumption by employing both conventional LCA and scenario-based pLCA for three cement types (OPC, MPC-MgO, and MPC-TUN) in the three essential formats (cement, cement paste, and mortar). Future changes are modelled by incorporating anticipated alterations in future electricity and heat usage within the processes of the evaluated materials. This research helps to understand and compare the emission reduction potential offered by innovative cements compared to conventional cements (Fig. 2), allowing environmental hotspots to be identified. It also provides valuable insights to guide the future development of sustainable materials in the cement industry.

2. Raw materials

The environmental impact of conventional cement is compared to other types of cements for the application as cement, cement paste, and mortar, all of which have been prepared following the UNE EN 196-1 standard (Normalización Española, 2018). The different products evaluated are.

- OPC CEM I 52,5 R.
- MPC formulated with pure MgO: MPC-MgO.
- MPC formulated with TUN as MgO source: MPC-TUN.

Clinker is the major component of OPC, simultaneously contributing the most to its emissions. The quantity of clinker used, and the types of materials employed are regulated by international standards, ensuring that cement is a standardized product that meets rigorous specifications for constructing durable structures with long lifetimes. Substituting clinker with alternative materials requires that the final product possesses similar mechanical and durability properties, as well as high availability. Rules and regulations play an important role in approving the introduction of new cements into this sector (Griffiths et al., 2023; Guo et al., 2024; Wang et al., 2021).

MPC-TUN is at Technology Readiness Level 3 (TRL3), indicating that it is a laboratory-scale development and not yet a fully mature technology (Alfocea-Roig et al., 2023). On the other hand, OPC CEM I, and MPC-MgO are at TRL9 because they are currently commercially available cements. Previously, a preliminary study was conducted to evaluate the properties of MPC-TUN, and the results showed that it possesses the necessary qualities for construction applications (Alfocea-Roig et al., 2023). Therefore, this study assumes that MPC-TUN can be used commercially, enabling a comprehensive comparison and full-scale environmental assessment (Batuecas et al., 2021).

3. Methodology

LCA is a tool utilized for analysing and assessing the environmental impacts of a product or service. By highlighting emission hotspots and comparing impacts between alternatives, the LCA methodology allows consumers and producers make more sustainable product choices.

This study was conducted following four primary stages (Pryshlakivsky and Searcy, 2013).

A. **Goal and scope:** This stage involves defining the main goal and determining the system boundary.
B. **Life cycle inventory (LCI):** In the LCI stage, data collection and calculations are performed to quantify the input and output of materials and energy.

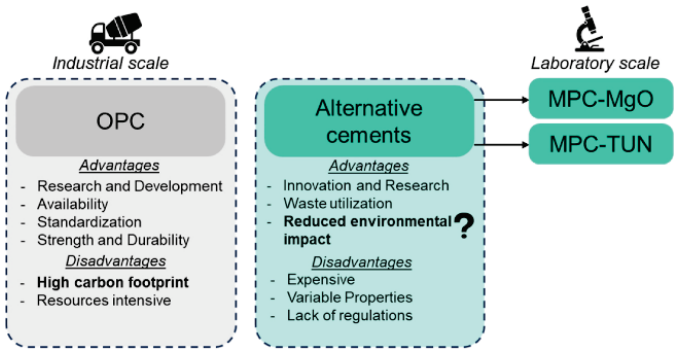

Fig. 2. Advantages and disadvantages of OPC and alternative cements under investigation.

C. **Life cycle impact assessment (LCIA):** During the LCIA stage, the potential environmental impact obtained from the LCI is evaluated.
D. **Interpretation:** The interpretation stage involves drawing conclusions based on the environmental impacts while considering the previously established objectives.

3.1. Goal and scope

The main goal of this study is to perform an LCA to compare the carbon footprint of different cements for construction applications. Consequently, the study aims to assess and compare the environmental impacts of OPC-CEM I, MPC-MgO, and MPC-TUN to identify the environmental hotspots.

The functional unit serves to quantify the specific product characteristics and defines the functions to be analysed (Batuecas et al., 2021; Panesar et al., 2017). In this study, three functional units are examined: 1 tonne of cement (dry powder), 1 m^3 of cement paste, and 1 m^3 of mortar. Three basic components are evaluated to cover the many commercialization strategies of cement: it is marketed as dry cement, which functions as a binder (cement paste), or as mortar for non-structural precast element. Although all three functional units are considered for impact assessment, particular attention will be given to the results obtained for 1 m^3 of mortar, which is a mix of cement, sand, and water, since mortar is a versatile material widely used in the construction industry. However, the functional unit of 1 m^3 of mortar allows to standardize the comparison between different materials and to enhance understanding of their carbon footprint impact per volume unit for the same applicability, which is an approach used within the research field. The geographical context of the study is the European Union (EU), and the time horizon is 2020–2050. This attributional LCA study uses the Ecoinvent 3.9 cut-off database.

The study adopts the Cradle-to-Gate system boundary. This system boundary considers the flow of materials, energy, and emissions from raw material extraction until manufacturing, excluding use and end of life. In addition, in this study, transport has not been considered, since it has been estimated that all materials are manufactured in the same location. It is important to note that the mixture design is tailored to the functional unit, resulting in different proportions of raw materials. However, despite the variations in proportions, all materials exhibit the essential properties to be applied by the same application. A fundamental prerequisite for materials intended for use in the construction industry is that they possess identical workability characteristics, among other requirements. Hence, the water/cement (W/C) ratio of these materials has been carefully adjusted to obtain a similar consistency during casting, i.e. moderate slump.

3.1.1. Future scenarios

The conducted LCA takes a prospective approach, for which it focuses on the anticipated evolution of the heat supply in cement industry and worldwide transformations in the global electricity sector related to sustainable development (Georgiades et al., 2023; Maes et al., 2023; Müller et al., 2024). The scenario development and analysis in this study are explorative, as it seeks to answer the question of how the situation in this sector could change if this alternative were to be introduced. Currently, this possibility is considered as a future simulation, although it has not yet been established as mandatory compliance regulations for the coming years.

The LCI is studied under policy scenarios for 2020, 2030 and 2050. Therefore, it is necessary to update and modify the Life Cycle Inventory database with respect to energy, efficiency, and other relevant factors based on these future pathways.

Specifically, this study focuses on the changes in emissions from conventional and alternative cements resulting from the use of alternative fuels and alternative electricity supply. The scenarios selected for each type of cement are based on the energy vision 2050 studies (Brugger et al., 2021). Two types of scenarios were evaluated.

1. **Electricity scenario**
   Scenarios that consider only the evolution of electricity production in cement production and the wider economic background system (Mendoza Beltran et al., 2020).
2. **Fuel and electricity scenario**
   Combined modelling of the background electricity scenario with foreground scenarios concerning fuel switch, developed by the decision-maker conducting the LCA (International Energy Agency, 2021).

Regarding the electricity scenario, this study considers multiple scenarios based on the Shared Socioeconomic Pathways (SSPs), which describe different potential future development pathways based on different assumptions about population, socio-economic conditions, energy use, and technology advancements (Riahi et al., 2017). Out of the five SSPs available, only SSP2 is considered in this study, as it represents a medium-level challenge for mitigation and adaptation, following the current development pathways (How 'Shared Socioeconomic Pathways, 2018; Meinshausen et al., 2020). The Representative Concentration Pathways (RCPs) are used to describe various levels of GHG (greenhouse gas) emissions that could occur in the next century. In this study, the Integrated Assessment Model (IAM) REMIND (REgional Model of Investments and Development) is employed for the electricity scenario (Potsdam Institute for Climate Impact Research, 2023; REMIND, 2023). The different IAM pathways evaluated are as follows.

- SSP2-Base (resulting in an increase of 3.5 °C by 2100): in this scenario, society and economic trends are projected based on historical developments, without considering any specific additional climate policy using the most recent projections of the European Commission and PRIMES (Price-induced market equilibrium system) projections, as the reference for energy consumption (Castillo et al., 2022).
- SSP2-RCP1.9 (resulting in an increase of 1.5 °C by 2100): this scenario extrapolates society and economic trends from historical developments while aligning with the climate policy objectives outlined in the Paris Agreement.

In addition to assessing the isolated influence of a decarbonized electricity system in the electricity scenarios, a second set of scenarios combines these with changes is future thermal fuels. In these joint scenarios, the same assumptions from REMIND for electricity are taken as in electricity scenario, and the fuel assumptions are presented in Table 1. It is important to highlight that in 2020 no alteration in the fuel mix has been accounted for, and the data solely encompasses the information from the preceding scenario (electricity scenario). Future fuel scenarios are considered by adapting fuel types from cement roadmaps and altering the fuel sources for the main sub-processes integrated into the database (Brugger et al., 2021; CEMBUREAU, 2021). In practice, it is assumed that the heat market is shared between cement manufacturing and the production of chemical reagents. Table 2 summarizes the combination of scenarios of this study.

3.2. Life cycle inventory analysis (LCI)

3.2.1. OPC-CEM I

OPC CEM I is frequently used for structures, products, and pavements in areas with low concentrations of sulphate ions in groundwater or soil. Among all the OPC families, CEM has been selected, as it is suitable material to be used as a non-structural precast element. Its composition consists of 95 wt% of clinker and 5 wt% of gypsum (Real et al., 2021). Fig. 3 illustrates the raw materials used of OPC-CEM I and the MPC-cements for the different functional units evaluated in this study, which was conducted based on data from both the literature and laboratory studies (Niewiadomski et al., 2021). Furthermore, it is possible to observe the raw materials utilized, the material density, and the water/cement (W/C) ratio.

Fig. 4 shows the flowchart to produce 1 m^3 of OPC mortar, with all steps passing through the stages of cement and cement paste and their respective functional units. It visually represents the different materials used in the cement mix and displays the various processes involved in obtaining clinker (95% of the total of OPC-CEM I). The main stages are.

- The acquisition of raw materials, which primarily involves sourcing limestone and clay.
- Quartering, grinding, and milling processes are employed to homogenize the raw materials and reduce their particle size.
- Preheating and calcination are carried out to induce a series of reactions that result in the formation of clinker.

3.2.2. MPC-MgO

MPC-MgO is conventionally produced using 22.85 wt% of pure MgO, and 77.15 wt% of MKP. Fig. 3 presents the raw materials of MPC-MgO for the different functional units examined. To achieve workability and consistency comparable to MPC-TUN, and considering the specific requirements and characteristics of the pure MgO used, a higher W/C ratio was selected than typically recommended in the literature (Ma et al., 2014; Meng et al., 2023). Additionally, the use of boric acid as a retarder was not required due to the different material requirements for the same application.

Currently, magnesium oxide is obtained from the calcination of magnesite ($MgCO_3$), resulting in the generation of 1.55 tonnes of CO_2 per ton of MgO produced (Ellis Gartner A, 2018). The specific type of magnesium oxide used in the development of MPC is referred to as Dead-Burned Magnesia (DBM) or sintered magnesia. DBM is obtained through another high-temperature calcination of magnesium oxide at approximately 1500 °C, which consumes 6546 MJ per one tonne of DBM (Mathias, 2009). This calcination process ensures the desired chemical reactivity characterized by low reactivity MgO and reduces the specific surface area (An et al., 2018; Luong et al., 2018; Ruan and Unluer, 2016; Sinka et al., 2018).

Fig. 5 shows the flowchart of the production of 1 m^3 of MPC-MgO mortar, including the MPC-MgO cement and cement paste stage. The flowchart includes the two-step calcination to obtain DBM and the other required materials (monopotassium phosphate, sand, and water).

3.2.3. MPC-TUN

In this case, the magnesium oxide source is obtained from tundish deskulling waste (TUN), which is a waste derived from steel manufacturing. This study incorporates the conditioning process required to transform TUN into useable raw materials with the desired quality and particle size for its use as a cement component. Magnesitas Navarras, S.A., a company located in Navarra (Spain), has provided information on the TUN conditioning process, starting from when it is considered waste until it is revalued as a primary component of MPC-TUN. The conditioning process involves screening, grinding, magnetic separation, and mixing, which are observed in Fig. 6. Based on the data supplied by the companies, the conditioning process is approximated to consume 64 kWh per tonne of TUN. These companies focus their activity on the recovery of refractory material from all types of industrial furnaces, for this reason, it is estimated that the values provided are reliable. The other raw materials used in MPC, being commercial materials, do not require a conditioning process. MPC-TUN is produced by combining 60 wt% of TUN with 40 wt% of MKP (Alfocea-Roig et al., 2023). Additionally, 1 wt% of boric acid (HB) is added to the total solid weight to enhance workability and delay the setting time. Fig. 3 shows the MPC-TUN raw materials, revealing the ratios derived from previous laboratory-scale studies. The DIOPMA research group has

Table 1
Heat fuel generation mix (Brugger et al., 2021; CEMBUREAU, 2021).

Type	2030 (%)	2050 (%)
Coal	30	0
Fuel oil	10	10
Biomass	30	50
Bio propane (GPL)	30	40

Table 2
Overview of scenario combinations.

	Electricity sector projections	Fuel mix projections
Electricity BAU	SSP2-Base (REMIND)	–
Electricity 1.5 °C	SSP2-RCP1.9 (REMIND)	–
Electricity and fuel BAU	SSP2-Base (REMIND)	Heat fuel mix, see Table 1
Electricity and fuel 1.5 °C	SSP2-RCP1.9 (REMIND)	Heat fuel mix, see Table 1

BAU (Business as usual); SSP2-Base1.5 °C; SSP2-RCP1.9.

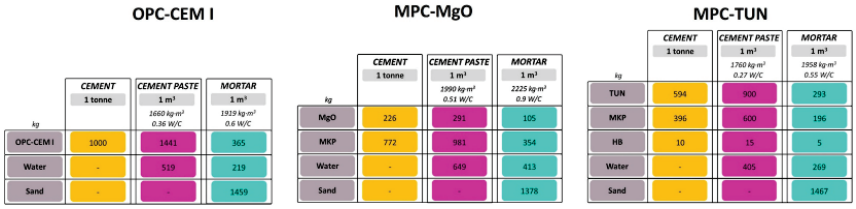

Fig. 3. Raw materials used in the functional units of the evaluated materials (see Appendix A, Table A.1).

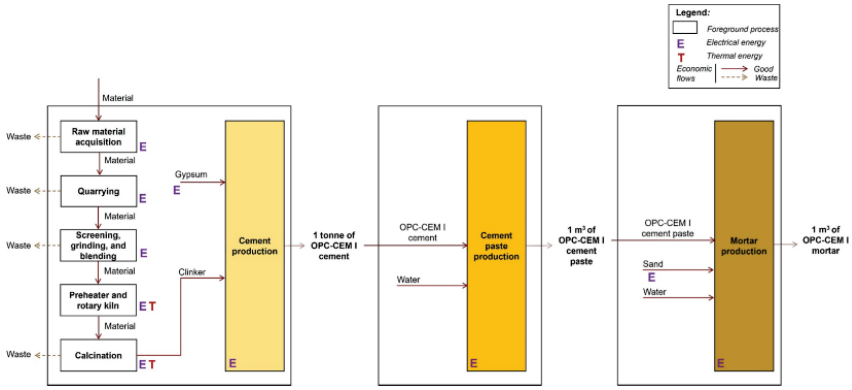

Fig. 4. OPC-CEM I flowcharts of the functional units assessed (see Appendix A, Table A.1).

considerable expertise in this field, having devoted extensive years to the advancement of MPCs.

It is essential to highlight that the collection of this data was difficult due to the low TLR of MPC-TUN. Particularly, data on the electricity consumption for an industrial-level conditioning of TUN was lacking and these gaps were filled with contains various assumptions. These data gaps have the potential to underestimate the ultimate results concerning the future production of this product. However, it is anticipated that the deviation from reality will be minimal, given that the assumptions have been carefully aligned with real-world conditions.

Allocation involves assigning the input and/or output streams of a multifunctional process to the product system under evaluation (H. A. Aguirre-Villegas et al., 2012; Heijungs and Guinée, 2007). In this case, allocation by cut-off is applied to divide the impacts of TUN between steel production and its later use in MPC-TUN. This means that the upstream impacts of TUN are counted towards steel, while the conditioning process to turn the TUN waste into a raw material is counted towards the cement life cycle (Turk et al., 2015). In other words, as depicted in Fig. 6, the TUN comes as a burden-free waste from the steel industry and is considered as a good after it undergoes conditioning, making it suitable for use as a magnesium source.

3.3. *Life cycle impact assessment (LCIA) methods*

The outcomes of the LCA are dependent on the choices and assumptions made regarding the data and methods employed. The specific impact category considered is the same across in both scenarios, which is.

- Climate change:

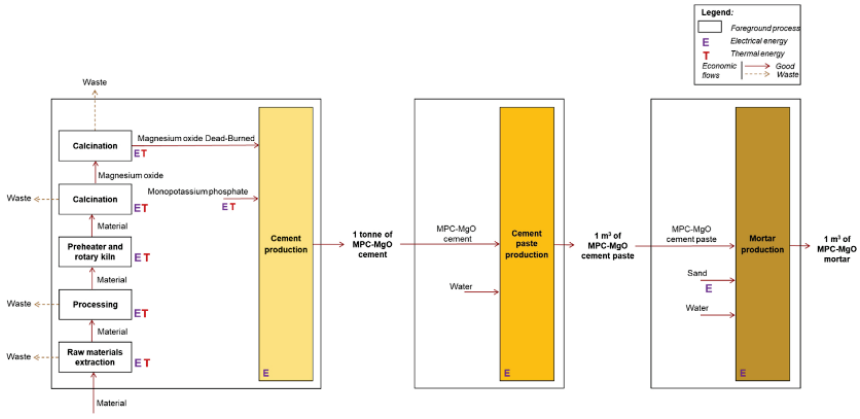

Fig. 5. Flow diagrams of the MPC-MgO functional units evaluated (see Appendix A, Table A.1).

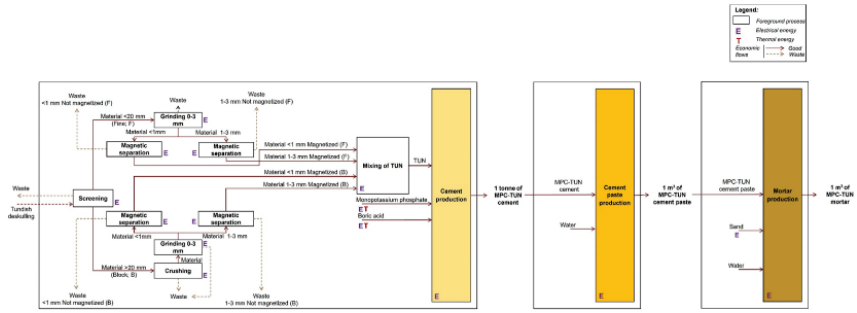

Fig. 6. Flow diagrams of the MPC-TUN functional units evaluated (see Appendix A, Table A.1).

- Global warming potential (GWP 100): this indicator quantifies the potential for global warming over a 100-year timeframe. The unit used is kg $CO_{2\text{-eq}}$. The used methods are part of the Environmental Footprint (EF) method family, which is the recommended impact assessment method family of the European Union (Fazio et al., 2018).

Future research shall explore how the investigated materials contribute to non-climate-change related environmental impacts, such as abiotic resource depletion and acidification potential, PM2.5, among other impact indicators. However, the focus and scope of this study has focused solely on the impact of climate change, this approach is justified by the assumption that if a material does not exhibit favourable characteristics in terms of GHG emissions, its market viability is compromised from the outset. Therefore, this study is the first investigation to assess its environmental footprint and subsequently study its feasibility.

3.4. Results

3.4.1. Current impact

Table 3 shows the results for cements, cement pastes and mortar for the year 2020, the starting year of the study. The slightly different values between SSP2-Base and SSP2-RCP1.9 can be explained by small modifications to the background electricity mix that have already been modelled in 2020 based on REMIND. The impact of mortars is lower compared to cement or cement pastes due to the different proportions and material dosages employed.

Table 4 shows the impacts on climate change for all scenarios considered for each material and functional unit evaluated.

3.4.2. Electricity scenario

Fig. 7 shows the climate change results for the electricity scenario for the different cements. In these scenarios, the electricity supply throughout the production processes of the cements has been replaced with the future projected electricity mix from the IAM REMIND. The electricity consumed in the mixing process of the three evaluated materials has been assumed to be uniform. It is shown that the environmental impact is lower when using MPC-TUN compared to the other materials for all cement applications studied: cement,

Table 3
Current impact in the year 2020.

		Climate change	
		kg $CO_{2-eq.}$	
		SSP2-Base	SSP2-RCP1.9
		2020	2020
Cement [tonne]	OPC-CEM I	830	820
	MPC-MgO	1160	1130
	MPC-TUN	430	420
Cement paste [m^3]	OPC-CEM I	1197	1186
	MPC-MgO	1478	1441
	MPC-TUN	657	632
Mortar [m^3]	OPC-CEM I	363	361
	MPC-MgO	591	577
	MPC-TUN	275	266

Table 4
Impacts of the different scenarios evaluated in the pLCA.

		Electricity scenario				Fuel and electricity scenario			
		Climate change							
		kg $CO_{2-eq.}$							
		SSP2-Base		SSP2-RCP1.9		SSP2-Base		SSP2-RCP1.9	
		2030	2050	2030	2050	2030	2050	2030	2050
Cement [tonne]	OPC-CEM I	820	810	810	810	760	700	750	700
	MPC-MgO	1100	1040	1000	960	1050	850	940	760
	MPC-TUN	400	370	350	330	370	290	320	250
Cement paste [m^3]	OPC-CEM I	1187	1169	1165	1162	1103	1014	1078	1004
	MPC-MgO	1401	1316	1266	1217	1331	1077	1195	972
	MPC-TUN	609	554	524	495	566	434	480	372
Mortar [m^3]	OPC-CEM I	361	356	354	353	339	316	332	313
	MPC-MgO	562	531	513	495	537	445	487	406
	MPC-TUN	259	240	230	220	245	201	216	180

cement paste and mortar. Conversely, MPC-MgO stands out as the material with the greatest environmental impact, higher than OPC. For OPC, the climate change impact stays almost constant over time despite a continuously cleaner electricity mix. This shows that electricity is only a minor driver for climate change for OPC, for which most impact stems from calcination and fuel combustion.

Concerning the development over time in the electricity scenario, more impact reduction is achieved, as expected, in the 1.5C-compliant scenario (SSP2-RCP1.9) than in the business as usual (SSP2-Base), which, however, also shows modest reductions. Focusing on the mortars in the SSP2-Base pathways in 2050, the following observations can be made for their climate change impact (Fig. 8).

i) Clinker production is responsible for 82.8% of the impact of OPC-CEM I mortar.
ii) For the MPC-MgO mortar, MKP production causes 60.2% of the impact, while 20.5% comes from MgO production. Additionally, 8.7% of the impact comes from the calcination process of magnesite, which is crucial for achieving the desired reactivity required for its use as a raw material.

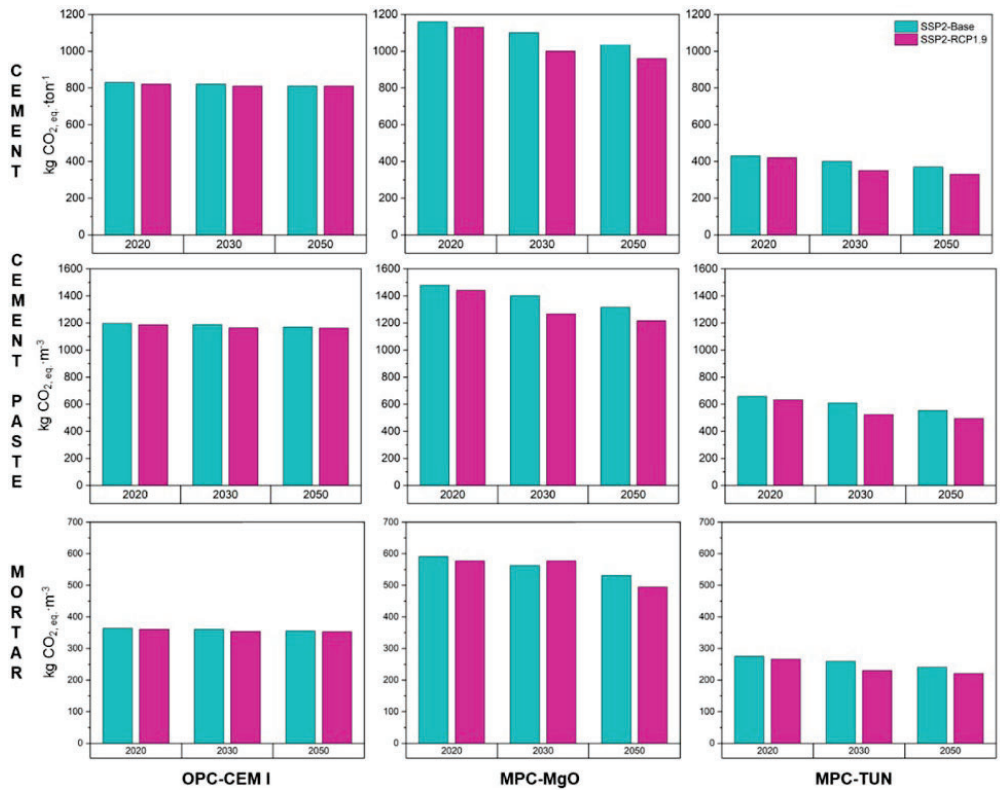

Fig. 7. Results for climate change category for electricity scenario.

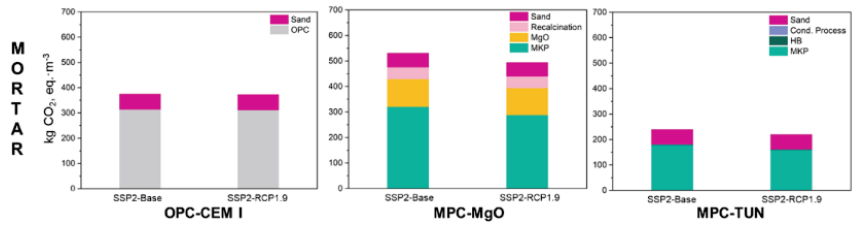

Fig. 8. Contributions of mortars to climate change impacts for the electricity scenario in the year 2050 (OPC, Ordinary Portland Cement; MgO, magnesium oxide; MKP, monopotassium phosphate; Cond. Process, conditioning process; HB, boric acid).

iii) For MPC-TUN mortar, MKP causes 73.5% of the impact. More precisely, 35.7% is attributed to phosphoric acid, and 37.8% to potassium hydroxide. Additionally, 1.2% of the impact is attributed to HB, while 0.4% is associated with the TUN conditioning process.

Moving forward to the SSP2-RCP1.9 pathway for the same year 2050, the following slight changes in impacts for the mortars can be observed.

i) For the OPC-CEM I mortar, 83% of the impact still comes from the production of clinker.

ii) For the MPC-MgO, 58% of the impact originates from MKP, 21.5% from MgO production, and 9.3% from the recalcination of magnesite to obtain the desired reactivity.
iii) For the MPC-TUN mortar, MKP causes 71.8% of the impact, HB 1.2%, and 0.1% stems from the TUN conditioning process.

It is crucial to highlight that the remaining impact on climate change of each material is associated with the use of silica sand (Fig. 8). These assessments provide valuable insights into the climate change impacts of the different mortars under consideration for the specified scenarios. First and foremost, it can be deduced from the different pathways evaluated that for the OPC-CEM I mortar, the impact comes mainly from the clinker. In the case of MPC-MgO, the production of DBM incurs a significant energy consumption and leads high CO_2 emissions, while the production of MKP is also a significant contributor. Lastly, in the context of MPCs, the MKP component stands out as having the most significant impact. The percentage shift in the impact contribution of MKP between MPC-MgO and MPC-TUN can be attributed to variations in their respective compositions.

Moreover, it is noticeable that in the future the different impacts are decreasing. This trend can be attributed to the continuous reduction in fossil-fuel based electricity generation in both scenarios. Besides, the impacts of SSP2-RCP1.9 are lower compared to SSP2-Base, as can be seen in Fig. 7. This difference could be because SSP2-RCP1.9 incorporates a faster phase-out of fossil-based electricity and higher shares of low-carbon energy sources to achieve the goals outlined in the Paris Agreement.

Finally, considering SSP2-RCP1.9 pathway and looking forward to the year 2050, it can anticipate the following mortar related changes. Specifically, MPC-TUN exhibits a 38% reduction in climate change impacts compared to OPC-CEM I and a 55% reduction in impacts compared to MPC-MgO mortar.

3.4.3. *Fuel and electricity scenario*

The trends of the combined scenario are consistent with the electricity-only scenario, but reductions over time are more pronounced. MPC-TUN shows the smallest footprint concerning the climate change impact category, followed by OPC-CEM I and MPC-MgO, as shown in Fig. 9.

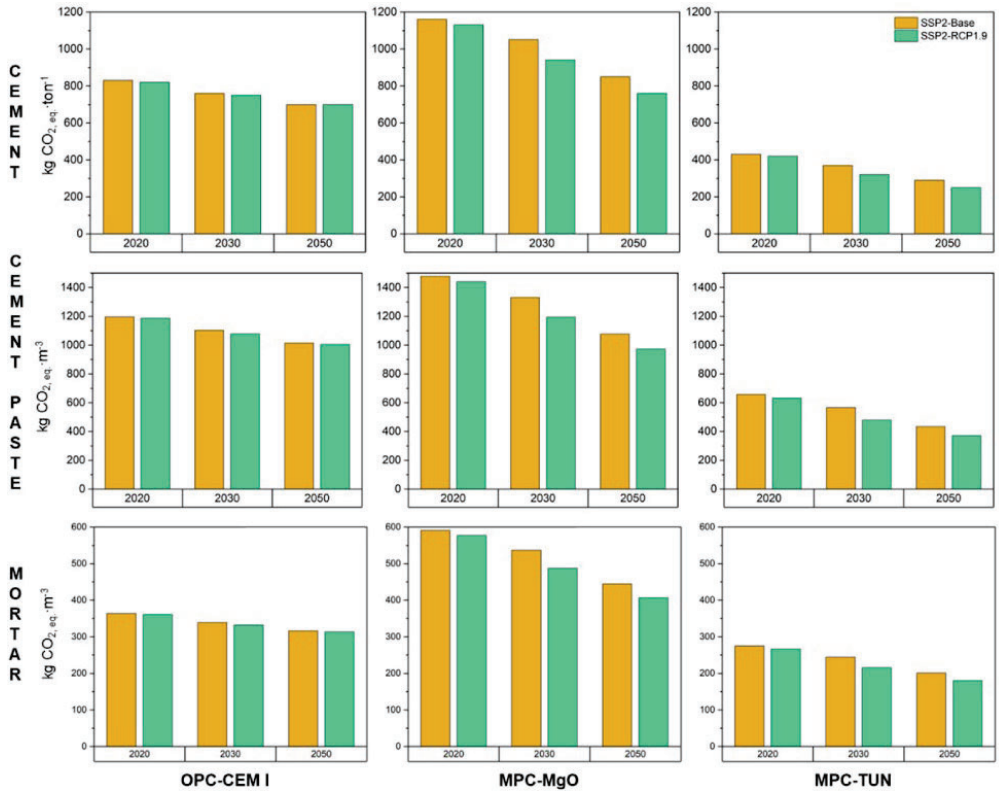

Fig. 9. Climate change category for electricity and fuel scenario.

Fig. 10 shows the environmental contributions of mortars for each material in the SSP2-Base and SSP2-RCP1.9 scenarios for 2050, considering future assumptions. The additional implementation of a cleaner fuel mix in cement production reduces the overall emissions compared to those of the previous scenario, which only included electricity decarbonisation. Nevertheless, it is noteworthy that the distribution of impact contributions remains similar to that of the previous scenario, as the primary contributors for each type of mortar remain consistent.

In the SSP2-RCP1.9 scenario, the $CO_{2\text{-eq}}$ emissions (Fig. 9) of the combined scenarios (electricity and fuel) display a decreasing trend for all mortars over the years.

i) For the OPC-CEM I, emissions are decreased from 361 kg CO_2 eq. in 2020 to 313 kg CO_2 eq. in 2050 (reduction of ≈13%).
ii) For the MPC-MgO, emissions descend from 577 kg CO_2 eq. in 2020 to 406 kg CO_2 eq. in 2050 (reduction of ≈30%).
iii) For the MPC-TUN, emissions fall from 266 kg CO_2 eq. in 2020 to 180 kg CO_2 eq. in 2050 (reduction of ≈32%).

A particularly significant aspect of this scenario lies in the notable decrease in impacts when compared to the previous scenario. In the context of mortars focusing on the fuel and electricity scenario for SSP2-RCP1.9 by 2050, there is a significant reduction compared to electricity scenario: 13% for OPC-CEM I, 22% for MPC-MgO, and 22% for MPC-TUN. This emphasizes the pivotal role that fuel sources play across various sectors and underscores their profound influence on environmental impact. Lastly, looking ahead to the year 2050 for the SSP2-RCP1.9 pathway, MPC-TUN causes 42% less climate change impacts than OPC-CEM I and 56% less impacts compared to MPC-MgO.

An assessment of emerging materials, despite their current low rate of application and the challenges they face to achieve industrial production, is significant as it describes their potential for climate change mitigation. However, these evaluations incorporate the scale-up of production at the industrial level of production, the study of the properties at the laboratory level so that they have the same applicability as commercial products, among others.

4. Discussion

The impact of climate change on society and the conservation of the natural world are intertwined; thus, it is impossible to resolve one without addressing the other. The LCA methodology is increasingly gaining more importance in the construction sector, as it allows to evaluate the environmental impacts associated with the materials or processes evaluated (AzariJafari et al., 2021; Jiang et al., 2023; Martínez-Rocamora et al., 2016).

4.1. Materials

This study adopts the LCA method to assess the climate change of using different types of cements in the construction sector as non-structural precast elements. The results show that the cement industry can reduce its emissions by adopting low-carbon cements, such as MPC-TUN, but also by considering low-carbon electricity and fuels. The results underscore the importance of utilizing recovered materials, such as MPC-TUN, instead of relying solely on pure materials or on by-products. By incorporating waste materials, the environmental impacts associated with sending materials to landfills and virgin resource extraction can be avoided. This can contribute both to climate change mitigation and a more circular economy (European Commission. Joint Research Centre. Institute for Environment and Sustainability, 2010). However, one must be aware of the limitations and uncertainty of this material, as it is currently at laboratory scale (TLR 3). Therefore, hypotheses have been made concerning its viability as a commercial product and its energy requirements during manufacture.

The results show that the MPC-TUN materials display the lowest CO_2 emissions score in all applications studied as they avoid calcination related GHG emissions. Thus, a climate benefit is observed for this novel material. Additionally, in all scenarios, it is evident that MPC-TUN demonstrates a reduced impact compared to MPC-MgO. This reduction can be attributed to the use of a waste as a source of MgO instead of using pure MgO, which contains substantial amounts of fossil fuel resources and CO_2 emissions in its supply chain.

However, the presence of MKP in all MPCs presents another significant environmental challenge. To ensure a sustainable development, it is essential to explore ways to reduce emissions associated with MKP production or find alternative sources for obtaining this material. The search for different residual sources or more environmental methods to obtain MKP is crucial to further enhance the sustainability of MPC-based mortars.

Focusing on the OPC-CEM I, main efforts in the upcoming years include to replace and reduce clinker usage, which are integral steps of the roadmap for the cement industry. The reduction of clinker content helps mitigate the carbon footprint associated with OPC production.

4.2. Scenarios

The electricity scenario has shown how an increasingly decarbonized electricity system reduces the climate change impact of the assessed materials for the same applicability. Here, a higher reduction is observed for the MPC-based materials than the OPC-cement based ones and a higher reduction in the more climate-ambitious scenario SSP2-RCP1.9 compared to the baseline scenario (SSP2-Base). The combined scenarios of electricity and fuel sector show the additional savings that can be achieved from a changing thermal fuel market in the upcoming years: the values obtained in the electricity and fuel scenario, as shown in Fig. 9, are better compared to the electricity-only scenario (Fig. 7). This improvement is based on the change in the fuel oil market (shift from coal to biomass and bio propane). Also, in the combined scenarios, which implement the same future heat mixes in both pathways, the deeper decarbonisation of the electricity mix in the SSP2-RCP1.9 pathway results in larger impact reductions compared to the SSP2-Base pathway.

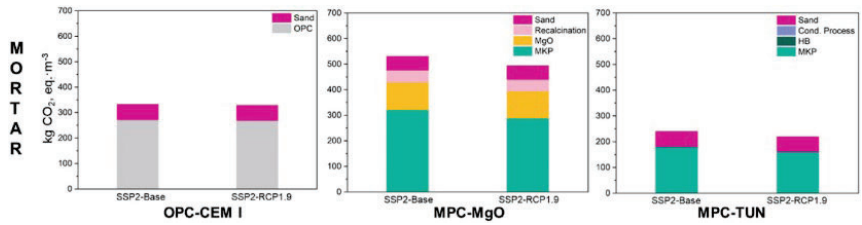

Fig. 10. Contributions of mortars to climate change impacts for the electricity and fuel scenario (OPC, Ordinary Portland Cement; MgO, magnesium oxide; MKP, monopotassium phosphate; Cond. Process, conditioning process; HB, boric acid).

The scenario assessment highlights the significant role played by the construction sector. The extent to which the projected more sustainable electricity and fuel supply can be achieved depends on the political frameworks, infrastructures development, and economic factors. This necessitates detailed studies to evaluate their viability and enhance facilities in terms of energy storage, demand response, network extension, and renewable sources (de Brito and Kurda, 2021; Munaro and Tavares, 2023; Scrivener et al., 2019; Wang et al., 2023). However, in a future study it would be of great interest to also introduce enhancements in efficiency, technological advancements, and other factors in cement production in the future projections. These projections would be related to a reduction in the assessed impacts.

Finally, this study demonstrates that the introduction of MPC-TUN aligns with the construction sector's roadmap in terms of exploring alternative materials. Then, it should be noted that.

- To allow the incorporation of different cements, it will be essential to have the regulations in place that guarantee their properties.
- The cement industry has several actions it can take to reduce the emissions, introduce low-carbon technologies, and embrace circularity. It is crucial to emphasize that this sector requires political and funding support to achieve the environmental goals since it cannot reach them on its own.

5. Conclusions

This study shows that all MPC-TUN materials demonstrate a significant reduction in climate change impacts compared their OPC-CEM I and MPC-MgO-based alternatives in all scenarios. Therefore, MPC-TUN is shown to be a more climate friendly cement type that simultaneously contributes to waste prevention, raw materials reduction, and a more circular economy by utilizing waste from the steel industry. Our results also show that MPC-MgO based materials have the highest impact on climate change, higher than OPC-CEM I. This highlights the fact that not all alternatives to clinker-based Portland cements necessarily result in a benefit for the climate. When assessing these findings, it is crucial to acknowledge that the MPC-TUN has not been developed for industrial use yet but is currently at laboratory scale (TLR3). This means that there are significant uncertainties concerning production parameters when upscaling MPC-TUN to industrial use, such as conditioning process. Nonetheless, efforts have been made to minimize the uncertainty by estimating the performance this process.

The scenario analysis in this study highlights the potential impact reductions over time that arise from using a decarbonized future electricity mix and greener thermal heat supply. This points to the significant reduction potential for the cement industry by switching to greener electricity and fuels, next to adopting low-carbon alternative cements, such as MPC-TUN.

To reduce the energy demand and climate change impact of MPC-TUN materials further, it will be necessary to seek new sources of MKP from residual and alternative sources. Simultaneously, this approach promotes the circular economy by utilizing waste as raw materials, thereby avoiding the need to send it to landfills. Moreover, utilizing these alternative sources of phosphate could significantly help in lowering the final cost of the product. As MPC-TUN is still at laboratory scale, it is essential to implement new regulations, do more research, and secure financial support to mature this novel, climate-friendlier construction material and overcome its barriers to adoption. For their future applicability as construction material, MPC-TUN must be thoroughly evaluated to verify technical requirements, including durability in different environments and the achievement of optimal mechanical properties, among other specifications.

CRediT authorship contribution statement

Anna Alfocea-Roig: Writing – original draft, Visualization, Investigation, Formal analysis, Data curation, Conceptualization. **Amelie Müller:** Writing – review & editing, Supervision, Software, Resources, Methodology. **Bernhard Steubing:** Writing – review & editing, Supervision, Resources, Methodology. **Sergio Huete-Hernández:** Writing – review & editing, Resources. **Jessica Giro-Paloma:** Writing – review & editing, Visualization, Supervision, Conceptualization. **Joan Formosa:** Writing – review & editing, Visualization, Supervision, Funding acquisition, Conceptualization.

Funding

This work is supported by the Spanish Government with the Grant PID2021-125810OB-C21 funded by MCIN/AEI/10.13039/

501100011033, by "ERDF A way of making Europe", CNS2022-135800 funded by MICIU/AEI/10.13039/501100011033 and by the "European Union NextGenerationEU/PRTR", and by the Catalan Government with the Grant 2021 SGR 00708. Furthermore, the Agència de Gestió d'Ajuts Universitaris i de Recerca (AGAUR) contributed through Ms A. Alfocea-Roig's PhD grant (FI-DGR, 2021). A. Alfocea-Roig wants to acknowledge Fundació Agustí Pedro i Pons for the financial support in her stage in Leiden (Netherlands) to execute this study. This work is also partially supported by Magnesitas Navarras, S.A. (FBG312160). Amelie Müller received funding from the European Union's Horizon Europe research and innovation programme under grant agreement No. 101056755.

Declaration of competing interest

The authors declare that they have no known competing financial interests or personal relationships that could have appeared to influence the work reported in this paper.

Data availability

Data will be made available on request.

Acknowledgments

The authors would like to thank Magnesitas Navarras, S.A. company for the information supply. Dr. Jessica Giro-Paloma wants to thank the Serra Húnter Program, DIOPMA is a certified agent TECNIO in the category of technology developers from the Government of Catalonia. We would like to express our sincere gratitude to Institute of Environmental Sciences (CML, Leiden University) for providing us with the opportunity to carry out a research stay at their facilities.

Appendix A. Supplementary data

Supplementary data to this article can be found online at https://doi.org/10.1016/j.scp.2024.101802.

References

Agrupación de fabricantes de cemento de España, 2021. Hoja de ruta de la industria cementera española para alcanzar la neutralidad climática en 2050. Oficemen.
Aguirre-Villegas, H.A., Milani, F.X., Kraatz, S., Reinemann, D.J., 2012. Life cycle impact assessment and allocation methods development for cheese and whey processing. Trans. ASABE (Am. Soc. Agric. Biol. Eng.) 55, 613–627. https://doi.org/10.13031/2013.41363.
Alfocea-Roig, A., Huete-Hernández, S., García-Zubiri, X., Giro-Paloma, J., Formosa, J., 2023. Can tundish deskulling waste be used as a magnesium oxide source to develop magnesium phosphate cement? J. Environ. Chem. Eng. 11. https://doi.org/10.1016/j.jece.2023.110618.
Amanatidis, G., 2019. European Policies on Climate and Energy towards 2020, 2030 and 2050.
An, J., Li, Y., Middleton, R.S., 2018. Reducing energy consumption and carbon emissions of magnesia refractory products: a life-cycle perspective. J. Clean. Prod. 182, 363–371. https://doi.org/10.1016/j.jclepro.2018.01.266.
Anna Nilsson, F.H., Legarreta, P.L., Lui, S., Röser, F., 2020. Decarbonisation Pathways for the EU Cement Sector: Technology Routes and Potential Ways Forward. New Climate Institute.
Arvidsson, R., Tillman, A.M., Sandén, B.A., Janssen, M., Nordelöf, A., Kushnir, D., Molander, S., 2018. Environmental assessment of emerging technologies: recommendations for prospective LCA. J. Ind. Ecol. https://doi.org/10.1111/jiec.12690.
AzariJafari, H., Guest, G., Kirchain, R., Gregory, J., Amor, B., 2021. Towards comparable environmental product declarations of construction materials: insights from a probabilistic comparative LCA approach. Build. Environ. 190. https://doi.org/10.1016/j.buildenv.2020.107542.
Batuecas, E., Ramón-Álvarez, I., Sánchez-Delgado, S., Torres-Carrasco, M., 2021. Carbon footprint and water use of alkali-activated and hybrid cement mortars. J. Clean. Prod. 319. https://doi.org/10.1016/j.jclepro.2021.128653.
Brugger, H., Eichhammer, W., Mikova, N., 2021. Energy Efficiency Vision 2050: how will new societal trends influence future energy demand in the European countries? Energy Pol. 152.
Castillo, V.Z., Boer, H.S. de, Muñoz, R.M., Gernaat, D.E.H.J., Benders, R., van Vuuren, D., 2022. Future global electricity demand load curves. Energy 258. https://doi.org/10.1016/j.energy.2022.124741.
CEMBUREAU, 2021. Reaching Climate Neutrality along the Cement and Concrete Value Chain by 2050. Cementing the European Green Deal.
de Brito, J., Kurda, R., 2021. The past and future of sustainable concrete: a critical review and new strategies on cement-based materials. J. Clean. Prod. 281. https://doi.org/10.1016/j.jclepro.2020.123558.
Eberhardt, L.C.M., van Stijn, A., Rasmussen, F.N., Birkved, M., Birgisdottir, H., 2020. Development of a life cycle assessment allocation approach for circular economy in the built environment. Sustainability 12, 1–16. https://doi.org/10.3390/su12229579.
El-Dieb, A.S., Kanaan, D.M., 2018. Ceramic waste powder an alternative cement replacement – characterization and evaluation. Sustainable Materials and Technologies 17. https://doi.org/10.1016/j.susmat.2018.e00063.
Ellis Gartner A, T.S.B., 2018. Alternative cement clinkers. Cement Concr. Res. 114, 27–39. https://doi.org/10.1016/j.cemconres.2017.02.002.
European Commission. Joint Research Centre. Institute for Environment and Sustainability, 2010. Framework and Requirements for Life Cycle Impact Assessment Models and Indicators. Publications Office.
Fazio, S., Biganzioli, F., De Laurentiis, V., Zampori, L., Sala, S., Diaconu, E., 2018. Supporting information to the characterisation factors of recommended EF Life Cycle Impact Assessment methods, version 2, from ILCD to EF 3.0. New Models and Differences with ILCD, EUR. https://doi.org/10.2760/002447.
Folliet, Michel, Milagros Rivas Saiz, J.S., 2017. Improving thermal and electric energy efficiency at cement plants. Improving Thermal and Electric Energy Efficiency at Cement Plants. https://doi.org/10.1596/28304.
Font, A., Soriano, L., de Moraes Pinheiro, S.M., Tashima, M.M., Monzó, J., Borrachero, M.V., Payá, J., 2020. Design and properties of 100% waste-based ternary alkali-activated mortars: blast furnace slag, olive-stone biomass ash and rice husk ash. J. Clean. Prod. 243. https://doi.org/10.1016/j.jclepro.2019.118568.
Formosa, J., Chimenos, J.M., Lacasta, A.M., Niubó, M., 2012. Interaction between low-grade magnesium oxide and boric acid in chemically bonded phosphate ceramics formulation. Ceram. Int. 38, 2483–2493. https://doi.org/10.1016/j.ceramint.2011.11.017.
Georgiades, M., Shah, I.H., Steubing, B., Cheeseman, C., Myers, R.J., 2023. Prospective life cycle assessment of European cement production. Resour. Conserv. Recycl. 194. https://doi.org/10.1016/j.resconrec.2023.106998.

Giro-Paloma, J., Mañosa, J., Maldonado-Alameda, A., Quina, M.J., Chimenos, J.M., 2019. Rapid sintering of weathered municipal solid waste incinerator bottom ash and rice husk for lightweight aggregate manufacturing and product properties. J. Clean. Prod. 232, 713–721. https://doi.org/10.1016/j.jclepro.2019.06.010.
Gong, X., Nie, Z., Wang, Z., Cui, S., Gao, F., Zuo, T., 2012. Life cycle energy consumption and carbon dioxide emission of residential building designs in Beijing: A comparative study. Journal of Industry Ecology 16, 576–587. https://doi.org/10.1111/j.1530-9290.2011.00415.x.
Griffiths, S., Sovacool, B.K., Furszyfer Del Rio, D.D., Foley, A.M., Bazilian, M.D., Kim, J., Uratani, J.M., 2023. Decarbonizing the cement and concrete industry: a systematic review of socio-technical systems, technological innovations, and policy options. Renew. Sustain. Energy Rev. https://doi.org/10.1016/j.rser.2023.113291.
Guo, Y., Luo, L., Liu, T., Hao, L., Li, Y., Liu, P., Zhu, T., 2024. A review of low-carbon technologies and projects for the global cement industry. J. Environ. Sci. (China). https://doi.org/10.1016/j.jes.2023.01.021.
Heijungs, R., Guinée, J.B., 2007. Allocation and "what-if" scenarios in life cycle assessment of waste management systems. Waste Manag. 27, 997–1005. https://doi.org/10.1016/j.wasman.2007.02.013.
Hossain, M.U., Poon, C.S., 2018. Comparative LCA of wood waste management strategies generated from building construction activities. J. Clean. Prod. 177, 387–397. https://doi.org/10.1016/j.jclepro.2017.12.233.
How 'Shared Socioeconomic Pathways, 2018. explore future climate change. URL. https://www.carbonbrief.org/explainer-how-shared-socioeconomic-pathways-explore-future-climate-change/.
Huete-Hernández, S., Maldonado-Alameda, A., Giro-Paloma, J., Chimenos, J.M., Formosa, J., 2021. Fabrication of sustainable magnesium phosphate cement micromortar using design of experiments statistical modelling: valorization of ceramic-stone-porcelain containing waste as filler. Ceram. Int. 47, 10905–10917. https://doi.org/10.1016/j.ceramint.2020.12.210.
International Energy Agency, 2021. World Energy Outlook 2021.
International Energy Agency, 2023. Technology Roadmap - Low-Carbon Transition in the Cement Industry.
Jiang, J., Chu, C., Song, L., Gao, X., Huang, B., Zhang, Yufei, Zhang, Yi, Liu, Y., Hou, L., Ju, M., Cao, Z., 2023. From prospecting to mining: a review of enabling technologies, LCAs, and LCCAs for improved construction and demolition waste management. Waste Manag. https://doi.org/10.1016/j.wasman.2023.01.017.
Kermeli, K., Edelenbosch, O.Y., Crijns-Graus, W., van Ruijven, B.J., Mima, S., van Vuuren, D.P., Worrell, E., 2019. The scope for better industry representation in long-term energy models: modeling the cement industry. Appl. Energy 240, 964–985. https://doi.org/10.1016/j.apenergy.2019.01.252.
Langkau, S., Steubing, B., Mutel, C., Permana, M., Lorenz, A., 2023. A stepwise approach for scenario - based inventory modelling for prospective LCA (SIMPL). Int. J. Life Cycle Assess. https://doi.org/10.1007/s11367-023-02175-9.
Luong, V.T., Amal, R., Scott, J.A., Ehrenberger, S., Tran, T., 2018. A comparison of carbon footprints of magnesium oxide and magnesium hydroxide produced from conventional processes. J. Clean. Prod. 202, 1035–1044. https://doi.org/10.1016/j.jclepro.2018.08.225.
Ma, H., Xu, B., Liu, J., Pei, H., Li, Z., 2014. Effects of water content, magnesia-to-phosphate molar ratio and age on pore structure, strength and permeability of magnesium potassium phosphate cement paste. Mater. Des. 64, 497–502. https://doi.org/10.1016/j.matdes.2014.07.073.
Ma, W., Liu, T., Hao, J.L., Wu, W., Gu, X., 2023. Towards a circular economy for construction and demolition waste management in China: critical success factors. Sustainable Chemistry and Pharmacy 35. https://doi.org/10.1016/j.scp.2023.101226.
Maes, B., Sacchi, R., Steubing, B., Pizzol, M., Audenaert, A., Craeye, B., Buyle, M., 2023. Prospective consequential life cycle assessment: identifying the future marginal suppliers using integrated assessment models. Renew. Sustain. Energy Rev. 188. https://doi.org/10.1016/j.rser.2023.113830.
Maldonado-Alameda, A., Lacasta, A.M., Giro-Paloma, J., Chimenos, J.M., Haurie, L., Formosa, J., 2017. Magnesium phosphate cements formulated with low grade magnesium oxide incorporating phase change materials for thermal energy storage. Construct. Build. Mater. 155, 209–216. https://doi.org/10.1016/j.conbuildmat.2017.07.227.
Maldonado-Alameda, A., Formosa, J., Chimenos, J.M., Huete-Hernández, S., Giro-Paloma, J., 2018. Geopolymer development based on the CSP residue as unique precursor. In: WASCON 2018. 10th International Conference on the Environmental and Technical Implications of Construction with Alternative Materials. Tampere, Finland.
Martínez-Rocamora, A., Solís-Guzmán, J., Marrero, M., 2016. LCA databases focused on construction materials: a review. Renew. Sustain. Energy Rev. https://doi.org/10.1016/j.rser.2015.12.243.
Mathias, T., 2009. Master of Science Thesis Principles of Benchmarking Criteria for the European Magnesia. University of Leoben, Austria.
Meinshausen, M., Nicholls, Z.R.J., Lewis, J., Gidden, M.J., Vogel, E., Freund, M., Beyerle, U., Gessner, C., Nauels, A., Bauer, N., Canadell, J.G., Daniel, J.S., John, A., Krummel, P.B., Luderer, G., Meinshausen, N., 2020. The shared socio-economic pathway (SSP) greenhouse gas concentrations and their extensions to 2500. Geosci. Model Dev. (GMD) 3571–3605. https://doi.org/10.5194/gmd-13-3571-2020, 2020.
Mendoza Beltran, A., Cox, B., Mutel, C., van Vuuren, D.P., Font Vivanco, D., Deetman, S., Edelenbosch, O.Y., Guinée, J., Tukker, A., 2020. When the background matters: using scenarios from integrated assessment models in prospective life cycle assessment. Journal of Industry Ecology 24, 64–79. https://doi.org/10.1111/jiec.12825.
Meng, X., Jiang, Y., Chen, B., Wang, L., 2023. Research progress on the setting time and solidification mechanism of magnesium phosphate cement: a review. Construct. Build. Mater. https://doi.org/10.1016/j.conbuildmat.2023.133612.
Müller, A., Harpprecht, C., Sacchi, R., Maes, B., van Sluisveld, M., Daioglou, V., Šavija, B., Steubing, B., 2024. Decarbonizing the cement industry: findings from coupling prospective life cycle assessment of clinker with integrated assessment model scenarios. J. Clean. Prod. 450. https://doi.org/10.1016/j.jclepro.2024.141884.
Munaro, M.R., Tavares, S.F., 2023. A review on barriers, drivers, and stakeholders towards the circular economy: the construction sector perspective. Cleaner and Responsible Consumption 8. https://doi.org/10.1016/j.clrc.2023.100107.
Niewiadomski, P., Karolak, A., Stefaniuk, D., Królicka, A., Szymanowski, J., Sadowski, Ł., 2021. Cement paste mixture proportioning with particle packing theory: an ambiguous effect of microsilica. Materials 14. https://doi.org/10.3390/ma14226970.
Normalización Española, 2018. UNE-EN_196-1:2018 Methods of Testing Cement - Part 1. Determination of strength.
Panesar, D.K., Seto, K.E., Churchill, C.J., 2017. Impact of the selection of functional unit on the life cycle assessment of green concrete. Int. J. Life Cycle Assess. 22, 1969–1986. https://doi.org/10.1007/s11367-017-1284-0.
Potsdam Institute for climate impact research - premise. https://premise.readthedocs.io/en/latest/introduction.html, 2023 (accessed 5.25.23).
Pryshlakivsky, J., Searcy, C., 2013. Fifteen years of ISO 14040: a review. J. Clean. Prod. https://doi.org/10.1016/j.jclepro.2013.05.038.
Real, S., Bogas, J.A., Carriço, A., Hu, S., 2021. Mechanical characterisation and shrinkage of thermoactivated recycled cement concrete. Appl. Sci. 11. https://doi.org/10.3390/app11062454.
Remind. https://github.com/remindmodel/remind, 2023 (accessed 7.28.23).
Riahi, K., Vuuren, D.P. Van, Kriegler, E., Edmonds, J., Neill, B.C.O., Fujimori, S., Bauer, N., Calvin, K., Dellink, R., Fricko, O., Lutz, W., Popp, A., Crespo, J., Kc, S., Leimbach, M., Jiang, L., Kram, T., Rao, S., Emmerling, J., Ebi, K., Hasegawa, T., Havlik, P., Humpenöder, F., Aleluia, L., Silva, D., Smith, S., Stehfest, E., Bosetti, V., Eom, J., Gernaat, D., Masui, T., Rogelj, J., Stre, J., Drouet, L., Krey, V., Luderer, G., Harmsen, M., Takahashi, K., Baumstark, L., Doelman, J.C., Kainuma, M., Klimont, Z., Marangoni, G., Lotze-campen, H., Obersteiner, M., Tabeau, A., Tavoni, M., 2017. The Shared Socioeconomic Pathways and their energy, land use, and greenhouse gas emissions implications. An overview 42, 153–168.
Ruan, S., Unluer, C., 2016. Comparative life cycle assessment of reactive MgO and Portland cement production. J. Clean. Prod. 137, 258–273. https://doi.org/10.1016/j.jclepro.2016.07.071.
Sacchi, R., Terlouw, T., Siala, K., Dirnaichner, A., Bauer, C., Cox, B., Mutel, C., Daioglou, V., Luderer, G., 2022. PRospective EnvironMental Impact assement (premise): a streamlined approach to producing databases for prospective life cycle assessment using integrated assessment models. Renew. Sustain. Energy Rev. 160. https://doi.org/10.1016/j.rser.2022.112311.
Scrivener, K., Habert, G., De Wolf, C.F.A., 2019. A Sustainable Future for the European Cement and Technology Assessment for Full Decarbonisation of the Industry by 2050.

Sinka, M., Van den Heede, P., De Belie, N., Bajare, D., Sahmenko, G., Korjakins, A., 2018. Comparative life cycle assessment of magnesium binders as an alternative for hemp concrete. Resour. Conserv. Recycl. 133, 288–299. https://doi.org/10.1016/j.resconrec.2018.02.024.

Sousa, V., Bogas, J.A., Real, S., Meireles, I., Carriço, A., 2023. Recycled cement production energy consumption optimization. Sustainable Chemistry and Pharmacy 32. https://doi.org/10.1016/j.scp.2023.101010.

Turk, J., Cotić, Z., Mladenovič, A., Šajna, A., 2015. Environmental evaluation of green concretes versus conventional concrete by means of LCA. Waste Manag. 45, 194–205. https://doi.org/10.1016/j.wasman.2015.06.035.

Valipour, M., Yekkalar, M., Shekarchi, M., Panahi, S., 2014. Environmental assessment of green concrete containing natural zeolite on the global warming index in marine environments. J. Clean. Prod. 65, 418–423. https://doi.org/10.1016/j.jclepro.2013.07.055.

Wang, Q., Xu, X., Liang, K., 2021. The impact of environmental regulation on firm performance: evidence from the Chinese cement industry. J. Environ. Manag. 299. https://doi.org/10.1016/j.jenvman.2021.113596.

Wang, N., Xu, Z., Liu, Z., 2023. Innovation in the construction sector: bibliometric analysis and research agenda. Journal of Engineering and Technology Management - JET-M 68. https://doi.org/10.1016/j.jengtecman.2023.101747.

3.3.4. Additional research contribution

In addition to the measurements presented in the publication, an initial analysis was carried out on the resources' consumption impact category, specifically focusing on cumulative energy demand from non-renewable fossil sources, to further complement the material investigation. The nomenclature used in this analysis follows that of *Publication 3*. Table 3.1 provides a summary of the impact category, including the respective indicator and units applied in this study.

Table 3.1. Impact categories used in this study.

Impact categories	Category Indicators	Units
Resource consumption	Energy resources: non-renewable, abiotic depletion potential (ADP), fossil fuels	MJ, net calorific value

In the first scenario, focused on electricity, the assessed impact category is fossil fuel resource consumption, measured in megajoules (MJ). For the mortars, Figure 3.9 illustrates the contributions of individual materials to the fossil fuel consumption indicator under the SSP2-Base and SSP2-RCP1.9 pathways for the year 2050. Specifically, the contributions under the SSP2-RCP1.9 pathway are further detailed to highlight specific trends and materials influences.

i) OPC-CEM I mortar: the majority of its environmental impact (64.1%) originates from OPC, with 61.1% of this specifically attributed to clinker production.
ii) MPC-MgO mortar: a significant portion of its impact (79.6%) is due to MKP, while 2.4% is associated with magnesium oxide production, and an additional 7.4% results from the secondary calcination process.
iii) MPC-TUN mortar: MKP accounts for 78.3% of the total impacts, with 44.9% attributed to phosphoric acid and 33.4% to potassium hydroxide. In addition, 1.3% of the impact is associated to HB, and 0.5% is associated with the TUN conditioning process.

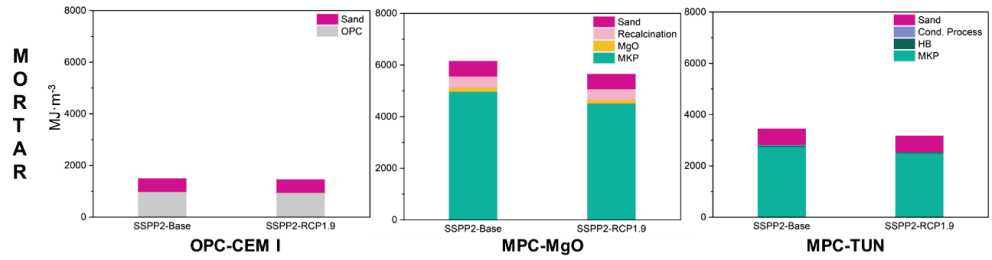

Figure 3.9. Contributions of mortars to the impacts on resource consumption (MJ) for the electricity scenario in 2050.

The results for all evaluated materials and timeframes are presented in Figure 3.10. The remaining contribution to the environmental impact of each material is associated with the use of silica sand. The findings for this impact category reveal the following trends:

- OPC-CEM I exhibits the lowest fossil fuel (MJ) impact, followed by MPC-TUN and MPC-MgO.
- Regarding energy consumption, the primary energy-intensive activity for OPC-CEM I is clinker production, while for MPC-MgO is the calcination of magnesium oxide and MKP production. For MPC-TUN, the predominant energy-consuming activity is MKP production. Therefore, the major contributors to fossil fuel consumption align with the previously mentioned factors.

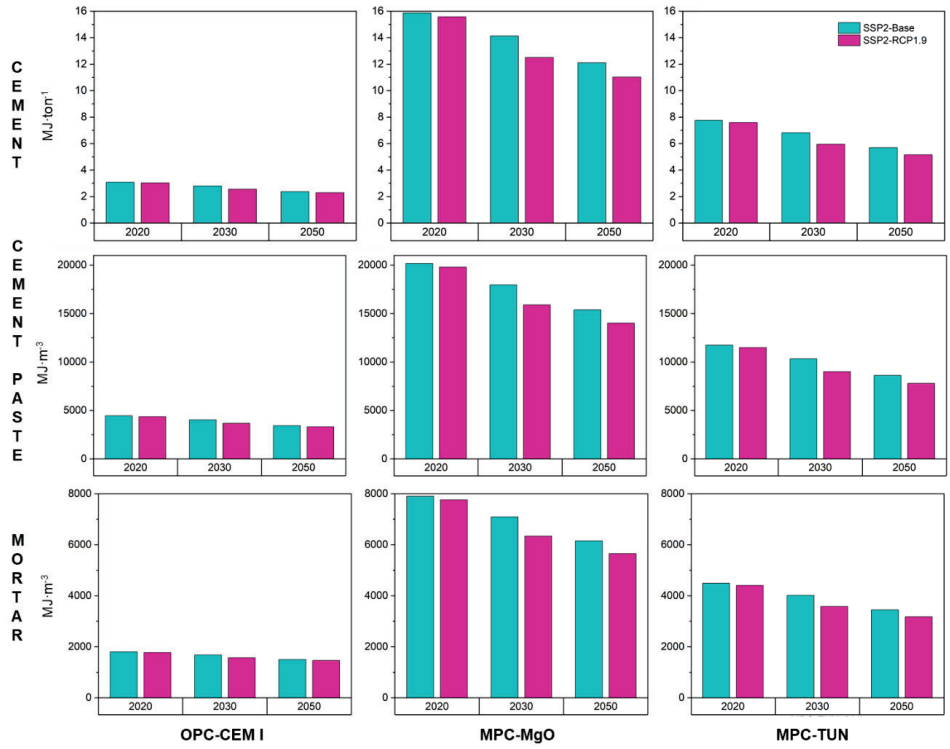

Figure 3.10. Results for the resource consumption category under electricity scenario.

Moreover, it is evident that the impacts decrease year after year. This trend can be attributed to the ongoing reduction in fossil-fuel based electricity generation in both scenarios. Besides, the impacts under SSP2-RCP1.9 pathway are consistently lower than those under the SSP2-Base pathway. This difference could be explained by the more rapid-out of fossil electricity and the greater integration of low-carbon energy sources in SSP2-RCP1.9, aligning with the objectives set forth in the Paris Agreement. Finally, it is important to note that MPC-TUN exhibits a 118% higher impact in terms of resource consumption (measured in MJ) compared to OPC-CEM I. Nevertheless, MPC-TUN shows a significantly reduction of 44%, when compared to MPC-MgO.

In the case of the second scenario, fuel and electricity scenario, the results measured in MJ, are illustrated in Figure 3.11. In addition, Figure 3.12 shows the environmental contributions of mortars for each material in the SSP2-Base and SSP2-RCP1.9 scenarios for 2050, considering future assumptions.

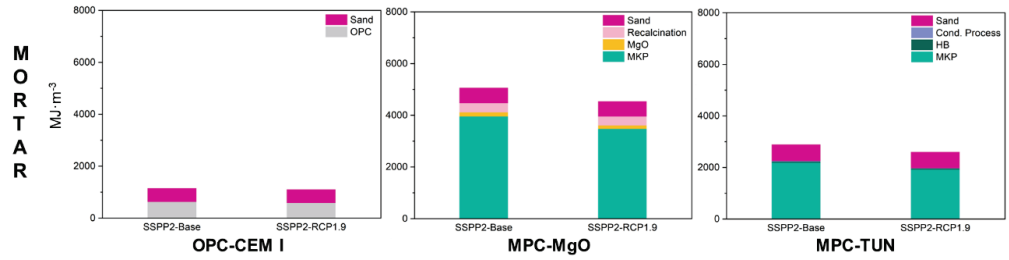

Figure 3.11. Contributions of resource consumption for the electricity and fuel scenario.

The mortar that exhibits the lowest environmental impact on fossil fuel resources consumption is OPC-CEM I, yet it has the highest carbon footprint. The following differences of impact contributions are observed for each mortar type for SSP2-RCP1.9 pathway:

i) For OPC-CEM I, fossil fuel consumption is reduced from 1775 MJ in 2020 to 1104 MJ in 2050 (reduction of ≈ 38%).

ii) For MPC-MgO, fossil fuel consumption decreases from 7765 MJ in 2020 to 4538 MJ in 2050 (reduction of ≈ 42%).

iii) For MPC-TUN, fossil fuel consumption diminishes from 4408 MJ in 2020 to 2602 MJ in 2050 (reduction of ≈ 41%).

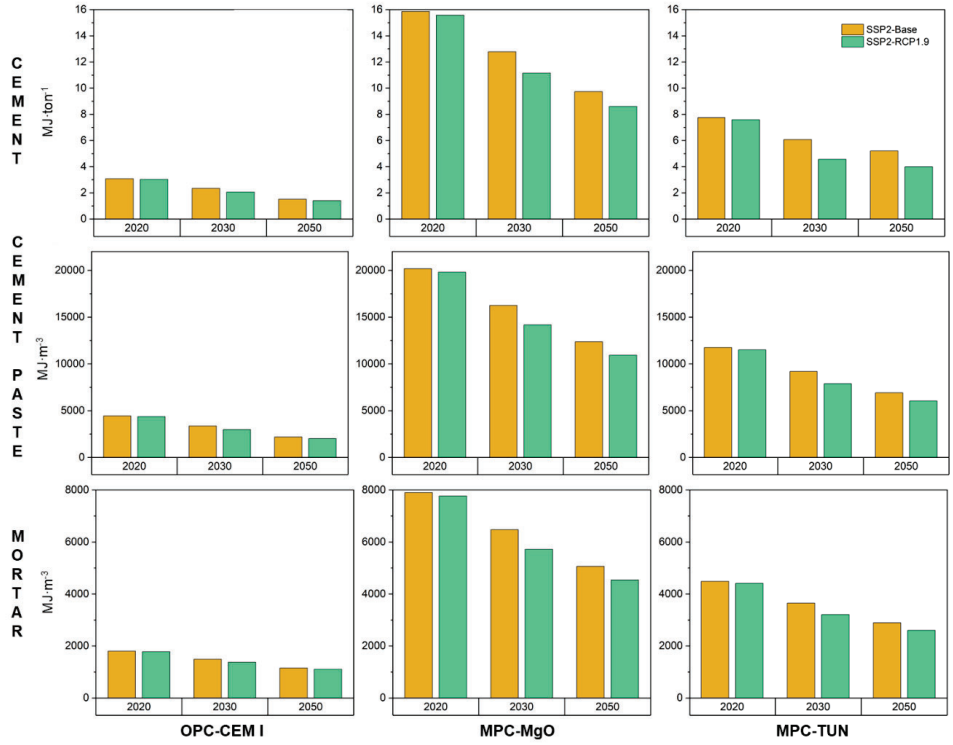

Figure 3.12. Resource consumption category for electricity and fuel scenario.

A particularly significant aspect of this scenario lies in the notable decrease in values when compared to the previous scenario. This emphasizes the pivotal role that fuel sources play across various sectors and underscores their profound influence on environmental impact.

However, the presence of MKP in MPC presents another significant environmental challenge. To promote sustainable development, it is vital to investigate methods for decreasing the emissions and energy demand linked to MKP production or to identify alternative sources for acquiring this material. The pursuit of various wastes sources or more eco-friendly methods for producing MKP is essential for further improving the sustainability of MPC-based mortars.

Finally, it is important to note that this is a preliminary study. As indicated in the publication, several assumptions have been made to scale up the alternative material

to an industrial level to assess environmental viability. These assumptions are essential for assessing the associated environmental impacts [30]. Environmental research adds significant value to the search for alternative materials [31]. The findings will support the development of new materials and promote their future standardization in the industrial construction sector [32].

3.4. References

[1] J. Formosa, J.M. Chimenos, A.M. Lacasta, M. Niubó, Interaction between low-grade magnesium oxide and boric acid in chemically bonded phosphate ceramics formulation, Ceramics International 38 (2012) 2483–2493. https://doi.org/10.1016/j.ceramint.2011.11.017.

[2] Y. Liu, Z. Qin, B. Chen, Influence of low-grade bauxite on the properties of magnesium phosphate cement, Construction and Building Materials 242 (2020). https://doi.org/10.1016/j.conbuildmat.2020.118052.

[3] Bo Pang, Jun Liu, Baomin Wang, Runqing Liu, Yuanquan Yang, Effects of K-struvite on hydration behavior of magnesium potassium phosphate cement, Construction and Building Materials 275 (2021).

[4] M. Le Rouzic, T. Chaussadent, G. Platret, L. Stefan, Mechanisms of k-struvite formation in magnesium phosphate cements, Cement and Concrete Research 91 (2017) 117–122. https://doi.org/10.1016/j.cemconres.2016.11.008.

[5] J.O. Ighalo, A.G. Adeniyi, A perspective on environmental sustainability in the cement industry, Waste Dispos. Sustain. Energy 2 (2020) 161–164. https://doi.org/10.1007/s42768-020-00043-y.

[6] A. Alfocea-Roig, S. Huete-Hernández, X. García-Zubiri, J. Giro-Paloma, J. Formosa, Can tundish deskulling waste be used as a magnesium oxide source to develop magnesium phosphate cement?, Journal of Environmental Chemical Engineering 11 (2023). https://doi.org/10.1016/j.jece.2023.110618.

[7] K. Sotiriadis, P. Mácová, A.S. Mazur, P.M. Tolstoy, A. Viani, A solid state NMR and in-situ infrared spectroscopy study on the setting reaction of magnesium sodium phosphate cement, Journal of Non-Crystalline Solids 498 (2018) 49–59. https://doi.org/10.1016/j.jnoncrysol.2018.06.006.

[8] A. Viani, P. Mácová, R. Ševčík, L. Zárybnická, Mechanism of magnesium phosphate cement retardation by citric acid, Ceramics International 49 (2023) 11112–11122. https://doi.org/10.1016/j.ceramint.2022.11.308.

[9] M.A. Goldberg, P.A. Krohicheva, A.S. Fomin, D.R. Khairutdinova, O.S. Antonova, A.S. Baikin, V.V. Smirnov, A.A. Fomina, A.V. Leonov, I.V. Mikheev, N.S. Sergeeva, S.A. Akhmedova, S.M. Barinov, V.S. Komlev, In situ magnesium calcium phosphate cements formation: From one pot powders precursors synthesis to in vitro investigations, Bioactive Materials 5 (2020) 644–658. https://doi.org/10.1016/j.bioactmat.2020.03.011.

[10] I. Kabdaşlı, A. Siciliano, C. Limonti, O. Tünay, Is K-Struvite Precipitation a Plausible Nutrient Recovery Method from Potassium-Containing Wastes?—A Review, Sustainability (Switzerland) 14 (2022). https://doi.org/10.3390/su141811680.

[11] R.C.D.S. Meira, S.P.A.D. Paz, J.A.M. Corrêa, XRD-Rietveld analysis as a tool for monitoring struvite analog precipitation from wastewater: P, Mg, N and K recovery for fertilizer production, Journal of Materials Research and Technology 9 (2020) 15202–15213. https://doi.org/10.1016/j.jmrt.2020.10.082.

[12] A. Moropoulou, A. Bakolas, K. Bisbikou, Investigation of the technology of historic mortars, Journal of Cultural Heritage 1 (2000) 45–58. https://doi.org/10.1016/S1296-2074(99)00118-1.

[13] A. Arizzi, G. Cultrone, Mortars and plasters—how to characterise hydraulic mortars, Archaeol Anthropol Sci 13 (2021) 144. https://doi.org/10.1007/s12520-021-01404-2.

[14] M.C. Bignozzi, Sustainable Cements for Green Buildings Construction, Procedia Engineering 21 (2011) 915–921. https://doi.org/10.1016/j.proeng.2011.11.2094.

[15] K.A. Knight, P.R. Cunningham, S.A. Miller, Optimizing supplementary cementitious material replacement to minimize the environmental impacts of concrete, Cement and Concrete Composites 139 (2023). https://doi.org/10.1016/j.cemconcomp.2023.105049.

[16] T. Santos, J. Almeida, J.D. Silvestre, P. Faria, Life cycle assessment of mortars: A review on technical potential and drawbacks, Construction and Building Materials 288 (2021). https://doi.org/10.1016/j.conbuildmat.2021. 123069.

[17] K. Krueger, A. Stoker, G. Gaustad, "Alternative" materials in the green building and construction sector: Examples, barriers, and environmental analysis, SASBE 8 (2019) 270–291. https://doi.org/10.1108/SASBE-09-2018-0045.

[18] H. AzariJafari, G. Guest, R. Kirchain, J. Gregory, B. Amor, Towards comparable environmental product declarations of construction materials: Insights from a probabilistic comparative LCA approach, Building and Environment 190 (2021). https://doi.org/10.1016/j.buildenv.2020.107542.

[19] D.N. Huntzinger, T.D. Eatmon, A life-cycle assessment of Portland cement manufacturing: comparing the traditional process with alternative technologies, Journal of Cleaner Production 17 (2009) 668–675. https://doi.org/10.1016/j.jclepro.2008.04.007.

[20] S. Nie, J. Zhou, F. Yang, M. Lan, J. Li, Z. Zhang, Z. Chen, M. Xu, H. Li, J.G. Sanjayan, Analysis of theoretical carbon dioxide emissions from cement production: Methodology and application, Journal of Cleaner Production 334 (2022). https://doi.org/10.1016/j.jclepro.2021.130270.

[21] A.V. Agbedahin, Sustainable development, Education for Sustainable Development, and the 2030 Agenda for Sustainable Development: Emergence, efficacy, eminence, and future, Sustainable Development 27 (2019) 669–680. https://doi.org/10.1002/sd.1931.

[22] C.L. Carpentier, H. Braun, Agenda 2030 for Sustainable Development: A powerful global framework, Journal of the International Council for Small Business 1 (2020) 14–23. https://doi.org/10.1080/26437015.2020.1714356.

[23] M.A.B. Omer, T. Noguchi, A conceptual framework for understanding the contribution of building materials in the achievement of Sustainable Development Goals (SDGs), Sustainable Cities and Society 52 (2020). https://doi.org/10.1016/j.scs.2019.101869.

[24] S. Fawzy, A.I. Osman, J. Doran, D.W. Rooney, Strategies for mitigation of climate change: a review, Environ Chem Lett 18 (2020) 2069–2094. https://doi.org/10.1007/s10311-020-01059-w.

[25] S.A. Miller, G. Habert, R.J. Myers, J.T. Harvey, Achieving net zero greenhouse gas emissions in the cement industry via value chain mitigation strategies, One Earth 4 (2021) 1398–1411. https://doi.org/10.1016/j.oneear.2021.09.011.

[26] Y. Guo, L. Luo, T. Liu, L. Hao, Y. Li, P. Liu, T. Zhu, A review of low-carbon technologies and projects for the global cement industry, Journal of Environmental Sciences (China) 136 (2024) 682–697. https://doi.org/10.1016/j.jes.2023.01.021.

[27] G. Terán-Cuadrado, F. Tahir, A. Nurdiawati, M.A. Almarshoud, S.G. Al-Ghamdi, Current and potential materials for the low-carbon cement production: Life cycle assessment perspective, Journal of Building Engineering 96 (2024). https://doi.org/10.1016/j.jobe.2024.110528.

[28] M. Georgiades, I.H. Shah, B. Steubing, C. Cheeseman, R.J. Myers, Prospective life cycle assessment of European cement production, Resources, Conservation and Recycling 194 (2023). https://doi.org/10.1016/j.resconrec.2023.106998.

[29] A. Alfocea-Roig, A. Müller, B. Steubing, S. Huete-Hernández, J. Giro-Paloma, J. Formosa, Life cycle assessment of the climate change impact of magnesium phosphate cements formulated with tundish deskulling waste compared to conventional cement, Sustainable Chemistry and Pharmacy 42 (2024). https://doi.org/10.1016/j.scp.2024.101802.

[30] O.E. Ige, O.A. Olanrewaju, K.J. Duffy, C. Obiora, A review of the effectiveness of Life Cycle Assessment for gauging environmental impacts from cement production, Journal of Cleaner Production 324 (2021). https://doi.org/10.1016/j.jclepro.2021.129213.

[31] N. Mohamad, K. Muthusamy, R. Embong, A. Kusbiantoro, M.H. Hashim, Environmental impact of cement production and Solutions: A review, Materials Today: Proceedings 48 (2022) 741–746. https://doi.org/10.1016/j.matpr.2021.02.212.

[32] P. Busch, A. Kendall, C.W. Murphy, S.A. Miller, Literature review on policies to mitigate GHG emissions for cement and concrete, Resources, Conservation and Recycling 182 (2022). https://doi.org/10.1016/j.resconrec.2022. 106278.

Chapter 4

CHAPTER 4

CHARACTERIZATION OF MPC FORMULATIONS

This chapter focuses on expanding the characterization of MPC formulations incorporating by-products and wastes. The objective is to study the physicochemical and mechanical properties while studying the synergy between these materials. In addition, the incorporation of natural fibres is examined in detail to expand strategies to optimize these formulations in different applications.

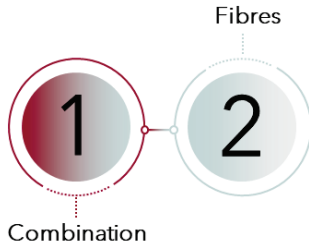

4.1. Combination

4.1.1. Introduction

Recent studies have highlighted the potential applications of alternative materials in the cement and construction industries, emphasizing the value of utilizing industrial by-products and wastes materials as sustainable raw materials. LG-MgO, a magnesium oxide-rich by-product, is collected in the exhaust gas system as a cyclone dust during the calcination of magnesite and/or dolomite ores for the industrial production of magnesium oxide mainly commercialized for refractory purposes. The production of such by-products tends to rise in response to the growing demand in various industries for magnesite [1–5]. A similar trend is observed with TUN, as steel production increases globally, the generation of TUN as a waste product also escalates [6–9].

Therefore, as discussed earlier, both LG-MgO and TUN have the potential to serve as alternative magnesium oxide sources in the development of MPC. In this study, mixtures of TUN and LG-MgO were prepared at weight ratios of 100/0, 75/25, 50/50, 25/75, and 0/100. These formulations were used to assess the impact of the magnesium

oxide source composition on the final properties of MPC binders, with a focus on their chemical, physical, mechanical, and environmental characteristics. Particular emphasis was placed on porosity characterization to understand its influence on the performance of the MPC and how the use of these two alternative raw materials affects the material's properties [10,11].

The main goal of the present PhD research was to evaluate the effect of secondary content and the final properties for evaluating the suitability of TUN and LG-MgO as sustainable replacements for traditional magnesium oxide, aiming to optimize binder performance while reducing the environmental impact. The next sections briefly describe the key points of this study, as well as the main contributions.

4.1.2. Relevance

The novelty of this investigation lies in the utilization of secondary magnesium oxide sources, specifically TUN and LG-MgO, marking a significant advancement in sustainable materials research as shown in Figure 4.1. Additionally, the synergistic behaviour of these precursors has been studied for the first time. A key contribution of this PhD research is the demonstration of the feasibility of formulating MPC binders using a combination of TUN and LG-MgO. In addition, this research emphasizes the characterization of porosity to analyse the type of pores present and their interconnectivity as an analysis conducted for the first instance with these specific materials.

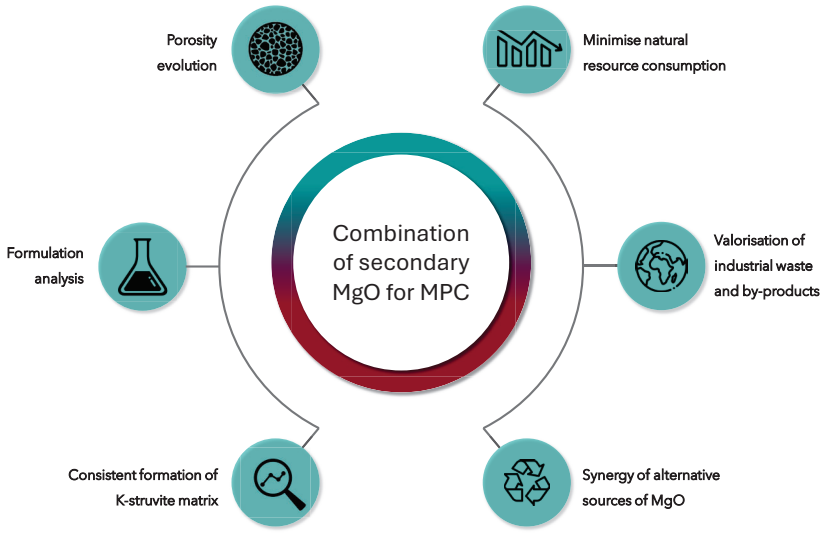

Figure 4.1. Advantages of research on MPC development using a combination of two alternative raw materials.

4.1.3. Publication 4

Publication 4, titled "Secondary sources of MgO for the development of magnesium phosphate cement: approach to sustainable construction" is currently under review in a high-ranked journal, Environmental Chemical Engineering (JIF of 7.4 in 2023, Q1), submitted on March 27th 2025. The publication's title is shown in Figure 4.2, and the full text is included in this manuscript.

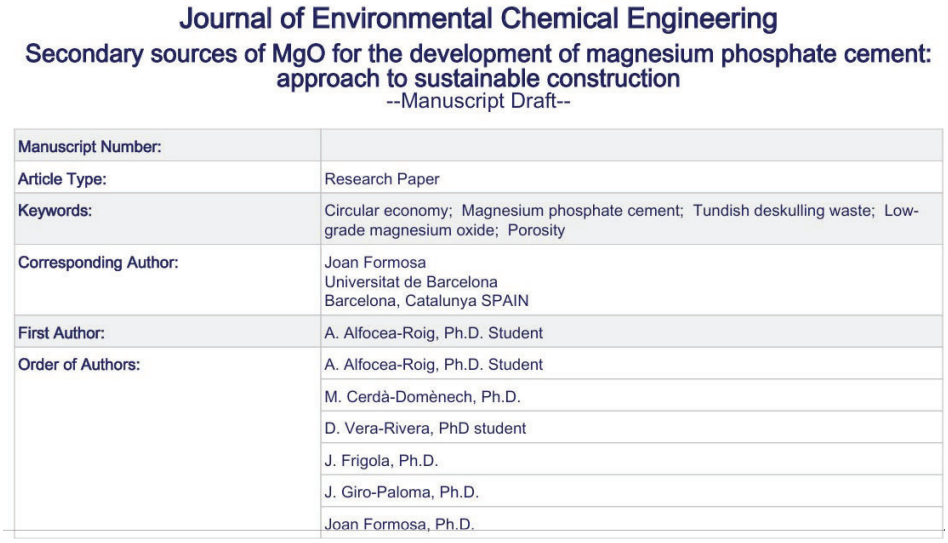

Journal of Environmental Chemical Engineering

Secondary sources of MgO for the development of magnesium phosphate cement: approach to sustainable construction

--Manuscript Draft--

Manuscript Number:	
Article Type:	Research Paper
Keywords:	Circular economy; Magnesium phosphate cement; Tundish deskulling waste; Low-grade magnesium oxide; Porosity
Corresponding Author:	Joan Formosa Universitat de Barcelona Barcelona, Catalunya SPAIN
First Author:	A. Alfocea-Roig, Ph.D. Student
Order of Authors:	A. Alfocea-Roig, Ph.D. Student
	M. Cerdà-Domènech, Ph.D.
	D. Vera-Rivera, PhD student
	J. Frigola, Ph.D.
	J. Giro-Paloma, Ph.D.
	Joan Formosa, Ph.D.

Figure 4.2. Headline of the article under review, entitled "Secondary sources of MgO for the development of magnesium phosphate cement: approach to sustainable construction".

Secondary sources of MgO for the development of magnesium phosphate cement: approach to sustainable construction

A. Alfocea-Roig[1], M. Cerdà-Domènech[2], D. Vera-Rivera[1], J. Frigola[2], J. Giro-Paloma[1], J. Formosa[1,*]

[1]Departament de Ciència de Materials i Química Física, Universitat de Barcelona, Martí i Franquès 1-11, 08028, Barcelona, Spain. Ph: +34-934021316

[2]GRC Geociències Marines, Dept. Dinàmica de la Terra i de l'Oceà, Facultat de Ciències de la Terra, Universitat de Barcelona, Martí i Franquès s/n, 08028, Barcelona, Spain

*Corresponding author

E-mail address: joanformosa@ub.edu

ABSTRACT

Magnesium phosphate cements (MPCs) are typically produced from pure raw materials, resulting in significant environmental impacts. This study evaluates five MPC formulations incorporating the combination of two secondary resources as MgO source: tundish deskulling waste (TUN) and low-grade MgO (LG). The hydration process was analysed using time-dependent in situ FTIR-ATR spectroscopy and isothermal conduction calorimetry, revealing distinct behaviours based on TUN and LG content. Micro-X-ray computed tomography showed that 100 wt.% TUN formulations exhibited higher porosity, decreasing from 13.25% at 2 days to 9.55% at 28 days, while 100 wt. % LG formulations maintained stable porosity (~2.38%) throughout curing times. These findings correlate with hydration observations and the indefinite phase detected by ^{31}P MAS NMR spectroscopy in 100 wt. % TUN formulations. These insights are supported by the higher compressive strength performance of formulations containing LG, which increased from 17 MPa to 30 MPa.

KEYWORDS

Circular economy; Magnesium phosphate cement; Tundish deskulling waste; Low-grade magnesium oxide; Porosity

1. INTRODUCTION

Cement stands as one of the most widely used materials in contemporary construction due to its pivotal role as the primary constituent in concrete, the globally dominant construction material. Specifically, it is a fine powder, which serves as a binding agent. Its significance arises from its property to harden through chemical interactions with water during a process known as setting. Cement offers several remarkable advantages, including cost-efficiency, exceptional strength, and durability, as well as versatile applications. It constitutes a crucial material directly related with societal progress [1]. Therefore, the dependency of global society on this material is irrefutable.

Ordinary Portland cement (OPC), the most used cement today, presents many benefits for the construction industry, but it also leads to enormous environmental and health hazards. In fact, the manufacture of cement is responsible for 8% of greenhouse gas emissions [2]. Consequently, a range of initiatives and commitments have been established to alleviate the industry's environmental impact, all with the ultimate goal of achieving carbon neutrality by 2050 [3]. One potential strategy for addressing this challenge is the development of new cements incorporating alternative materials. Through technological progress and increased demand, alternative construction materials are regularly found [1], [4], [5]. For example, magnesium phosphate cement (MPC) is one of those alternative cements, which includes MKPCs (magnesium potassium phosphate cements) [6]. MKPCs are obtained from mixing a source of magnesium oxide (MgO), a source of potassium-phosphate (usually KH_2PO4) and water to obtain a phosphate salt known as K-struvite ($MgKPO_4 \cdot 6H_2O$) [7], [8], [9].

Research into novel materials has special significance as it seeks to determine their viability as crucial components in the construction industry to mitigate climate change and reduce the depletion of natural resources, among other aspects. It is imperative to recognize that cement will persist as the primary building material both presently and in the foreseeable future, due to its pivotal role in shaping our urban and suburban landscapes in the coming years. Therefore, it is necessary to make efforts and changes, to move towards the transition of an ethical, fair, sustainable, and economically viable cement [1].

For this reason, it is necessary to search new cements with a different composition but which at the same time have the appropiate properties to be applicable in the construction sector. One of the aspects limiting the use and applications of MKPCs is their high cost [10], [11], [12], [13]. These costs are mainly due to two factors. On the one hand, the high price of raw materials, mainly because of the increase in the price of phosphate chemicals. On the other hand, when using primary sources of MgO, it must be thermal treated to adjust its reactivity for the correct formation of the cementitious material [14], [15]. In the latter case, the authors have developed in recent years MKPCs from secondary MgO sources, such as TUN and LG [8], [16], [17]. These secondary sources allow a

substantial reduction in the cost of the cement finally developed, since they avoid the conventional heat treatment necessary when using high purity MgO. Furthermore, studies have demonstrated that these cements could result in a lower CO_2 footprint compared to traditional formulations [16]. This thermal treatment is usually carried out at around 1200 ºC (which entails not only economic costs, but also energy costs and CO_2 emissions).

Porosity is an important property to examine and understand since it is directly connected to resistance and durability [18], [19]. This study is focused on exploring alternative secondary sources of MgO from wastes and industrial by-products to develop MKPCs with the aim of advancing the principles of the circular economy while minimizing reliance on landfills. Particularly, we investigate the porosity by micro X-ray computed tomography (mCT) of the different alternative cements to evaluate their potential to be applicable in the construction and building sector [19], [20], [21], [22]. Therefore, this research sheds light on the formation mechanism and performance of MKPCs formulated by using secondary sources of MgO.

2. MATERIALS AND METHODS

2.1. Raw materials

The MgO sources used in the research of this paper are a waste named tundish deskulling waste (TUN) and an industrial by-product known as Low Grade-MgO (LG) [23], [24]. Both materials were comprehensively characterized in previous studies by the authors to verify the viability to achieve K-struvite (MKPC) [8], [25]. Specifically, TUN and LG composition are 61 wt.% and 50 wt.% of MgO, respectively, as shown in Table 1. In addition, the following major phases can also be visualized in Table 1, which are magnesium hydroxide and calcium oxide for the TUN, and magnesium carbonate and calcium carbonate for the LG, among other compounds. Furthermore, although TUN has a density comparable to LG (3.06 ± 0.04 $g \cdot cm^{-3}$), it is characterized by smaller particle dimensions and a reduced surface area. Specifically, the BET analysis reveals values of 3.6 $m^2 \cdot g^{-1}$ for TUN and 12.9 $m^2 \cdot g^{-1}$ for LG. The reactivity of both secondary MgO sources is considered adequate for MPC development, as both are classified as dead burned magnesite (DBM) with low reactivity according to the citric acid reactivity test (CART). However, LG demonstrates slightly shorter times, indicating higher reactivity. Magnesitas Navarras, S.A. company located in Navarra (Spain) supplied the materials.

Table 1. Estimated composition (wt.%) of TUN, and LG by XRD-TG/DTG-XRF performed in previous studies sorted by element and reactivity [8], [25].

TUN (wt.%)							
MgO	$Mg(OH)_2$	$CaMg_{0.27}Fe_{0.73}(CO_3)_2$	CaO	$Ca(OH)_2$	$CaCO_3$	$CaSO_4$	Others
61.42	6.9	5.27	6.05	1.04	1.27	2.51	15.54
LG (wt.%)							
MgO	$Mg(OH)_2$	$MgCO_3$	$MgCa(CO_3)_2$	$MgSO_4$	$CaCO_3$	$Ca_5Si_6O_{16}(OH)_2$	Others
50.13	2.11	21.21	5.19	2.12	13.7	2.21	3.33

On the one hand, TUN is a refractory material used in the last metallurgical container before the steel solidification. After its useful life, this material is conditioned to remove undesired components and reach the appropriate granulometry. On the other hand, LG is a by-product produced in the calcination of $MgCO_3$ to generate MgO. It is mainly a dust generated by the cyclone filters, which separate the partially calcined solid particles from the gas stream [19], [20].

2.2. Samples preparation

A total of five formulations have been developed by adjusting the proportions of the two sources of MgO used in this research. Based on the preliminary studies from the authors, all the formulations were developed with a 60 wt.% of MgO source and 40 wt.% phosphate sources (monopotassium phosphate, MKP, KH_2PO_4) [8], [16], [25]. In addition, 1 wt.% relative to the total solid mass of boric acid (H_3BO_3) was added as a setting retarder and to limit thermal expansion [26]. Additionally, throughout the formulation of the samples, a mixing protocol was maintained, which involved mixing the solid components for 60 seconds, followed by an additional 180 seconds of mixing after the addition of water. Samples were prepared with varying W/C (water/cement) ratios, as detailed in Table 2, ensuring that all pastes maintained a uniform consistency within 10% of the reference value of 110 mm. This approach was adopted to ensure uniform workability and applicability across all samples.

Table 2. Formulation proportions, mean consistencies, and setting times determined by the Vicat needle method.

Formulations	TUN (wt.%)	LG (wt.%)	W/C	Mean consistency (mm)	IST (min)	FST (min)
100TUN-0LG	100	0	0.22	119 ± 2	32.5 ± 0.5	34.5 ± 0.5
75TUN-25LG	75	25	0.26	111 ± 0	42.5 ± 0.5	46.0 ± 1.0
50TUN-50LG	50	50	0.26	104 ± 1	44.5 ± 0.5	47.5 ± 0.5
25TUN-75LG	25	75	0.27	108 ± 3	41.5 ± 0.5	50.5 ± 0.5
0TUN-100LG	0	100	0.28	109 ± 2	69.5 ± 0.5	81.5 ± 0.5

The mixtures were poured in moulds of 4 x 4 x 4 cm^3. The moulds were removed after 24 hours, and the samples were cured at room temperature (20 ± 1 ºC) with a controlled relative humidity of ~60 ± 5% for different period times, 2, 7, and 28 days, for further characterization.

2.3. Characterization

The fresh state of the mixtures was evaluated by determining the slump test following the UNE-EN 1015-9, and the initial and final setting time (IST and FST, respectively) from the Vicat needle test based on EN 196-3.

Furthermore, Isothermal Conduction Calorimetry (ICC) experiments were performed using an isothermal calorimeter TAM Air 8-channel (TA Instruments). The calorimeter was maintained at a constant temperature of 20 ºC throughout the experiment. For this procedure, the batches were prepared directly within the calorimeter. Water was introduced into the solid powder using an Ad-Mix system, which included a sealed glass ampoule fitted with a stirring rotor and a syringe for injecting the liquid. Data collection began at the moment of water injection, marking the first interaction between the water and the powder, thereby initiating the reaction. The paste was then mixed for 180 seconds, and the heat flow was monitored over a period of 70 hours. On the other hand, in situ Fourier transform infrared spectroscopy in attenuated total reflectance mode (FTIR-ATR) have been collected using the Spectrum Two™ instrument from PerkinElmer to analyse the symmetric and asymmetric stretching vibration bonds during setting. To perform this analysis, a specialized device known as the Top Plate SP2 UATR Arrow is required. The spectral range 4000-450 cm^{-1} with a resolution of 4 cm^{-1} was acquired by averaging 4 scans for each spectrum. The total number of spectra collected was 1008 with approximately 15-second intervals between spectra, concluding the experiment after 360 minutes.

The five formulations (each 4 x 4 x 4 cm^3) at different curing times (2, 7 and 28 days) were scanned using a multiresolution micro-CT system at the CORELAB Laboratory from the Faculty of Earth Sciences of the University of Barcelona. It includes an X-ray source type open microfocus

XWT 190 SE with a maximum energy of 180kV, 300W and 1.6 mA, which allows an optimum maximum resolution less than 4 □m, and a flat panel detector of 20 cm in size. The samples were scanned at tube conditions of 120 kV and 35 W using a 0.5 mm Cu filter, for a total of 1200 projections of 400 ms exposure time each, recorded over a 360º rotation, resulting in a scan duration of 46 minutes per sample, and obtaining a voxel size resolution of 35 µm.

The image analysis was achieved using Avizo® software at the CORELAB Laboratory. Post-processing images workflow was developed to perform a morphometric analysis of the sample porosity. The initial step involved applying a bilateral filter algorithm to denoise the scalar volume data, followed by implementing a delineate filter to enhance the edges of objects, thereby improving object differentiation. The second step was segmentation of the 3D data to divide the image into various materials (i.e., matrix and porosity – air), which was obtained through the application of multiple morphological transformations including masking and closing de scalar volume data and removing small holes (Figure 1). Finally, the detailed characterization of the porosity was carried out by measuring the length, volume, and sphericity of the porous in an inner subregion of 2 x 2 x 4 cm^3 within the samples to reduce border effects during the formulation process within the mould.

The pore volume can be determined by summing the voxels that constitute each pore. Given the image volume resolution is 35 µm, this study defines the minimum pore size as a pore composed of 4 x 4 x 4 voxels, excluding pores of smaller sizes. The sphericity of a pore (S) (Eq. 1) can be defined as the ratio of the equivalent spherical surface area relative to the measured surface area [27]:

$$S = \sqrt[3]{\frac{36\pi V_p^2}{S_P^3}} \qquad \text{Eq. 1}$$

Where V_p is the volume of the pore, and S_p is the surface area of the pore, and values close to 1 correspond to more spherical pore. The pore network model was extracted from the segmented images using the MATLAB package developed by Rabbani and Jamshidi (2014) [28].

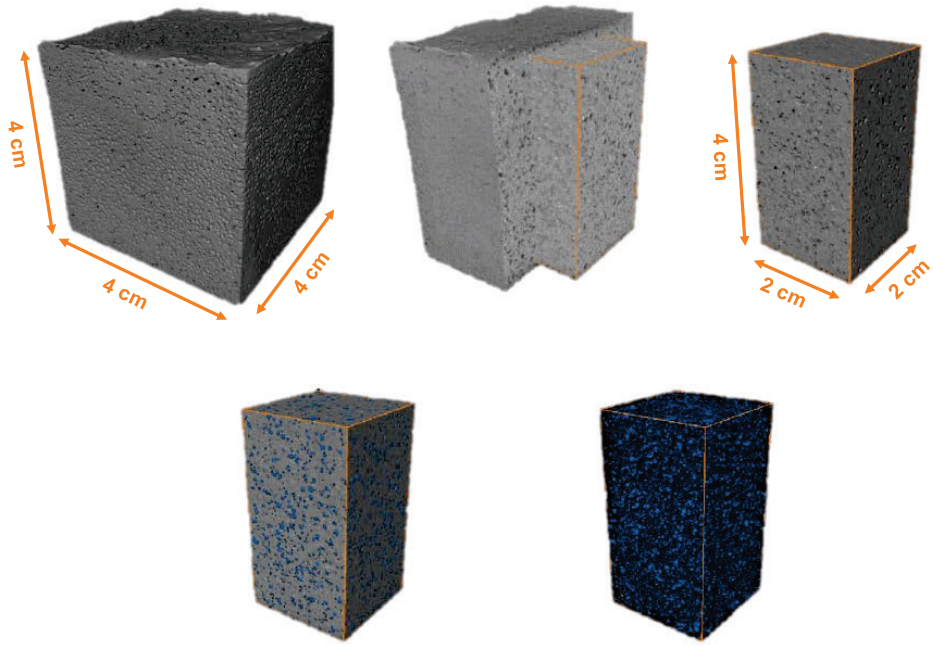

Figure 1. Example of a 3D model and the segmentation process of the 3D data to isolate the porosity, which is coloured in blue.

The compressive strength tests, at 2, 7, and 28 days, were carried out according to the UNE-EN 196-1 standard using the Incotecnic MULTI-R1 universal machine.

After 28 days of curing, each sample underwent the isopropanol (IPA) exchange method to preserve the microstructure of the hydrated cementitious materials [29]. Subsequently, the samples were ground into powder form to enable further analyses.

X-Ray diffraction (XRD) was used to identify the main crystalline phases present in the samples at 28 days of curing employing the Bragg-Brentano PANalytical X'Pert PRO MPD alpha1 powder diffractometer (CuKα_1) using the X'Pert HighScore software. The TGA 550 (TA Instruments) was used to perform thermogravimetric analysis (TG) at 28 days of curing time with derivative thermogravimetry (TG/DTG) with a HiRes Ramp of 10 ºC·min^{-1} to 1000 ºC, with a flow rate of 50 mL·min^{-1} in air atmosphere. ^{31}P MAS-NMR (Magic Angle Spinning Nuclear Magnetic Resonance) spectra were recorded at RT in an AVANCEIII HD 600 (Bruker AXS) spectrometer, using a triple resonance Cross Polarization Magic Angle Spinning (CP-MAS) probe of 2.5 mm at a spinning rate of 12.5 kHz, to determine the formation of K-struvite. The magnetic field was 14.1 T corresponding

to a ^{31}P resonance frequency of 242.92 MHz. The ^{31}P chemical shifts are referenced to $NH_4H_2PO_4$. ^{31}P MAS NMR spectra were recorded with a length pulse of 0.7 us and 5-s delay with 1H decoupling (^{31}P Hpdec with spinal 64 decoupling sequence for P) and summing up 380 scans.

The scanning electron microscope (SEM) used in this study was the QUANTA-200 model from the *Centres Científics i Tecnològics de la Universitat de Barcelona* (CCiTUB). In addition to employing the imaging mode of the microscope, elemental distribution maps were obtained using the energy dispersive spectroscopy (EDS) system for microanalysis. The imaging mode of the SEM allows for the observation of the different phases within the sample. Specifically, the backscattered electron (BSE) mode, which is sensitive to the atomic number (Z), enables the differentiation of phases based on atomic weight, as each phase exhibits varying shades of grey.

3. RESULTS AND DISCUSSION

3.1. Consistency, and Vicat needle test

Table 2 presents the average consistencies, IST, and FST. As shown, increasing the LG content also increases the W/C ratio to maintain the consistency within the desired range (110 mm ± 10%). The need to increase the W/C ratio generally results in higher IST values and, consequently, longer FST values. Increasing the water content extends the setting time, as water acts as a cooling agent in the reaction [25]. This behaviour is well-documented in MKPC-type cements, where higher water content leads to extended setting times due to the cooling effect of water [30], [31]. In particular, as the LG content increases, the open time (difference of time between FST and IST) also increases. However, it is important to note that although F1 exhibits the highest consistency, its short IST, FST and open time make it more difficult to work with. This problem is alleviated by increasing the LG content in the mix. Furthermore, variations in open time are expected to affect the final pore structure of the material.

3.2. Isothermal calorimetry

Figure 2 compares the isothermal calorimetry results of the MKPC formulations. The normalized to the amount of cement calorimetric curves of the samples shown in Figure 2.A present an initial endothermic peak (Phase I) followed by two exothermic peaks (Phase II, and Phase III), and finally the further continuous precipitation of K-struvite (Phase IV). The balance equations of the hydration are listed in Table 3. This study was conducted under controlled conditions, as the reaction was restricted from proceeding freely due to the closed system and the constant temperature maintained throughout the analysis.

The endothermic peak, Phase I, is attributed to the dissolution of the MKP in water, releasing amount of hydrogen ions, potassium ions and phosphate ions into the solution, as shown in Eq. 2, Eq. 3 and Eq. 4. The endothermic peak is distinctly observed in the 100TUN-0LG formulation, attributed to the slower dissolution rate of MgO in TUN compared to that in LG. This behaviour is

closely linked to the lower BET surface area of TUN relative to the higher BET value of LG, as previously mentioned. Consequently, the MKP dissolution endothermic peak is only identified in the 100TUN-0LG and 75TUN-25LG formulations, as highlighted in the zoomed region of Figure 2.A. Formulations with more than 50% LG rapidly reach the first exothermic peak, preventing the observation of the MKP dissolution endothermic peak.

Following, an increasing trend over times is observed of the first exothermic peak, with the maximum reached within the first 15 minutes [7], [32], [33], [34], [35]. The first exothermic peak is ascribed to the dissolution of the MgO particles by the H^+ present in the medium (Eq. 5). And the second one is related to the reaction of the ions present in the medium for the formation of K-struvite (Eq. 6) [32]. In this phase, a change in slope is observed after the first exothermic peak, which is associated with the formation of K-struvite.

Variations in the slope and timing of the exothermic peaks were observed, which do not follow a clear pattern. This phenomenon requires further investigation, as it may be related to the compatibilities between raw materials with different degrees of reactivity. In addition, factors such as competition between calcium (Ca) coming from TUN and magnesium (Mg) in the raw materials in the precipitation initiation phase, solubility differences, and closed system conditions could contribute to these irregularities. Despite these complexities, it is clear that an increase in LG content leads to a higher heat flow in both the first and second exothermic peaks. This behaviour is likely attributable to the higher reactivity of LG compared to TUN, which influences the thermal behaviour of the system. Further studies are needed to explore these interactions in more detail and to better understand their implications for material performance.

This initial peak is observed in a shorter time for the 100TUN-0LG formulation, occurring immediately after the first reaction phase, with the two exothermic peaks overlapping. This rapid succession is consistent with the behaviour noted above in the difference between IST and FST, confirming a fast reaction of this formulation. Next, the two samples with the highest LG content (0TUN-100LG and 25TUN-75LG) exhibit a steeper slope, indicating faster reaction kinetics. This tendency helps differentiate the thermal profiles of the various formulations and provides insights into the cement setting process. In contrast, the two remaining formulations present a peak with a gentler slope and a broader shape, suggesting a slower and more progressive reaction. This variation in the peak profiles may reflect differences in the reaction dynamics and crystallization rates influenced by the composition of the mixtures. However, it is also detected that the formulation of 50TUN-50LG present the interval between the two exothermal peak wider and that the second exothermic peak characteristic of K-struvite formation appears with a longer time. Finally, in phase IV, the precipitation of K-struvite continues slowly [32].

Table 3. Balance equation of the MKPC hydration [36].

Phase I	
$KH_2PO_4 \rightarrow K^+ + H_2PO_4^-$	*Eq. 2*
$H_2PO_4^- \rightarrow H^+ + HPO_4^{2-}$	*Eq. 3*
$HPO_4^{2-} \rightarrow H^+ + PO_4^{3-}$	*Eq. 4*
Phase II	
$MgO + H_2O \rightarrow Mg^{2+} + 2OH^-$	*Eq. 5*
Phase III and Phase IV	
$Mg^{2+} + PO_4^{3-} + K^+ + 6H_2O \rightarrow MgKPO_4 \cdot 6H_2O$	*Eq. 6*

The formation of K-struvite and the dissolution of MgO is accompanied by a significant release of heat, therefore, the cumulative normalised heat (Figure 2.B) released is proportional to the quantity of the reaction products formed [37]. Furthermore, the accumulated heat reveals that higher LG content leads to greater heat release, even at a lower W/C ratio, indicating a more exothermic reaction between MgO and phosphate during K-struvite formation. The results highlight the greater reactivity of MgO, which can be attributed to its inherent LG characteristics.

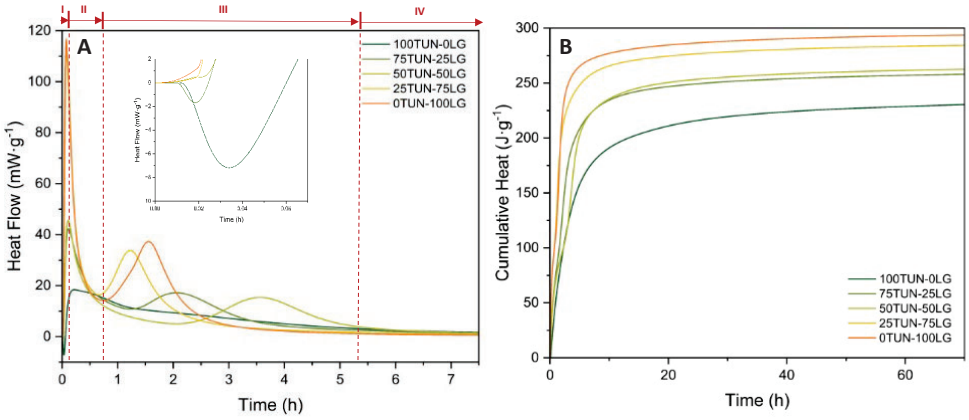

Figure 2. Isothermal calorimetry of the MKPC formulations. (A) Normalized heat flow, (B) Cumulative normalized heat.

3.3. FTIR-ATR spectroscopy

The time-dependent FTIR-ATR spectra, displayed in Figure 3, highlight the progressive appearance of the primary phosphate group vibrations as the cementation reaction advances. These findings demonstrate that the dominant phosphate vibrations (1200–800 cm^{-1}) become noticeable during the later stages of the experiment's initiation phase. The results presented in Figure 3 were calculated using the same analysis time. However, it is observed that the 50TUN-50LG formulation lost contact as it was washed, which is why the data appears to be cut off. Despite this limitation, the general trend can still be estimated.

The stretching region of H_2O (3700–2600 cm^{-1}) and the water bending vibration spectral region (1900–1400 cm^{-1}) are observed in all the samples. In all cases, an evolution in these regions is noted as time progresses. This trend suggests a progressive transformation of water from free to confined or bound states, likely associated with the formation of reaction products [38], [39].

The interval of 1200–400 cm^{-1} corresponds to the primary vibrations of phosphate groups. A tetragonal penta-atomic molecule, PO_4^{3-}, exhibits four different vibrations (i) the symmetric stretching (930-995 cm^{-1}), (ii) the symmetric bending (404-470 cm^{-1}), (iii) the asymmetric stretching (1017-1163 cm^{-1}) and (iv) the asymmetric bending (509-554 cm^{-1}) [40], [41], [42]. The FTIR-ATR analysis reveals that the bands at approximately ~998 cm^{-1} increase in intensity over time. Notably, as the LG content increases, the shift in the intensity of this band occurs later. This behaviour aligns with the trends observed in the IST and FST results, which, while not perfectly matching in exact timing, follow a consistent order with comparable values. These findings further support the correlation between LG content and the reaction dynamics. The evolution of the phosphate band suggests progressive changes in the interactions or structural organization of the phosphate groups as the reaction progresses. Specifically, the growth of the phosphate band is associated with water coordination, which is directly linked to the formation of K-struvite. This is evident in the 100TUN-0LG and 0TUN-100LG formulations, which exhibit higher intensity in the band associated with water stretching bands. This indicates that the OH^- ions present in the raw materials, originating from Mg and Ca in the case of TUN and from Mg in the case of LG, undergo coordination to contribute to the formation of the final product.

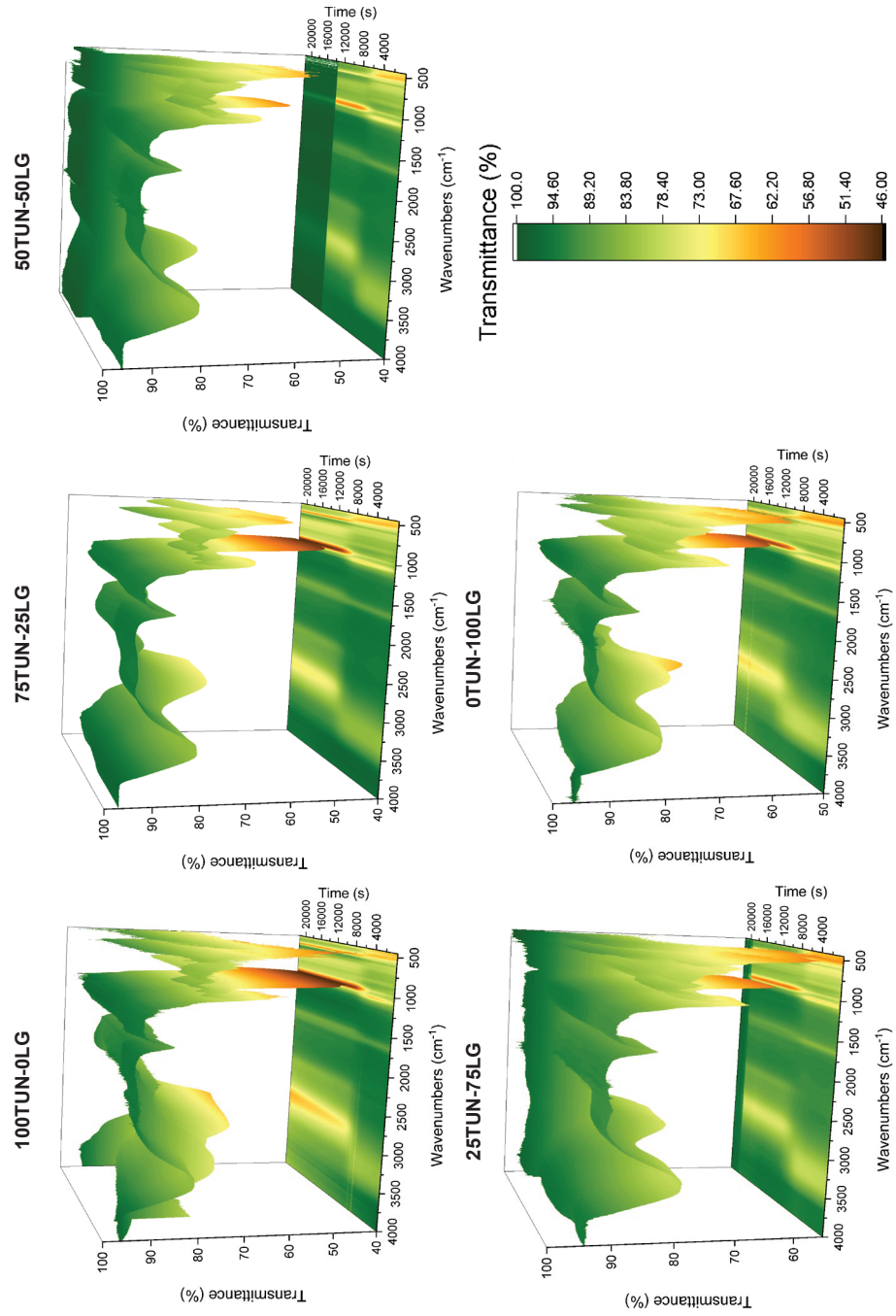

Figure 3. Time evolution of FTIR-ATR spectra.

3.4. Porosity

The porosity measurements conducted by micro-CT scan at three distinct curing times, 2 days (2d), 7 days (7d), and 28 days (28d), are summarized in Table 4 and shown in Figure 4. The results reveal a clear trend in the porosity values across the different formulations and curing times. The formulation containing 100% TUN by weight (100TUN-0LG) exhibited the highest porosity values at all curing times, with a significant reduction of 28%, the value decreased from 13.25% at 2 days to 9.55% at 28 days. Conversely, the formulation with 100% by weight of by-product (0TUN-100LG) showed the lowest porosity values, maintaining a remarkably consistent porosity around 2.38% across all curing times. The reduction in porosity over time on 100TUN-0LG samples could be an indicative of the ongoing slow hydration process and the resultant densification of the cement matrix. Indeed, the presence of the low-density material inside the pore reinforces this observation. Oppositely, the porosity consistence of the 0TUN-100LG samples suggests a rapid initial setting and stabilization of the material, potentially due to the chemical interactions within the alternative cement matrix. Intermediate formulations, such as 75TUN-25LG and 50TUN-50LG, displayed porosity values that decreased with increasing proportions of the LG. For instance, the 50TUN-50LG formulation demonstrated a significant 22% reduction in porosity, decreasing from 5.84% at 2 days to 4.53% at 28 days. Otherwise, the 25TUN-75LG and 75TUN-25LG formulations showed more stable porosity values, with a minimal reduction of 0.6% (from 9.82% at 2 days to 9.76% at 28 days) and a modest reduction of 6% (from 5.30% at 2 days to 4.98% at 28 days), respectively.

The volume, length, and sphericity of the pores were also analyzed (Table 4). The 100TUN-0LG formulation exhibited the highest initial pore volume, which decreased over time from 4.05 x 10^{-2} mm^3 at 2d to 3.79 x 10^{-2} mm^3 at 28d. Nevertheless, the pore length increases from 0.43 mm at 2d to 0.45 mm at 28d, while sphericity remained relatively stable around 0.92. The presence of unreacted cement on the pore walls (Figure 4) at 2d could explain the initially higher volume, which diminishes as the hydration process progresses and the cement matrix densifies over time. The results of volume pore distribution for classes confirm this observation, showing a significant reduction in the proportion of smaller pores with lower length, which are filled during the hydration and densifies process over time (Figure 5). Consistent with previous IST and FST results, the 100TUN-0LG formulation sets more rapidly, which could explain its higher porosity. A plausible explanation is that water becomes trapped within the matrix during the rapid setting process, preventing it from escaping and contributing to the observed porosity. In contrast, the 0TUN-100LG formulation showed the lowest pore volume and length, with constant values at three curing times around 1.8 x 10^{-2} mm^3 and 0.38 mm, respectively, and high sphericity values around 0.94. These results suggest a more compact and uniform pore structure, which aligns with the broader time range observed between IST and FST. This extended interval likely facilitates water escape during the

setting process, contributing to the compact nature of the matrix. Intermediate formulations showed gradual decreases in pore volume and length with increasing W/C ratios.

Table 4. Measurements of volume, length, and sphericity of the pores on the different formulation and different curing times.

Formulation	Curing times	Porosity	Pore length *(mm)*	Pore volume *(mm^3)*	Pore Sphericity
100TUN-0LG	2d	13.25	0.43	4.05×10^{-2}	0.93
	7d	10.02	0.46	3.94×10^{-2}	0.92
	28d	9.54	0.45	3.79×10^{-2}	0.92
75TUN-25LG	2d	9.82	0.42	3.28×10^{-2}	0.94
	7d	9.54	0.43	3.39×10^{-2}	0.94
	28d	9.76	0.42	3.22×10^{-2}	0.94
50TUN-50LG	2d	5.84	0.37	2.15×10^{-2}	0.95
	7d	4.31	0.36	2.06×10^{-2}	0.95
	28d	4.53	0.36	2.01×10^{-2}	0.95
25TUN-75LG	2d	5.3	0.36	2.11×10^{-2}	0.95
	7d	5.3	0.36	2.10×10^{-2}	0.95
	28d	4.98	0.36	2.08×10^{-2}	0.95
0TUN-100LG	2d	2.37	0.38	1.90×10^{-2}	0.94
	7d	2.39	0.38	1.82×10^{-2}	0.94
	28d	2.38	0.38	1.83×10^{-2}	0.94

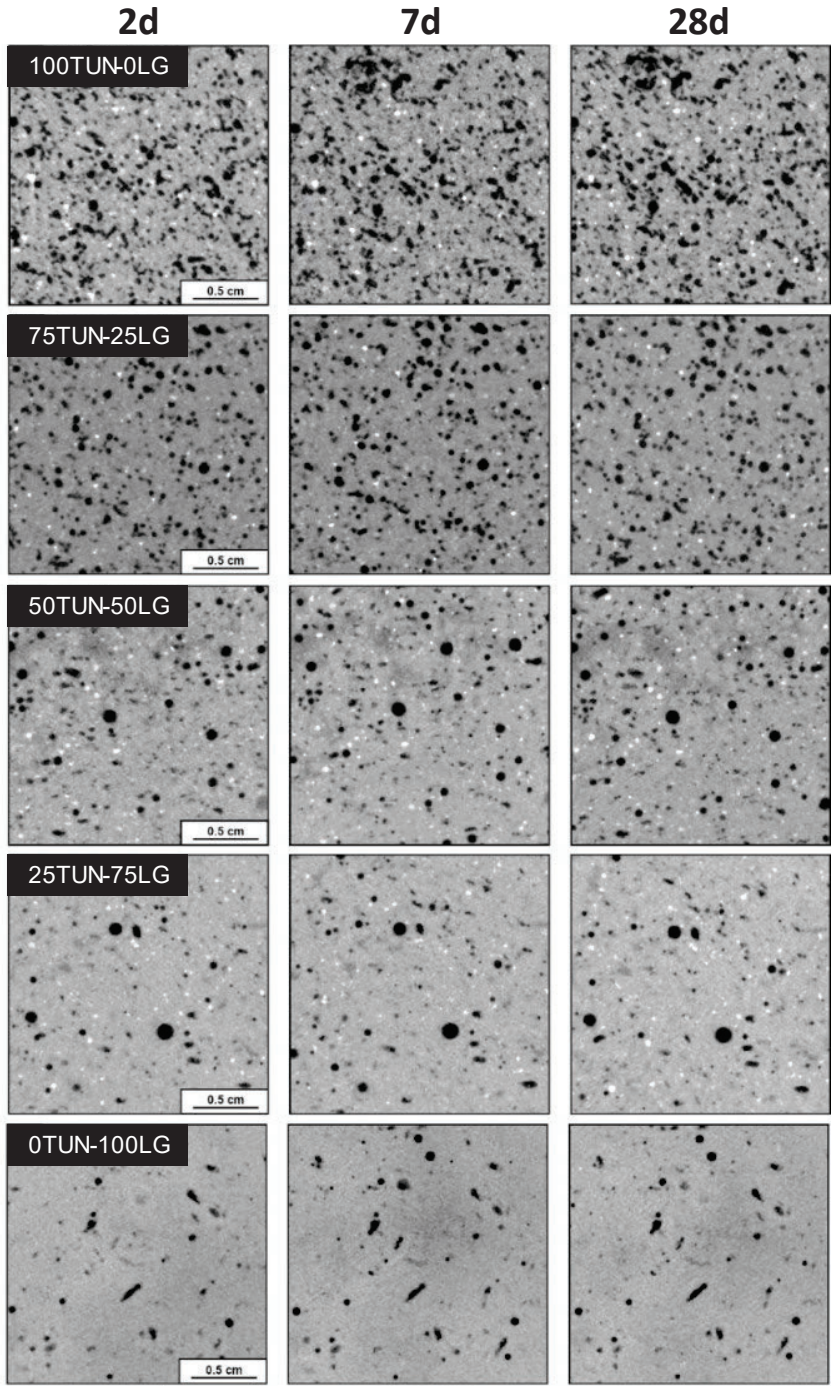

Figure 4. Slice taken from the tomographic 3D reconstruction of the cement pastes.

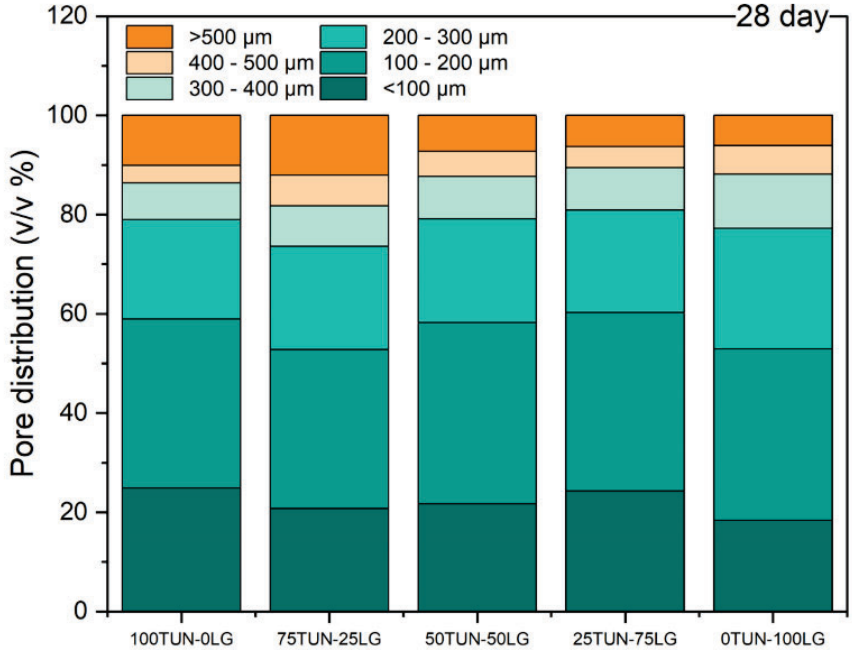

Figure 5. Pore length distribution after 28 days of curing time.

The pore connectivity, quantified as the coordination number, characterizes the topology of the pore structure by indicating the number of pore connections with surrounding pores. An increase in the coordination number denotes a higher number of connected pores, which can significantly impact, for example, the fluid permeability through the material. The frequency distribution of the coordination number is illustrated in Figure 6 and Figure 7. The results show that the dominant coordination number is higher for the 100TUN-0LG sample, ranging from 0 to 10, and lower for the 0TUN-100LG sample, ranging from 0 to 4. Otherwise, the 75TUN-25LG, 50TUN-50LG, and 25TUN-75LG samples have coordination numbers ranging from 0 to 6, 0 to 4, and 0 to 6, respectively. This distribution could be related to the porosity distribution, which decreases in samples with lower LG content. Indeed, the low-density pores increase the distances between pores (Figure 6), and the increased sphericity in the 0TUN-100LG sample contributes to reduced connectivity.

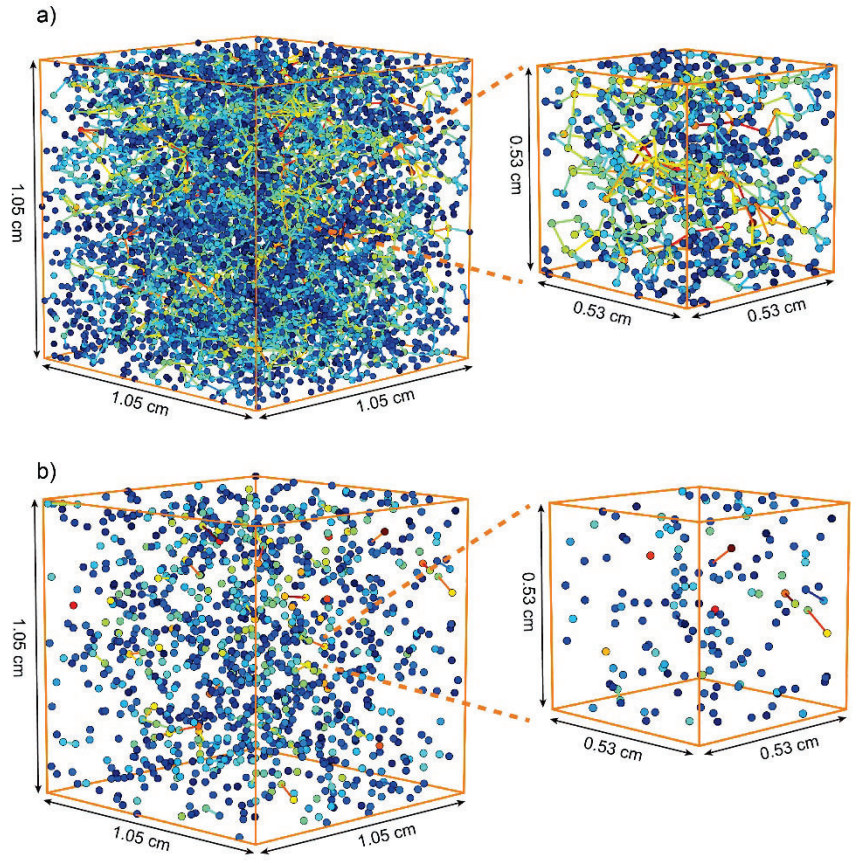

Figure 6. 3-D pore network model. The points represent pores, the lines indicate connectivity, and the blue to red colour gradient represents the increase in coordination number. (a) 100TUN-0LG and (b) 0TUN-100LG after 28 days of curing time.

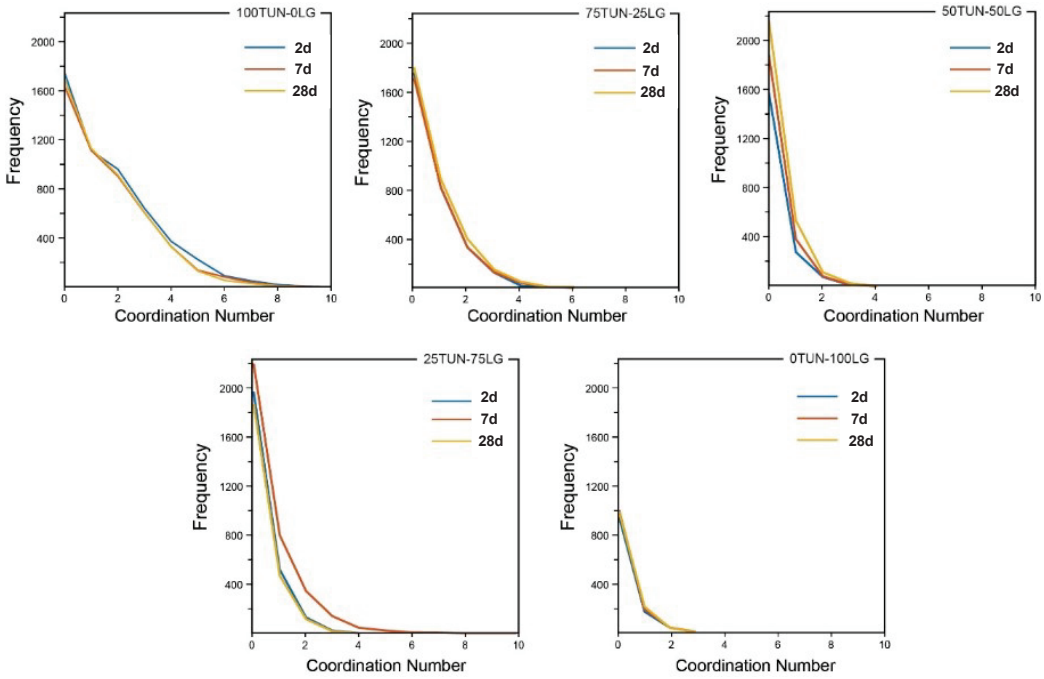

Figure 7. Distribution of coordination numbers in the pore network model for each formulation and curing time.

3.5. Mechanical compressive strength

The influence of the different raw materials used as MgO source and curing age on the compressive strength were evaluated. The compressive strengths at different ages of the formulations are shown in Figure 8. The results indicate that the strength increases with longer curing times until 28 days.

The higher the LG content the higher the compressive strength. This increase could be explained by the smaller particle size of LG, the distinct phases formed, and the different total porosity of the final product. However, an exception is observed in the 25TUN-75LG sample, which deviates from the expected trend. This anomaly suggests that the composition or interaction of components in this specific proportions may influence the results differently compared to the others.

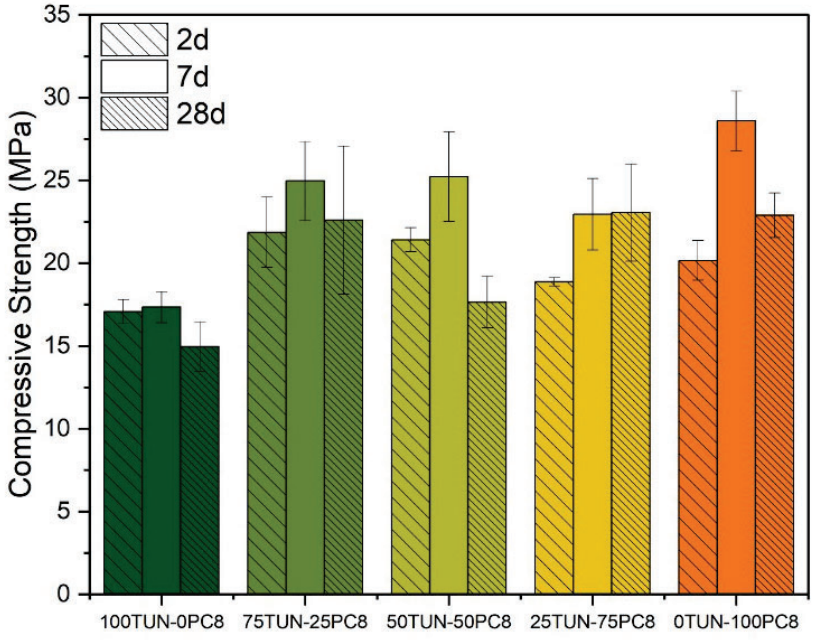

Figure 8. Results of compressive strength at different ages.

3.6. X-Ray Diffraction (XRD)

Figure 9 shows the diffraction patterns of specimens of the different samples cured at 28 days. The XRD results reveal the main crystalline hydration product present in the MKPC samples is K-struvite ($MgKPO_4 \cdot 6H_2O$), along with unreacted MgO, brucite ($(Mg(OH)_2$), and arcanite (K_2SO_4) [40], [43], [44]. Previous studies have demonstrated that there is MgO unreacted coming from the raw materials [8], [45].

In addition, there are other characteristics peaks related to calcite ($CaCO_3$) determined in all the samples. For formulations with high TUN content, the appearance of calcite can be attributed to the hydration of CaO, which forms the corresponding hydroxide that subsequently undergoes carbonation during the curing process. The increasing of LG resulting in a gradual increase of the secondary phases such as magnesite ($MgCO_3$) and dolomite ($CaMg(CO_3)_2$) coming from the LG, except for the 100TUN-0LG formulation.

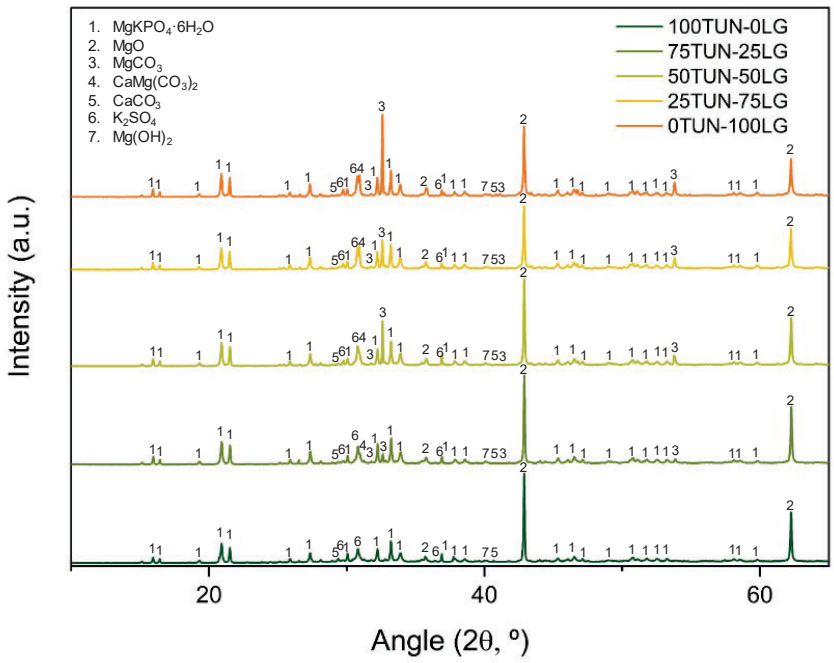

Figure 9. X-ray diffraction patterns of MPCs at 28 days.

3.7. Thermogravimetric analysis (TG)

The TG/DTG curves of the samples at 28 days of age, and the corresponding TG losses, are shown in Figure 10. The first weight loss between 25 and 300 ºC is related to the dehydration decomposition of the main hydration product K-struvite, and the second loss pertains to the dehydration process of brucite [46], [47], [48], [49].

The mass loss occurred in the range of 450-900 ºC is attributed to the carbonates decomposition of $MgCO_3$, $CaMg(CO_3)_2$ and $CaCO_3$ respectively. The last mass loss presents in all the samples located above 900 ºC is characterized by the decomposition of sulphates, specifically K_2SO_4, as characterized in the XRD.

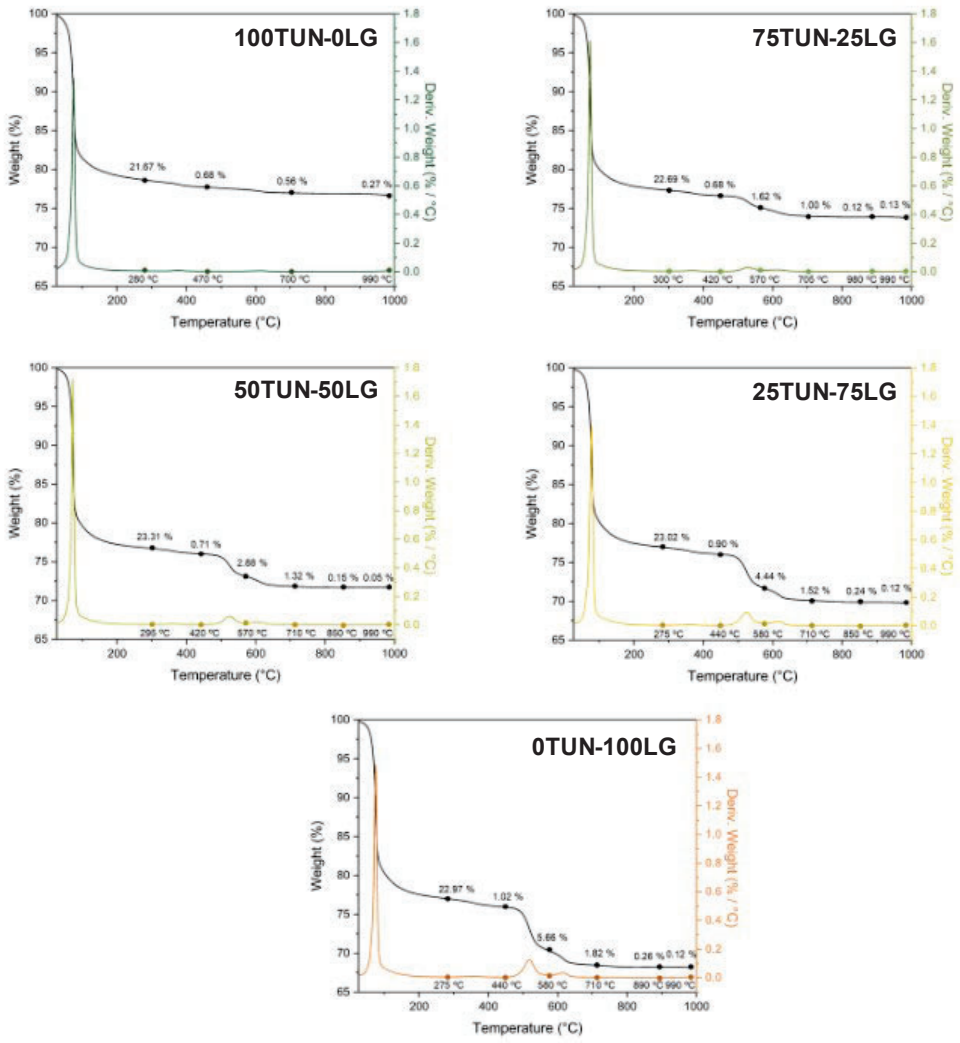

Figure 10. Thermogravimetric analysis of MPC cements.

Specifically, a high-resolution TG study was conducted over the temperature range of 25-1000ºC under the specified analysis conditions. As shown in Figure 11, it was possible to visualize in detail the characteristic mass loss associated with K-struvite and the carbonates. In addition, Figure 11 demonstrate the decomposition behaviours and highlighting the presence of different compounds.

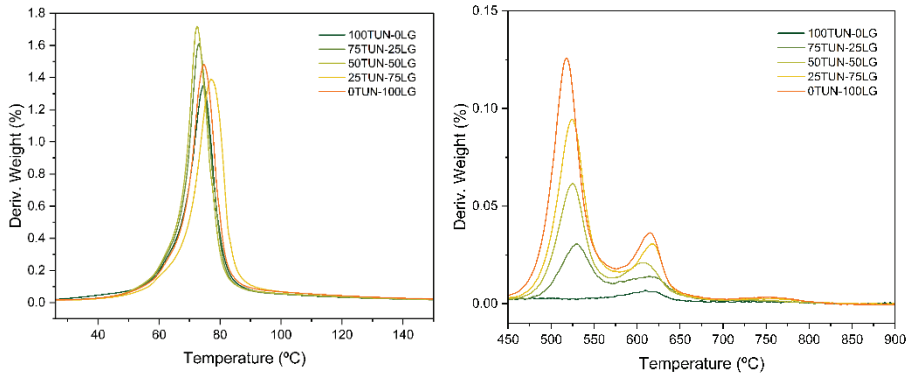

Figure 11. Derivative weight in percentage of the K-struvite phase (right) and carbonates (left) at 28 days of curing by high resolution TG analysis.

By comparing the mass losses of the different samples and the phases determinate by XRD analyses at 28 days of curing, it can be visualized an estimation in percentage of the distinct phases shown in Table 5, in which all the formulations have a similar K-struvite phase content. However, a trend is observed in which samples with higher LG content generally show a higher K-struvite phase, with the exception of sample 50TUN-50LG. An increase in the brucite content is observed as the LG content increases. Due to the inherent nature of the raw materials, the increasing of LG resulting in a gradual increase of $MgCO_3$, and $CaMg(CO_3)$, except for the 100TUN-0LG formulation, as TUN does not possess these phases (Table 1). Carbonates exhibit inert behaviour and function as fillers, improving the mechanical strength of the material, as evaluated in the mechanical properties results. In contrast, the 100TUN-0LG presents the highest content of $CaCO_3$ and K_2SO_4.

In addition, Table 5 reveals a significant weight percentage of non-decomposed phases, probably attributed to non-reactive MgO, sulphates, silicates among other phases. Notably, while formulations with higher TUN content exhibit a lower W/C ratio, suggesting the potential for a more exothermic reaction and improved product formation, the observed results indicate the opposite. Specifically, as the TUN proportion increases, the weight percentage of undecomposed material also increases. This phenomenon may be related to the inherent characteristics of the raw material, including the lower reactivity of MgO, as corroborated by the TAM-AIR test (Figure 2.B), and the higher content of unreactive MgO.

Table 5. Compounds estimation at 28 days through XRD and high resolution TG/DTG results.

	Wt. %							
Formulation	**$MgKPO_4 \cdot 6H_2O$**	**$Mg(OH)_2$**	**$MgCO_3$**	**$CaMg(CO_3)$**	**$CaCO_3$**	**K_2SO_4**	**MgO unreacted**	**Others**
100TUN-0LG	53.42	2.19	-	-	1.26	0.58	12.91	29.64
75TUN-25LG	55.93	2.21	3.09	2.10	0.28	0.35	12.12	23.92
50TUN-50LG	57.47	2.31	5.51	2.76	0.34	0.14	12.18	19.29
25TUN-75LG	56.74	2.90	8.50	3.18	0.54	0.34	10.54	17.26
0TUN-100LG	56.64	3.29	10.85	3.82	0.59	0.32	9.25	15.24

3.8. ^{31}P MAS-NMR

All the formulations were characterized by ^{31}P MAS NMR spectroscopy. The spectra analyses provided significant insights into the composition of the cement pastes. The characteristic peaks corresponding to K-struvite (δ= 6.5 ppm) were identifiable in all formulations, as shown in Figure 12 [50]. The ^{31}P chemical shift of K-struvite observed in the current study correlates well with the previously results that validated its presence. Additionally, a poorly ordered phosphate zone between -5 and approximately 5 ppm, and a broad hump-shaped peak was detected around 2 ppm in the 100TUN-0PC8 formulation. Although its exact nature remains unclear, one plausible explanation following the bibliography could be the presence of a phosphorösslerite ($MgHPO_4 \cdot 7H_2O$) peak [50]. Identifying the exact phosphate present is challenging due to the overlapping chemical changes characteristic of different magnesium phosphates, which complicates precise distinction [51] [52].

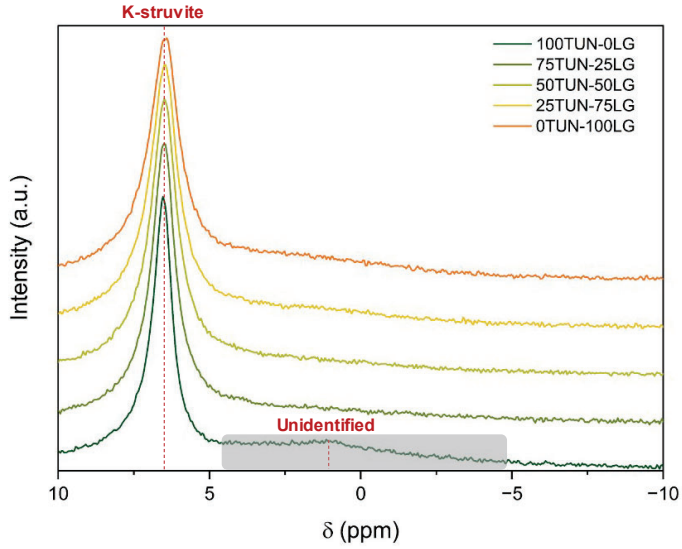

Figure 12. ^{31}P MAS-NMR spectra of the cement pastes.

3.9. SEM-EDS

SEM-EDS elemental mapping of the micrographs at 28 days provides a detailed analysis using different colours to represent elemental distributions, as shown in Figure 13. Significant microcracking is evident in the 100TUN-0LG and 75TUN-25LG formulations, characterized by their high TUN content. This can be attributed to water evaporation during the curing period, likely intensified by the thermal effects of the reaction. These formulations also exhibit shorter setting times and lower W/C ratios, which may contribute to the observed behaviour. Conversely, the other formulations display a smaller number and size of microcracking, likely due to the extended setting times that mitigate thermal stress during curing.

A dominant K-struvite matrix is evident in all five formulations. However, unreacted MgO particles are also observed, especially in samples with higher TUN content. This can be attributed to the inherent nature of TUN and its lower reactivity, as corroborated by previous analyses.

In addition, two other notable features are evident. First, an increase in Ca-rich particles is observed in the formulations with higher TUN content. Second, Si-rich particles are more abundant in formulations with higher LG content, reflecting compositional differences and their influence on the phase distribution within the matrix.

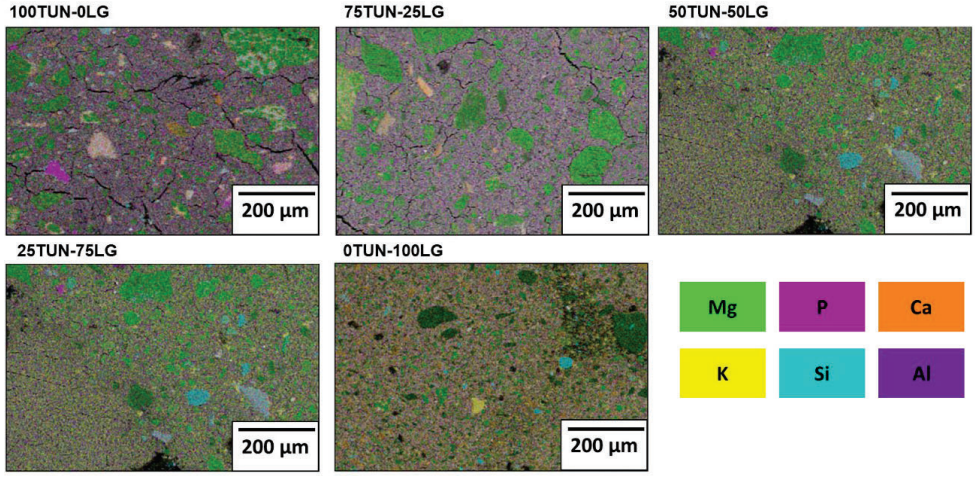

Figure 13. SEM-EDS general elemental mapping and the elemental mapping colours of MPC formulations (x200µm).

4. CONCLUSIONS

The findings of this study highlight the differences in the porosity network of paste samples under the using of different MgO source. MPC was formulated with various MgO sources, incorporating waste and by-products in different proportions from 0 to 100 wt.%. A thorough study was presented, concerning first the compressive strength and then physicochemical properties of the cements. In addition, the alternative cements were fully characterised with assess their porosity. This research work led to the following conclusions:

- The use of alternative sources of MgO represents the beginning of research into alternative binders, which could play an important role in the development of sustainable construction materials that foster the principles of the circular economy.
- The physicochemical characterization reveals that the primary hydration product in the samples is the K-struvite matrix ($MgKPO_4 \cdot 6H_2O$), alongside other phases like unreacted MgO, magnesium hydroxide, sulphates, and carbonates. However, the estimation of K-struvite content, based on XRD and TG analysis, indicates that all samples contain similar amounts of K-struvite.
- Higher LG content increases compressive strength due to its smaller particle size and composition, whereas higher TUN content results in lower compressive strength. Micro-CT analyses confirm this relationship, showing that samples formulated exclusively with TUN exhibit the highest porosity, which significantly decreases with curing time. Conversely, increasing LG content leads to lower porosity levels. In these formulations, porosity decreases only slightly over time, with the 0TUN-100LG samples maintaining an almost stable porosity throughout the curing process.
- The volume pore distribution results for the 100TUN-0LG indicates a significant reduction in the proportion of smaller pores with shorter lengths, which are filled during the hydration and densification process over time with a higher connectivity. In the contrast, the 0TUN-0LG suggest a more dense and consistent pore structure with lower porosity connectivity.

Overall, the results obtained in this work proved the feasibility of using different alternative magnesium source to produce MPC. The various combinations of waste and by-product contents not alter the matrix formation; hence the K-struvite was obtained. The main effect of TUN compared to LG was decreasing of mechanical properties, increasing porosity and connectivity of their pore network. However, the adoption of waste and by-products recovery strategies not only enhances the efficient use of natural resources but also signifies a shift towards sustainable practices.

Although a total of five formulations were studied, this research highlights the potential of utilizing formulations that incorporate a waste material currently destined for landfill. While the 0TUN-100LG formulation yielded the best overall performance, the 50TUN-50LG formulation also exhibited promising characteristics, striking an optimal balance between mechanical properties and porosity,

among other parameters. From an environmental perspective, the 50TUN-50LG formulation is particularly advantageous, as it enables half of the MgO source to be derived from a waste material and the other half from a by-product. This contributes to reducing the environmental impact associated with raw material extraction. Future research should focus on a more detailed examination of the interactions between these two raw materials to better understand their behaviour and potential compatibility. This deeper understanding could further optimize the formulations and enhance their performance and sustainability.

Acknowledgments

The authors would like to thank Magnesitas Navarras, S.A. company for the information supply. Dr. Jessica Giro-Paloma is a Serra Húnter Fellow.

Funding

This work is supported by the Spanish Government with the Grant PID2021-125810OB-C21 funded by MCIN/AEI/10.13039/501100011033 and by “ERDF A way of making Europe”. Grant CNS2022-135800 funded by MICIU/AEI /10.13039/501100011033 and by the "European Union NextGenerationEU/PRTR”. The authors would like to thank the Catalan Government for the quality accreditation and funding given to their research group DIOPMA (2021 SGR 00708). DIOPMA is a certified agent TECNIO in the category of technology developers from the Government of Catalonia. Furthermore, the Agència de Gestió d’Ajuts Universitaris i de Recerca (AGAUR) contributed through Ms A. Alfocea-Roig’s PhD grant (FI-DGR 2021). This work is also partially supported by Magnesitas Navarras, S.A. (FBG312160).

Credit authorship contribution statement

A. Alfocea-Roig: Data curation, Formal analysis, Visualization, Investigation, Writing - original draft. M. Cerdà-Domènech: Data curation, Visualization, Writing - review & editing. D. Vera-Rivera: Data curation, Visualization, Investigation, Writing - review & editing. J. Frigola: Visualization, Writing - review & editing. J. Giro-Paloma: Conceptualization, Visualization, Supervision, Writing - review & editing, Funding acquisition. J. Formosa: Conceptualization, Visualization, Supervision, Methodology, Writing - review & editing, Funding acquisition.

Declaration of competing interest

The authors declare that they have no known competing financial interests or personal relationships that could have appeared to influence the work reported in this paper.

References

[1] J. de Brito, R. Kurda, The past and future of sustainable concrete: A critical review and new strategies on cement-based materials, Journal of Cleaner Production 281 (2021). https://doi.org/10.1016/j.jclepro.2020.123558.

[2] E. Khankhaje, T. Kim, H. Jang, C.-S. Kim, J. Kim, M. Rafieizonooz, A review of utilization of industrial waste materials as cement replacement in pervious concrete: An alternative approach to sustainable pervious concrete production, Heliyon 10 (2024). https://doi.org/10.1016/j.heliyon.2024.e26188.

[3] S. Sourmelis, Y. Pontikes, R.J. Myers, M. Tennant, Business models for symbiosis between the alumina and cement industries, Resources, Conservation and Recycling 205 (2024). https://doi.org/10.1016/j.resconrec.2024.107560.

[4] H. AzariJafari, G. Guest, R. Kirchain, J. Gregory, B. Amor, Towards comparable environmental product declarations of construction materials: Insights from a probabilistic comparative LCA approach, Building and Environment 190 (2021). https://doi.org/10.1016/j.buildenv.2020.107542.

[5] M. Schneider, M. Romer, M. Tschudin, H. Bolio, Sustainable cement production-present and future, Cement and Concrete Research 41 (2011) 642–650. https://doi.org/10.1016/j.cemconres.2011.03.019.

[6] D. Wang, Y. Yue, J. Qian, Effect of carbonation on the corrosion behavior of steel rebar embedded in magnesium phosphate cement, Composites Part B: Engineering 268 (2024). https://doi.org/10.1016/j.compositesb.2023.111088.

[7] J. Zhao, J. Shi, Y. Li, P. Hou, S. Liang, H. Chen, Y. Huang, S. Adu-Amankwah, X. Zhou, X. Cheng, Phase and microstructure evolution of the hydration products of magnesium phosphate cements under sulfuric acid environments, Construction and Building Materials 418 (2024). https://doi.org/10.1016/j.conbuildmat.2024.135465.

[8] A. Alfocea-Roig, S. Huete-Hernández, X. García-Zubiri, J. Giro-Paloma, J. Formosa, Can tundish deskulling waste be used as a magnesium oxide source to develop magnesium phosphate cement?, Journal of Environmental Chemical Engineering 11 (2023). https://doi.org/10.1016/j.jece.2023.110618.

[9] L. Diaz Caselles, C. Cau Dit Coumes, P. Antonucci, A. Rousselet, A. Mesbah, V. Montouillout, Chemical degradation of magnesium potassium phosphate cement pastes during leaching by demineralized water: Experimental investigation and modeling, Cement and Concrete Research 178 (2024). https://doi.org/10.1016/j.cemconres.2024.107456.

[10] J. Nobre, H. Ahmed, M. Bravo, L. Evangelista, J. De Brito, Magnesia (MgO) Production and Characterization, and Its Influence on the Performance of Cementitious Materials: A Review, Materials 13 (2020). https://doi.org/10.3390/ma13214752.

[11] N. McQueen, P. Kelemen, G. Dipple, P. Renforth, J. Wilcox, Ambient weathering of magnesium oxide for CO_2 removal from air, Nat Commun 11 (2020). https://doi.org/10.1038/s41467-020-16510-3.

[12] S.A. Walling, J.L. Provis, Magnesia-Based Cements: A Journey of 150 Years, and Cements for the Future?, Chemical Reviews 116 (2016) 4170–4204. https://doi.org/10.1021/acs.chemrev.5b00463.

[13] I. Ahmed Raza, Navdeep, R. Maaze, G. Kumar Attri, S. Shrivastava, Comparative life cycle assessment of recycled soil-stabilized bricks and traditional bricks, Materials Today: Proceedings 80 (2023) 532–537. https://doi.org/10.1016/j.matpr.2022.11.042.

[14] X. Shen, X. Wang, K. Li, X. Hu, C. Shi, Life cycle assessment of magnesium phosphate cement production, Journal of Cleaner Production 467 (2024). https://doi.org/10.1016/j.jclepro.2024.142981.

[15] Q. Zhang, X. Cao, R. Ma, S. Sun, L. Fang, J. Lin, J. Luo, Solid waste-based magnesium phosphate cements: Preparation, performance and solidification/stabilization mechanism, Construction and Building Materials 297 (2021). https://doi.org/10.1016/j.conbuildmat.2021.123761.

[16] A. Alfocea-Roig, A. Müller, B. Steubing, S. Huete-Hernández, J. Giro-Paloma, J. Formosa, Life cycle assessment of the climate change impact of magnesium phosphate cements formulated with tundish deskulling waste compared to conventional cement, Sustainable Chemistry and Pharmacy 42 (2024). https://doi.org/10.1016/j.scp.2024.101802.

[17] S. Huete-Hernández, A. Maldonado-Alameda, A. Alfocea-Roig, J. Giro-Paloma, J.M. Chimenos, J. Formosa, Sustainable magnesium phosphate micromortars formulated with PAVAL® alumina by-product as micro-aggregate, Boletin de La Sociedad Espanola de Ceramica y Vidrio (2023) 1–15. https://doi.org/10.1016/j.bsecv.2023.02.001.

[18] Z.-L. Jiang, Y.-J. Pan, J.-F. Lu, Y.-C. Wang, Pore structure characterization of cement paste by different experimental methods and its influence on permeability evaluation, Cement and Concrete Research 159 (2022). https://doi.org/10.1016/j.cemconres.2022.106892.

[19] Z. Jiang, Y. Pan, C. Fu, W. Li, Y. Wang, W.-J. Long, Three-dimensional pore structure characterization of cement paste by X-ray computed tomography (XCT) and focused ion beam/scanning electron microscopy (FIB/SEM), Construction and Building Materials 383 (2023). https://doi.org/10.1016/j.conbuildmat.2023.131379.

[20] G. Zhang, Y. Li, S. Naderi, Z. Wang, M. Zhang, Two-scale modelling of fracture of magnesium phosphate cement under bending using X-ray computed tomography characterisation, Cement and Concrete Composites 121 (2021). https://doi.org/10.1016/j.cemconcomp.2021.104099.

[21] M.K. Mohan, A.V. Rahul, J.F. Van Stappen, V. Cnudde, G. De Schutter, K. Van Tittelboom, Assessment of pore structure characteristics and tortuosity of 3D printed concrete using mercury intrusion porosimetry and X-ray tomography, Cement and Concrete Composites 140 (2023). https://doi.org/10.1016/j.cemconcomp.2023.105104.

[22] W. Kong, Y. Wei, S. Wang, J. Chen, Y. Wang, Research progress on cement-based materials by X-ray computed tomography, Int. J. Pavement Res. Technol. 13 (2020) 366–375. https://doi.org/10.1007/s42947-020-0119-8.

[23] M. Niubó, J. Formosa, A. Maldonado-Alameda, R. del Valle-Zermeño, J.M. Chimenos, Magnesium phosphate cement formulated with low grade magnesium oxide with controlled porosity and low thermal conductivity as a function of admixture, Ceramics International 42 (2016) 15049–15056. https://doi.org/10.1016/j.ceramint.2016.06.159.

[24] A.C. Quintero-Payan, S. Huete-Hernández, V.B. Aguilar-Pozo, S. Astals, J.M. Chimenos, Stabilization of metal and metalloids from contaminated soils using magnesia-based tundish deskulling waste from continuous steel casting, Chemosphere 348 (2024). https://doi.org/10.1016/j.chemosphere.2023.140750.

[25] S. Huete-Hernández, A. Maldonado-Alameda, J. Giro-Paloma, J.M. Chimenos, J. Formosa, Fabrication of sustainable magnesium phosphate cement micromortar using design of experiments statistical modelling: Valorization of ceramic-stone-porcelain containing waste as filler, Ceramics International 47 (2021) 10905–10917. https://doi.org/10.1016/j.ceramint.2020.12.210.

[26] J. Formosa, J.M. Chimenos, A.M. Lacasta, M. Niubó, Interaction between low-grade magnesium oxide and boric acid in chemically bonded phosphate ceramics formulation, Ceramics International 38 (2012) 2483–2493. https://doi.org/10.1016/j.ceramint.2011.11.017.

[27] L. Kong, M. Ostadhassan, C. Li, N. Tamimi, Pore characterization of 3D-printed gypsum rocks: a comprehensive approach, J Mater Sci 53 (2018) 5063–5078. https://doi.org/10.1007/s10853-017-1953-1.

[28] A. Rabbani, S. Jamshidi, Specific surface and porosity relationship for sandstones for prediction of permeability, International Journal of Rock Mechanics and Mining Sciences 71 (2014) 25–32. https://doi.org/10.1016/j.ijrmms.2014.06.013.

[29] Z. Zhang, G.W. Scherer, Physical and chemical effects of isopropanol exchange in cement-based materials, Cement and Concrete Research 145 (2021). https://doi.org/10.1016/j.cemconres.2021.106461.

[30] Y. Li, B. Chen, Factors that affect the properties of magnesium phosphate cement, Construction and Building Materials 47 (2013) 977–983. https://doi.org/10.1016/j.conbuildmat.2013.05.103.

[31] M.A. Haque, B. Chen, Research progresses on magnesium phosphate cement: A review, Construction and Building Materials 211 (2019) 885–898. https://doi.org/10.1016/j.conbuildmat.2019.03.304.

[32] B. Xu, B. Lothenbach, A. Leemann, F. Winnefeld, Reaction mechanism of magnesium potassium phosphate cement with high magnesium-to-phosphate ratio, Cement and Concrete Research 108 (2018) 140–151. https://doi.org/10.1016/j.cemconres.2018.03.013.

[33] B. Xu, H. Ma, H. Shao, Z. Li, B. Lothenbach, Influence of fly ash on the compressive strength and micro-characteristics of magnesium potassium phosphate cement mortars, Cement and Concrete Research 99 (2017) 86–94. https://doi.org/10.1016/j.cemconres.2017.05.008.

[34] B. Xu, C.C.D. Coumes, D. Lambertin, B. Lothenbach, Compressive strength and hydrate assemblages of wollastonite-blended magnesium potassium phosphate cements exposed to different pH conditions, Cement and Concrete Composites 143 (2023). https://doi.org/10.1016/j.cemconcomp.2023.105255.

[35] H. Lahalle, C. Cau Dit Coumes, A. Mesbah, D. Lambertin, C. Cannes, S. Delpech, S. Gauffinet, Investigation of magnesium phosphate cement hydration in diluted suspension and its retardation by boric acid, Cement and Concrete Research 87 (2016) 77–86. https://doi.org/10.1016/j.cemconres.2016.04.010.

[36] E.M. Van Der Merwe, C.A. Strydom, Hydration of medium reactive magnesium oxide using hydration agents, J Therm Anal Calorim 84 (2006) 467–471. https://doi.org/10.1007/s10973-005-7291-6.

[37] F. Qiao, C.K. Chau, Z. Li, Calorimetric study of magnesium potassium phosphate cement, Materials and Structures/Materiaux et Constructions 45 (2012) 447–456. https://doi.org/10.1617/s11527-011-9776-z.

[38] P. Mácová, A. Viani, Investigation of setting reaction in magnesium potassium phosphate ceramics with time resolved infrared spectroscopy, Materials Letters 205 (2017) 62–66. https://doi.org/10.1016/j.matlet.2017.06.063.

[39] K. Sotiriadis, P. Mácová, A.S. Mazur, P.M. Tolstoy, A. Viani, A solid state NMR and in-situ infrared spectroscopy study on the setting reaction of magnesium sodium phosphate cement, Journal of Non-Crystalline Solids 498 (2018) 49–59. https://doi.org/10.1016/j.jnoncrysol.2018.06.006.

[40] I. Kabdaşlı, A. Siciliano, C. Limonti, O. Tünay, Is K-Struvite precipitation a plausible nutrient recovery method from potassium-containing wastes?- A Review, Sustainability (Switzerland) 14 (2022). https://doi.org/10.3390/su141811680.

[41] C. Sun, D. Xue, Physical Chemistry of Crystalline $(K,NH_4)H_2PO_4$ in Aqueous Solution: An in Situ Molecule Vibration Spectral Observation of the Early Formation Stage, J. Phys. Chem. C 118 (2014) 16043–16050. https://doi.org/10.1021/jp504830u.

[42] R.C.D.S. Meira, S.P.A.D. Paz, J.A.M. Corrêa, XRD-Rietveld analysis as a tool for monitoring struvite analog precipitation from wastewater: P, Mg, N and K recovery for fertilizer production, Journal of Materials Research and Technology 9 (2020) 15202–15213. https://doi.org/10.1016/j.jmrt.2020.10.082.

[43] Y. Wang, B. Lin, F. He, J. Zhou, C. Chen, Z. He, L. Wang, Understanding hydration process and paste viscosity evolution of magnesium potassium phosphate cement, Cement and Concrete Research 169 (2023). https://doi.org/10.1016/j.cemconres.2023.107177.

[44] M. Le Rouzic, T. Chaussadent, G. Platret, L. Stefan, Mechanisms of k-struvite formation in magnesium phosphate cements, Cement and Concrete Research 91 (2017) 117–122. https://doi.org/10.1016/j.cemconres.2016.11.008.

[45] L. Diaz Caselles, C. Cau Dit Coumes, P. Antonucci, A. Rousselet, A. Mesbah, V. Montouillout, Leaching of magnesium potassium phosphate cement pastes under alkaline conditions, Applied Geochemistry 170 (2024). https://doi.org/10.1016/j.apgeochem.2024.106067.

[46] J.L. Bo Pang Baomin Wang, Runqing Liu, Yuanquan Yang, Effects of K-struvite on hydration behavior of magnesium potassium phosphate cement, Construction and Building Materials 275 (2021).

[47] C. Xu, J. Han, Y. Yang, A review on magnesium potassium phosphate cement: Characterization methods, Journal of Building Engineering 82 (2024). https://doi.org/10.1016/j.jobe.2023.108284.

[48] L.J. Gardner, S.A. Walling, S.M. Lawson, S. Sun, S.A. Bernal, C.L. Corkhill, J.L. Provis, D.C. Apperley, D. Iuga, J.V. Hanna, N.C. Hyatt, Characterization of and Structural Insight into Struvite-K, $MgKPO_4 \cdot 6H_2O$, an Analogue of Struvite, Inorganic Chemistry 60 (2021) 195–205. https://doi.org/10.1021/acs.inorgchem.0c02802.

[49] B. Pang, J. Liu, B. Wang, R. Liu, Y. Yang, Enhancement of magnesium phosphate cement solidification of Pb^{2+} by K-struvite whisker in lead-contaminated solution, Journal of Cleaner Production 320 (2021). https://doi.org/10.1016/j.jclepro.2021.128848.

[50] H. Lahalle, C. Cau Dit Coumes, C. Mercier, D. Lambertin, C. Cannes, S. Delpech, S. Gauffinet, Influence of the w/c ratio on the hydration process of a magnesium phosphate cement and on its retardation by boric acid, Cement and Concrete Research 109 (2018) 159–174. https://doi.org/10.1016/j.cemconres.2018.04.010.

[51] B. Xu, F. Winnefeld, B. Lothenbach, Effect of temperature curing on properties and hydration of wollastonite blended magnesium potassium phosphate cements, Cement and Concrete Research 142 (2021). https://doi.org/10.1016/j.cemconres.2021.106370.

[52] B. Xu, F. Winnefeld, B. Ma, D. Rentsch, B. Lothenbach, Influence of aluminum sulfate on properties and hydration of magnesium potassium phosphate cements, Cement and Concrete Research 156 (2022). https://doi.org/10.1016/j.cemconres.2022.106788.

4.2. Fibres

4.2.1. Introduction

LG-MgO has been extensively studied in the field of MPC due to its suitability as a source of magnesium oxide. While its composition makes it a viable candidate, recent investigations have also explored novel applications of the MPC binder formulated by using LG-MgO as a magnesium oxide source [3,12].

The increasing prevalence of synthetic fibres in the textile industry, coupled with the high quality of certain sheep wool fibres (SWF) from various regions worldwide, has led to a decline in demand for SWF produced in Europe [13,14]. Nevertheless, this natural, animal-derived fibres continue to be generated since sheep must be regularly sheared throughout their lifecycle [15]. Consequently, alternative uses for locally produced wool are being explored. One promising application is using SWF for developing insulation materials due to their low thermal conductivity [16–20]. This type of insulation offers a balance between efficiency and sustainability, making it an increasingly notable option in the construction sector [21–24].

The fifth research of this doctoral thesis explores the potential of locally produced SWF from Spain to develop improved MPC formulated with LG-MgO. Its low-pH environment, compared to conventional cement's high alkalinity, enhances the compatibility with natural fibres, making it ideal for creating durable, and alternative binders. Thirteen formulations were developed using an experimental design (Design of experiment; DoE) that varied the ratio of SWF to cement and the proportion of SWF to additional water. The main objective of this study was to evaluate the physical, thermal, and mechanical properties of the formulations to identify the optimal composition with the best performance for competitive market applications. To achieve this, tests were conducted on specimens of varying dimensions to assess key parameters, including thermal conductivity, apparent density, modulus of elasticity (MoE), flexural strength, and acoustic insulation. Moreover, this research demonstrates the feasibility of developing MPC using industrial by-products, specifically LG-MgO,

combined with natural fibres to enhance insulation performance. The following sections provide a concise overview of the study's key aspects and its primary contributions.

4.2.2. Relevance

The relevance of this research, Figure 4.3, lies in its pioneering approach to incorporate natural fibres, specifically SWF, into MPC formulated with LG-MgO. This research opens the way for exploring improved properties, such as thermal and acoustic insulation, while also laying the foundation for further studies on natural fibres-reinforced cements, thereby expanding their applicability and importance in sustainable construction practices. By incorporating locally sourced SWF, this research demonstrates the feasibility of producing sustainable cements with superior insulating properties while also promoting efficient waste management practices and supporting environmental sustainability goals.

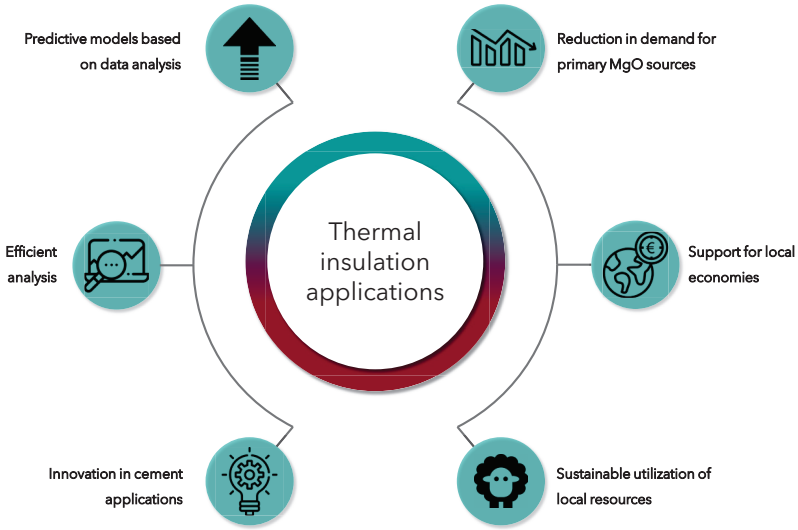

Figure 4.3. Advantages of research on development of MPC with LG-MgO and natural fibres.

4.2.3. Publication 5

Publication 5, titled "Magnesium phosphate cement incorporating sheep wool fibre for thermal insulation applications", was published as an open access article in the October 2023, volume 76 of Building Engineering journal (JIF of 6.7 in 2023, Q1). The title of the publication is presented in Figure 4.4, and the completed text is included in this manuscript.

Figure 4.4. Headline of the article, titled "Magnesium phosphate cement incorporating sheep wool fibre for thermal insulation applications", was published in the journal of Building Engineering in 2023 [25].

Journal of Building Engineering 76 (2023) 107043

Contents lists available at ScienceDirect

Journal of Building Engineering

journal homepage: www.elsevier.com/locate/jobe

Magnesium phosphate cement incorporating sheep wool fibre for thermal insulation applications

A. Maldonado-Alameda, A. Alfocea-Roig, S. Huete-Hernández, J. Giro-Paloma, J.M. Chimenos, J. Formosa *

Department de Ciència de Materials I Química Física, Universitat de Barcelona, C/ Martí I Franquès, 1-11, 08028, Barcelona, Spain

ARTICLE INFO

Keywords:
Magnesium phosphate cement
Low-grade magnesium oxide
By-product
Valorisation
Sheep wool fibre
Design of experiments

ABSTRACT

The increasing use of synthetic fibres in clothing and the high quality of sheep wool fibre (SWF) from the Australian and New Zealand market leads to a decline in the interest in SWFs produced in European countries, considering them as waste that could be valorised within the framework of a circular economy. The use of natural fibre in cement-based composites presents the main issue of durability due to the alkaline pH media of conventional cement. The use of a low-pH cement could improve the viability of combining natural fibres in this low-pH cement as matrix for developing composites. One of these low-pH cements is magnesium phosphate cement (MPC). As a ceramic material the MPC presents high thermal conductivity (~1 W m^{-1} K^{-1}) to be used as isolating material. The present work combines MPC formulated with an industrial by-product (low-grade magnesium oxide; LG-MgO) and Spanish SWF, to develop new sustainable cement-based materials (Sust-MPC-SWF) for thermal building insulation applications. The physical, thermal, and mechanical properties of Sust-MPC-SWF were evaluated to determine the optimal formulation through a design of experiments (DoE). Thirteen formulations designed by DoE were conducted with different sheep wool fibre/cement (SWF/C) and sheep wool fibre/extra water (SWF/EW) ratios. A statistical model was obtained and the optimal formulation (SWF/C = 0.36 and SWF/EW = 0.25) was validated. The increase in SWF content led to an enhancement of thermal and acoustic insulation properties of Sust-MPC-SWF, with similar results to other building materials commercialized with these features.

1. Introduction

There is an undeniable fact that climate change and energy demand are the main threats facing society and planet earth in the coming decades [1,2]. Many industrial and urban activities require complex processes which consume a high amount of energy and carbon dioxide (CO_2) emissions. These processes contribute to the gradual increase in the planet's average annual temperature due to the greenhouse effect, leading to severe environmental problems [3]. In this sense, the building field is one of the highest-polluting industrial sectors due to its carbon and energy-intensive activities and manufacturing processes [4].

On the one hand, among the most polluting industries encompassed in this sector is the cement industry [5,6]. Ordinary Portland cement (OPC) is the most worldwide produced material due to its cost, availability, and mechanical properties. Nowadays, the global production capacity of OPC is more than 4100 Mt per year [7]. OPC industry is currently the third-largest industrial energy consumer

* Corresponding author.
E-mail address: joanformosa@ub.edu (J. Formosa).

https://doi.org/10.1016/j.jobe.2023.107043
Received 4 April 2023; Received in revised form 31 May 2023; Accepted 7 June 2023
Available online 14 June 2023
2352-7102/© 2023 The Authors. Published by Elsevier Ltd. This is an open access article under the CC BY-NC-ND license (http://creativecommons.org/licenses/by-nc-nd/4.0/).

and the second-largest industrial CO_2 emitter globally [8]. For this reason, the OPC industry is increasingly striving to minimise its impact on the environment and the population [9]. The current solutions focus on improving resource and energy efficiency and the development of novel binders based on low carbon manufacturing [10]. Accordingly, new alternative binders have emerged in recent years, extending their application range in diverse technology areas [11]. These alternative cements can contribute to the EU 2050 strategic policy, based on a low-carbon economy, circular economy, and efficiency in using natural resources and energy [12,13].

On the other hand, buildings are responsible for 40% of global CO_2 emissions [14] and consume approximately 40% of global primary energy [15], mainly due to the use of heating, ventilating, and air conditioning (HVAC) systems to provide thermal comfort in both residential and non-residential buildings [16]. For this reason, the search for solutions to the minimisation of energy consumption in buildings becomes crucial to mitigate local and global climate change [17]. In this sense, the EU is recasting its regulations for energy performance in buildings, aiming to promote the building sector decarbonisation and move towards zero-emission building development [18]. Finally, from a materials engineering perspective, it is important to continue developing alternative insulation materials, which can contribute to energy savings in buildings [19].

In this context, this research approaches the development of new sustainable cement-based materials to reduce the use of the OPC as a building material and favour the energy efficiency of buildings. Concretely, this work formulates magnesium phosphate cement (MPC) incorporating sheep wool fibre (SWF) to enhance its thermal insulation properties and decrease energy consumption in buildings. MPC is an acid-base cement being part of the family of Chemically Bonded Phosphate Ceramics (CBPCs) [20]. Its manufacturing presents ecological and environmental benefits compared with OPC manufacturing [21]. MPC offers numerous advantages, including excellent biocompatibility, fast setting, and high early strength, which allow its application as a rapid repair material, hazardous and toxic waste stabiliser, and biomedical material [22]. Moreover, the neutral pH of MPCs cementitious matrixes can be interesting to incorporate natural fibres [23,24] compared to OPC (pH ~ 12–13) since high alkalinity leads to the degradation of the fibres [25]. Regarding SWF, the increasing use of synthetic fibres in clothing and low-quality wool led to a decline in the commercial interest and value of SWF produced in European countries [26]. Nowadays, SWF generates high expenses for the farms and the administrations since it is classified as special waste because it needs a sterilisation treatment to remove pathogenic organisms before its disposal [27]. For this reason, the scientific community are seeking alternatives to valorise this residue in other production sectors such as the building and construction fields. One of these alternatives is the incorporation of SWF in cement-based materials [28]. Most of the studies in the literature incorporate SWF in an OPC matrix to assess their thermal and mechanical properties. SWF stand out for its thermal and acoustic insulation properties, non-flammability and non-toxicity, and the possibility of enhancing the bending properties of cement-based materials [29]. The obtained results generally demonstrated a substantial enhancement of thermal insulation. However, the alkalinity of the cement matrix implies the degradation of SWF, which leads to a decrease in mechanical performance [27,29,30]. In this sense, using a neutral cement-based matrix such as MPC could enhance the final properties of SWF cement composites.

This study aimed to assess the potential use of MPC and SWF to develop a new sustainable insulation material to maintain thermal comfort in buildings. The originality of this work mainly lies in the incorporation of SWF in an alternative cement-based material with a lower pH than OPC. In addition, a low-grade magnesium oxide (LG-MgO) was used to formulate a more sustainable MPC (Sust-MPC) with a lower CO_2 footprint [31]. Hence, this is the first time that SWFs are used in this kind of matrix, MPC and/or Sust-MPC, for developing a composite material. In a previous study conducted by the authors the lowest thermal conductivity achieved with Sust-MPC formulation as a function of W/C ratio and a setting retardant additive was 0.89 $W\,m^{-1}\,K^{-1}$ [32]. The present investigation evaluated Sust-MPC-SWF properties as a function of sheep wool fibre/cement (SWF/C) and sheep wool fibre/extra water (SWF/EW) ratios using a design of experiments (DoE). Thermal, physical, and mechanical properties were determined and then evaluated through the analysis of variance (ANOVA) to determine the optimal formulation for its use as a passive thermal panel.

2. Experimental procedure

2.1. Materials

The LG-MgO was provided by Magnesitas Navarras, S.A. company (Navarra, Spain). This by-product is generated during the calcination of natural magnesite ($MgCO_3$) to produce magnesia (MgO). Furthermore, the food-grade monopotassium phosphate (MKP) was supplied by J. Norken S.L. (Barcelona, Spain). This phosphate source is commonly used as fertiliser and has a purity of 99.8%. The authors previously reported the characterisation of LG-MgO and MKP [33,34]. The SWF used in this research proceeds from the Spanish production of sheep wool, which is considered a residue of the livestock industry due to its low interest. This research aims to modify the Sust-MPC thermal and acoustic properties by incorporating natural fibres, which offer excellent thermal and acoustic insulation [35,36]. For this purpose, the fibres were previously washed and then minced (<5 mm) with a mincer machine (Moulinex A320R1) to favour the mix with MPC paste.

2.2. Design of experiments: optimal formulation

Design of Experiments (DoE) is an efficient method that allows designing a material's ideal dosage, which depends on several factors and restrictions, using the minimum number of experiments or tests [32]. The present research used a response surface methodology (RSM) with a quadratic design to determine optimal formulation using previously obtained results. RSM allowed generating of a response surface plot calculated from statistical polynomic equations derived from the obtained results. Each surface plot represents the results obtained for each evaluated property (response) of the Sust-MPC-SWF. Thermal conductivity, apparent density, modulus of elasticity (MOE), and flexural strength were the responses evaluated to obtain the optimal Sust-MPC-SWF formulation. LG-MgO and MKP to cement (LG-MgO/C and MKP/C) ratios were kept constant in all the experiments, consisting of

Table 1
DoE formulations, fixed ratios and variable factors.

Run	Formulations	Fixed ratios			Variable Factors	
		LG-MgO/*C*	*MKP/C*	*W/C*	*SWF/C*	*SWF/EW*
1	30SWF-25 E W	0.6	0.4	0.4	0.30	0.25
2	20SWF-20 E W	0.6	0.4	0.4	0.20	0.20
3	30SWF-32 E W	0.6	0.4	0.4	0.30	0.32
4	16SWF-25 E W	0.6	0.4	0.4	0.16	0.25
5	20SWF-30 E W	0.6	0.4	0.4	0.20	0.30
6	30SWF-25 E W	0.6	0.4	0.4	0.30	0.25
7	30SWF-25 E W	0.6	0.4	0.4	0.30	0.25
8	30SWF-18 E W	0.6	0.4	0.4	0.30	0.18
9	40SWF-20 E W	0.6	0.4	0.4	0.40	0.20
10	30SWF-25 E W	0.6	0.4	0.4	0.30	0.25
11	44SWF-25 E W	0.6	0.4	0.4	0.44	0.25
12	30SWF-25 E W	0.6	0.4	0.4	0.30	0.25
13	40SWF-30 E W	0.6	0.4	0.4	0.40	0.30

Table 2
Step-by-step procedure for Sust-MPC-SWF formulation.

Stages	Time (s)
Precursors and kneading water addition	0
Mixing start	1
Stop mixing + wool addition	120
Mixing	130
Stop mixing + extra water addition	190
Mixing	200
Stop mixing + wool addition	260
Mixing	270
Stop mixing + pouring	360
Compaction	370
Curing	970

0.6 and 0.4, respectively. The water/cement (W/C) ratio was fixed at 0.4. Two variable factors were considered. On the one hand, the sheep wool fibre/cement (SWF/C) ratio was fixed between 0.2 and 0.4. On the other hand, the sheep wool fibre/extra water (SWF/EW) ratio was fixed between 0.2 and 0.3. SWF was used dried in order to facilitate the study and to avoid a lack of consistency in the results. As it is well known SWF adsorbs part of the kneading water, hence extra water is needed for obtaining the proper workability in the range of study. Hence, both ranges were selected by conducting a preliminary study taking into account the workability during the mixture with a planetary mixer for mortars as well as the final aspect of the product. Table 1 summarises the formulations under study, where the fixed ratios were the same for all the formulations meanwhile the effect of the variable factors were evaluated by means of the software (Design Expert®). The ratios and the statistical approach were conducted by following the methodology reported in previous studies published by the authors [32,37].

Once measured and analysed the obtained responses (thermal conductivity, apparent density, modulus of elasticity (MOE), and flexural strength) for each run, the optimal formulation is determined through a statistical model, assigning the constraints (goals and importance) of each variable factor and response studied. Finally, the preparation of the optimal formulation is performed to validate the feasibility of DoE.

2.3. Sust-MPC-SWF preparation

The preparation of Sust-MPC-SWF was performed through a strict protocol to avoid possible errors and changes caused by the complexity of the preparation process, which could directly affect their final properties. SWF was previously washed, dried in an oven at 60 °C for 24 h and then minced with a mincer machine. Table 2 summarises the chronology steps for the formulation of Sust-MPC-SWF samples and the time when the corresponding stage starts. Before the mixing process, the solid cement components (LG-MgO and MKP) must be weighed and homogenised in the mortar planetary mixer for 1 min. The preparation process starts when the first drop of water contacts the homogenised solids (time 0). Then, i) solids binder precursors (LG-MgO and MKP) and kneading water are mixed for 120 s. Subsequently, ii) half of the SWFs are added and mixed for 60 s. Afterwards, iii) extra water is added and mixed for 60 s. iv) The other half of the SWFs are added and mixed for 90 s. Finally, the fresh Sust-MPC-SWF paste is poured into plate-shaped (150 × 150 × 50 or 300 × 300 × 30 mm) wood moulds and then pressed (for 10 min) in a universal compression test machine until the sample reaches 30 mm of thickness. Then the specimens are cured at laboratory conditions (23 °C ± 2 °C and 50% ± 5% relative humidity) for 24 h.

After 24 h of curing, the specimens are demoulded and dried at 40 °C for three days to remove the “free water” in Sust-MPC-SWF. Finally, the specimens are placed in a container with silica gel until the experimental trials to avoid humidity absorption by the SWF. Fig. 1 depicts the final appearance of Sust-MPC-SWF specimens.

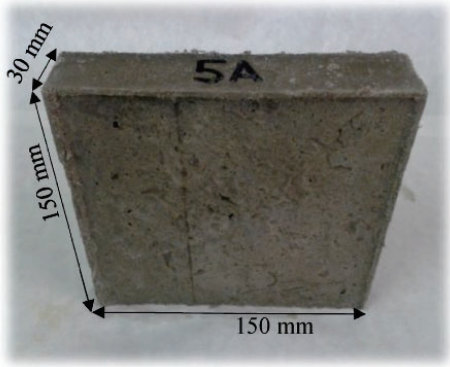

Fig. 1. Final appearance of Sust-MPC-SWF specimen.

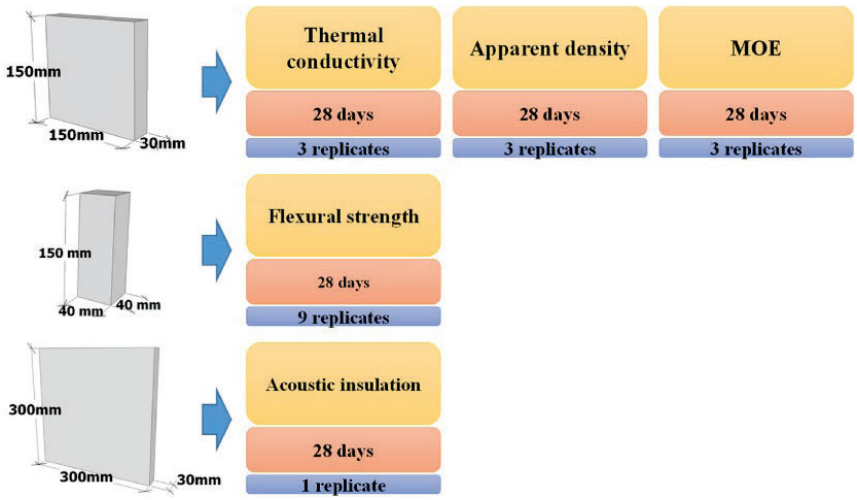

Fig. 2. Flowsheet of the experimental trials.

2.4. Property measurements

Fig. 2 shows the flowsheet of the experimental trials conducted. The property measurements were carried out using different-shaped specimens. The plate-shaped specimens of 150 × 150 × 30 mm were used to evaluate the thermal conductivity (λ), apparent density (ρ), and Modulus of Elasticity (MOE), while the prismatic-shaped specimens (150 × 40 × 40 mm) were used to determine the flexural strength (σ). Finally, the largest plate-shaped specimen (300 × 300 × 30 mm) was performed just for the proposed optimal formulation to assess the acoustic insulation. The properties considered in the statistical study were thermal conductivity (λ), apparent density (ρ), Modulus of Elasticity (MOE), and flexural strength (σ), while acoustic insulation was just evaluated for the proposed optimal formulation.

2.4.1. Thermal conductivity (λ)

Thermal conductivity was measured using Quickline™-30, Anter Corporation (USA), equipment. The equipment follows a dynamic measurement method based on the ASTM D5930 standard to determine thermal conductivity [38]. Two surface probes with a measuring range of 0.01–0.3 W m^{-1} K^{-1} and 0.3–2.0 W m^{-1} K^{-1} were used. During samples measurements, the ambient temperature was 23.0 °C ± 2.0 °C, and the relative humidity was 50% ± 5%. The thermal conductivities of each plate-shaped specimen (150 × 150 × 30 mm) were computed from two measured values. This thermal property allowed assessing the effect of wool content on the

Table 3
Responses of the DoE.

Formulations	Responses			
	λ (W·m^{-1}·K^{-1})	ρ (kg·m^{-3})	MoE (GPa)	σ (MPa)
30SWF-25 E W	0.152	830	0.24	0.31
20SWF-20 E W	0.173	905	0.62	1.01
30SWF-32 E W	0.216	993	0.67	2.54
16SWF-25 E W	0.209	1015	0.88	2.01
20SWF-30 E W	0.227	1050	0.97	2.68
30SWF-25 E W	0.140	840	0.24	0.46
30SWF-25 E W	0.141	820	0.24	0.33
30SWF-18 E W	0.189	876	0.43	1.78
40SWF-20 E W	0.154	813	0.20	1.99
30SWF-25 E W	0.140	850	0.22	0.45
44SWF-25 E W	0.164	833	0.18	2.19
30SWF-25 E W	0.160	860	0.24	0.77
40SWF-30 E W	0.157	850	0.28	1.51

thermal behaviour of Sust-MPC-SWF.

2.4.2. Bulk density (ρ)

The plate-shaped specimens used for the thermal conductivity test were previously conditioned to measure the bulk density, which was determined by weighing and measuring each specimen. The sample dimensions were computed from the average thickness, width, and length (8 measures per dimension).

2.4.3. Modulus of elasticity (MoE)

Modulus of Elasticity (MoE) was determined using an ultrasonic pulse velocity tester (C368, Matest, Italy) following the UNE-EN 12504-4 standard. The equipment consisted of an emitter transducer (T_x) and a receiver transducer (R_x) operating at 50 Hz. The emitter applies an acoustic wave transmitted throughout the thickness of each plate-shaped specimen. Then, the receiver detects the wave signal, and the equipment can measure the delay time. MoE was calculated (five measurements per specimen) through Eqs. (1) and (2):

$$MoE = \rho \cdot V^2 \quad \text{Eq. 1}$$

$$V = 2 \cdot T \cdot f \quad \text{Eq. 2}$$

where ρ (kg·m^{-3}) is the bulk density, V (m·s^{-1}) is the wave passage velocity, T (m) is the thickness of the specimen, and f (Hz) is the vibration frequency.

2.4.4. Flexural strength (σ)

The flexural strength measurement was carried out using technical equipment (Zmart-PRO, ZwickRoell, Germany) following the standard UNE-EN 196-1 method. The plate-shaped specimens (150 × 150 × 30 mm) used in the previously described tests were cut to obtain three prism-shaped specimens (40 × 40 × 150 mm) using a cutting machine. A progressive load until fracture was applied with a loading rate of 10 mm min^{-1}. Flexural strength was computed by nine specimens of each formulation using Eq. (3):

$$Flexural\ strength = \frac{1.5 \cdot F \cdot L}{b \cdot h^2} \quad \text{Eq. 3}$$

where F is the maximum load applied, L is the distance between the two support rods, b is the length of the specimen, and h *is* the height of the prism-shaped specimen.

2.4.5. Sound reduction index

The acoustic insulation level was evaluated through a standardized test according to the UNE-EN 140–1. Two interconnected cabins with a square hole of 300 × 300 mm were used. The largest plate-shaped specimen (300 × 300 × 30 mm) was placed in the square hole. A loudspeaker (noise emitter) was placed in one of the cabins. Two microphones were placed in each cabin to obtain the emission (Le) and immission (Lr) levels. The microphones (MI 17 type of ¼'') allow recording the decibel data at different frequencies (20 Hz-4kHz (±0.5 dB); 4–20 kHz (±1 dB)) to compare the noise level between the two cabins and thus obtain the sound reduction index [39]. The data acquisition was recorded with the help of a DA-20 equipment and DA-20PA1 v2.0 software from RION Co., Ltd. In this case, the test was only performed on the optimal formulation and a MPC without sheep wool fibre as reference material.

3. Results and discussion

3.1. DoE: analysis of responses

The DoE analysis is based on the analysis of variance (ANOVA) to predict an optimal response. The p-value allows interpretation of the obtained results. This parameter represents the lowest level of significance that would lead to rejection of the null hypothesis,

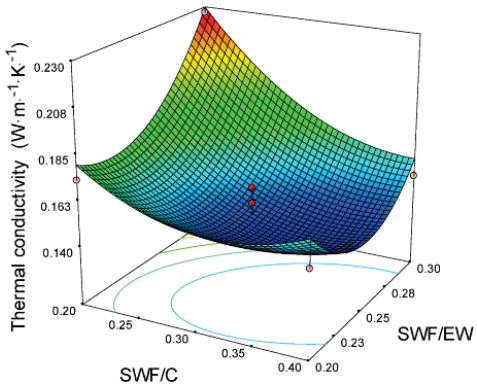

Fig. 3. Surface plot of the thermal conductivity.

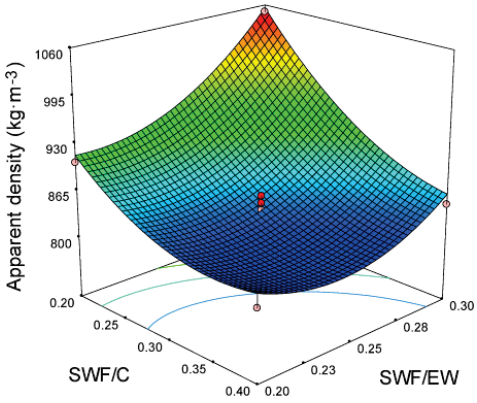

Fig. 4. Surface plot of the bulk density.

indicating that the controllable factor does not affect the response under study. Therefore, this factor will be statistically significant with a confidence level above 95% if the p-value is smaller than 0.05. The DoE was significant for all the responses analysed in the present study. Table 3 summarises the experimental values obtained for each response. All the equations of the statistical model were mathematically fitted. Thus, each response analysed allowed for determining a mathematical formula, which adjusted to the response surface. The following sub-sections discuss and present the proposed models (in terms of actual factors) for each response under study.

3.1.1. Thermal conductivity (λ)

Thermal conductivity (λ) is an important parameter to determine the thermal insulation capability of a construction material [40]. Therefore, the main goal of this investigation was to minimise thermal conductivity through the incorporation of SWF (Table 3). As a result of formulations proposed by DoE, the lowest thermal conductivity was 0.140 W m^{-1} K^{-1} in the 30SWF-25 E W formulation, while the highest was 0.227 W m^{-1} K^{-1} in the 20SWF-30 E W formulation (Table 3). The experimental values of the thermal conductivity allowed determining the mathematical model (Eq. (4)) and the surface plot (Fig. 3). The model presented a standard deviation and an R^2 value of 0.01 and 0.91, respectively. Focusing on the surface plot of thermal conductivity depending on variable factors studied (Fig. 3), the authors expected a linear trend based on the decrease in thermal conductivity when increase the amount of SWF fibres and vice-versa. However, the minimum thermal conductivity is around the median value of SWF/C (0.3) and SWF/EW (0.25) ranges. This fact agrees with the quadratic adjustment presented by both variable factors shown in Eq. (4) and reveals that both the increase and decrease in EW negatively affect the objective of minimising thermal conductivity. On the one hand, a lower EW content leads to less evaporation of "free water" during the curing process of Sust-MPC-SWF, generating less porosity and increasing thermal conductivity [32]. On the other hand, the unexpected increase in thermal conductivity as increased EW content is probably due to the high hygroscopicity of SWF [27], which leads to moisture trapping and the consequent increase in thermal conductivity as

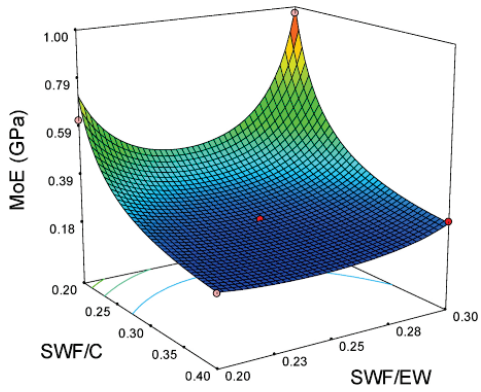

Fig. 5. Surface plot of the MoE.

reported elsewhere [41]. However, it could also be due to the high compaction of SWF during the sample preparation [42]. The excess of water favours the compaction of SWF, reducing their voids and leading to an increase in the thermal conductivity.

$$\lambda\left(\frac{W}{m\cdot K}\right)=0.69-0.50\cdot\frac{SWF}{C}-3.75\cdot\frac{SWF}{EW}-2.55\cdot\frac{SWF}{C}\cdot\frac{SWF}{EW}+1.58\cdot\left(\frac{SWF}{C}\right)^2+9.5\cdot\left(\frac{SWF}{EW}\right)^2 \quad \text{Eq. 4}$$

3.1.2. Bulk density (ρ)

The bulk density is significant in defining potential materials applications in the building field. Table 3 summarises bulk density responses, where the lowest (813 kg m^{-3}) was obtained in the 40SWF-20 E W formulation, while the highest (1050 kg m^{-3}) was in the 20SWF-30 E W formulation. The mathematical model of bulk density revealed a quadratic adjustment between the two variable factors (SWF/C and SWF/EW), as shown in Eq. (5). The standard deviation and R^2 values were 18.62 and 0.97, respectively. The bulk density surface plot (Fig. 4) tendency was similar to the thermal conductivity surface plot (Fig. 3). As expected, the higher the amount of the fibres, the lower the bulk density obtained since the SWF is less dense than the cement. In addition, the increase in EW leads to a decrease in bulk density due to the increase of porosity generated by the evaporation of "free water" during the sample curing [32]. However, as it occurred in thermal conductivity, the maximum SWF/C ratio and the minimum SWF/EW ratio slightly increased bulk density. This behaviour is attributable to the increase in humidity due to the hygroscopicity of SWF. The higher the SWF content, the higher the moisture trapped in the specimens. Therefore, the increase in humidity leads to an increase in bulk density due to the higher density of water compared SWF [36].

$$\rho\left(\frac{kg}{m^3}\right)=1.78-1.48\cdot\frac{SWF}{C}-5.74\cdot\frac{SWF}{EW}-5.42\cdot\frac{SWF}{C}\cdot\frac{SWF}{EW}+3.59\cdot\left(\frac{SWF}{C}\right)^2+16.47\cdot\left(\frac{SWF}{EW}\right)^2 \quad \text{Eq. 5}$$

3.1.3. Modulus of elasticity (MoE)

The material's density and stiffness are intimately related to MoE. Therefore, the authors expected that the increase in SWF would lead to a decrease in MoE of Sust-MPC-SWF formulations. As a result of analysing the formulations proposed by DoE, the lowest MoE (0.20 GPa) was obtained in the 40SWF-20 E W formulation, while the highest (0.97 GPa) in the 20SWF-30 E W formulation, as shown in Table 3. Eq. (6) shows the mathematical model for fitting the response values of the MoE. The standard deviation and R^2 values were 0.20 and 0.99, respectively. Fig. 5 represents the surface plot of the MoE, where it is observed that the maximum value is obtained when the amount of EW and SWF decreases, as expected. The decrease in EW implies a lower porosity in the MPC matrix, causing higher densification and, therefore, a higher MoE value. The surface plot also revealed that the lower the amount of the fibres, the stronger the influence of the extra water percentage in MoE. In this sense, the increase in MoE as the SWF/EW ratio decreases is probably due to the higher compaction of fibres, which leads to a densification of the material. In contrast, it is observed that the increase in fibre amount leads to MoE stabilised values, as evidenced by the plateau as the SWF/C ratio approaches 0.4.

$$MoE^{-1}(GPa)=-33.2+50.1\cdot\frac{SWF}{C}+229\cdot\frac{SWF}{EW}-42.3\cdot\frac{SWF}{C}\cdot\frac{SWF}{EW}-40.4\cdot\left(\frac{SWF}{C}\right)^2-449\cdot\left(\frac{SWF}{EW}\right)^2 \quad \text{Eq. 6}$$

3.1.4. Flexural strength (σ)

The flexural strength responses of Sust-MPC-SWF formulations are shown in Fig. 6. The minimum flexural strength was presented by the 30SWF-25 E W formulation (0.31 MPa) and the maximum by the 20SWF-30 E W (2.68 MPa) formulation. Eq. (7) shows the adjusted formula to obtain the flexural strength according to the selected SWF/C and SWF/EW ratios. The standard deviation and R^2 values were 0.23 and 0.96, respectively. Fig. 6 depicts the surface plot of the flexural strength. Two maximums can be considered in

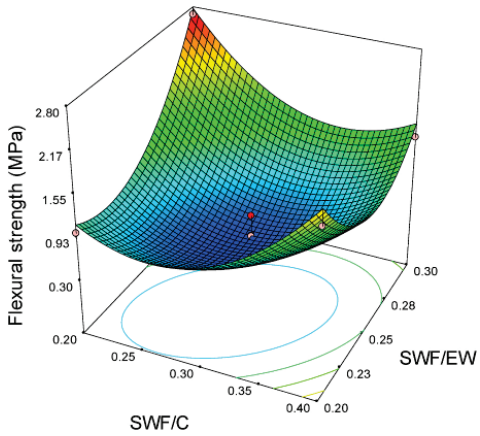

Fig. 6. Surface plot of the flexural strength.

Table 4
Optimisation criteria and optimal formulation.

Constraints			Predicted range		Optimal formulation	
Parameters	Goal	Importance	Lower	Upper	Experimental value	Predicted value
SWF/C	In the range	3	0.20	0.40	0.36	
SWF/EW	In the range	3	0.20	0.30	0.25	
λ ($W{\cdot}m^{-1}{\cdot}K^{-1}$)	Minimise	5	0.130	0.150	0.148	0.141
ρ ($kg{\cdot}m^{-3}$)	Minimise	5	791	829	818	810
MoE (GPa)	In the range	3	0.18	0.21	0.23	0.2
σ (MPa)	In the range	3	0.47	0.95	0.54	0.77

this parameter, one of them when the SWF and EW decrease and the other when these two factors increase. In the first case, the main reason is the lower proportion of EW and SWF, which reduces the porosity, causing a higher stiffness and enhancing the mechanical performance. The second case is due to the higher proportion of SWF since fibres act as a reinforcement of the cement matrix, enhancing flexural capacity before reaching fracture.

$$\sigma(MPa) = 16.7 - 17.1 \cdot \frac{SWF}{C} - 115 \cdot \frac{SWF}{EW} - 107.25 \cdot \frac{SWF}{C} \cdot \frac{SWF}{EW} + 73.5 \cdot \left(\frac{SWF}{C}\right)^2 + 306 \cdot \left(\frac{SWF}{EW}\right)^2 \quad \text{Eq. 7}$$

3.2. Optimal formulation

The optimal formulation (Table 4) was determined using the statistical models of each response presented above. However, as mentioned before, it was necessary to prepare the optimal formulation to validate the DoE, comparing the values obtained experimentally for each response with the values predicted by using the mathematical equations (Eq. 4-7). Moreover, considering that this research aimed to enhance the thermal properties of Sust-MPC-SWF for its use as a thermal passive construction system, the main goal was to minimise the thermal conductivity and bulk density (Table 4). The rest of the factors and responses were assigned within the range limits. Finally, the importance of each parameter was fixed at 3 (on a scale of 5), except thermal conductivity and bulk density, which were fixed at 5. Table 4 also shows that the statistical responses predicted by the mathematical model and the experimental responses values (thermal conductivity, bulk density, and flexural strength) matched, except for MoE. The difference in MoE may be due to the difference in laboratory temperature and humidity conditions during the curing of the DoE formulations shown in Table 1 and the optimal formulation (Table 4). The variation of these two parameters affects the densification of the material and, therefore, the stiffness. However, the MoE value is very close to the upper limit of the predicted value. Hence, it can conclude that DoE was performed successfully. Thermal conductivity, bulk density, and MoE of a Sust-MPC without SWF are 0.89 $W\,m^{-1}\,K^{-1}$, 1925.2 $kg\,m^{-3}$, and 16.50 GPa, respectively [32]. As it was expected thermal conductivity, bulk density, and MoE are significantly reduced when Sust-MPC-SWF are formulated in the proportions indicated in Table 4 and compared with previous works, (i.e.: 83.4%, 57.1%, and 98.6%, respectively).

3.2.1. Sound reduction index

Fig. 7a and b show the emission (Le) and immission (Li) noise levels of reference MPC and optimal formulation (36SWF-25 E W),

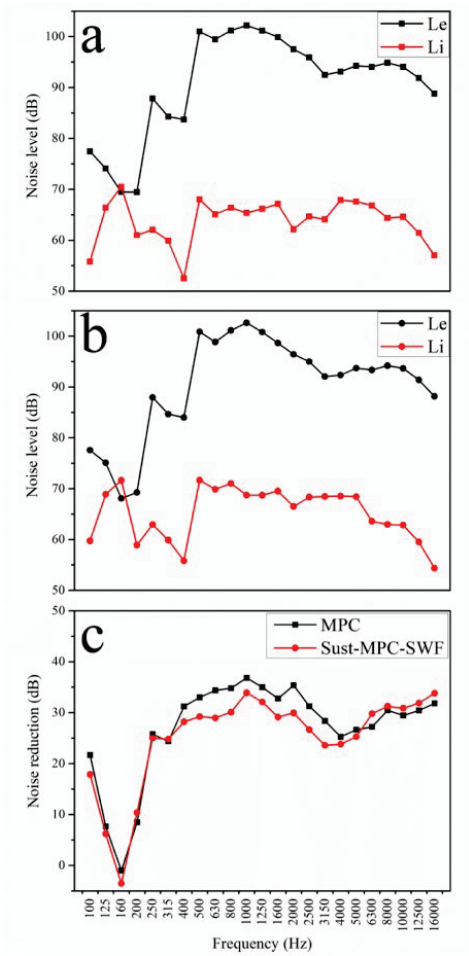

Fig. 7. (a) Emission and immission noise levels of reference MPC (b) Emission and immission noise levels of optimal formulation (c) Noise reduction achieved by reference MPC and optimal formulation.

respectively. A substantial reduction of level emissions in low, intermediate, and high frequencies can be observed, except in 120, 160, and 200 Hz. On the other hand, the sound reduction index in reference MPC is slightly higher than the optimal formulation, as shown in Fig. 7c. This fact is attributed to the difference in bulk density since the higher the density, the higher the acoustic insulation. In this sense, the reference MPC has a bulk density of around 1800 kg m^{-3}, as reported elsewhere [43]. Finally, it was demonstrated that the sound reduction index of the optimal formulation is similar to other materials such as wood wool and cellulose [29].

4. Conclusions

This research evidenced that it is possible to formulate a sustainable MPC with magnesium oxide by-product incorporating SWF as an admixture to improve thermal insulation properties (Sust-MPC-SWF). Furthermore, the formulation of Sust-MPC-SWF also promotes sustainability criteria using special waste and industrial by-products such as SWF and LG-MgO. In addition, Sust-MPC-SWF can contribute as potential insulation material in passive energy buildings to optimise energy efficiency and thermal comfort.

The DoE and the ANOVA statistical analysis allowed obtaining a model for further optimisation of Sust-MPC-SWF formulation, minimising thermal conductivity and apparent density. Therefore, the optimal dosage was obtained by considering mixing variables such as sheep wool fibres/cement (SWF/C) and sheep wool fibres/extra water (SWF/EW) ratios. The range, factors and responses

under study were appropriately adjusted to quadratic equations. The work demonstrated that it is possible to control the dosages by following the proposed methodology to diminish thermal conductivity and apparent density.

Both SWF/C and SWF/EW ratios evidenced a synergistic interaction as demonstrated in the surface plots of each response studied, where no linear trend is observed. The unexpected increase in thermal conductivity and apparent density in formulations with high fibre content is due to the hygroscopic nature of the SWF, leading to moisture absorption. The unexpected increase in MoE when the EW proportion increase is probably due to the high "free water" content, which favours the compaction of SWF and the densification of Sust-MPC-SWF. It was also revealed that SWF enhances the bending capacity when the SWF/EW ratio decrease.

The optimal formulation proposed a SWF/C ratio of 0.36 and a SWF/EW of 0.25. The experimental results obtained in this formulation validated the DoE performed in this investigation. The use of SWF for developing Sust-MPC-SWF allows to reduce of the thermal conductivity of Sust-MPC without SWF (83% of reduction for the optimal formulation), with a remarkable reduction of the mechanical properties. Considering the mechanical results of the optimal formulation, it would be concluded that the Sust-MPC-SWF composite could be used just as a non-structural material. For instance, it would be used a part for developing External Thermal Insulation Composite System (ETICS). Finally, the sound reduction index determined in the optimal formulation showed similar values to other building materials.

CRediT authorship contribution statement

A. Maldonado-Alameda: Data curation, Formal analysis, Investigation, Writing - original draft. **A. Alfocea-Roig**: Data curation, Formal analysis, Visualization, Writing - review & editing. **S. Huete-Hernández**: Resources, Visualization. **J. Giro-Paloma**: Visualization, Supervision, Writing - review & editing. **J. M. Chimenos**: Visualization, Supervision, Writing - review & editing, Funding acquisition. **J. Formosa**: Conceptualization, Visualization, Supervision, Methodology, Writing - review & editing, Funding acquisition.

Declaration of competing interest

The authors declare that they have no known competing financial interests or personal relationships that could have appeared to influence the work reported in this paper.

Data availability

Data will be made available on request.

Acknowledgements

This work is partially supported by Social Innova (FGB308411) company, by the Spanish Government with the Grant PID2021-125810OB-C21 funded by MCIN/AEI/10.13039/501,100,011,033 and by "ERDF A way of making Europe", and by the Catalan Government with the Grant 2021 SGR 00708. Furthermore, the Agència de Gestió d'Ajuts Universitaris i de Recerca (AGAUR) contributed through Ms A. Alfocea-Roig's PhD grant (FI-DGR 2021). The authors would like to thank Magnesitas Navarras, S.A. company for material supply. Dr. Jessica Giro-Paloma is a Serra Húnter Fellow.

References

[1] S.R. Paramati, U. Shahzad, B. Doğan, The role of environmental technology for energy demand and energy efficiency: evidence from OECD countries, Renew. Sustain. Energy Rev. 153 (2022), https://doi.org/10.1016/j.rser.2021.111735.
[2] D. Degroot, K. Anchukaitis, M. Bauch, J. Burnham, F. Carnegy, J. Cui, K. de Luna, P. Guzowski, G. Hambrecht, H. Huhtamaa, A. Izdebski, K. Kleemann, E. Moesswilde, N. Neupane, T. Newfield, Q. Pei, E. Xoplaki, N. Zappia, Towards a rigorous understanding of societal responses to climate change, Nature 591 (2021) 539–550, https://doi.org/10.1038/s41586-021-03190-2.
[3] L. Al-Ghussain, Global warming: review on driving forces and mitigation, Environ. Prog. Sustain. Energy 38 (2019) 13–21, https://doi.org/10.1002/ep.13041.
[4] E.W.L. Cheng, Y.H. Chiang, B.S. Tang, Exploring the economic impact of construction pollution by disaggregating the construction sector of the input-output table, Build. Environ. 41 (2006) 1940–1951, https://doi.org/10.1016/j.buildenv.2005.06.020.
[5] H.G. Van Oss, A.C. Padovani, Cement manufacture and the environment Part I: chemistry and technology, J. Ind. Ecol. 6 (2002) 89–105, https://doi.org/10.1162/10881980232097165O.
[6] H.G. Van Oss, A.C. Padovani, Cement Manufacture and the Environment Part II: environmental Challenges and Opportunities Keywords alternative fuels carbon dioxide clinker greenhouse gases (GHG) industrial symbiosis portland cement, J. Ind. Ecol. 7 (2003) 93–126, https://doi.org/10.1162/108819803766729212.
[7] J.F. Reilly, Mineral commodity summaries 2020, Reston, VA. https://doi.org/10.3133/mcs2020, 2020.
[8] M.B. Ali, R. Saidur, M.S. Hossain, A review on emission analysis in cement industries, Renew. Sustain. Energy Rev. 15 (2011) 2252–2261, https://doi.org/10.1016/j.rser.2011.02.014.
[9] J. Lehne, F. Preston, Making Concrete Change: Innovation in Low-Carbon Cement and Concrete, 2018.
[10] I.E.A. International, E. Agency, Technology Roadmap for Cement, SpringerReference, 2011.
[11] M.C.G. Juenger, F. Winnefeld, J.L. Provis, J.H. Ideker, Advances in alternative cementitious binders, Cement Concr. Res. 41 (2011) 1232–1243, https://doi.org/10.1016/j.cemconres.2010.11.012.
[12] Institute for Sustainability Leadership, Industrial Transformation 2050 - Pathways to Net-Zero Emissions from EU Heavy Industry, 2019.
[13] P. Hoddinott, The Role of Cement in the 2050 Low Carbon Economy, 2013.
[14] A. Tallini, L. Cedola, A review of the properties of recycled and waste materials for energy refurbishment of existing buildings towards the requirements of NZEB, Energy Proc. 148 (2018) 868–875, https://doi.org/10.1016/j.egypro.2018.08.108.
[15] G. Martinopoulos, K.T. Papakostas, A.M. Papadopoulos, A comparative review of heating systems in EU countries, based on efficiency and fuel cost, Renew. Sustain. Energy Rev. 90 (2018) 687–699, https://doi.org/10.1016/j.rser.2018.03.060.
[16] Sholahudin Nasruddin, P. Satrio, T.M.I. Mahlia, N. Giannetti, K. Saito, Optimization of HVAC system energy consumption in a building using artificial neural network and multi-objective genetic algorithm, Sustain. Energy Technol. Assessments 35 (2019) 48–57, https://doi.org/10.1016/j.seta.2019.06.002.

[17] M. Santamouris, Innovating to zero the building sector in Europe: minimising the energy consumption, eradication of the energy poverty and mitigating the local climate change, Sol. Energy 128 (2016) 61–94, https://doi.org/10.1016/j.solener.2016.01.021.
[18] European Commission, DIRECTIVE of the EUROPEAN PARLIAMENT and of the COUNCIL on the Energy Performance of Buildings (Recast), European Union, 2021.
[19] B. Abu-Jdayil, A.H. Mourad, W. Hittini, M. Hassan, S. Hameedi, Traditional, state-of-the-art and renewable thermal building insulation materials: an overview, Construct. Build. Mater. 214 (2019) 709–735, https://doi.org/10.1016/j.conbuildmat.2019.04.102.
[20] A.S. Wagh, Introduction to Chemically Bonded Ceramics, in: E.S. Publishing (Ed.), Chem. Bond. Phosphate Ceram, Elsevier, 2016, pp. 1–16, https://doi.org/10.1016/B978-0-08-100380-0.00001-4.
[21] A.S. Wagh, Environmental Implications of Chemically Bonded Phosphate Ceramic Products, in: E.S. Publishing (Ed.), Chem. Bond. Phosphate Ceram, Elsevier, 2016, pp. 359–372, https://doi.org/10.1016/B978-0-08-100380-0.00020-8.
[22] M.A. Haque, B. Chen, Research progresses on magnesium phosphate cement: a review, Construct. Build. Mater. 211 (2019) 885–898, https://doi.org/10.1016/j.conbuildmat.2019.03.304.
[23] S. Manso, G. Mestres, M.P. Ginebra, N. De Belie, I. Segura, A. Aguado, Development of a low pH cementitious material to enlarge bioreactivity, Construct. Build. Mater. 54 (2014) 485–495, https://doi.org/10.1016/j.conbuildmat.2014.01.001.
[24] R. del Valle-Zermeño, J.E. Aubert, A. Laborel-Préneron, J. Formosa, J.M. Chimenos, Preliminary study of the mechanical and hygrothermal properties of hemp-magnesium phosphate cements, Construct. Build. Mater. 105 (2016) 62–68, https://doi.org/10.1016/j.conbuildmat.2015.12.081.
[25] J. Wei, C. Meyer, Degradation mechanisms of natural fiber in the matrix of cement composites, Cement Concr. Res. 73 (2015) 1–16, https://doi.org/10.1016/j.cemconres.2015.02.019.
[26] B. Petek, R. Marinšek Logar, Management of waste sheep wool as valuable organic substrate in European Union countries, J. Mater. Cycles Waste Manag. 23 (2021) 44–54, https://doi.org/10.1007/s10163-020-01121-3.
[27] M.C.M. Parlato, S.M.C. Porto, Organized framework of main possible applications of sheep wool fibers in building components, Sustain. Times 12 (2020), https://doi.org/10.3390/su12030761.
[28] R. Alyousef, H. Alabduljabbar, H. Mohammadhosseini, A.M. Mohamed, A. Siddika, F. Alrshoudi, A. Alaskar, Utilization of sheep wool as potential fibrous materials in the production of concrete composites, J. Build. Eng. 30 (2020), 101216, https://doi.org/10.1016/j.jobe.2020.101216.
[29] D. Jóźwiak-Niedźwiedzka, A.P. Fantilli, Wool-reinforced cement based composites, Materials 13 (2020), https://doi.org/10.3390/MA13163590.
[30] M.T. Marvila, H.A. Rocha, A.R.G. de Azevedo, H.A. Colorado, J.F. Zapata, C.M.F. Vieira, Use of natural vegetable fibers in cementitious composites: concepts and applications, Innov. Infrastruct. Solut. 6 (2021) 1–24, https://doi.org/10.1007/s41062-021-00551-8.
[31] R. del Valle-Zermeño, J. Giro-Paloma, J. Formosa, J.M. Chimenos, Low-grade magnesium oxide by-products for environmental solutions: characterization and geochemical performance, J. Geochem. Explor. 152 (2015), https://doi.org/10.1016/j.gexplo.2015.02.007.
[32] M. Niubó, J. Formosa, A. Maldonado-Alameda, R. del Valle-Zermeño, J.M. Chimenos, Magnesium phosphate cement formulated with low grade magnesium oxide with controlled porosity and low thermal conductivity as a function of admixture, Ceram. Int. 42 (2016), https://doi.org/10.1016/j.ceramint.2016.06.159.
[33] S. Huete-Hernández, A. Maldonado-Alameda, J. Giro-Paloma, J.M. Chimenos, J. Formosa, Fabrication of sustainable magnesium phosphate cement micromortar using design of experiments statistical modelling: valorization of ceramic-stone-porcelain containing waste as filler, Ceram. Int. 47 (2021) 10905–10917, https://doi.org/10.1016/j.ceramint.2020.12.210.
[34] S. Huete-hernández, A. Maldonado-alameda, A. Alfocea-roig, J. Giro-paloma, J.M. Chimenos, J. Formosa, Sustainable magnesium phosphate micromortars formulated with PAVAL ® alumina by-product as, Boletín La Soc. Española Cerámica y Vidr (2023) 1–15, https://doi.org/10.1016/j.bsecv.2023.02.001.
[35] T. Michael, S. Kumar, L. Kumar, M.P. Shettar, S. Pal, Materials Today : proceedings Assessing the potentials of Bamboo and sheep wool fiber as sustainable construction materials : a review, Mater. Today Proc. (2021), https://doi.org/10.1016/j.matpr.2021.05.322.
[36] O. Dénes, I. Florea, D.L. Manea, Utilization of sheep wool as a building material, Procedia Manuf. 32 (2019) 236–241, https://doi.org/10.1016/j.promfg.2019.02.208.
[37] J. Formosa, J.M. Chimenos, A.M. Lacasta, M. Niubó, Interaction between low-grade magnesium oxide and boric acid in chemically bonded phosphate ceramics formulation, Ceram. Int. 38 (2012) 2483–2493, https://doi.org/10.1016/j.ceramint.2011.11.017.
[38] A.H.-C. Shin, U. Kodide, Thermal conductivity of ternary mixtures for concrete pavements, Cem. Concr. Compos. 34 (2012) 575–582, https://doi.org/10.1016/j.cemconcomp.2011.11.009.
[39] R. del Rey, J. Alba, J.C. Rodríguez, L. Bertó, Characterization of new sustainable acoustic solutions in a reduced sized transmission chamber, Buildings 9 (2019), https://doi.org/10.3390/buildings9030060.
[40] L.D. Hung Anh, Z. Pásztory, An overview of factors influencing thermal conductivity of building insulation materials, J. Build. Eng. 44 (2021), https://doi.org/10.1016/j.jobe.2021.102604.
[41] D. Bosia, L. Savio, F. Thiebat, A. Patrucco, S. Fantucci, G. Piccablotto, D. Marino, Sheep wool for sustainable architecture, Energy Proc. 78 (2015) 315–320, https://doi.org/10.1016/j.egypro.2015.11.650.
[42] T.T. Nguyen, V. Picandet, P. Carre, T. Lecompte, S. Amziane, C. Baley, Effect of compaction on mechanical and thermal properties of hemp concrete, Eur. J. Environ. Civ. Eng. 14 (2010) 545–560, https://doi.org/10.1080/19648189.2010.9693246.
[43] A. Maldonado-Alameda, A.M. Lacasta, J. Giro-Paloma, J.M. Chimenos, L. Haurie, J. Formosa, Magnesium phosphate cements formulated with low grade magnesium oxide incorporating phase change materials for thermal energy storage, Construct. Build. Mater. 155 (2017) 209–216, https://doi.org/10.1016/j.conbuildmat.2017.07.227.

4.3. References

[1] Y. Liu, Z. Qin, B. Chen, Influence of low-grade bauxite on the properties of magnesium phosphate cement, Construction and Building Materials 242 (2020). https://doi.org/10.1016/j.conbuildmat.2020.118052.

[2] J. Formosa, J.M. Chimenos, A.M. Lacasta, M. Niubó, Interaction between low-grade magnesium oxide and boric acid in chemically bonded phosphate ceramics formulation, Ceramics International 38 (2012) 2483–2493. https://doi.org/10.1016/j.ceramint.2011.11.017.

[3] A. Maldonado-Alameda, A.M. Lacasta, J. Giro-Paloma, J.M. Chimenos, L. Haurie, J. Formosa, Magnesium phosphate cements formulated with low grade magnesium oxide incorporating phase change materials for thermal energy storage, Construction and Building Materials 155 (2017) 209–216. https://doi.org/10.1016/j.conbuildmat.2017.07.227.

[4] Future Market Insights, Calcite market, (2022). https://www.futuremarketinsights.com/reports/calcite-market.

[5] Statista, Market volume of magnesium oxide worldwide from 2015 to 2022, with a forecast for 2023 to 2030, (2022). https://www.statista.com/statistics/1310514/magnesium-oxide-market-volume-worldwide/.

[6] D. Mazumdar, Review, Analysis, and Modeling of Continuous Casting Tundish Systems, Steel Research Int. 90 (2019). https://doi.org/10.1002/ srin.201800279.

[7] F. Ravazzolo, J. Vespignani, World steel production: A new monthly indicator of global real economic activity, Canadian J of Economics 53 (2020) 743–766. https://doi.org/10.1111/caje.12442.

[8] World Steel Association, World Steel in Figures, (2024). https://worldsteel.org/data/world-steel-in-figures-2024/.

[9] Statista, Steel industry - Statistics & Facts, (2024). https://www.statista.com/topics/1149/steel-industry/topicOverview.

[10] H. Ma, B. Xu, Z. Li, Magnesium potassium phosphate cement paste: Degree of reaction, porosity and pore structure, Cement and Concrete Research 65 (2014) 96–104. https://doi.org/10.1016/j.cemconres.2014.07.012.

[11] A. Rabbani, S. Jamshidi, Specific surface and porosity relationship for sandstones for prediction of permeability, International Journal of Rock Mechanics and Mining Sciences 71 (2014) 25–32. https://doi.org/10.1016/j.ijrmms.2014.06.013.

[12] S. Huete-Hernández, A. Maldonado-Alameda, J. Giro-Paloma, J.M. Chimenos, J. Formosa, Fabrication of sustainable magnesium phosphate cement micromortar using design of experiments statistical modelling: Valorization of ceramic-stone-porcelain containing waste as filler, Ceramics International 47 (2021) 10905–10917. https://doi.org/10.1016/j.ceramint.2020.12.210.

[13] R. Nayak, L.V.T. Nguyen, T. Panwar, L. Jajpura, Sustainable technologies and processes adapted by fashion brands, in: Sustainable Technologies for Fashion and Textiles, Elsevier, 2020: pp. 233–248. https://doi.org/10.1016/B978-0-08-102867-4.00011-6.

[14] B. Petek, R. Marinšek Logar, Management of waste sheep wool as valuable organic substrate in European Union countries, J Mater Cycles Waste Manag 23 (2021) 44–54. https://doi.org/10.1007/s10163-020-01121-3.

[15] X. Xueliang, Animal Fibers: Wool, in: J. Hu, B. Kumar, J. Lu (Eds.), Handbook of Fibrous Materials, 1st ed., Wiley, 2020: pp. 37–74. https://doi.org/10.1002/9783527342587.ch2.

[16] T. Cardinale, G. Arleo, F. Bernardo, A. Feo, P. De Fazio, Thermal and mechanical characterization of panels made by cement mortar and sheep's wool fibres, Energy Procedia 140 (2017) 159–169. https://doi.org/10.1016/j.egypro.2017.11.132.

[17] M.S. Imbabi, C. Carrigan, S. McKenna, Trends and developments in green cement and concrete technology, International Journal of Sustainable Built Environment 1 (2012) 194–216. https://doi.org/10.1016/j.ijsbe.2013.05.001.

[18] B. Abu-Jdayil, A.-H. Mourad, W. Hittini, M. Hassan, S. Hameedi, Traditional, state-of-the-art and renewable thermal building insulation materials: An overview, Construction and Building Materials 214 (2019) 709–735. https://doi.org/10.1016/j.conbuildmat.2019.04.102.

[19] T.M. Tiza, S.K. Singh, L. Kumar, M.P. Shettar, S.P. Singh, Assessing the potentials of Bamboo and sheep wool fiber as sustainable construction materials: A review, Materials Today: Proceedings 47 (2021) 4484–4489. https://doi.org/10.1016/j.matpr.2021.05.322.

[20] H. Maleki, H. Barani, Acoustic properties of wool: sound insulation properties of wool fiber, in: The Wool Handbook, Elsevier, 2024: pp. 487–500. https://doi.org/10.1016/B978-0-323-99598-6.00007-4.

[21] O. Bili, K. El Kalaaoui, A. Boukhriss, S. Gmouh, Industrial properties and advancements of synthetic and mineral fibers, in: Synthetic and Mineral Fibers, Their Composites and Applications, Elsevier, 2024: pp. 679–695. https://doi.org/10.1016/B978-0-443-13623-8.00025-3.

[22] E.K. Doyle, J.W.V. Preston, B.A. McGregor, P.I. Hynd, The science behind the wool industry. The importance and value of wool production from sheep, Animal Frontiers 11 (2021) 15–23. https://doi.org/10.1093/af/vfab005.

[23] G. Midolo, M. Del Zoppo, S.M.C. Porto, F. Valenti, Recycling of wasted wool fibers from sheep shearing for green building components: A review, Case Studies in Construction Materials 21 (2024). https://doi.org/10.1016/j.cscm.2024. e03623.

[24] S. Hetimy, N. Megahed, O.A. Eleinen, D. Elgheznawy, Exploring the potential of sheep wool as an eco-friendly insulation material: A comprehensive review and analytical ranking, Sustainable Materials and Technologies 39 (2024). https://doi.org/10.1016/j.susmat.2023.e00812.

[25] A. Maldonado-Alameda, A. Alfocea-Roig, S. Huete-Hernández, J. Giro-Paloma, J.M. Chimenos, J. Formosa, Magnesium phosphate cement incorporating sheep wool fibre for thermal insulation applications, Journal of Building Engineering 76 (2023) 107043. https://doi.org/10.1016/j.jobe.2023.107043.

Chapter 5

CHAPTER 5

CONCLUSIONS

The conclusions section of each appended publication provides the specific outcomes of the respective chapters. This chapter synthesizes the main findings in their entirety, analysing the significance of the results and emphasizing the most impactful implications of the study.

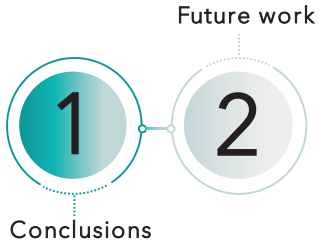

5.1. Conclusions

The cement industry faces significant challenges, including rising demand particularly from developing nations while balancing environmental sustainability with economic feasibility. Projections through 2050 highlight the growing need for innovative approaches to address these demands. As the global economy shifts towards decarbonization, cementitious solutions are anticipated to play a pivotal role in transitioning the cement industry towards sustainability.

In this context, alternative materials can contribute to this transition by maturing technologically to become viable options for use in the cement sector. These emerging materials are expected to become key solutions for decarbonization in various regions over the coming years, providing an effective means to reduce the industry's carbon footprint.

Despite the absence of a mature, established industry with fully sustainable production, magnesia-based cement has steadily attracted growing interest. While research into many magnesia-based cement is still in its early stages, these solutions are

rapidly gaining progress, with various approaches actively being developed and scaled up on a global scale. However, advancing this research area requires focusing on reducing environmental impacts, promoting a circular economy, and improving the management of industrial by-products and wastes. A key strategy in this regard is to replace primary sources of magnesium oxide with alternative secondary sources. This research line has been thoroughly investigated in this thesis, and the main findings are summarized below.

5.1.1. Main findings

The key conclusions presented in order following the specific objectives of the doctoral thesis are summarized as follows:

- Alternative secondary magnesium oxide sources

Secondary sources of magnesium oxide represent a promising alternative to reduce the environmental impact associated with high-purity magnesium oxide. The valorisation of both TUN and LG-MgO contributes to promoting circular economy practices and adds value through improved management of resources.

While LG-MgO has been utilized in previous applications, this PhD thesis is the first of evaluating the feasibility of using TUN for various construction solutions with promising results.

- Development of MPC-TUN

The extensive physicochemical characterization of TUN has demonstrated its suitability as a raw material for the development of MPC. TUN exhibits properties that make it appropriate for MPC formulation without requiring calcination to enhance its reactivity, thus significantly reducing production and energy costs. This research successfully employed TUN to develop both cements and mortars formulations, demonstrating for the first time its feasibility in achieving a K-struvite matrix binder for a range of construction applications.

Critical parameters for cement formulation were identified, including the optimal dosage of TUN and phosphate source, as well as the W/C ratio, among others. For mortars, different W/C ratios were systematically evaluated to analyse their impact on

mechanical and chemical performance, leading to the determination of the optimal formulation. These findings were substantiated through extensive characterization, providing a robust basis for further development.

For alternative materials to be truly viable, they must meet technological, engineering, and environmental criteria. The results indicate that MPC-TUN achieves a substantial reduction in carbon dioxide emissions and resource consumption compared to those formulated with high-purity magnesium oxide, presenting a more sustainable alternative. In addition, the environmental impact assessment reveals that MPC-TUN has a lower contribution to climate change compared to conventional cement, such as OPC CEM I.

These advances highlight the potential of MPC-TUN to positively influence the environmental performance of construction materials. Future scenario changes and continuous optimization in this area will further reduce the environmental footprint of these materials, contributing to sustainable construction practices and aligning with global decarbonization goals.

- Characterization of MPC developed with secondary magnesium oxide sources

The synergy between the two alternative magnesium oxide sources marks an initial step toward exploring the potential of mixing different secondary materials in varying proportions. This approach allows for the observation of the direct effects of each raw material's nature, as well as the synergistic interactions between the two sources, which still require further investigation.

It was observed that LG-MgO exhibits higher reactivity and a smaller particle size. Additionally, the inclusion of LG-MgO slows the setting process due to the heterogeneous nucleation effect induced by the fine particles during the nucleation and growth of K-struvite crystals. This results in increased K-struvite formation, reduced porosity, a less interconnected pore structure, and a higher presence of carbonates, leading to improved compressive strength.

The compatibility of sheep wool fibres (SWFs) with the MPC developed in this PhD thesis opens new possibilities for their application as materials with insulating properties. Through the statistical models generated using a DoE approach, the relationships between variables were statistically optimized within the studied ranges,

aiming to minimize thermal conductivity and apparent density. Both evaluated ratios demonstrated a clear synergistic interaction across all the formulations developed. However, the optimal formulation was identified, offering valuable insights into the material's behaviour.

These findings not only pave the way for the implementation of experimental designs in future research but also highlight the potential for incorporating natural fibres into cement-based materials. The present research opens new avenues for the development of more sustainable and efficient building materials, contributing to advances in both material science and environmental sustainability.

5.1.2. Future work

This PhD thesis establishes a foundation for advancing the integration of by-products and wastes into the construction and building industry. To enhance confidence and demonstrate feasibility, several potential directions for future research are proposed below:

- Complementary characterization to identify phases and evaluate cement hydration

Although extensive characterization has been performed, further analysis is required to gain a more detailed understanding of the different phases present in these materials, quantifying the crystalline phases. In addition, a detailed study of the electrical conductivity, pH, and ionic activity of potassium (K^+) and magnesium (Mg^{2+}) would provide a comprehensive description of the crystalline phases present in the cements, helping to comprehend their behaviour and hydration mechanisms.

- Curing conditions

Apart from evaluating the impact of curing conditions of the final materials' properties, it would be important to explore the influence of temperature, humidity, and curing time, among others. These factors play a crucial role in determining the hydration kinetics, microstructural development, and mechanical performance of the cements.

- Durability

While good mechanical properties are essential for construction materials, their durability against external agents must also be thoroughly assessed. Future studies should focus on the impact of environmental factors such as freeze-thaw cycles, salt crystallization, and capillarity on cement performance.

Further investigations could include evaluating porosity changes after accelerated aging tests and using characterization performances to confirm the stability of K-struvite matrices in various formulations. These studies will help to enhance the long-term durability and sustainability of cementitious materials.

- Use of secondary phosphate sources

The LCA study has revealed that the MKP source is the largest contributor to carbon dioxide emissions and resource consumption in the development of alternative cements. Given the environmental impact associated with this source, it would be both advantageous and environmentally beneficial to explore the use of alternative phosphate sources derived from wastes materials. Utilizing such sources not only reduces the carbon footprint but also promotes the principles of circular economy by revaluating industrial by-products or wastes.

Chapter 6

CHAPTER 6

APPENDIX

This chapter focuses on expanding the publications and conferences directly related to the PhD thesis research, as well as additional publications and conferences that explore topics aligned with those addressed in the doctoral work.

A. Publications and conferences

A.1. Contributions to conferences associated with thesis results

A.1.1. Conferences from Chapter 3

Some of the results from *Chapter 3* focused on *Cement* were presented as an oral communication at the conference *LVIII Congreso Nacional de la SECV (Sociedad Española de Cerámica y Vidrio),* held in Madrid (Spain), in September 2022. The presentation, titled "*Revalorización de residuos refractarios para la formulación de cementos de fosfato de magnesio*" highlighted key findings from the study. The abstract headline of the presentation is shown in Figure A.1.

LVIII Congreso Nacional de la SECV

Revalorización de residuos refractarios para la formulación de cementos de fosfato de magnesio

A. Alfocea-Roig[1*], S. Huete-Hernández[1], J. Giro-Paloma[1], J.M. Chimenos[1], J. Formosa[1]

[1]Departament de Ciència de Materials i Química Física, Universitat de Barcelona, Martí i Franquès 1-11, 08028, Barcelona. Tel.: +34-934037244
*E-mail: annaalfocea@ub.edu

Figure A.1.Oral communication presented at *LVIII Congreso Nacional de la SECV* in 2022.

Additionally, the cement research results were presented as an oral communication at the X *Jornadas Cátedra Acerinox "Acerinox Circular"*, held in Algeciras (Spain), in March 2023. The presentation, titled "*Valoración de residuos refractarios para el diseño y desarrollo de nuevos materiales sostenibles (Eco diseño)*", is showed in Figure A.2.

UCA Universidad de Cádiz
Cátedra Acerinox

ACERINOX

X JORNADAS CÁTEDRA ACERINOX:
"ACERINOX CIRCULAR"

CERTIFICADO DE PARTICIPACIÓN

ANNA ALFOCEA

ha participado como ponente en las X Jornadas Cátedra Acerinox: "ACERINOX CIRCULAR", celebradas en Acerinox Europa, S.A.U. (Los Barrios) los días 22 y 23 de marzo de 2023, con la comunicación:

"VALORACIÓN DE RESIDUOS REFRACTARIOS PARA EL DISEÑO Y DESARROLLO DE NUEVOS MATERIALES SOSTENIBLES (ECO DISEÑO)"

Y para que así conste, y surta los efectos oportunos donde proceda, expido el presente certificado en Algeciras, a 23 de marzo de 2023

Sra. Dña. María del Mar Cerbán Jiménez
Vicerrectora del Campus Bahía de Algeciras

Sr. D. Francisco Fernández de la Mata
Director de la Fábrica Campo de Gibraltar
de Acerinox Europa, S.A.U

UCA Universidad de Cádiz

Cátedra Acerinox
Escuela Técnica Superior de Ingeniería de Algeciras
Avda. Ramón Puyol, s/n
11202 Algeciras (Cádiz)

Figure A.2.Certificate of attendance at the *X Jornadas cátedra Acerinox: "Acerinox Circular"*.

Moreover, an additional study on the durability of the optimal formulation of MPC-TUN was presented as an oral communication at the 7th International Conference Non-Traditional Cement & Concrete, held in Brno (Czech Republic), in June 2023. The presentation, titled "Durability of magnesium phosphate cement using refractory waste as a magnesium oxide source", is summarized in the abstract shown in Figure A.3.

7th International Conference
Non-Traditional Cement & Concrete
June 25-28, 2023
Brno, Czech Republic

Durability of magnesium phosphate cement using refractory waste as a magnesium oxide source

A. Alfocea-Roig[1*], S. Huete-Hernández[1], J. Giro-Paloma[1], J. Formosa[1]

[1]Departament de Ciència de Materials i Química Física, Universitat de Barcelona, Martí i Franquès 1-11, 08028, Barcelona. Tel.: +34-934037244
*E-mail: annaalfocea@ub.edu

Figure A.3. Oral communication presented at the 7th International Conference Non-Traditional Cement & Concrete in 2023.

Some of the results related to the mortar's formulation were presented as an oral communication at the conference *V Jornadas de Jóvenes Científicos en Materiales de Construcción* held in Madrid (Spain), in November 2023. The work presented was titled *"Valoración de un residuo de la industria siderúrgica para la elaboración de morteros a partir de cementos de fosfato de magnesio"*. The abstract headline for the presentation is presented in Figure A.4.

Valorización de un residuo de la industria siderúrgica para la elaboración de morteros a partir de cementos de fosfato de magnesio

A. Alfocea-Roig[1], D. Vera-Rivera[1], S. Huete-Hernández[1], J. Giro-Paloma[1], J. Formosa[1]

[1] *Departament de Ciència de Materials i Química Física, Universitat de Barcelona*
Corresponding author: *Joan Formosa Mitjans, joanformosa@ub.edu*

Figure A.4. Oral communication presented at the *V Jornadas de Jóvenes Científicos en Materiales de Construcción* in 2023.

In addition, the mortars study was presented as an oral communication entitled "Development of mortars using magnesium phosphate cement formulated with tundish deskulling as a MgO source" at the 11th International Conference on the Innovative Valorization of Alternative Materials and Waste Towards Circular Construction WASCON 2023 in Hong Kong (China), in December 2023. The abstract headline is displayed in Figure A.5.

WASCON – Hong Kong, 13-16 December 2023

Development of mortars using magnesium phosphate cement formulated with tundish deskulling as a MgO source

Alfocea-Roig, A[1], Vera-Rivera, D[1], Formosa, J[1], Chimenos, J.M.[1], and Giro-Paloma, J[1]

[1] Departament de Ciència de Materials i Química Física, Universitat de Barcelona

joanformosa@ub.edu (corresponding author)

Figure A.5. Oral communication presented at the 11th International Conference on the Innovative Valorization of Alternative Materials and Waste Towards Circular Construction WASCON 2023 in 2023.

The LCA research was presented as a poster communication at the 11th International Conference on the Innovative Valorization of Alternative Materials and Waste Towards Circular Construction WASCON 2023 (Hong Kong, China) in December 2023. The work presented was titled "Evaluation and comparison of the environmental footprint of two repair mortars through a Life Cycle Assessment". The abstract headline is shown in Figure A.6.

WASCON – Hong Kong, 13-16 December 2023

Evaluation and comparison of the environmental footprint of two repair mortars through a Life Cycle Assessment.

Alfocea-Roig, A[1], Pompido-Pujol, G[1], **Formosa, J[1]**, and Giro-Paloma, J[1]

[1] Departament de Ciència de Materials i Química Física, Universitat de Barcelona

joanformosa@ub.edu (corresponding author)

Figure A.6. Poster communication presented at the 11th International Conference on the Innovative Valorization of Alternative Materials and Waste Towards Circular Construction WASCON 2023 in 2023.

A.2. Contributions associated with alternative construction materials

A.2.1. Publications

A.2.1.1. Sustainable magnesium phosphate micromortars formulated with PAVAL alumina by-product as micro-aggregate

This investigation study was published in *Boletín de la Sociedad Española de Cerámica y Vidrio* (JIF of 3.4 in 2023, Q1) in November-December 2023. The publication headline is shown in Figure A.7. The publication explores the effect of adding a by-product rich in alumina to developed new sustainable magnesium phosphate cement – PAVAL® micromortars.

Figure A.7. Article published in *Boletín de la Sociedad Española de Cerámica y Vidrio* in 2023.

A.2.1.2. Ecotoxicity assessment of sustainable magnesium phosphate cements (Sust-MPCs) using luminescent bacteria and sea urchin embryo-larval development tests

This work was published in the journal of Environmental Chemical Engineering (JIF of 7.4 in 2023, Q1) in October 2024. The publication headline is shown in Figure A.8. The publication assesses the potential ecotoxicity over marine biological life of two

alternative magnesium phosphate cements obtained from secondary sources of magnesium oxide.

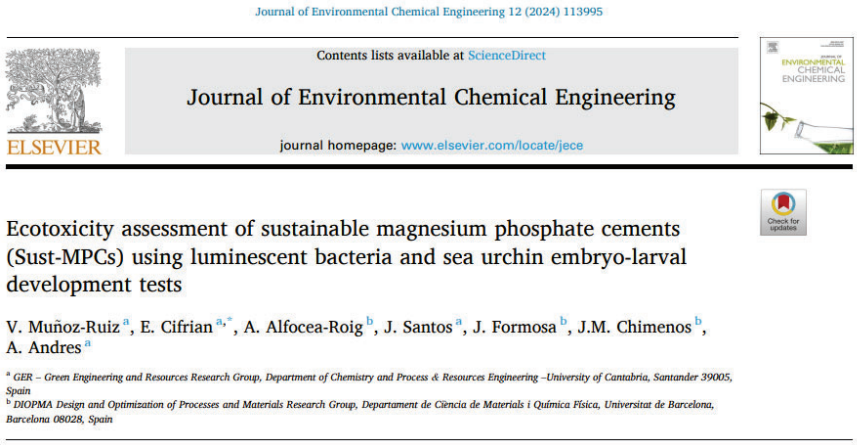
Journal of Environmental Chemical Engineering 12 (2024) 113995

Contents lists available at ScienceDirect

Journal of Environmental Chemical Engineering

journal homepage: www.elsevier.com/locate/jece

Ecotoxicity assessment of sustainable magnesium phosphate cements (Sust-MPCs) using luminescent bacteria and sea urchin embryo-larval development tests

V. Muñoz-Ruiz [a], E. Cifrian [a,*], A. Alfocea-Roig [b], J. Santos [a], J. Formosa [b], J.M. Chimenos [b], A. Andres [a]

[a] GER – Green Engineering and Resources Research Group, Department of Chemistry and Process & Resources Engineering –University of Cantabria, Santander 39005, Spain
[b] DIOPMA Design and Optimization of Processes and Materials Research Group, Departament de Ciència de Materials i Química Física, Universitat de Barcelona, Barcelona 08028, Spain

Figure A.8. Article published in the journal of Environmental Chemical Engineering in 2024.

A.2.2. Conferences

A.2.2.1. Magnesium phosphate micromortars developed with industrial aluminium waste

This work was presented as an oral communication at the conference *IV Jornadas de Jóvenes Científicos en Materiales de Construcción* (Madrid, Sapin) in September 2021. The abstract headline is shown in Figure A.9. In the oral communication, an overview of the properties of magnesium phosphate micromortars produced with industrial aluminium waste was presented.

IV Jornadas de Jóvenes Científicos en Materiales de Construcción

Magnesium phosphate micromortars developed with industrial aluminium waste

A. Alfocea-Roig[1], S. Huete-Hernández[1], A. Maldonado-Alameda[1], J. Giro-Paloma[1], J.M. Chimenos[1], J. Formosa[1]
[1]*Departament de Ciència de Materials i Química Física, Universitat de Barcelona, Martí i Franquès 1, 08028, Barcelona, Spain*
Joan Formosa Mitjans: joanformosa@ub.edu

Figure A.9. Oral communication presented at the *IV Jornadas de Jóvenes Científicos en Materiales de Construcción* in 2021.

A.2.2.2. Life cycle assessment of alkali activated cement compared to ordinary Portland cement

This work was presented as an oral communication and poster at the WasteLCA_3 Life Cycle Assessment for Waste Management and Resource Optimization (Cetraro, Italy) in June 2022. The abstract headline is shown in Figure A.10. The life cycle assessment of alternatives cements compared to conventional cements were exposed.

WasteLCA_3 Life Cycle Assessment for Waste Management and Resource Optimization

LIFE CYCLE ASSESSMENT OF ALKALI ACTIVATED CEMENT COMPARED TO ORDINARY PORTLAND CEMENT

A. Alfocea-Roig, Departament de Ciència de Materials i Química Física, Universitat de Barcelona, Martí i Franquès, 08028, Barcelona, Spain
annaalfocea@ub.edu
A. Maldonado-Alameda, Departament de Ciència de Materials i Química Física, Universitat de Barcelona, Martí i Franquès, 08028, Barcelona, Spain
J. Giro-Paloma, Departament de Ciència de Materials i Química Física, Universitat de Barcelona, Martí i Franquès, 08028, Barcelona, Spain
J.M. Chimenos, Departament de Ciència de Materials i Química Física, Universitat de Barcelona, Martí i Franquès, 08028, Barcelona, Spain
J. Formosa, Departament de Ciència de Materials i Química Física, Universitat de Barcelona, Martí i Franquès, 08028, Barcelona, Spain

Figure A.10. Poster and oral communication presented at the WasteLCA_3 Life Cycle Assessment for Waste Management and Resource Optimization in 2022.

A.2.2.3. Eco-toxicity assessment of sustainable magnesium phosphate cements (Sust-MPCs) using luminescent bacteria and sea urchin embryogenesis bioassays

This work was presented as a poster at the 11th International Conference on the Innovative Valorization of Alternative Materials and Waste Towards Circular Construction WASCON 2023 (Hong Kong, China) in December 2023. The abstract headline is shown in Figure A.11. The analysis of the eco-toxicity assessment of alternative materials developed with secondary raw materials was proposed.

WASCON – Hong Kong, 13-16 December 2023

ECO-TOXICITY ASSESSMENT OF SUSTAINABLE MAGNESIUM PHOSPHATE CEMENTS (Sust-MPCs) USING LUMINESCENT BACTERIA AND SEA URCHIN EMBRYOGENESIS BIOASSAYS

V. Muñoz-Ruiz[1], A. Alfocea-Roig[2], J. Santos[1], **E. Cifrian**[1], J. Formosa[2], J.M. Chimenos[2] and A.Andres[1]

[1] GER – Green Engineering and Resources Research Group, Department of Chemistry and Process & Resources Engineering – ETSIIT, University of Cantabria, 39005, Santander, Spain.
[2] DIOPMA Design and Optimization of Processes and Materials Research Group, Departament de Ciència de Materials i Química Física, Universitat de Barcelona, 08028 Barcelona, Spain
andresa@unican.es (corresponding author)

Figure A.11. Oral communication presented at the 11th International Conference on the Innovative Valorization of Alternative Materials and Waste Towards Circular Construction WASCON 2023 in 2023.

A.2.2.4. Sustainable building solutions: advancements in microencapsulated phase change materials and alternative cements

This work was presented as an oral communication at the 2nd international workshop on net zero carbon buildings, held in Bath (England) in January 2024. The abstract headline, shown in Figure A.12, focuses on innovative materials for sustainable construction and thermal management, with an emphasis on the development of phase change materials.

Sustainable Building Solutions: Advancements in Microencapsulated Phase Change Materials and Alternative Cements

J. Giro-Paloma, A. Alfocea-Roig, J. Formosa

Departament de Ciència de Materials i Química Física, Universitat de Barcelona, Martí i Franquès 1-11, 08028, Barcelona, Spain.

Corresponding autor: jessicagiro@ub.edu

Figure A.12. Oral communication presented at the 2nd international workshop on net zero carbon buildings in 2024.

A.2.2.5. Durability of reinforcements in new eco-friendly phosphate mortars

This work was presented as an oral communication at the *LIX Congreso Nacional de la SECV,* held in Zaragoza (Spain) in June 2024. The abstract headline is shown Figure A.13. In the oral communication, the durability of reinforcements of alternative construction materials was proposed.

LIX Congreso Nacional de la SECV

Durabilidad de armaduras en nuevos morteros ecológicos de fosfatos

Angily Paola Cruz Hernández[1], Joan Formosa Mitjans[2], Jessica Giro Paloma[2], Anna Alfocea Roig[2], Francisco J. Velasco López[1], Manuel Torres Carrasco[1], Asunción Bautista Arija[1*]

[1]Universidad Carlos III de Madrid, [2] Universidad de Barcelona,
Av. de la Universidad, 30, 28911 Leganés, Madrid
E-mail: mbautist@ing.uc3m.es

Figure A.13. Oral communication presented at the *LIX Congreso Nacional de la SECV* in 2024.